# Supramolecular Association of Hydrogen-bonded Polybutadienes Functionalized with Ureidopyrimidone

**A Dissertation Presented for the**

**Doctor of Philosophy**

**Degree**

**The University of Tennessee, Knoxville**

**Sachin Laxman Bobade**

**December 2014**

## Bhagavad-Gita 2.47

**कर्मण्येवाधिकारस्ते मा फलेषु कदाचन |**
**मा कर्मफलहेतुर्भूर्मा ते सङ्गोऽस्त्वकर्मणि ||**

karmaṇyevādhikāraste mā phaleṣu kadācana |
mā karmaphalaheturbhūrmā te saṅgo.astvakarmaṇi ||

***Translation***

Your right is to work only, but never to the fruit thereof. Be not instrumental in making your actions bear fruit, nor let your attachment be to inaction.

## Dedications

*This thesis is dedicated to my late Grandparents, Parents and my Family.*

## Acknowledgements

First of all, I would like to thank, Dr. Durairaj Baskaran for his role as my mentor in scientific research at the NCL, Pune, India and at the University of Tennessee, Knoxville. He will always remain as an ideal scientist and teacher in my life, and unending source of inspiration in my research career. I would like to express my sincere gratitude to my advisor Prof. Jimmy Mays for giving me an opportunity to work in his group, his constant support, and encouragement. I thank both of them for their guidance throughout my graduate school.

I would like to thank my research committee members for their valuable time, suggestions and guidance. I thank, Dr. Alexei Sokolov, Dr. Sheng. Dai, Dr. Gajanan Bhat and Dr. Jimmy Mays for being on my research committee.

Journey of doctoral study seems to be never ending and at a time painful and frustrating, though a constant support and encouragement from family members and close friends provide a much needed comfort and a force to focus and eventually succeed. I would like to thank my family members, my sisters (Archana, and Kalpana), my brother (Nitin) and my wife Laxmi and my in-laws Mr. Mohan Avatade and Mrs. Mangala Avatade, for providing an essential dose of constant support and encouragement. I would especially thank all my relatives for their affection, love and inspiration to succeed in my life.

I would like to thank Dr. Yangyang Wang, ORNL, for his help with polymer characterization and his thoughtful views into understanding polymer rheology. I would also like to thank Dr. Brad Lokitz, for help with polymer characterization at ORNL.

Only a synthetic chemist can better understand the role of proper functioning polymer characterization lab. I really appreciate work of Mr. Tom Malmgren for his constant help with maintaining the PCL lab always ready to use, and running characterization of my samples.

I would also like to thank other staff members at the chemistry department for their help during my stay at UTK. I thanks, Rhonda, Pam and Susan (administrative work); Jessica, Beverly, and Gail (chemstore), Gurley, and John (PC support), Art Patt, and Bo Bishop (glass workshop).

Throughout my time in the graduate school at the University of Tennessee, Knoxville, I have been very fortunate to work with many talented and creative fellow graduate students in our research group. I want to thank ex- and current lab members, Holley Wade, Ravi Aggarwal, Justin Roop, Vikram Srivastava, Andrew Goodwin, Christopher Hurley, Weiyu Wang, Wei Lu, Xinyi Lu, Hongbo Feng, Benjamin Ripy, and Huiqun Wang for making my time pleasurable at UTK.

I would like to thank Adam Imel, and Brad Miller for their help with polymer characterization.

Alongwith graduate students, I also had privilege to work with fellow postdoc and research staff. I would like to thank them all, Dr. Shahinur Rahman, Dr. Suxiang Deng, Dr. Kostas Mischronis, Dr. Beomgoo Kang, and Dr. Namgoo Kang.

I would like to thank Dr. Prakash Wadgaonkar, Mr. Shamal Menon, and Dr. R. A. Kulkarni for their support while my stay at NCL, Pune, India.

I extend my thanks to my all friends at NCL, including group members of Dr. PPW group, and Dr. Baskaran group, for making my stay memorable at NCL.

Non-covalent and covalent interactions play significant roles in a living matter. Covalent bond provides the essential chemical structure and makes backbone of a molecule and non-covalent bonding helps in supramolecular activities. Both are essential for functioning of a life and often not separable from each other. Similarly, during my doctoral study the presences of many people have helped me either directly or indirectly, which was vital for my growth as a good scientist and a good person.

I would like to thank them all!

Finally, I would like to thank my father (Mr. Laxman Bobade), and mother (Mrs. Hirabai Bobade). Without their hard work, struggle, sacrifice, and love, this day would not have been made possible.

Sachin Bobade

## Abstract

Ureidopyrimidone (UPy) is a well-known self-complementary quadruple hydrogen bonding unit, extensively applied in the preparation of supramolecular polymers with enhanced physical properties. The property enhancement is assigned partly to linear chain extension and fibrillar nanophase separation due to secondary hydrogen bonding by urethane and urea linker, though a clear distinctive structure property relationship has not be reported. In this work, two distinct sets of UPy functional polymers, a series of monochelic polybutadienes (PBd) and telechelic polybutadienes, were synthesized and analyzed by solution and bulk characterization techniques to probe the role of polymer chain mobility and polarity on the UPy chain-end association.

ω [omega]-UPy terminated polybutadiene was semi-solid waxy material, indicating association beyond dimers. Solution studies indicate the presence of star-like micelles that are in equilibrium with dimers. These aggregated micellar clusters have distinct endothermic transitions in differential scanning calorimetry (DSC). Atomic force microscopy (AFM) studies show an evidence of micellar-clusters forming associated parallel line-like structures on a mica surface with the well-defined order.

A series of α [alpha], ω [omega]-di-UPy terminated polybutadienes and hydrogenated polybutadienes were synthesized, and their properties was evaluated as a function of *1,2-vinyl* content. Telechelic UPy-PBd differs strongly in their physical properties, PBd with low $T_g$ [glass transition temperature] (-90 °C) forms semi-solid and brittle material, whereas PBd with moderate $T_g$ (-45 °C) gave strong thermoplastic elastomer. AFM images give parallel association of micellar clusters. Dynamics of micellar-cluster associated UPy domains with unassociated chain extended dimers lead to gelation at specific temperature depending on the characteristics of the linker precursor oligomers. Supramolecular gel transition temperature ($T_{SG}$) was identified in rheological studies on various UPy telechelics. In addition, polystyrene and poly(*n*-butylacrylate) UPy telechelics were also prepared by copper (I) catalyzed alkyne azide coupling (CuAAC) "click" reaction. The triazole linker in these polymers interferes with the UPy association and reduces the size of the hydrogen bonded UPy aggregates, which was found to improve the physical property of the supramolecular polymers. An attempt was made to examine the role of polymer chain mobility and its polarity was used to correlate structure and property with reference to room temperature.

# Table of Contents

**Chapter 1: Ureidopyrimidone Based Supramolecular Polymers** ..... 1
1.1 Background ..... 2
1.2 Significance of self-assembly ..... 3
1.3 Supramolecular polymerization ..... 4
1.3.1 Mechanism of the formation of supramolecular polymers ..... 5
1.3.2 Classification of supramolecular polymers ..... 8
1.4 Hydrogen bonded supramolecular polymers ..... 9
1.4.1 Multiple hydrogen bonding in bifunctional small molecules ..... 11
1.4.2 Multiple hydrogen bonding in telechelic oligomers ..... 13
1.5 Nucleobases based supramolecular materials ..... 13
1.6 The need for high $K_a$ system: Ureidopyrimidone (UPy) functionality ..... 17
1.6.1 UPy functionalized supramolecular polymers ..... 19
1.6.2 Supramolecular materials by chain extensions with UPy ..... 23
1.6.3 Non-linear supramolecular polymers using pendant UPy group ..... 29
1.7 Recent development in the UPy supramolecular materials ..... 32
1.8 Conclusions ..... 36
1.9 References ..... 38
**Chapter 2: Scope of the Thesis** ..... 47
2.1 Proposed research ..... 48
2.2 Outline of the thesis ..... 50
2.3 References ..... 51
**Chapter 3: Experimental Techniques and Characterization Tools** ..... 52
3.1 Introduction ..... 53
3.2 Controlled Radical Polymerization ..... 55
3.3 Experimental ..... 59
3.3.1 Typical Schlenk Technique for ATRP and RAFT ..... 60
3.4. High Vacuum Techniques for Anionic Polymerization ..... 60
3.5 Apparatus ..... 62
3.6 Purification of Solvents ..... 63
3.6.1 Benzene ..... 63
3.6.2 Hexanes ..... 64
3.6.3 Tetrahydrofuran ..... 64
3.6.4 Methanol ..... 65

3.7 Purification of monomers ..... 65
3.7.1 Butadiene ..... 65
3.7.2 Styrene ..... 67
3.7.3 Ethylene oxide ..... 68
3.8 Ampulization of initiator solution ..... 68
3.9 Polymerizations ..... 70
3.10 Polymer Characterization Methods ..... 72
3.11 Dilute solution viscometry ..... 73
3.12 Mark-Houwink-Sakurada Equation ..... 75
3.13 Measurement of solution viscosity ..... 75
3.14 Size Exclusion Chromatography ..... 76
3.15 Dynamic Light Scattering ..... 77
3.16 References ..... 82
**Chapter 4: Micellar Cluster Association of Ureidopyrimidone Functionalized Monochelic Polybutadiene** ..... 86
Abstract ..... 87
4.1 Introduction ..... 88
4.2 Experimental Section ..... 91
4.2.1 Materials ..... 91
4.2.2 Characterization ..... 91
4.3.1 Synthesis of monochelic hydroxyl-polybutadiene (MPBd-OH) ..... 92
4.3.2 Synthesis of monochelic UPy-Polybutadiene (MPBd-UPy) ..... 93
4.4 Results and discussion ..... 95
4.4.1 Synthesis of Monochelic polybutadienes with UPy tag ..... 95
4.4.2 Aggregation of monochelic PBd-UPys in SEC elution profile ..... 97
4.4.3 Solution viscosity studies and effect of UPy aggregation ..... 101
4.4.4 Micellar structure and their temperature dependence ..... 105
4.4.5 Solid-state morphology of MPBd-UPy ..... 107
4.4.6 Morphology of MPBd-UPy by Atomic Force Microscopy (AFM) ..... 110
4.5 Conclusions ..... 113
4.6 References ..... 114
**Chapter 5: Synthesis and Characterization of Telechelic Polybutadienes Functionalized with Ureidopyrimidone** ..... 117
Abstract ..... 118
5.1 Introduction ..... 119

5.2 Experimental Section ..... 120
5.2.1 Synthesis of telechelic hydroxyl-polybutadiene (HO-PBd-OH) ..... 121
5.2.2 Synthesis UPy-synthon ..... 122
5.2.3 UPy functionalization of telechelic Polybutadiene (UPy-PBd-UPy) 122
5.3 Results and discussion ..... 123
5.3.1 Intrinsic viscosity of telechelic polymers ..... 130
5.3.2 Effect of addition of end-capping agents in UPy association ..... 133
5.3.3 Bulk properties of telechelic UPy-PBd-UPy polymers: DSC Studies ..... 135
5.3.4 Dynamics of UPy domain aggregation in hydrogenated polymers ... 137
5.3.5 Surface morphology of UPy-PBd-UPy samples ..... 139
5.3.6 Bulk morphology of UPy-PBd-UPy ..... 142
5.4 Conclusions ..... 144
5.5 References ..... 145
**Chapter 6: Synthesis and Characterization of Ureidopyrimidone Telechelics by CuAAC "Click" Reaction: Effect of $T_g$ and Polarity** ..... 147
Abstract ..... 148
6.1 Introduction ..... 149
6.2 Experimental Section ..... 151
6.2.1 Materials ..... 151
6.2.2 Characterization ..... 152
6.3 Synthesis of functional UPy tags ..... 153
6.3.1 NCO-UPy ..... 153
6.3.2 Propargyl-UPy (UPy-Pg) ..... 153
6.3.3 Azido-UPy (UPy-N3) ..... 154
6.4 Synthesis of telechelic functional polymers ..... 154
6.4.1 α, ω-*Bis*-bromo polystyrene (Br-PS-Br) ..... 154
6.4.2 α, ω-*Bis*-azido polystyrene ($N_3$-PS-$N_3$) ..... 155
6.4.3 α, ω-*Bis*bromo poly(*n*-butyl acrylate) (Br-P*n*BA-Br) ..... 155
6.4.4 α, ω-*Bis*azido poly(*n*-butyl acrylate) ($N_3$-P*n*BA-$N_3$) ..... 156
6.4.5 α, ω-*Bis*-propargyl polybutadiene (PgO-PBd-OPg) ..... 156
6.4.6 α, ω-*Bis*-azido poly(ethylene-co--butylene) ($N_3$-P*E*-*co*-*PB*-$N_3$) ..... 157
6.4.7 α,ω-*Bis*-UPy polybutadiene (UPy-PBd-UPy) ..... 157
6.4.8 α,ω-*Bis*-UPy hydrogenated polybutadiene (UPy-(PE-*co*-PB)-UPy). 158

6.5 UPy functionalization of telechelic polymers using CuAAC click chemistry ..... 158
6.5.1 Synthesis of UPy-Tz-polymer-Tz-UPy ..... 158
6.5.2 UPy-Tz-PS-Tz-UPy ..... 158
6.5.3 UPy-Tz-P*n*BA-Tz-UPy ..... 159
6.5.4 UPy-Tz-PBd-Tz-UPy ..... 159
6.6 Results and Discussion ..... 159
6.6.1 Multiple aggregation in SEC elution profile ..... 166
6.6.2 Solution viscosity ..... 167
6.6.3 Effect of heating rate and aging on DSC analysis of UPy Telechelics ..... 169
6.6.4 Network structure by AFM and DMTA ..... 173
6.7 Conclusions ..... 177
6.8 Appendix Information ..... 177
6.9 References ..... 178
Appendix A6 ..... 181
**Chapter 7: Dynamics of Ureidopyrimidone Telechelics: Role of Chain Mobility and Polarity** ..... 185
Abstract ..... 186
7.2 Experimental section ..... 190
7.2.1 Rheology and Dynamic Mechanical Analysis ..... 190
7.3 Results and Discussion ..... 191
7.3.1 Gelation in UPy Telechelics ..... 191
7.3.2 Effect of *1,2 vinyl* contents and hydrogenation on the melt viscosity of UPy telechelics ..... 198
7.3.3 Influence of low $T_g$, polar and high $T_g$, nonpolar linker ..... 204
7.4 Dynamics of UPy-Supramolecular Associations ..... 207
7.5 Conclusions ..... 209
7.6 References ..... 210
Appendix 7A ..... 212
**Chapter 8: Conclusions and Feature Perspective of UPy Hydrogen Bonded SPs** ..... 213
Vita ..... 216

# List of Tables


**Table 3. 1:** Common terms used in definition of viscosity[56,57] ..... 73
**Table 3. 2:** Common equations used for determination of intrinsic viscosity [η][59] ..... 74
**Table 4. 1:** Characterization of monochelic polybutadiene with hydroxyl (MPBd-OH) and ureidopyrimidone (MPBd-UPy) functional groups .....97
**Table 4. 2:** Concentration dependent GPC of the MPBd-UPy-2 and MPBd-OH-2 .... 101
**Table 4. 3:** Viscosity measurements of MPBd-OH and MPBd-UPy samples in toluene ..... 102
**Table 4. 4:** Enthalpy values of MPBd-UPy..... 109
**Table 5. 1:** $^{1}$H NMR and SEC characterization of the functional (X) polybutadienes with the hydroxyl (HO-PBd-OH) and ureidopyrimidone (UPy-PBd-UPy) .....125
**Table 5. 2:** Effect of microstructure of PBd on DSC characterization of UPy-PBd-UPy ..... 136
**Table 6. 1:** Characterization UPy telechelics prepared by combination of ATRP and CuAAC click reactions .....165
**Table 6. 2**: DSC analysis of UPy-PBd-UPy, effect of triazole on hydrogen bonded aggregation of UPy groups ..... 169
**Table 6. 3:** Modulus enhancement of Triazole linker in UPy telechelics..... 176
**Table 7. 1:** DSC characterization of UPy-PBd-UPy and UPy-(PE-*co*-PB)-UPy samples.....192
**Table 7. 2** Gelation temperature for UPy-PBd-UPy and UPy-(PE-*co*-PB)-UPy ..... 197

# List of Figures


**Figure 1. 1:** Theoretical plot of the degree of polymerization as a function of association constant and concentration (for an isodesmic polymerization mechanism) (section 1.4)[28] ..... 5

**Figure 1. 2:** Schematic representations of the major supramolecular polymerization mechanism (ditopic monomer).[33] ..... 6

**Figure 1. 3:** Qualitative plot of degree of polymerization vs concentration of the monomer (discotic), a) multistage open association (MSOA) or isodesmic, b)nucleation elongation (NE) with helical growth concentration (c*), c)open supramolecular liquid crystal (SLC) with mesophase formation concentration ($c^i$).[33,39] ..... 8

**Figure 1. 4:** Schematic representations of supramolecular polymers a) main-chain supramolecular polymers and b) side-chain supramolecular polymers.[39].... 9

**Figure 1. 5:** Influence of the secondary interactions on the stability of the triple hydrogen bonding motif.[71,73] ..... 10

**Figure 1. 6:** Lehn's main chain supramolecular polymerization with ditopic molecules functionalized with triply hydrogen bonding unit.[16,17,78]..... 12

**Figure 1. 7:** Schematic representation of phase transition for molecular liquid crystals.[24] ..... 12

**Figure 1. 8:** Supramolecular associations by single hydrogen bond a) Griffin's supramolecular polymer network formation by tetrakis-pyridine and bis-benzoic acid derivatives[80], b) Kato's side chain liquid crystalline supramolecular polymer[26] ..... 13

**Figure 1. 9:** (Left) Recognition motif or thymine and diaminotriazine, and proposed mechanism for the aggregation, (right) schematic representation of aggregates particle and effect of length of functional block on size of aggregates.[89] ..... 15

**Figure 1. 10:** i) PTHF end functionalized with adenine, and thymine, ii) optical microcopy of fiber and film formation made from melt of **35**, iii) proposed mechanism for transition from gel-like to linear polymer.[93,94] ..... 16

**Figure 1. 11:** Selected examples of the multiple hydrogen bonding motif containing more than four hydrogen bonds (association or dimerization constant are determined in chloroform solutions).[19,46,109,116,118,126,128-135] ..... 18

**Figure 1. 12:** Schematic syntheses of 2-ureidompyrididone, and two self-complementary tautomeric forms 4[1H] keto and 4[1H] enol.[46] ..... 19

**Figure 1. 13:** Structures of small building blocks with di-and tri-functional UPy group.[19] ..... 20

**Figure 1. 14:** Effect of monofuctional UPy (14) addition on the specific viscosity of 40 mM solution of monomer **12** in chloroform, and unidirectional chain extension vs multidirectional aggregates or gelation.[19,138] ..... 21

**Figure 1. 15:** Effect of spacer and monomer concentration on the linear-chain, ring-chain, and network formation.[19,138] ..... 22

**Figure 1. 16:** DMTA and rheology analysis, a) DMTA showing the presence of two $T_g$s, (single $T_g$ by DSC at 10 °C), b) A plot of G' and G" vs frequency at 40 °C

showing a rubbery plateau, and c) the melt viscosity of the monomer **13** vs frequency at various temperatures.[19,138] ..... 23
**Figure 1. 17:** Two approaches for the synthesis of UPy-telechelic, and the formation or urethane or urea linkages from hydroxyl and amino telechelic precursors, respectively.[19,28,138,142,143] ..... 24
**Figure 1. 18:** Schematic representations of UPy-functionalized polymers. a) UPy telechelics by reacting UPy-synthon with various hydroxyl precursors, and the pictures of viscous precursor and solid UPy elastomer of ethylene-*co*-butylene, b) telechelic PDMS-UPy c) trifunctional PEO-b-PPO, and d) monofuctional PS-b-PI-UPy.[41,47,142,143] ..... 25
**Figure 1. 19:** DSC traces of telechelic poly(ethylene-*co*-butylene) reported by Meijer et al.[47] ..... 27
**Figure 1. 20:** Schematic representation of free radical co-polymerization of UPy-methacrylate monomers[149,160] ..... 29
**Figure 1. 21:** Relationship between $T_g$ and UPy wt%.[148,149] ..... 30
**Figure 1. 22:** Biomimetic design of titin protein by UPy group; a) concept and design, b) two modular monomeric units, c) stress-strain curves of UPy based polymer (A), control polymer (b), and a reference polyurethane ( inset - hysteresis of single extension and retention).[164] ..... 31
**Figure 1. 23:** i) Tapping mode AFM images of poly(ethylene-co-butylene, $M_n$-3,500 g/mol) end functionalized with various functional groups (a, b, c, and e), ii) schematic representation of theoretical aggregation driven by nano-fiber formation, iii) rheological master curves for polymer d and e, with reference temperature of 125 °C, and 110 °C, respectively.[174] ..... 33
**Figure 1. 24:** a) Scheme for the synthesis of PnBA-ran-PnBA-UPy, b) linear relationship between UPy content and $T_g$ (at a constant polymer backbone molecular weight of ~ 24 kg/mol), c) storage modulus for the copolymer with various UPy contents, and d) effective H-bond life time with increasing UPy content (for random copolymer).[151] ..... 34
**Figure 1. 25:** Schematic representations of polynorbornene based nanoparticles synthesis, photolysis leading to collapse, and acidification leading to expansion, and AFM height image of the nanoparticles (right down).[173] .. 35
**Figure 2. 1:** Presence of micellar-clusters in UPy functionalized polybutadiene supramolecular polymer. The illustration is based on the AFM image obtained in our preliminary studies. .....48
**Figure 2. 2:** Proposed synthesis of mono- and telechelic polybutadienes, polystyrene, and poly(*n*-butyl acrylate) with UPy functionality, $f$ = 1, and 2. ..... 49
**Figure 3. 1:** Schlenk reactor with ground glass joint for attaching to high-vacuum line and with the Young's Teflon stopcocks (B), and flask with additional joint for septum. .....60
**Figure 3. 2:** High vacuum line set up ..... 62
**Figure 3. 3:** Break-seal and glass constriction ..... 63
**Figure 3. 4:** Purification of benzene for anionic polymerization (a), removable solvent reservoir with stopcock and color indication for pure solvents with

recommended solvent fill line to prevent bumping of solvent onto stopcock (b) (necessary for THF) ..... 64
**Figure 3. 5:** Apparatus for the distillation of butadiene ..... 67
**Figure 3. 6:** Ampules for distillation of styrene ..... 68
**Figure 3. 7:** Split-down apparatus for the dilution of initiator (structures of *sec*-butyllithium and 3-(*ter*-butyldimethylsilyloxy)-1-propyllithium are shown in the inset) ..... 69
**Figure 3. 8:** Polymerization reactor (A) with purge section and (B) after detaching from the vacuum line and distilling pure benzene from purge section. ..... 70
**Figure 3. 9:** Correlation function and corresponding spectrum of relaxation times for, single exponential decay (a), and theoretical multimodal curve for associating polymers with corresponding spectrum of relaxation times (b)[65] ..... 79
**Figure 3. 10:** Schematic diagram of light scattering apparatus and theoretical correlation as a function of size ..... 80
**Figure 4. 1:** $^{1}$H NMR spectrum of UPy- Synthon ..... 93
**Figure 4. 2:** $^{1}$H NMR spectrum of a) precursor MPBd-OH-4 and b) after chain-end functionalization with UPy, MPBd-UPy-4. The signals marked as * indicate residual solvent and antioxidant. ..... 95
**Figure 4. 3:** Picture of MPBd-OH-2 (liquid) and MPBd-UPy-2 (non-flowing semisolid) ..... 97
**Figure 4. 4:** GPC traces of a) MPBd-OH-4 and MPBd-UPy-4 and b) other MPBd-UPy samples showing presence of dimeric peak. ..... 98
**Figure 4. 5:** Concentration dependent (1-5 mg/mL) GPC eluogram of the MPBd-UPy-2 (a) and MPBd-OH-2 (b) ..... 100
**Figure 4. 6:** Plot of reduced viscosity vs concentration for a) MPBd-UPy-2 (i and ii) and MPBd-$(UPy)_2$-1 (iii and iv) in comparison with respective precursors and b) MPBd-UPy-4 (i and iv) and mixed with 55 wt % and 16 wt % precursor. ..... 103
**Figure 4. 7:** Temperature dependent DLS histogram of a) MPBd-UPy-1 and b) plot of $R_h$ over temperature for different populations observed in MPBd-UPy-4. ..... 106
**Figure 4. 8:** Representive histograms of the a) MPBd-UPy-4 and b) MPBd-$(UPy)_2$-1 at 25 °C ..... 107
**Figure 4. 9:** DSC traces of repeated heating cycles of (a) MPBd-UPy-1 and (b) MPBd-$(UPy)_2$-1 systems. ..... 110
**Figure 4. 10:** DSC profile of MPBd-UPy 7 kg/mol (*1,2-vinyl* contents ~94 %), a) after first run, b) after ~3 months at 30 °C ..... 110
**Figure 4. 11:** Phase images of i) MPBd-UPy-1, ii) MPBd-UPy-3, and iii) MPBd-UPy-4 b) zoomed in image of MPBd-UPy-3 and an illustration representing features of micellar-cluster morphology. ..... 111
**Figure 4. 12:** Time dependent morphology of MPBd-UPy-4 (from left to right, 15 min, 24 h, and 48 h after drop coating a thin film on freshly cleaved mica). The images were taken without changing the position of the sample in the AFM over 48 h. The size of the fibrous looking associated micellar clusters changes gradually over time indicating surface mobility of the associates

induced by PBd segments (low $T_g$) at room temperature. Micellar cluster sizes are in the range of ~ 25-27 nm..... 112
**Figure 5. 1:** $^1$H NMR spectra of a) UPy-PBd-UPy-1 and b) HO-PBd-OH-1 .....126
**Figure 5. 2:** $^1$H NMR spectra of a) UPy-PBd-UPy-5 and b) HO-PBd-OH-5 ..... 127
**Figure 5. 3:** $^1$H NMR spectrum of a) UPy-(PE-*co*-PB)-UPy-1 and b) HO-(PE-*co*-PB)-OH-1 ..... 127
**Figure 5. 4:** $^1$H NMR showing a) UPy-(PE-*co*-PB)-UPy-4 and b) HO-(PE-*co*-PB)-OH-4 ..... 128
**Figure 5. 5:** SEC traces of telechelic UPy, black like indicates hydroxyl precursor, and colored line indicates UPy functionalized polymers (arrow indicates presence of dimeric peak)..... 129
**Figure 5. 6:** SEC traces of hydroxyl and UPy telechelics of PBd with *1,2-vinyl* contents of ~57% ..... 129
**Figure 5. 7:** Double logarithmic plots for the solution viscosity of UPy-PBd-UPy samples with slope values reported in the bracket are for the similar concentration range for all the polymers (a); and effect of monofunctional impurity (chain stopper) and hydroxyl functional impurities (b)..... 131
**Figure 5. 8:** Plot of specific viscosity vs concentration for X-PBd-X-7 (a) and double logarithmic plots for the UPy-PBd-UPy-7 with slope value as function of concentration range (b)..... 131
**Figure 5. 9:** Double logarithmic plots of solution viscosity of UPy-PBd-UPy samples in the presence of chain-stoppers in chloroform. (a) in the presence of 8 mol % monofunctional oligomer impurity, MPBd-UPy and b) low molecular weight C6-UPy impurity. ..... 134
**Figure 5. 10:** DSC profile of UPy-PBd-UPy-1 (a) and UPy-PBd-UPy-4 (b)..... 137
**Figure 5. 11:** AFM phase images of UPy-PBd-UPy-2 (a) Scan size 1μm (b) zoomed image scan size 594 nm, and c) size of cluster domains. ..... 140
**Figure 5. 12:** AFM micrographs of UPy-PBd-UPy-1 (a) and UPy-PBd-UPy-4 (b)..... 142
**Figure 5. 13**: AFM phase images of UPy-PBd-UPy-4 a) thin film cast on mica surface, and b) bulk morphology (zoomed). ..... 142
**Figure 5. 14:** UPy-PBd-UPy-5, a) AFM of bulk phase from cryo-cut film, b) thermoplastic film forming ability from melt, and c) proposed micellar cluster network formation ..... 143
**Figure 6. 1:** $^1$H NMR spectra of (a) UPy-$N_3$ and (b) UPy-Pg. The star (*) indicates residual protons of $CDCl_3$. .....160
**Figure 6. 2:** $^1$H NMR spectra of UPy-telechelics prepared by CuAAC click reaction. a) UPy-Tz-PBd-Tz-UPy, b) UPy-Tz-P*n*BA-Tz-UPy, and c) UPy-Tz- PS-Tz-UPy. The star (*) indicates residual solvent $CDCl_3$. ..... 163
**Figure 6. 3:** a) $^1$H NMR and b) ATR-IR spectra of various stages of UPy-Tz-(PE-*co*-PB)-Tz-UPy synthesis. ..... 164
**Figure 6. 4:** SEC eluograms of UPy telechelics prepared by CuAAC click reaction using RI detector. a) UPy-Tz-PS-Tz-UPy-UPy, b) UPy-Tz-PBd-Tz-UPy, and c) UPy-Tz-P*n*BA-Tz-UPy, all SEC sample concentration are 1 mg/mL. ..... 166
**Figure 6. 5:** a) SEC traces showing effect of concentration on the aggregation of UPy groups in UPy-Tz-PS-Tz-UPy (i) 1 mg/mL and (ii) 2 mg/mL and b) a plot

of peak-maximum molecular weight at different injection sample concentration with light scattering detector using $d_n/d_c$ of 0.186. ..... 167
**Figure 6. 6:** Viscosity profile of UPy telechelics and the effect of triazole on UPy chain end association of UPy-Tz-PBd-Tz-UPy and UPy-Tz-PS-Tz-UPy. ..... 168
**Figure 6. 7:** DSC profile of telechelic PBd UPy, (i) heating rate (5 °C), UPy-PBd-UPy (a) and UPy-Tz-PBd-Tz-UPy (b); (ii) heating rate 20 °C, UPy-PBd-UPy (a) and UPy-Tz-PBd-Tz-UPy (b). ..... 171
**Figure 6. 8:** DSC plot of UPy-Tz-(PE-*co*-PB)-Tz-UPy ..... 171
**Figure 6. 9:** AFM Phase images of UPy-PBd-UPy (a) and UPy-Tz-PBd-Tz-UPy (b), and size of aggregated domains (from chloroform solution). ..... 172
**Figure 6. 10:** Complex viscosity master curves of UPy-Tz-PBd-Tz-UPy and UPy-PBd-UPy at reference temperature 90 ºC. ..... 174
**Figure 6. 11:** Temperature dependence of modulus for UPy-PBd-UPy and UPy-Tz-PBd-Tz-UPy ..... 175
**Figure 6. 12:** DMTA plot of Tan delta for UPy-Tz-(PE-*co*-PB)-Tz-UPy and UPy-(PE-*co*-PB)-UPy ..... 177
**Figure A6. 1:** FTIR (ATR) spectrums of UPy-Pg and UPy-$N_3$ .....181
**Figure A6. 2:** SEC traces of UPy-Tz-PS-Tz-UPy, the effect of concentration on the aggregation of UPy groups (1 mg/mL (a) to 6 mg/mL (e) (values are reported with the light scattering detector using $d_n/d_c$ of 0.186) ..... 181
**Figure A6. 3:** FTIR (ATR) spectra of end group transformations. a) UPy-Tz-P*n*BA-Tz-UPY, b) UPy –TZ-PS-Tz-UPy ..... 182
**Figure A6. 4:** FTIR (ATR) spectrum of UPy-Tz-PBd-Tz-UPy ..... 182
**Figure A6. 5:** Glass transition temperatures of the three polymers prepared by CuAAC click ..... 183
**Figure A6. 6:** Viscosity profile of UPy telechelics and the effect of triazole on UPy chain end association a) UPy-Tz-PBd-Tz-UPy and b) UPy-Tz-PS-Tz-UPy ..... 183
**Figure A6.7:** DSC profile (at heating rate 10 °C/min) showing effect of triazole on the UPy-group association in the UPy-PBd-UPy ..... 184
**Figure 7. 1:** Schematic representation of lateral aggregation of UPy dimers: (a) through π–π stacking in hydrogen bonded UPy dimer, (b) additional 1D stacking in H-bonding UPy dimer via a urethane linker, and (c) additional 1D staking by bifurcated H-bonding in UPy coupled via a urea linker.[14] .....189
**Figure 7. 2:** Dynamic mechanical spectra of UPy-PBd-UPy-4, 57% *1,2-vinyl* before and after gelation ..... 193
**Figure 7. 3:** Linear viscoelastic data of UPy-PBd-UPy-4 before gelation. SAOS measurements were performed at every 5 °C between 95 and 35 °C. The data are shifted to 90 °C according to the time-temperature superposition principle. Circles: Storage modulus (G′); Squares: Loss modulus (G″)... 195
**Figure 7. 4:** Temperature dependence of zero-shear viscosity (η). UPy-(PE-*co*-PB)-UPy-1 (16 % *1,2-vinyl* could not melt completely at the three testing temperatures (150, 145, and 140 °C), and did not strictly exhibit Newtonian behavior. The data for UPy-PBd-UPy-16 % *1,2-vinyl* should only be regarded as rough apparent viscosities. ..... 199

**Figure 7. 5:** Temperature dependence of viscosity for PBd-based (57 % *1,2-vinyl*) polymers. Solid symbols: UPy-terminated telechelic polymers. Open symbols: hydroxyl-terminated telechelic polymers. Red circles: polybutadienes (PBd). Blue diamonds: hydrogenated polybutadienes (PE-*co*-PB). ..... 200
**Figure 7. 6:** Temperature dependence of viscosity for PBd-based (16% *1,2-vinyl*) polymers. Solid symbols: UPy-terminated telechelic polymers. Open symbols: hydroxyl-terminated telechelic polymers. Red circles: polybutadienes (UPy-PBd-UPy-1). Blue diamonds: hydrogenated polybutadienes (UPy-(PE-*co*-PB)-UPy-1). ..... 201
**Figure 7. 7:** Comparison of the viscosities of different PBd precursors. ..... 202
**Figure 7. 8:** Comparison of the viscosities of PBd-UPys of different microstructures and molecular weight distributions ..... 203
**Figure 7. 9:** Comparison of the viscosities of different hydrogenated PBd-UPys..... 203
**Figure 7. 10:** DMTA curve of UPy-PBd-UPy with 57% *1,2-vinyl* groups and with different molecular weight. ..... 204
**Figure 7. 11:** Glass transition temperature of PBd-UPy-4 and PS-UPy and P*n*BA-UPy 205
**Figure 7. 12:** Comparison of the viscoelastic spectra of UPy-based supramolecular polymers of different backbones. (a) PBd-4. (b) PS. (c) P*n*BA. ..... 206
**Figure 7. 13:** Temperature dependence of viscosity for UPy-based supramolecular polymers of different backbones. (a) 2.3 kg/mol Polybutadiene (PBd) with 16 % *1,2-vinyl* groups. (b) 2.4 kg/mol PBd with 57 % *1,2-vinyl* groups. (c) 3.2 kg/mol Poly(*n*-butyl acrylate) (P*n*BA). (d) 2.4 kg/mol Polystyrene (PS) ..... 207
**Figure 7A. 1:** Temperature dependence of viscosity for P*n*BA-UPy and P*n*BA-Br. .....212
**Figure 7A. 2:** Temperature dependence of viscosity for PS-UPy and PS-Br. ..... 212

# List of Schemes


**Scheme 3. 1:** Anionic polymerization of styrene using sodium naphthalenide as initiator in THF at – 78 °C (a), and anionic polymerization of styrene using sec-butyllithium as initiator in cyclohexane at RT (b)..... 54

**Scheme 3. 2:** Three main groups of controlled radical polymerization based on the mechanism of reversible activation: (1) stable free radical polymerization (SFRP), examples (a), and (b), (2) atom transfer radical polymerization (ATRP), examples (c) and (d), and (3) degenerative chain transfer polymerization (DT), examples e), (f) and (g)..... 57

**Scheme 3. 3:** Key components of ATRP (a) and RAFT (b) ..... 58

**Scheme 4. 1:** UPy dimerization in the case of monochelic and linear supramolecular polymerization of telechelic functionalized oligomers.....89

**Scheme 4. 2:** Synthesis of monochelic polybutadienes by anionic polymerization and their chain-end transformation with a) monochelic polybutadiene with monofunctional UPy (MPBd-UPy) and b) monochelic polybutadiene with difunctional UPy (MPBd-$(UPy)_2$). ..... 94

**Scheme 4. 3:** Proposed dynamic equilibrium of micellar cluster aggregates in toluene solution of MPBd-UPy ..... 104

**Scheme 5. 1:** Synthesis of hydroxyl telechelic polybutadienes by anionic polymerization (a) and chain-end transformation of various hydroxyl terminated polybutadienes (HO-PBd-OH) and hydrogenated polybutadienes (HO-(PE-*co*-PB)–OH) into UPy-telechelics (b).....124

**Scheme 5. 2:** Representation of UPy-PBd-UPy polymers undergoing linear chain-extension via UPy hydrogen-bonding dimerization extending to multiple hydrogen bonded aggregates. ..... 132

**Scheme 5. 3:** Proposed equilibrium of associated micellar clusters and their alignment into parallel lines with unassociated linear molecules..... 141

**Scheme 6. 1:** Synthesis of UPy telechelics of PS, P*n*BA, and PBd by combination of ATRP and CuAAC click reactions .....151

**Scheme 6. 2:** Schematic synthesis of UPy telechelic polybutadiene, with and without triazole ring. ..... 161

**Scheme 6. 3:** Synthesis of triazole containing hydrogenated PBd telechelics (UPy-Tz-(PE-*co*-PB)-Tz-UPy). ..... 162

**Scheme 7. 1:** Different equilibrium states of mono- and telechelic associating systems**.**.....188

**Scheme 7. 2:** Proposed structures of UPy-PBd-UPy as function of supramolecular gelation temperature ..... 198

# Chapter 1: Ureidopyrimidone Based Supramolecular Polymers

## 1.1 Background

Synthetic organic macromolecules are indispensable for modern life and they find applications everywhere. Macromolecules are high molecular weight compounds formed via linking vinyl or bifunctional monomers with covalent bonds such as, C-C, C-O, C-N, and C-Si, etc. In general; they are synthesized using addition or step-growth polymerization methods.[1] A long linear chain structure of polymers and their high molecular weights provide enhanced inter/intra-molecular interactions to yield bulk material properties that are useful in all fields of engineering. The properties of polymers both in solution and solid state are governed by the structure or the composition of monomers, molecular weight, molecular weight distribution, branching, morphology, tacticity, microstructure, and functionality of the polymeric chain.[2] On the other hand, concepts of supramolecular chemistry (the chemistry beyond the molecules) based on self-assembly or self-recognition of molecules, primarily driven by non-covalent interactions, has been used to form various host-guest systems to understand biological function.[3-15] In the last three decades, such a molecular recognition phenomenon using non-covalent interactions has been extended to produce supramolecular polymers (SPs) for bulk physical property exploitation.[7,16-32]

In supramolecular chemistry, specially functionalized organic small molecules and oligomers are held together by non-covalent interactions resulting in macromolecular assemblies that exhibit specific physical and chemical properties. In general, secondary interactions such as ionic (50-200 kJ/mol), hydrogen bonding (4-120 kJ/mol), dipole-dipole (4-40 kJ/mol), pi-pi (1-20 kJ/mol) and van-der Waals (dispersion)(1-10 kJ/mol) interactions have been used to 'glue' the small or oligomers together to form SPs.[18,25,28,32-39]

Self-assembly of SPs rely strongly on the combination and cooperativity of many such weak secondary interactions. Initial studies in the field of SPs were focused on the liquid crystalline properties of complex macromolecules.[16,40] In the last two decades the attention is focused on the synthesis of polymeric materials targeting to exhibit superior mechanical properties in solid-state.[41] The first SP was synthesized by Lehn and co-workers in 1990.[16] Subsequently, Kato and Fréchet also reported the synthesis of complex macromolecular architectures based on the non-covalent interactions.[20,22] Hydrogen bonding is an ideal choice for non-covalent interaction due to specificity, directionality and reversibility by external stimuli such as, temperature, pressure, and solvent polarity.[42] π-π interactions and ionic

interactions were also employed to enhance self-assembly.[28] However, ionic interactions are not suitable due to their irreversibility, and pi-pi interactions are not strong enough to make SPs on their own.

The most commonly used non-covalent interaction is hydrogen bonding, and it gives dynamically interacting SPs. A molecular system consisting of either two or three hydrogen bonds with weak to moderate hydrogen bonding strength is required to form SPs. Earlier examples of SPs were derived from the nucelobases such as thymine, uracil, adenine, and diaminopyridines functionality.[16,43] Recently, Beijer and co-workers showed the formation of supramolecular polymer based on ureidopyrimidone (UPy), a strong quadruple hydrogen bonding motif, containing four hydrogen bonds.[19,44-47]

This introductory chapter will give an overview of the development of SPs based on multiple hydrogen bonding, their scope and limitations. It will also review the current state of the art synthesis of UPy containing SPs and their material properties.

## 1.2 Significance of self-assembly

The process of self-assembly requires molecules to have a specific shape and charge distribution in order to selectively, non-covalently, and reversibly interact to form thermodynamically stable pre-organized hierarchical structures. The development of supramolecular chemistry originated from the earlier understanding of host-guest interaction, ion-transport in biology, and molecular assemblies of crown ethers[5,6,48-50], cryptands[7,12,13,51,52], cyclodextrins[53], clathrates, and spherands. The pioneering contributions of Pedersen[5], Cram[3,4,54,55], and Lehn[7-9,17,56-58] led a new way of transforming small molecular association into supramolecular association.[3-5,7]

Supramolecular chemistry thrives on the inspiration from the nature and the desire to synthesize hierarchical molecular assemblies that are otherwise difficult to make solely based on covalent bonding to have complex environmental responsive materials. Directed associations of synthetic molecules driven by multiple non-covalent interactions lead to thermodynamically stable self-assembled SPs.[59,60] Weak non-covalent interactions are primary forces to construct dynamically, reversibly interacting SPs.

A well-known natural biopolymer, a SP and an ‘identity card’ of the living system, is the deoxyribonucleic acid (DNA), whose double helix structures and other properties are the results of cooperative non-covalent interactions between multiple hydrogen bonding units of

nucleobases, and hydrophobic interactions. Biomimetics though replication of self-assembly is crucial for sustaining life on the earth. Biological SPs can respond to external forces of the environment by virtue of equilibrium reversibility of self-assembly. In a similar fashion, synthetic molecules self-assembled via reversible non-covalent interactions can lead to the formation of 'smart SPs'. Biological systems use supramolecular association for the purpose of various mechanistic processes such as peptide folding, aggregation, ion-transport, receptor–ligand interactions as well as the construction of cells.[61-65] For examples, silk fibroin and collagen are well known natural proteins. Fibroin's unique strength is governed by the physical crosslink by micro-crystalline domains held in the flexible matrix, and collagen strength arises from covalent cross-linking of the hydrogen bonded triple helix into helical rod. Therefore silk is amongst the widely studied biomaterials.[66]

Similarly, secondary interactions also play a significant role in man-made polymers. Properties of synthetic polymers like nylon, *Kevlar*, *Nomex* have exceptional strength as a result of hydrogen bonding between the polymer chains (amide bond).[67] Unique properties of polyethylene are the result of weak van der Waals interactions.[39] Thus, non-covalent interactions have been used extensively and exploited in self-assembly processes in many areas of supramolecular research such as molecular recognition, ion-complexation, template directed synthesis, biomimetics, ligand co-ordination, and study of the amphiphlic systems. Currently, SPs are one of the interesting topics in the field of polymer chemistry with applications ranging from biochemistry, material chemistry and nanotechnology.

## 1.3 Supramolecular polymerization

Supramolecular polymerization is a process of self-assembling bi-functional monomer(s) (small building blocks, AB or $A_2$ type) or oligomer(s) containing two or more reversible and highly directional associating non-covalent interaction sites to form SPs. SPs are a class of polymers, which possess properties of long macromolecular chains. As the polymerization is a reversible equilibrium process that makes the SPs co-exists dynamically with small molecular weight fractions. In addition to the similarity to covalent polymeric materials, the SPs are held by reversible dynamic non-covalent bonds, which make them suitable for tuning their properties by the external forces such as temperature and pH, etc.

In principle, the polymerization can be divided into three steps; 1) selective dimerization through non-covalent bonds, 2) propagation through sequential binding-a linear

chain extension or formation of rings, spheres, and large assemblies; and 3) termination by addition of mono-functional interacting capping molecules also called as chain-stoppers. Properties of the conventional covalent polymers are highly dependent on the degree of polymerization (DP); similarly, molecular weight of SP is dependent on the degree of polymerization set by the association constants, $K_a$, between the secondary interaction sites. **Figure 1.1** gives the theoretical correlation between $K_a$ and the degree of polymerization (DP).

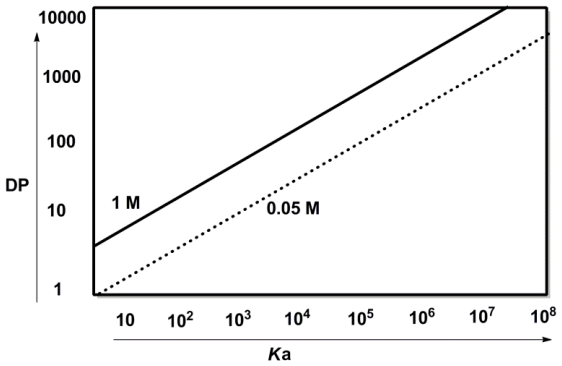



**Figure 1. 1:** Theoretical plot of the degree of polymerization as a function of association constant and concentration (for an isodesmic polymerization mechanism) (section 1.4)[28]

### 1.3.1 Mechanism of the formation of supramolecular polymers

As stated above supramolecular polymerization involves self-assembly process that links non-covalently interacting monomers into SPs. Association of secondary interactions between bifunctional molecules (ditopic, AB or AA) can be either by complementary (A-B) or self-complementary (A-A).The supramolecular polymerization is an equilibrium polymerization primarily driven by the strength of association constants, $K_a$ of interacting monomers. Thus, the degree of polymerization (DP) is a strong function of association strength of non-covalent interaction, concentration, and temperature of polymerization. The polymerization mechanism can be divided into three types; i) isodesmic, ii) ring-chain, and iii) co-operative growth (**Figure 1.2**).[33]

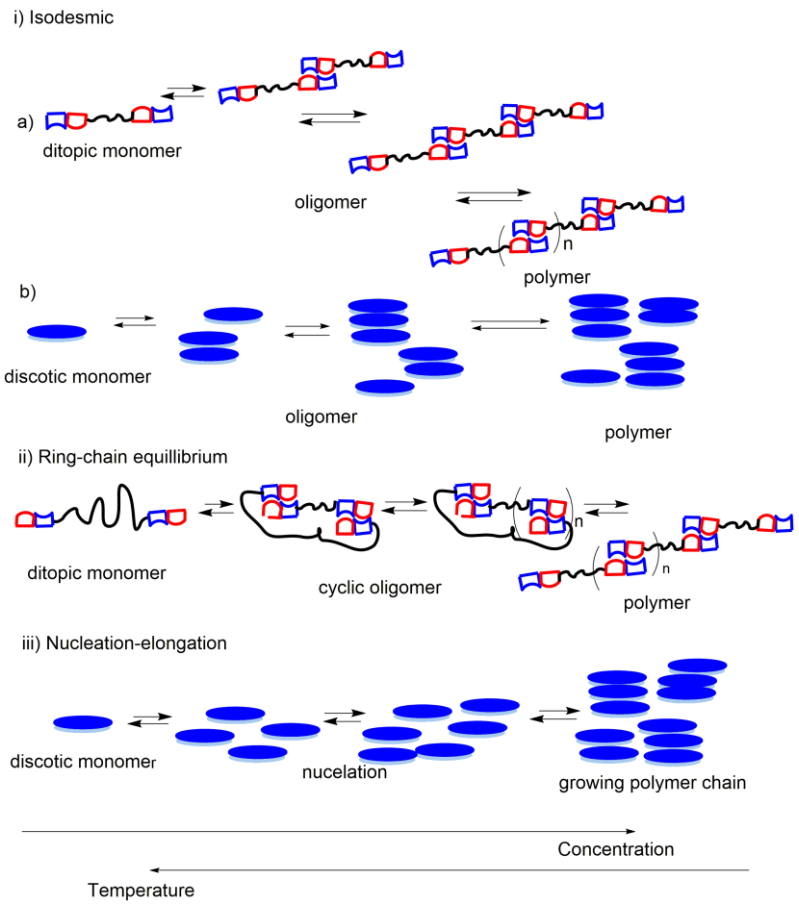



**Figure 1. 2:** Schematic representations of the major supramolecular polymerization mechanism (ditopic monomer).[33]

The isodesmic polymerization mechanism is also called as multistage open association (MSOA) or free association model. MSOA follows the Flory's principles of condensation polymerization of polyesters.[2,68] Addition of monomeric unit to a growing polymer chain is independent of the chain length and critical temperature, and strongly dependent on the strength of supramolecular interactions between ditopic monomers or oligomers. In systems where the cyclization is absent, the DP of polymerization is approximately propositional to ($\sim 2K_a$ [M] $^{1/2}$), where [M] is the total monomer concentration. Thus, higher values of $K_a$ are needed to obtain higher molecular weight and DP. The monomer can also be discotic in nature in this mechanism.

The ring-chain mechanism is governed by the thermodynamic stabilization of ditopic monomer by cyclization. A critical concentration of monomers creates the boundary between cyclic polymer and linear chain-extension polymerization. Cyclization of the monomer is

dependent on both the chain length and strength of supramolecular interaction. Furthermore, the rings versus chains population is governed by the factors: monomer shape, length and flexibility of the covalent spacer, strength and orientation of hydrogen bonding motif. Chain length in-turn correlates with the concentration.

Cooperative growth or nucleation-elongation mechanism is a non-linear polymerization associated with discotic monomers and involves two steps. First step is the association of molecules with low association strength into a nucleus which is less favorable due to high energy associated with it.[69] In the second step, the assemblies of nucleus occur to give polymer with higher association strength. These dramatic changes are often brought by the presence of additional secondary interactions such as, pi-pi stacking, hydrophobic and solvophobic effects, and van der Waals interactions. A long elongated polymer chain can be obtained only at critical temperature and monomer concentration. At a critical temperature, a sharp transition from the regime of monomer to small aggregates and to polymer takes place. However, polymerization mechanism of discotic molecules can be explained by: i) isodesmic, ii) nucleation elongation (NE) or helical growth, and growth coupled or supramolecular liquid crystal (SLC) (**Figure 1.3**). All the polymerization mechanisms except MSOA are characterized by critical step of self-assembly above which the polymers are formed.

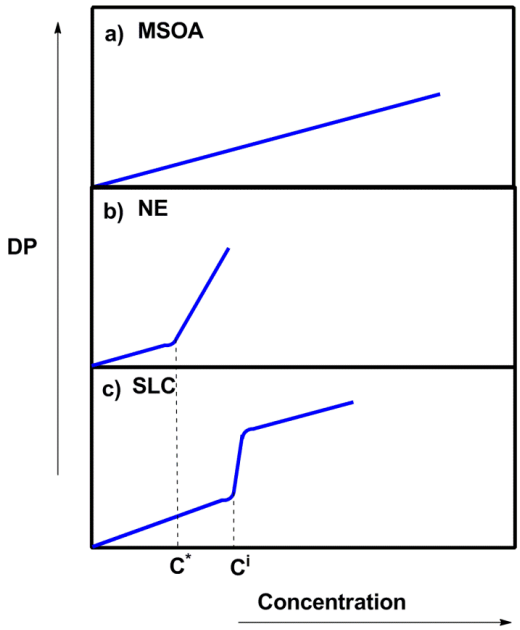



**Figure 1. 3:** Qualitative plot of degree of polymerization vs concentration of the monomer (discotic), a) multistage open association (MSOA) or isodesmic, b)nucleation elongation (NE) with helical growth concentration (c*), c)open supramolecular liquid crystal (SLC) with mesophase formation concentration ($c^i$).[33,39]

### 1.3.2 Classification of supramolecular polymers

Supramolecular polymers can be classified by the types of physical interactions or by the position of the supramolecular interaction sites on the monomer or oligomer unit (**Figure 1.4a**).[39] However, they are commonly classified by the position of supramolecular association sites into, main-chain supramolecular polymer and side-chain supramolecular polymers. Main chain polymerization is further classified into, i) linear chain extension, ii) network formation, and iii) linear main-chain based on bidirectional unit. Whereas, side chain polymers are classified as, i) polymer with associating groups on the side-chain and ii) polymer with associating groups in the main chain. **Figure 1.4b** gives the schematic representation of main chain *vs* side chain polymerization.[39]

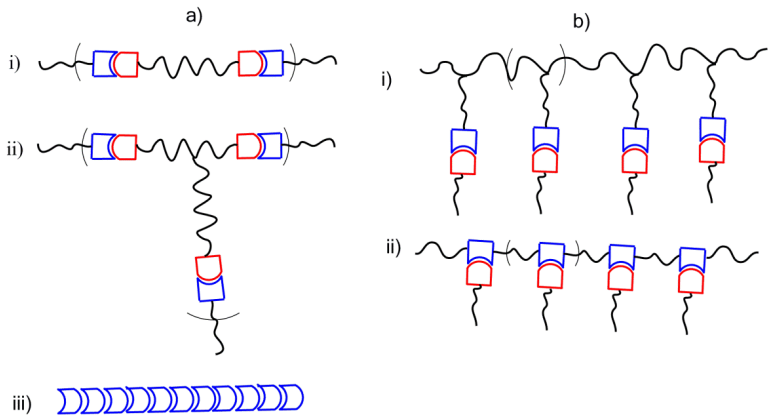



**Figure 1. 4:** Schematic representations of supramolecular polymers a) main-chain supramolecular polymers and b) side-chain supramolecular polymers.[39]

## 1.4 Hydrogen bonded supramolecular polymers

Among other non-covalent interactions with a moderate to high strength such as, metal-ligand interactions, ionic-interaction, and pi-pi interaction, the hydrogen bonding interaction is versatile and more suitable for the synthesis of supramolecular assemblies and SPs. Hydrogen bonding has features of specificity, directionality and tunability of strength using temperature and concentration of protons.

Hydrogen bond is defined as an electrostatic attraction between dipoles of a hydrogen attached to a heteroatom (O-H, N-H) with an electronegative heteroatom (C=O, C=N-). The strength of a single hydrogen bond is dependent on the basicity of the hydrogen acceptor (denoted as A) and the acidity of the hydrogen donor (denoted as D), and it ranges from very weak for neutral molecules (10-65 kJ/mol) such as,-CH-π to very strong $FH^{-}F^{-}$ ionic interactions (40-190 kJ/mol).[70] Due to a low energy associated with the hydrogen bonding, single hydrogen bonds are seldom used in the supramolecular chemistry; rather multiple arrays of hydrogen bonds are preferred to enhance, $K_a$. The stability of multiple hydrogen bonding array also termed as hydrogen bonding motif, increases with increasing number of hydrogen bonds; two hydrogen bonds are stronger than one. For example, in DNA nucleotide, hydrogen bonding between nucleobases pairing of adenine and thymine via two hydrogen bonds have association constant of, $K_a = 10^2\ M^{-1}$, whereas, nucleobases pair of guanidine and cytosine assembles via three hydrogen bonds with higher association constant ($K_a = 10^4$-$10^5\ M^{-1}$).[71] Gong *et al*. have synthesized a highly stable dimeric complex from an array of six-hydrogen

bonds with the $K_a$ of 1.3 x $10^9$ $M^{-1}$.[72] Moreover, the strength of hydrogen bonding motif is dependent on the sequence in which hydrogen bonding pairs are arranged. Jorgensen et *al.* have shown that a number of hydrogen bonding arrays, attractive and repulsive secondary interactions, arising from an adjacent hydrogen bonding pair, have a strong influence on the overall strength of supramolecular interactions.[73] For example, a hydrogen bonding motif with an array of three hydrogen bonds has varying association constant depending on the number and type of secondary interactions (**Figure 1.5**).

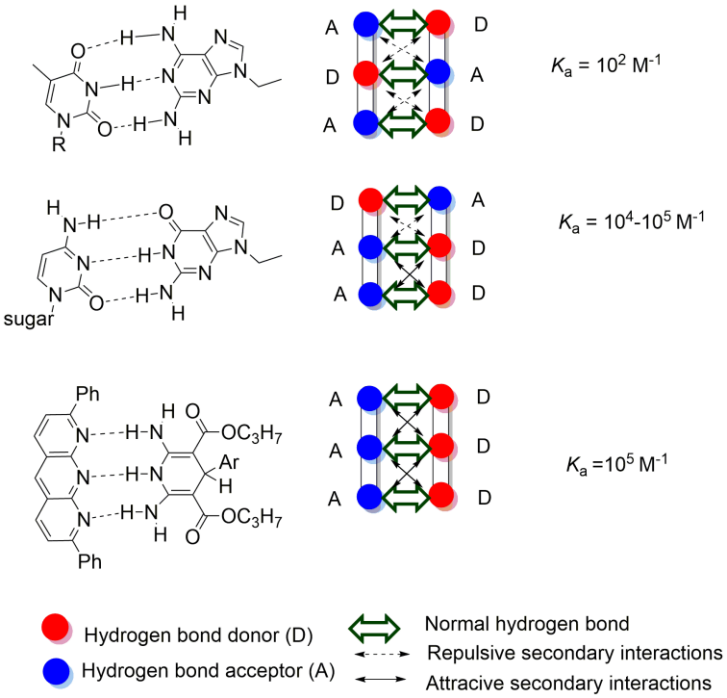



**Figure 1. 5:** Influence of the secondary interactions on the stability of the triple hydrogen bonding motif.[71,73]

The magnitude of $K_a$ is highest for a molecule containing an ideal array of hydrogen bonding with multiple A and D sequence such as AAA-DDD, and lowest for ADA-DAD sequence. Free energy analysis method developed by Schneider *et al.* showed a normal hydrogen bonding contributes to ~8 kJ/mol, and an attractive secondary hydrogen bonding contributes to results ~2.9 kJ/mol.[74] Zimmerman *et al*. confirmed the model and its predicted free-energies by synthesizing an ideal motif for three-fold hydrogen bonding (AAA-DDD), which gave $K_a$ in excess of $10^5$ $M^{-1}$.[75,76] In general, the hydrogen boding motifs with odd

number of hydrogen bonds require the necessity of hetero-complementary pair (ADA needs DAD). Motif with even number of hydrogen bonds can act as self-complementary (AD can pair with itself). The use of hydrogen bonding motif with multiple hydrogen bonds has been widely employed in the supramolecular assemblies as well as supramolecular polymers. More recently Slawin *et al*. have utilized ionic groups for making of AAA-DDD assemblies with much higher binding constant.[77]

### 1.4.1 Multiple hydrogen bonding in bifunctional small molecules

Lehn *et al.* presented for the first time the formation of multiple hydrogen bonded SP using small molecules that are appropriately designed to engage in multiple hydrogen bonding.[16,17,78] Supramolecular assemblies were formed by mixing two ditopic molecules (1:1) functionalized with complementary triple hydrogen bonding motif based on substituted diaminopyridine and uracil (array of DAD:ADA) with $K_a$ of $10^3$ $M^{-1}$ (**Figure1.6**).[17,58] Individual ditopic molecules are solids and had a specific melt-point without exhibiting liquid crystallinity. When the covalent spacer was a chiral tartaric acid, the resultant polymer showed thermotropic hexagonal columnar mesophase, which melted over a broad temperature range, and fibers could be drawn from the melt. Furthermore, helicity of the fiber was dependent on the optical activity of the spacer. On the other hand, anthracene based core gave rigid polymer with birefringent lytropic liquid crystallinity. **Figure 1.7** illustrates the ordering of the molecules in the liquid crystalline domains.

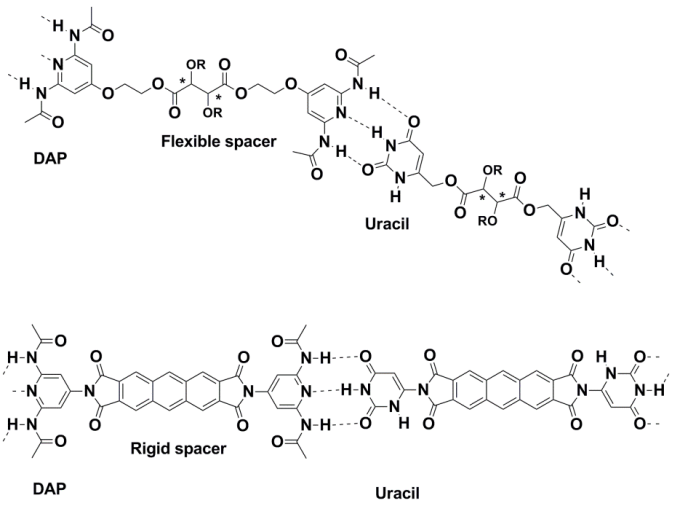



**Figure 1. 6:** Lehn's main chain supramolecular polymerization with ditopic molecules functionalized with triply hydrogen bonding unit.[16,17,78]

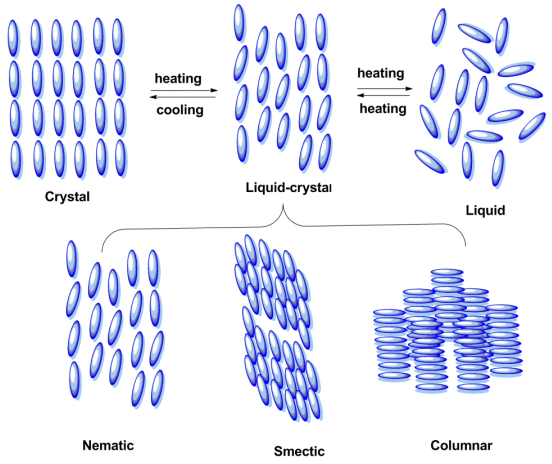



**Figure 1. 7:** Schematic representation of phase transition for molecular liquid crystals.[24]

Griffin *et al*. have synthesized liquid crystalline polymer from assemblies of bis-pyridine and bis-benzoic acid with single hydrogen bond.[79] Furthermore, network and ladder structures were made from pyridine with *tri*-and-*tetra*-functionality and benzoic acid with difunctionality (**Figure 1.8a**).[80] Polymeric assemblies were made possible by suppressing the rate of crystallization either by rapid cooling from the melt or introducing lateral bulky

substituent on the pyridine and benzoic acid. Polymer-like properties were present in the mesophase, but a limited DP in the isotropic solution. Though, $K_a$ of single hydrogen bond is weak, crystalline domain formations are necessary for mesophase liquid crystallinity.

### 1.4.2 Multiple hydrogen bonding in telechelic oligomers

Initial studies of Lehn *et al*. and Griffin *et al*. have focused on the small building blocks end functionalized with supramolecular associating sites.[16,79] Whereas, Lillya *et al.* have synthesized semicrystalline benzoic acid end functionalized poly (tetraethylene oxide) (PTHF) from viscous precursor of PTHF diol.[81] Crystalline aggregation of dimeric-carboxylates chain ends creates hard phase as physical cross links, which are stable up to 60 °C, and are responsible for elastomeric property. However, carboxylic chain end functionalized polydimethylsiloxane (PDMS) had the inferior strength than polytetrahydrofuran (PTHF).[82-85] Kato and Frechet synthesized side chain liquid crystalline polymer with single hydrogen bonding between pyridine and benzoic acid (**Figure 1.8b**).[20,26,86]

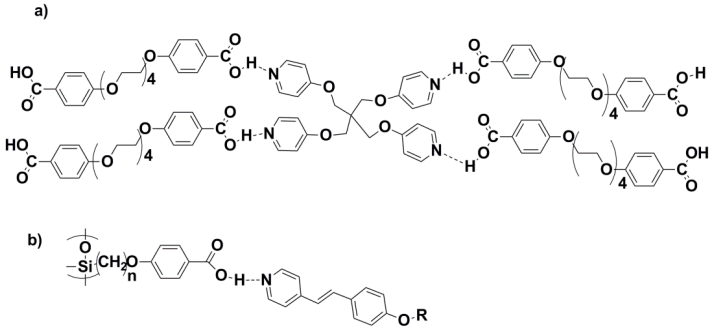



**Figure 1. 8:** Supramolecular associations by single hydrogen bond a) Griffin's supramolecular polymer network formation by tetrakis-pyridine and bis-benzoic acid derivatives[80], b) Kato's side chain liquid crystalline supramolecular polymer[26]

## 1.5 Nucleobases based supramolecular materials

Nucleobases based polymers also have been widely applied in the synthesis of SPs.[71,87] The $K_a$ for nucelobase pair's self-dimerization or complementary association is small. For examples, $K_a$ of thymine-thymine, adenine-adenine, cytosine-cytosine, and guanine-guanine hydrogen bonding associations is $K_{TT}$ = 3.5 $M^{-1}$, $K_{AA}$ = 2.4 $M^{-1}$, $K_{CC}$ = 40 $M^{-1}$, and $K_{GG}$ = $10^2$ to $10^4$ $M^{-1}$, respectively in $CDCl_3$.[71] Various nucleobases are incorporated into vinyl monomers such as

styrene, methacrylate and have been utilized in the preparation of random, and block copolymers.[88] Also, post polymer modifications and functional initiator that contains nucleobasehave also have been used for the synthesis of well-defined telechelics polymer. Synthesis of SPs using nucleobases as hydrogen bonding motif often requires complementary hydrogen bonding systems. Therefore, two separate polymers with complementary hydrogen bonding motif are needed for the synthesis of SPs. For example, polymer end functionalized with adenine will form 1:1 complex with thymine end functionalized polymer, and guanine functional polymer will form 1:1 complex with cytosine end functionalized polymer. In order to have better hydrogen bonding, it is preferable to have all the nucleobases with a single structure to avoid the complication due to the tautomerism.

Rotello *et al.* have applied the brick and mortar methodology for the synthesis of nanoparticles made by complementary triple hydrogen boding between thymine functionalized colloid (act as mortar), and diaminotriazine functionalized polystyrene (act as brick) (**Figure 1.9**).[89] Large, highly regular, spherical clusters with diameters of ~ 100 nm were observed. SAXS analysis indicated ~ 4.4 nm interparticle distance between thymine-Au aggregates and the functional polymer. A temperature-dependent association was reported. In another study, Rotello *et al*. applied block-copolymer of styrene and styrene containing diaminotriazine for controlling the size of aggregates in solution and in thin films by varying the length of the block.[90]

Van Hest *et al*. have synthesized methacrylate monomers containing adenine, thymine, cytosine and guanine.[91] ATRP of all the monomers shows pseudo-first order kinetics. Adenine, thymine, and guanine monomers were polymerized to give controlled molecular weight polymers ($M_n$ = 7 kg/mol) with narrow polydispersity. In the case of guanine containing monomer, the copper catalyst coordination doesn't have much detrimental effect on the ATRP, whereas cytosine containing monomer, the polymerization required addition of $CuCl_2$ and ligand. This work was extended to prepare block copolymer by using PEG-macroinitiaor. Diblock copolymer formed micelles (20 nm) and large micelles (150-200 nm). Association of adenine and thymine was assigned to either of hydrogen bonding or π-π stacking.[92]

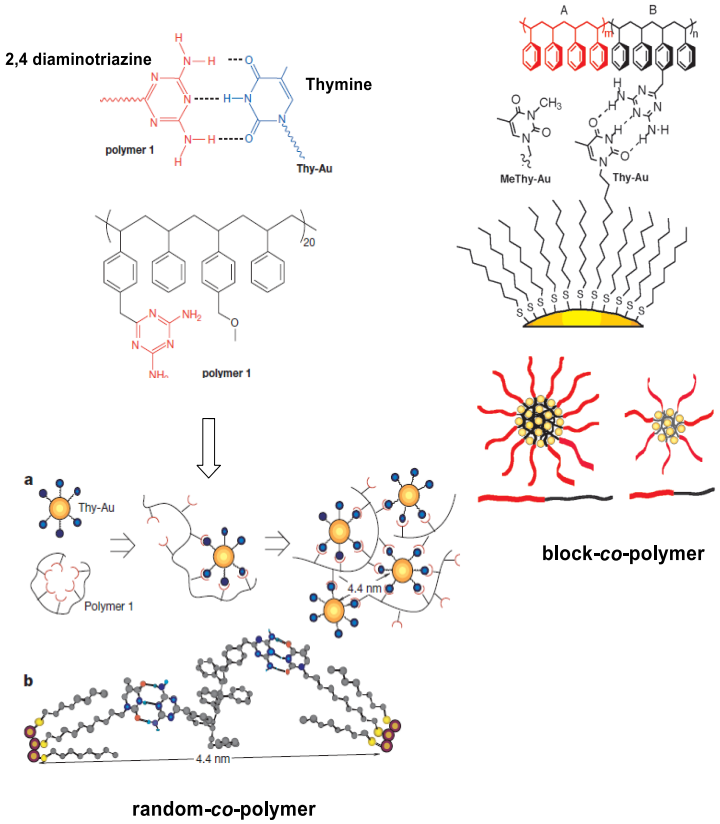



**Figure 1. 9:** (Left) Recognition motif or thymine and diaminotriazine, and proposed mechanism for the aggregation, (right) schematic representation of aggregates particle and effect of length of functional block on size of aggregates.[89]

Rowan *et al*. have synthesized nucelobase-functionalized telechelic polymers. Low molecular weight amino functional poly (tetramethyleneoxide) (PTHF) was converted into PTHF end functionalized with adenine and thymine groups (**Figure 1.10**).[93,94] Precursor PTHF-$NH_2$ was a viscous solid with a melting point of 21 °C, and the polymers with end functional thymine **34**, and adenine functional **35**, groups have melting point above 100 °C.

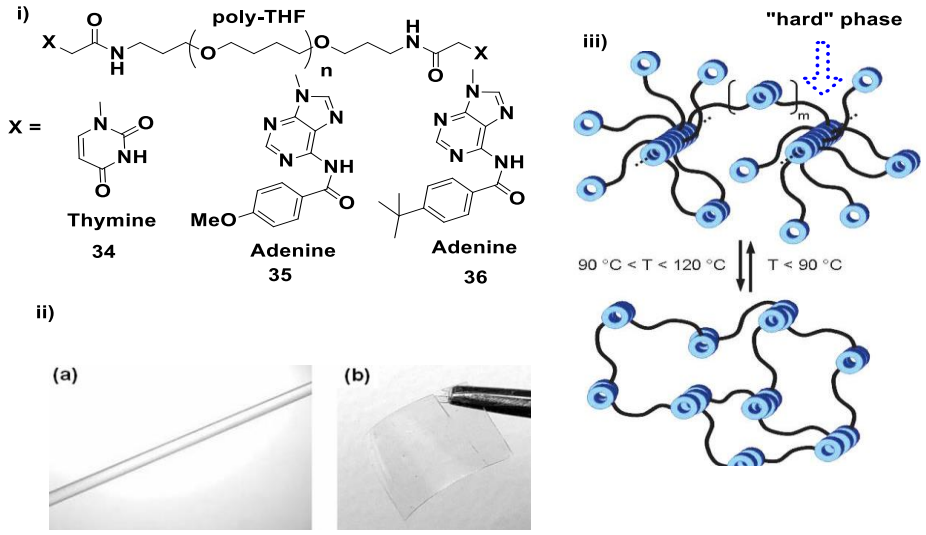



**Figure 1. 10:** i) PTHF end functionalized with adenine, and thymine, ii) optical microcopy of fiber and film formation made from melt of **35**, iii) proposed mechanism for transition from gel-like to linear polymer.[93,94]

They were able to form film and fiber from the melt of adenine end functionalized polymer. This was attributed to the cumulative effect of pi-pi stacking (observed in case of **35**), dipole-dipole interaction and phase segregation.[93,94] The authors further explained the presence of the gel-like transition, below which a phase-segregated linear polymer chains with unassociated chain-ends exist without complete chain extensions. Their system also contains long "hard" semicrystalline stacks of adenine chain end association within the "soft" PTHF matrix. Whereas, no such behavior was obtained for thymine end functional polymer, due to the absence of π-π stacking and high crystallization temperature (145 °C). In another study, a rigid backbone, *bis*-4-alkoxy-substituted bis(phenylethynyl)-benzene, was end functionalized with adenine and thymine, and it underlined the importance of 1:1 complementary motifs on LC phases and their stability were evaluated.[95]

Cheng *et al.* have synthesized well-defined P*n*BA with low percent of nucleobases.[96] Blending of adenine- and thymine-containing P*n*BA gave higher melt viscosity compared to the P*n*BA samples. Mather *et al*. have synthesized ABA triblock-*co*-polymer, with end block made of nucleobases monomer by using difunctional initiator and nitroxide mediated polymerization.[97]

In summary, nucelobase have very weak-hydrogen bonding and cannot form polymers by MSOA (linear chain extension) mechanism; however, the combination of polar group segregation, and nucelobase interactions (hard phase), and telechelic soft linking chain can give rise to very interesting supramolecular properties.

## 1.6 The need for high $K_a$ system: Ureidopyrimidone (UPy) functionality

Supramolecular chain assemblies synthesized using weak hydrogen bonding, for example, dimerization of carboxylic acid and nucleobases, gave high DP in the solid or crystalline state, whereas very low DP was obtained in solution. Therefore, in order to achieve SPs with high molecular weight (high DP) in solution, supramolecular associating functional group with very high $K_a$ is needed. This is achieved by increasing the strength of supramolecular association with high $K_a$ in excess of $10^3$ $M^{-1}$ by incorporation of hydrogen bonding motif containing more than three hydrogen bonds.

Various research groups have applied this methodology and synthesized multiple hydrogen bonding motifs. Notable contributions in this area were made by the groups of Lehn[40], Ghadiri[98], Hamilton[99-101], Boden[102-105], Rebek[64,106-108], and Zimmerman[75,76,109,110]. Boden, Ghadiri, and Rebek, studied the self-assemblies of peptides into polymeric β-sheet tapes, nanotubes from peptides, and capsules from calixarenes, respectively. Whereas, groups of Lehn[29,30,40,110-112], Hamilton[99-101,113], Meijer[19,41,42,46,114-118], Zimmerman[76,109,110,119-125] and contributed by the synthesis of complementary and self-complementary hydrogen bonding motifs for SPs.

Most important hydrogen bonding motifs with very high $K_a$ was synthesized by Beijer Sijbesma, and Meijer.[19,114] They synthesized and characterized several substituted ureidopyrimidone (UPy) (**1**) with the array of four hydrogen bonds arranged in the self-complementary fashion to form AADD bonding (**Figure 1.11**). Among the various compounds synthesized, simple UPy (**1**) is well-known as it has high $K_a$ and readily synthesized from inexpensive commercial reagents. Moreover, recent literature repots show synthesis of much stronger hydrogen bonding units based on six and eight hydrogen bonds.[126-128] However, all of them could not be incorporated in the polymer preparation due to their synthetic inaccessibility. **Figure 1.11** shows few selective examples of the building blocks capable of forming very robust hydrogen bonded complexes.

In the last two decades, the UPy group was widely used for the synthesis of main-chain SPs by telechelic chain extension, as well as for the synthesis of copolymers of UPy functionalized monomers. UPy group incorporation in telechelic chain extension led to the materials with very interesting properties.[19,47] The following section will discuss the scope and limitations along with the salient features and applications of UPy containing SPs.

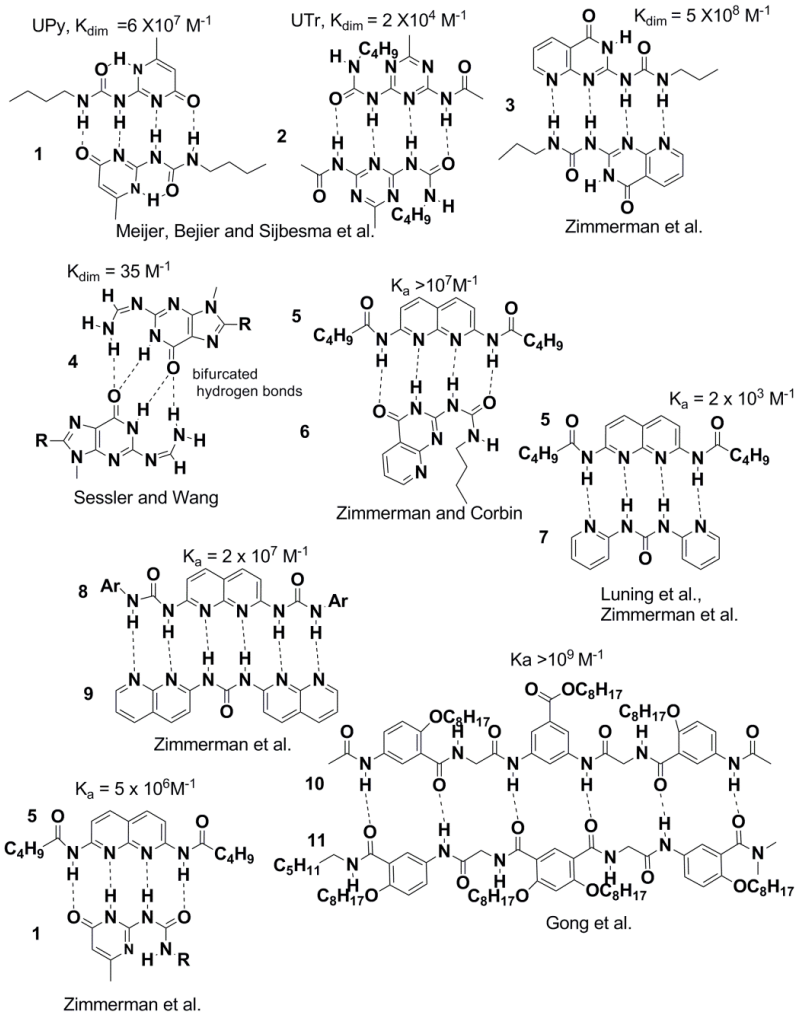



**Figure 1. 11:** Selected examples of the multiple hydrogen bonding motif containing more than four hydrogen bonds (association or dimerization constant are determined in chloroform solutions).[19,46,109,116,118,126,128-135]

### 1.6.1 UPy functionalized supramolecular polymers

An important stage in the preparation of isodesmic supramolecular polymers came through the development of UPy functionality.[19,46] UPy and its derivatives are easy to synthesize from inexpensive starting material, isocytosine and isocyanate or amine. It contains array of four hydrogen bonds (quadruple) arranged in the sequence of AADD. The UPy group is capable of forming three different tautomers as a function of solvent polarity and substituents on the pyrimidone ring. Single crystal XRD of monofuctional UPy group (**Figure 1.12**) shows planar structure and it self-assemble through AADD. Its dimerization or association constant was calculated to be $K_{dim}$= 6 × $10^7$ $M^{-1}$ in $CHCl_3$ with a lifetime of 170 ms at 298 K. This value corresponds to a $\Delta G$ of -44 kJ/mol, which is 0.125 times of the C-C covalent bond.[118,136]

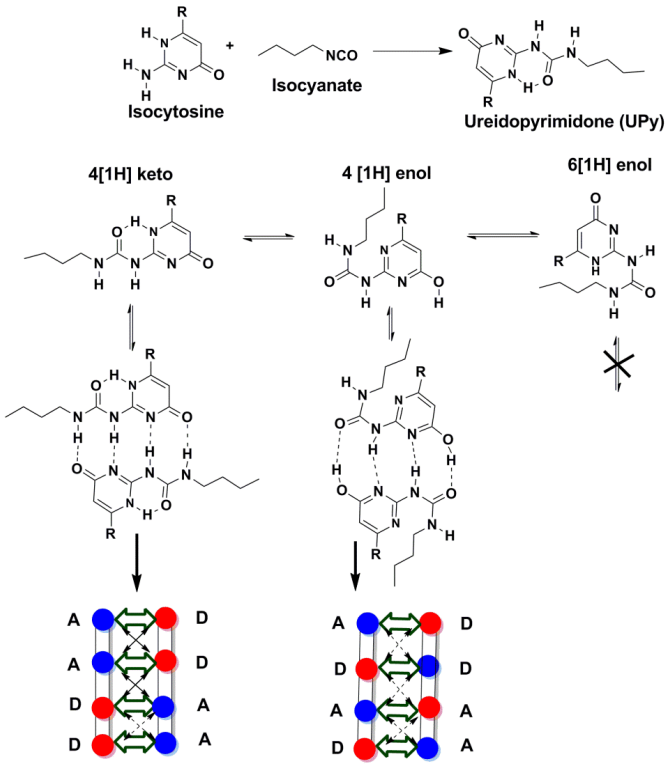



**Figure 1. 12:** Schematic syntheses of 2-ureidompyrididone, and two self-complementary tautomeric forms 4[1H] keto and 4[1H] enol.[46]

After a thorough investigation and the determination of high $K_a$ values for several UPy derivatives that are suitable for self-complementary AADD interaction, Meijer *et al.* applied UPy in the synthesis of bifunctional tags with UPy end groups.[19] A series of small building blocks including bifunctional and trifunctional UPy group were made and analyzed for its

supramolecular properties (**Figure 1.13**). The bifunctional compounds (with C6-linkers) contained linear (**12**) and branched (**13**) alkyl chain spacers. A trifunctional compound was made with a linear alkyl spacer **(15**). Solution viscosity and bulk analysis by rheology and dynamic mechanical analysis (DMA) were utilized to investigate the dynamics and properties of polymeric assemblies made by interactions of UPy group.

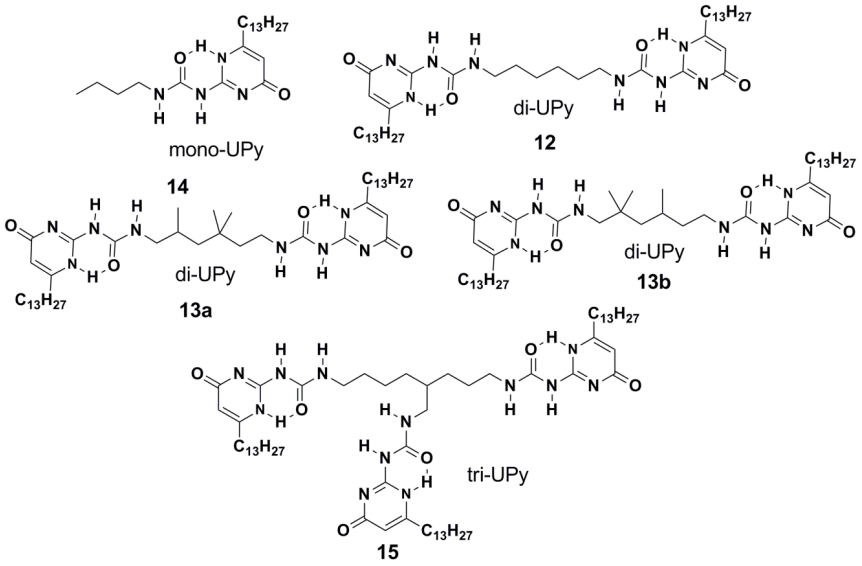



**Figure 1. 13:** Structures of small building blocks with di-and tri-functional UPy group.[19]

A 40 mM solution of compound **12** in chloroform exhibited large specific viscosity, which indicated the presence of linear or branched polymeric chains.[19] Addition of monofuctional UPy **14** leads to a dramatic change in the viscosity behavior indicating an absence of multidirectional aggregation and the formation of more unidirectional hydrogen bonded long chain polymer (**Figure 1.14**). This observation also underlines the importance of monomer purity, likewise in condensation polymers, where bifunctional monomers need to have 100 % functionality to build high molecular weight polymer. Monofuctional monomer can act as chain stoppers and hinder the growth of DP. On the other hand, the addition of trifunctional UPy compound will lead to network formations.[19] Furthermore, a logarithmic specific viscosity plot of **12** was linear with a slope of 3.76 versus 1 for the starting precursor. These values for supramolecular polymer agree well with the theoretical model of Cates[137] for reversible polymers. Compound **2a**, with the methyl substitution next to UPy group show the

presence of ring-chain equilibrium, and the linear polymer formation took place only at very high concentration.

A double logarithmic plot of the solution viscosity of trifunctional compound **15** with concentration was complex indicating multiple interactions.[138] At low concentration, it forms linear chains along with some cyclic aggregates, whereas at high concentration, trifunctionality enables formation of a reversible network. Studies carried out with photo-induced depolymerization with monofuctional oxy-protected UPy group confirm unidirectionality as a driving force for the linear polymerization.[139] Compound **12** in solution was shown to form a high molecular weight linear polymer with an estimated DP of 700. However, theoretical value for UPy group dimerization in chloroform is 6 x $10^7$ $M^{-1}$ and it corresponds to DP of 3000 (using $\eta_{sp} = k \times DP$).[19,28] Differences in these values was attributed to the trace amount of monofuctional impurities. Furthermore, its spin-cast film is leathery and becomes very brittle due to crystallization.

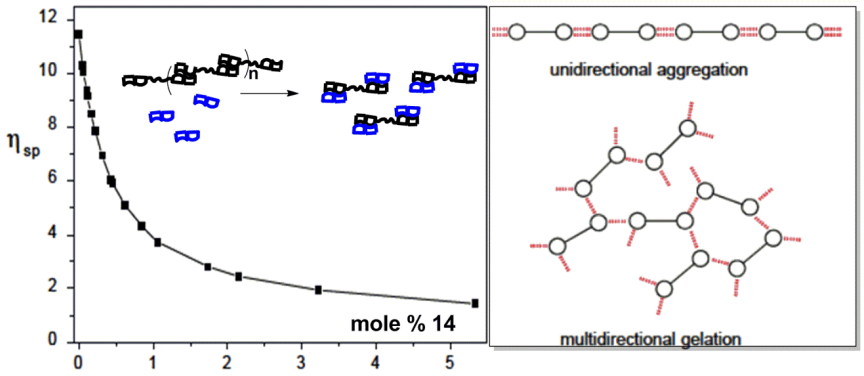



**Figure 1. 14:** Effect of monofuctional UPy (14) addition on the specific viscosity of 40 mM solution of monomer **12** in chloroform, and unidirectional chain extension vs multidirectional aggregates or gelation.[19,138]

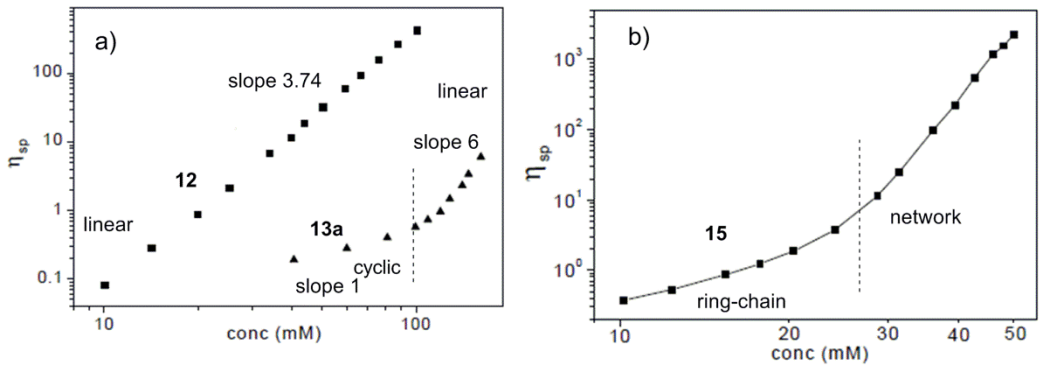



**Figure 1. 15:** Effect of spacer and monomer concentration on the linear-chain, ring-chain, and network formation.[19,138]

Intermolecular hydrogen bonding of **13** produced a transparent film, which behaved as an elastic solid at room temperature.[19,138] Low melt viscosity was obtained at high temperature indicating its thermoreversibilty. Flexible fibers were drawn from the melt. Both rheology and DMTA analyses further support the formation of very high 'virtual' molecular weight (**Figure 1.14** and **Figure 1.15**). Rheology analysis shows the presence of rubbery-plateau with a plateau modulus similar to soft rubber (**Figure 1.16**).[19,138,140] Furthermore, the estimated energy for viscous melt flow was 105 kJ/mol, which indicates a strong temperature dependent viscosity behavior.[39] This value is much higher than the conventional covalent bonded macromolecules (80 kJ/mol) and enables processing at temperature slightly above the $T_m$ or $T_g$. The high energy of activation also indicates enhanced relaxation of the SPs, which is assisted by breaking and recombining of chain end (by hydrogen bonding) without alerting effective strain. Hydrogen bonds break with increase in temperature and, therefore, SPs show a strong temperature-dependent behavior. Factors leading to the crystallization of monomer **12** were not addressed further.[19] Difference in monomer **12** and **13** has some similarity to the work of Griffin and co-workers, where lateral substitutions were used to avoid crystallization.[141] Studies on the covalent spacer end-functionalized with multiple end groups like *bis*-and *tris*-UPy functionality lead to the formation of linear polymer and network polymer, respectively.

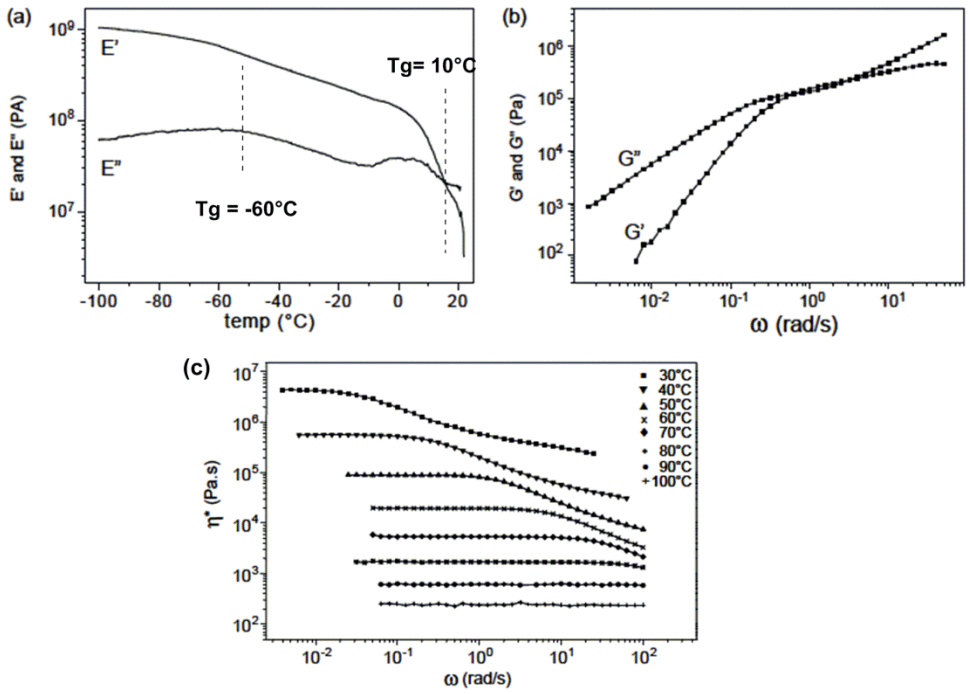



**Figure 1. 16:** DMTA and rheology analysis, a) DMTA showing the presence of two $T_g$s, (single $T_g$ by DSC at 10 °C), b) A plot of G' and G" vs frequency at 40 °C showing a rubbery plateau, and c) the melt viscosity of the monomer **13** vs frequency at various temperatures.[19,138]

These studies established the importance of UPy group for the synthesis of supramolecular materials and opened new opportunities for the synthesis of SPs from oligomer backbone made up of different monomers. Moreover, UPy group could be incorporated as pendants in side chain or as telechelic unit. Following section will review the literature on the SPs made from telechelic oligomers end functionalized with UPy.

### 1.6.2 Supramolecular materials by chain extensions with UPy

Synthesis of telechelic oligomers and polymers (hereafter will be termed as unimer) end capped with UPy group could be achieved by two approaches. First approach involves two steps. In the first step hydroxyl or amine functionality of the unimer is reacted with an equimolar amount of diisocyanates such as, isophorane diisocyanate (IPDI), 3(4)-isocyanatomethyl-l-methylcyclohexylisocyanate (IMCI). In the second step UPy group is

attached via coupling of isocyanate functionalized unimer with an excess of 2-amino-4-methyl-6-hydroxy-pyrimidine (Me-Iso) (**Figure 1.17**).

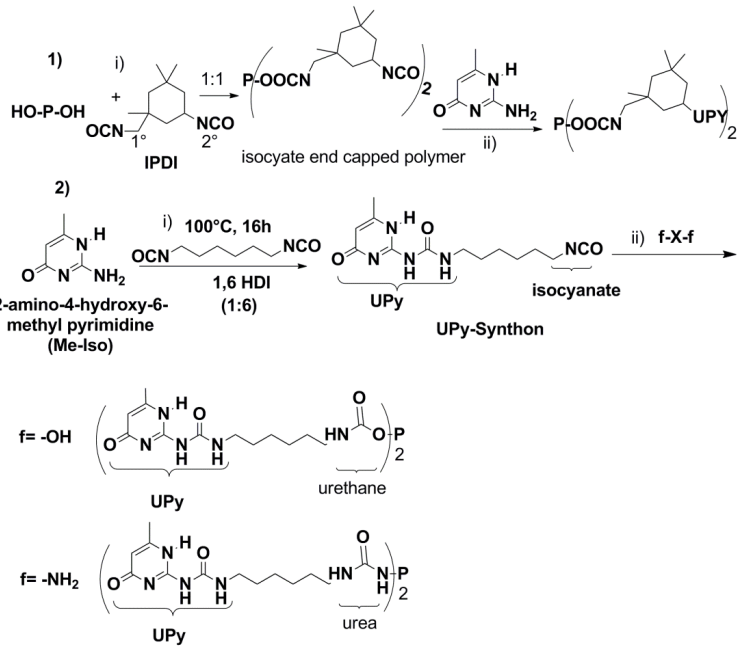



**Figure 1. 17:** Two approaches for the synthesis of UPy-telechelic, and the formation or urethane or urea linkages from hydroxyl and amino telechelic precursors, respectively.[19,28,138,142,143]

Unimer can be formed either with urethane or with urea bond, as per the precursor functionality (hydroxyl or amine). The significance of urethane and urea linkers in the formation of SPs will be addressed later. Although this approach works well, the reactive isocyanate may undergo unwanted side reactions with polar impurities such as water to prevent 100 % chain end functionalization.[144] Furthermore, IPDI and IMCI lead to various stereoisomers and may require further separation. However, this approach was used by various groups, in particular Long *et al.* have employed this approach for synthesis of SPs.[142,144] Due to the above mentioned problems, the reported functionalization efficiency for this approach is between 75-95 %.

In a second approach, a high functionalization efficiency and easy purification of telechelic-UPys are achieved using reactive preformed UPy-synthon as reported by Meijer and co-workers (**Figure 1.18**).[47,145] UPy-synthon is an UPy group pre-functionalized with reactive

isocyanate. UPy-synthon is synthesized by reacting commercially available Me-Iso with an excess of 1,6 hexane diisocyanate (1,6 HDI). Unimer end functionalization reaction is carried out by the reaction of hydroxyl telechelic oligomers with two mole excess of UPy-synthon in chloroform or toluene using dibutyltindilaurate (DBDTL) as catalyst. In the approach, the unreacted UPy-synthon is easily removed using silica gel at 60 °C. By using this approach Meijer and coworkers synthesized a set of UPy end functional telechelic compounds comprised of non-polar and polar backbone chains (**Figure 1.18a**). In all the polymers, UPy-chain end functionalization was complete within 16 h and the efficiency of the functionalization is 98 %.

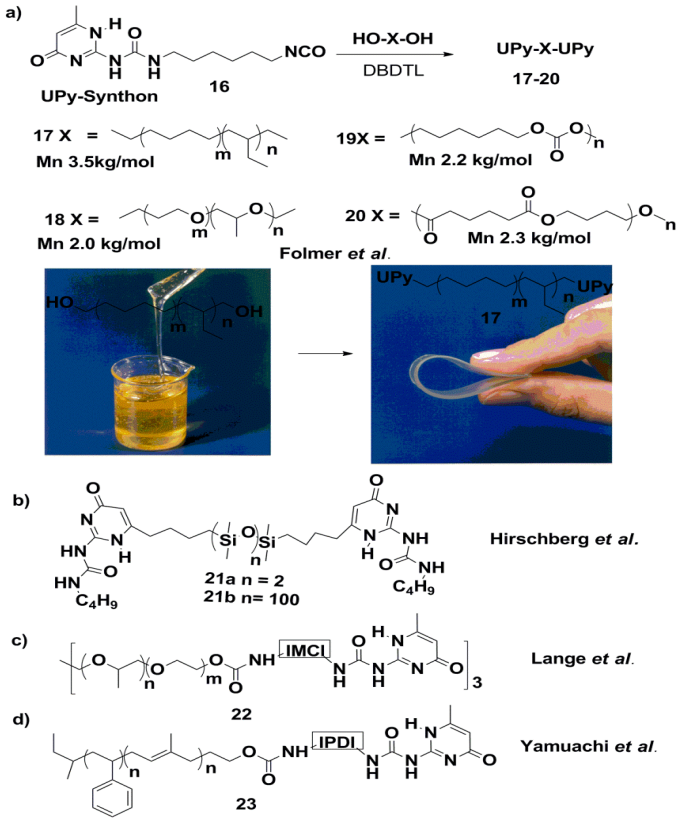



**Figure 1. 18:** Schematic representations of UPy-functionalized polymers. a) UPy telechelics by reacting UPy-synthon with various hydroxyl precursors, and the pictures of viscous precursor and solid UPy elastomer of ethylene-*co*-butylene, b) telechelic PDMS-UPy c) trifunctional PEO-b-PPO, and d) monofuctional PS-b-PI-UPy.[41,47,142,143]

The SPs formed using the UPy telechelics showed dramatic improvements in mechanical property when compared to the starting materials. As seen in the picture (**Figure 1.18a)**, precursor diol of poly(ethylene-*co*-butylene) was a viscous liquid whereas its UPy derivative was a soft elastic solid, from which self-standing films were made.[47] Moreover, **Figure 1.18** also shows some selective examples of unimer with trifunctional **22**, and monofuctional **23,** UPy functionality.[142,143]

Rheology and DMTA analysis of the UPy telechelics made by Meijer et *al*. have shown very interesting behavior.[47] Upon compositional modification in non-polar poly(ethylene-*co*-butylene) segments, significant changes in physical property of SPs were observed.[47] However, polar backbone polymers such as polycarbonate and polyester, which are waxy and brittle solids, gave strong and slightly less elastic materials, **18** and **20,** respectively.[47] And a low viscous liquid polyether-diol gave **19** as an elastic solid. A chloroform solution of **17** was highly viscous but the viscosity dropped substantially on the addition of trifluoroacetic acid (TFA), indicating reversibility of the chain extension. DMTA of the polymer **17** had a distinct $T_g$ of -50 °C with a rubbery plateau at $5 \times 10^6$ Pa. In general, a high modulus of SPs was considered as an effect of very high 'virtual' molecular weight (high DP) via supramolecular polymerization.[47]

Remarkably, the improvements in the properties can arise either due to the formation of very high DP of SPs or an improved interchain interaction in between the supramolecular chains leading to physical crosslinking. However, a clear appearance of the film lead to the conclusion of an absence of large hydrogen bonded clusters in SPs. Furthermore, an absence of melting endothermic peak that is present in the precursor poly(ethylene-*co*-butylene) diol also indicated the formation of SP, **17** (**Figure 1.19**). The absence of melting endothermic peak without significant difference in the $T_g$ was attributed to the increase of 'virtual' molecular weight or high DP, which in turn led to a decrease in the diffusional freedom preventing the formation of crystalline clusters.

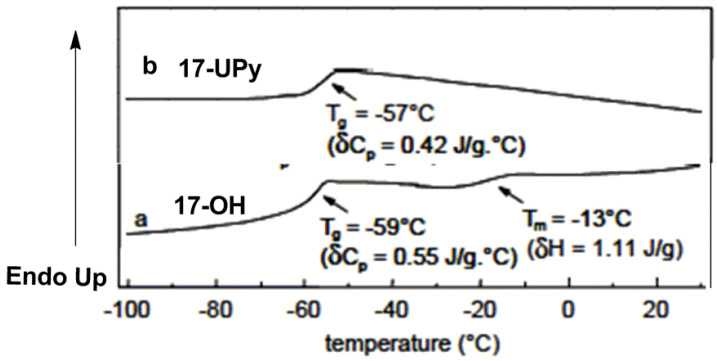



**Figure 1. 19:** DSC traces of telechelic poly(ethylene-*co*-butylene) reported by Meijer et al.[47]

However, the rheology analysis of UPy **17** shows a strong viscoelastic behavior; the modulus and viscosity were strongly frequency dependent. Reported zero shear viscosity was $2\times10^6$ Pa.s.[47] Moreover, the presence of rubbery-plateau at high frequency and the failure of time temperature superposition (TTS) were attributed to the presence of small clusters of the hydrogen bonded motif. In contrast to UPy-**17**, telechelic UPy with polar backbone (**18** and **20**) showed the presence of distinct endothermic peaks in the DSC analysis. In the case of 1**9,** a small endothermic peak was observed. This was attributed to either semicrystallinity of the polyether spacer or the presence of clustered hydrogen bonded units. Though, the results of rheology and DMTA studies indicate the presence of a small amount of hydrogen bonded clusters, the formation of clear/transparent film from these materials was interpreted to the absence of large hydrogen bonding clusters in these systems.[47,138]

Trifunctional UPy telechelic **23** forms reversible network in bulk, whereas its solution viscosity is strongly dependent on the chain stoppers. In conclusion, studies of Meijer *et al*. showed that the incorporation of UPy groups in telechelic chain extension supramolecular polymerization lead to the SPs with promising properties such as thermoplastic elastomers and temperature sensitive materials.[18,28,33,39]

The initial understanding of SPs using telechelic UPy groups was primarily based on the interpretation of formation of high molecular weight linear polymers via hydrogen bonded chain-extension and the property enhancement of SPs was attributed to the chain-entanglement of high molecular weight linear polymers.[19] At the same time, Hirschberg reported the synthesis of polydimethylsiloxane functionalized UPy, with a short (**22a**) and long chain

segments (**22b**) by coupling of silanol and protected UPy derivatives (**Figure 1.18b**).[41] An estimated DP of **22a** and **22b** was 100 and 20, respectively. Though **22a** can crystallize due to short segment of siloxane, it was amorphous, which was attributed to the high viscosity and the entanglement of SP. In the case of **22b**, the presence of small endothermic peak in the DSC was assigned to micro-crystalline domains resulting from association of UPy, and these domains disappeared above -25°C.For the first time this study recognized the formation of microcrystalline domain due to the hydrogen bonded UPy association. UPy associated crystalline domains in SP can only form when dimerized UPy associates intermolecularly and form a crystalline phase consisting of multiple UPys (physical crosslinks). However, explanation for the formation of physical UPy cross-links**,** and factors responsible for their formation was not provided, unambiguously. Furthermore, the determined DP of **22b** was just 20, far less than the theoretical value.[41] This discrepancy was assigned to the presence of monofuctional impurity, which can act as chain stopper.

Yamuachi *et al*. synthesized narrowly dispersed monochelic polystyrene-UPy (PS-UPy), poyisoprene-UPy (PS-UPy), and PS-*b*-PI-UPy and found the presence of multiple aggregation behavior of UPy group in SPs.[142] Monofunctional UPy polymers were expected to form only dimer with twice the molecular weight of the precursor. However, DSC and rheology analysis of PS-UPy and PI-UPy led to the conclusion that these polymers have aggregated UPy domains due to multiple hydrogen bonding. Again, an attempt was not made to provide a detailed explanation on the origin of these aggregates. On contrary, Guan *et al*. synthesized PS-b-P*n*BA block-copolymer, where poly(P*n*BA) contains UPy head group, with pyrimidone ring modified with bulky substituent to avoid planarity, results in tri-block-copolymer PS-*b*-P*n*BA-b-PS, a self-healing polymer.[146] Thus, the UPy groups have shown their versatility in the formation of SPs which possess macromolecular properties, including shear thinning, viscoelastic, and glass transition. These enhanced supramolecular properties of SPs were largely attributed to 'virtual' high molecular weight polymer formation, though a clear distinction between supramolecular entanglements and physical cross-links has not been established yet. In the following section we will discuss the side-chain supramolecular polymers made by UPy group association.

### 1.6.3 Non-linear supramolecular polymers using pendant UPy group

Chain-end functionalization of linear telechelic oligomers with UPy group is generally performed by post-polymer analogous reaction and it results mostly into linear-chain extended SPs. On the other hand, block copolymers as well as random copolymers made with UPy functional monomers give an opportunity for formation of non-linear SPs.[147-152] Free radical polymerization as well as controlled radical polymerizations such as atom transfer radical polymerization (ATRP),[150,151,153,154] reversible addition fragmentation (RAFT) polymerization[155-157] have been used for the incorporation of UPy groups either as chain end groups or as pendant groups. Initiator containing UPy functionality has also been used for the use in controlled polymerization methods.[150,154,158,159] This section will discuss the scope and limitation of this strategy to produce non-linear SPs.

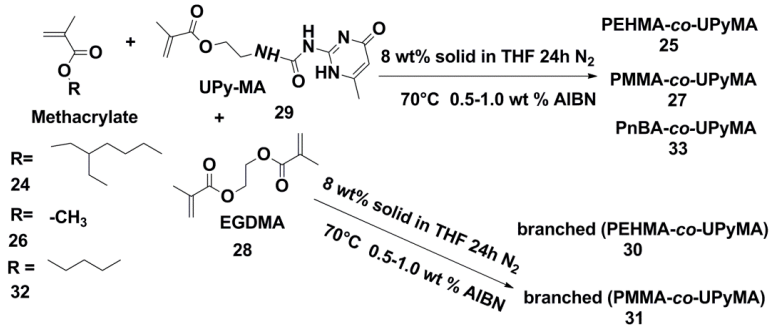



**Figure 1. 20:** Schematic representation of free radical co-polymerization of UPy-methacrylate monomers[149,160]

Long *et al.* reported free radical copolymerization of UPy-methacrylate **29** with methyl methacrylate (MMA **26**) and, ethylhexylmethacrylate (EHMA, **24**) and *n*-butyl acrylate (*n*BA, **32**) and synthesized random copolymers of **27**, **25**, and **33** with varying percent of pendant UPy groups, respectively (**Figure 1.20**).[147-149] Furthermore, to evaluate the effect of topology on the UPy group association, branched polymers of PMMA and PEHMA were also made by incorporation of ethylene glycol dimethacrylate (EGDMA).[160] Irrespective of topology both the branched and linear polymers showed similar enhancement of the relative viscosity, especially for the polymers with high UPy wt. % content.[160]

Solubility of the UPy-MA and the polymer containing pendant UPy groups limits the wt. % of UPy group (15 %) incorporation during the polymerization. This characteristic (low

wt. % of UPy loading) also limits the direct usage of UPy-MA monomer in the controlled radical polymerization, though there are other factors such as copper catalyst coordination with UPy, which also interferes with the ATRP.[151] Property enhancement due to the incorporation of UPy groups was clearly evident from the increased viscosity of the obtained SPs in non-polar solution, and increased zero shear melt viscosity.[160] Both solution and bulk studies of UPy containing copolymers indicated the presence of aggregation at temperatures even at 80 °C. Moreover, the glass transition temperature increased linearly with the UPy wt % (**Figure 1.21**). Moreover, Long *et al.* also synthesized PMMA-*co*-PMAA to compare the effect of dimeric hydrogen bonding of carboxylic acid group vs quadruple hydrogen bonding of UPy.[161] Improvements in the mechanical properties were ten times more for the copolymer with UPy-containing monomer than MAA, for a similar composition. Electrospinnig fiber formation was improved by the presence of UPy groups. Larger fibers were produced due to higher molecular weight of the copolymers as a result of lower apparent entanglement concentration ($C_e$).The UPy group associations served as interlinks and results in the formation of a dense and thermodynamically stable network.[161]

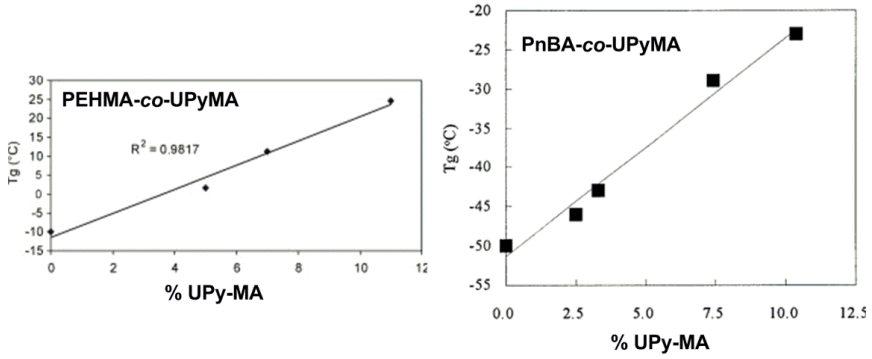



**Figure 1. 21:** Relationship between $T_g$ and UPy wt%.[148,149]

In short, Long *et al.* were able to make random copolymers of various methacrylates and found that UPy group aggregations are present despite the polar ester functionality of the polymer. Although, copolymer of P*n*BA-*co*-UPy-MA showed three times more adhesion on glass substrate than P*n*BA homopolymer, it formed a brittle film indicating vital role of glass transition on the UPy aggregation (P*n*BA $T_g$~ -50 °C).[148] Moreover, PEHMA–co-UPy-MA formed a film that showed improved creep performance and tensile properties (PEHMA ($T_g$~

-10 °C).[149] Recently Kuo *et al.* prepared copolymer of PMMA and UPy-MA for increasing the $T_g$ of PMMA.[162]

Coates *et al*. has synthesized polyolefin with pendant UPy groups from copolymerization of 1-hexene and 1-hexene-UPy.[163] Elastomeric properties obtained at room temperature were attributed to the cross-linking due to the dimerization of pendant UPy groups. In addition to a clear appearance of the material, they observed in the presence of a chain stopper, the viscosity of the copolymer dropped to that of the homopolymer and it led to the conclusion of the absence of a significant amount of stacks or clusters in SP.

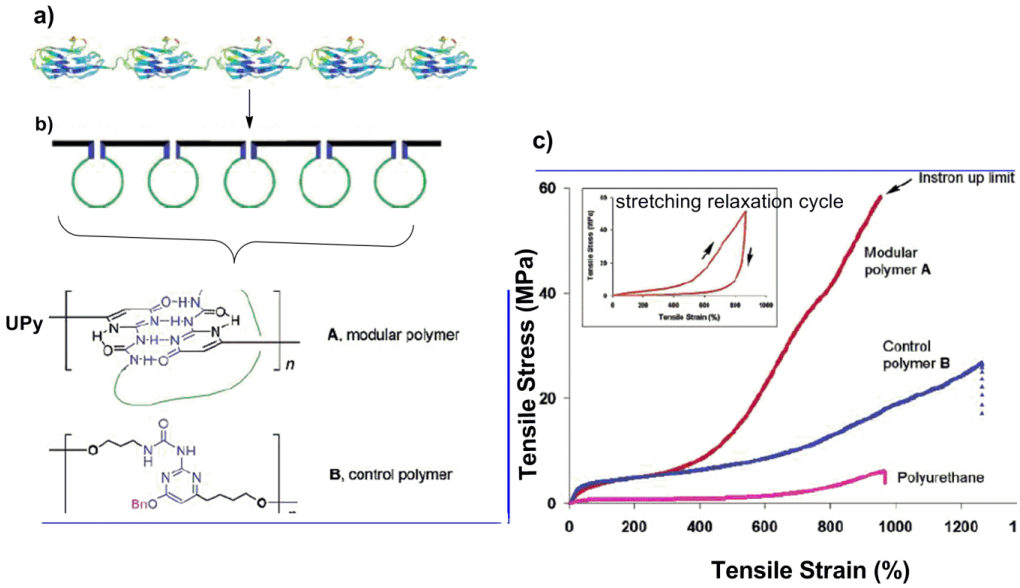



**Figure 1. 22:** Biomimetic design of titin protein by UPy group; a) concept and design, b) two modular monomeric units, c) stress-strain curves of UPy based polymer (A), control polymer (b), and a reference polyurethane ( inset -hysteresis of single extension and retention).[164]

In contrast to the above side chain polymers, Guan *et al*. elegantly synthesized poly-THF containing UPy groups in the backbone as a part of main-chain (**Figure 1.22b**).[164] Nanomechanical properties studied by atomic force microscopy (AFM) demonstrated a sequential unfolding of the UPy dimers upon polymer stretching. Bulk stress-strain analysis revealed high mechanical strength, toughness, and elasticity. Elastomeric property upto 900 % strain with a complete recovery to its original length was obtained. More recently, a modular

polymer with high modulus, toughness, and resilience, with shape memory properties were also made by Guan *et al.* by ADMET polymerization of main chain UPy containing bifunctional olefin.[165]

Similar concept of main-chain (loops) and end-chain UPy modification was applied by Dankers *et al*. for the biopolymer applications.[166] The crystallization of oligocaprolactones in the polymer was not observed, and optimum properties were obtained for the 4:1 mixture of main-chain and end-chain functional polymers. Excellent biocompatibility and high stability were obtained by selective manipulation of the functionality and the blend composition. In another study, biomaterial for tissue engineering was obtained by mixing UPy functionalized oligo (trimethylene) carbonate and polypeptides.[167]

Long *et al*. studied telechelic UPy functionalized linear and star-shaped poly(ethylene-*co*-propylene)s by SAXS and AFM.[168] It was concluded that a maxima in the X-ray scattering observed was a result of aggregation by microphase separated UPy-rich domains.

## 1.7 Recent development in the UPy supramolecular materials

Apart from thermoplastic elastomer applications, UPy hydrogen based SPs have also been also utilized in the preparation of biomaterial[166,167,169], polymer blends,[150,153,159] organic diode[170], self-healing and shape memory solid[146,157,171,172], and more recently nanoparticles synthesis[173]. In more recent studies by Kautz *et al*. and Appel *et al*., have indicated that the one dimensional stacking of UPy dimers is one of dominating factors for determining the outcome of the material properties.[174,175] The properties of SPs were attributed to the crystallization of dimeric urea-UPy into one dimensional stack. The presence of additional lateral interaction of urea or urethane linkers forms phase segregated nanometer-sized fibers. These fibers act as crosslinking points in the polymer matrix (**Figure 1.23**). Recent research is devoted to the understanding the role of secondary factors, such as interaction of urea *vs* urethane linkages, and the nature of spacer separating the UPy group and the type of linking chains. These factors were not considered earlier; rather the formation of very high molecular weight polymer devoid of any crystalline aggregates was thought to be a solo factor governing the property of SPs. Studies show clearly that the understanding of these factors is crucial for determining the properties of supramolecular materials.

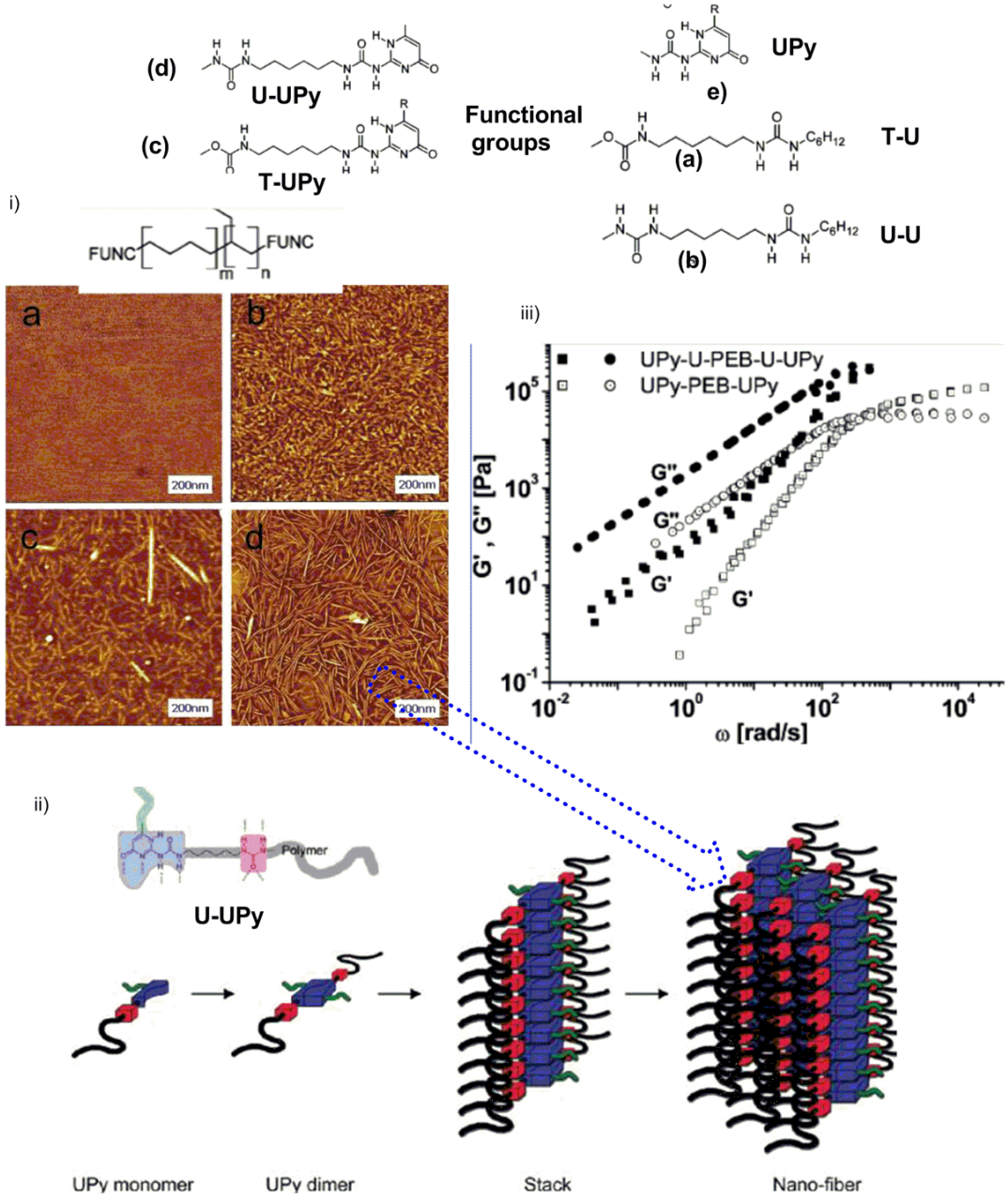



**Figure 1. 23:** i) Tapping mode AFM images of poly(ethylene-*co*-butylene, $M_n$-3,500 g/mol) end functionalized with various functional groups (a, b, c, and e), ii) schematic representation of theoretical aggregation driven by nano-fiber formation, iii) rheological master curves for polymer d and e, with reference temperature of 125 °C, and 110 °C, respectively.[174]

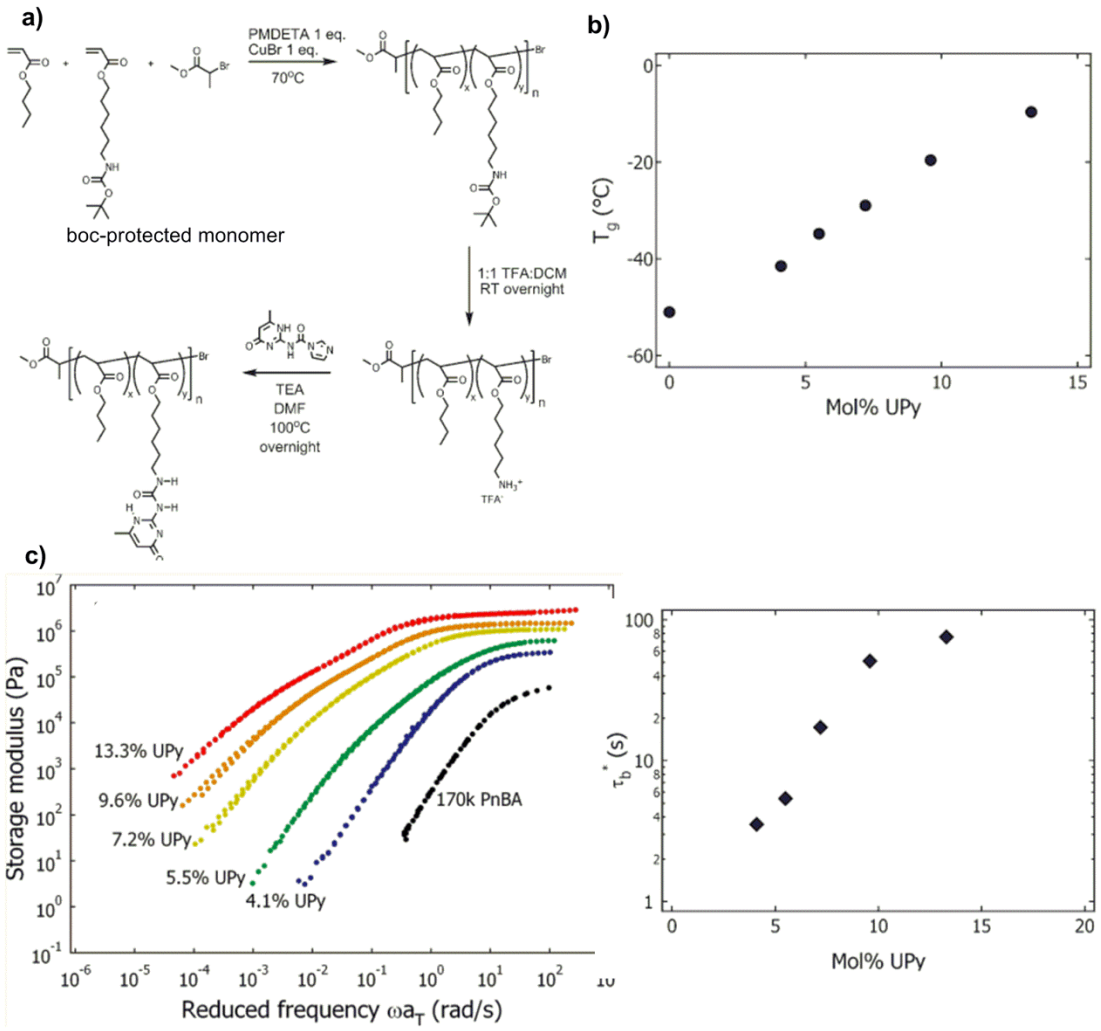



**Figure 1. 24:** a) Scheme for the synthesis of P*n*BA-*ran*-P*n*BA-UPy, b) linear relationship between UPy content and $T_g$ (at a constant polymer backbone molecular weight of ~ 24 kg/mol), c) storage modulus for the copolymer with various UPy contents, and d) effective H-bond life time with increasing UPy content (for random copolymer).[151]

As stated in earlier section, the controlled radical polymerization of UPy containing vinyl monomers was difficult due to the insufficient monomer solubility and interactions with copper catalyst in the case of ATRP. To eliminate these problems, Feldman *et al*. carried out ATRP of *boc*-protected amine functional monomer.[151] Subsequently, UPy group was introduced by post-polymer modification involving deprotection of amine and the reaction with 2-(1-imidazolylcarbonylamino)-6-methyl-4-[1H]-pyrimidinone (**Figure 1.24a**).

Copolymers obtained showed a linear increase in $T_g$ with increasing % of UPy content (**Figure 1.24b**) and it confirmed the previous work of Long *et al.*[147-149,160] Furthermore, no phase separation of the UPy groups was found by DSC and SAXS analysis. An estimated H-bond life time ($\tau_s$) indicated that the diffusion of UPy groups in the SPs decreased with increasing effective tying points. In their recent studies, monochelic P*n*BA-UPys were synthesized using UPy-functionalized initiator with different alkyl spacer (C2 and C6) between the initiator and the UPy group via ATRP.[154]

Scherman *et al*. have used ring opening metathesis polymerization (ROMP) to synthesize UPy telechelics by using chain-transfer agent functionalized with UPy.[176] The association of UPy group during the polymerization was protected with addition of another tautomeric UPy functional tag molecule. Upon completion of the reaction, protecting UPy additive was cleaved by precipitation. Tom de Geef *et al*. studied the effect of number of oligoethylene oxide units and the alkyl spacer between UPy groups and showed that a short spacer (C2, and C3) with two and three oligoethylene oxide units reduces the dimerization constant by intramolecular hydrogen bonding through the oxygen atom of ethylene oxide segment.[177]

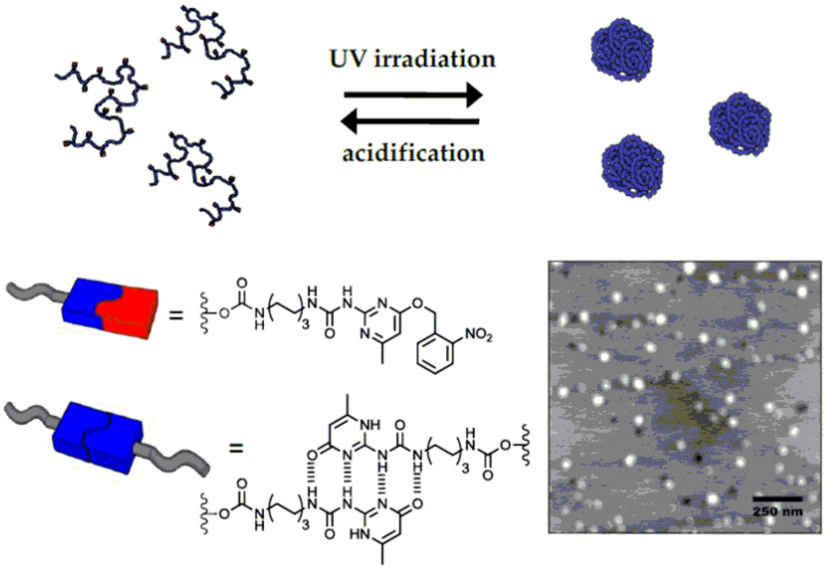



**Figure 1. 25:** Schematic representations of polynorbornene based nanoparticles synthesis, photolysis leading to collapse, and acidification leading to expansion, and AFM height image of the nanoparticles (right down).[173]

In a recent study, a photo-liable benzyl protection of UPy-keto group, to reduce its dimeric association during the polymerization, has been employed.[173,178,179] This approach was elegantly used in the synthesis of a novel class of materials with single-chain polymeric nanoparticles (SCPNs). Foster *et al.* synthesized polynorbornenes with protected UPy group (**Figure 1.25**).[173] On irradiation with a light, UPy groups were reformed to produce linear polymer with pendent UPy groups, which in dilute solution intramolecularly collapsed to formed nanometer-sized particles of approximately the size of a single polymer chain. Recently Chen *et al*. synthesized stable, high internal phase emulsion gels (HIPE-gels) by using PMMA-*co*-PBA latex particle loaded with 1.2mol % UPy.[180,181] More recently Chen *et al*. prepared waterborne poly(*N*-isopropylacrylamide) nanogel dispersions to make moldable, thermoresopnsive HIPE-hydrogels by incorporating non-covalent crosslinking with UPy groups.[182] It is clearly evident that, the UPy derivatives have been widely utilized in the preparation of supramolecular materials.

## 1.8 Conclusions

Supramolecular polymerization based on hydrogen bonding interaction is a new methodology to produce novel dynamic materials that exhibit tunable multiple-functionality. Simple organic molecules and oligomers having bifunctional or multifunctional hydrogen bonding moiety can be easily converted into supramolecular materials. Different types of hydrogen bonding motifs, from weak to strong association constants, have been utilized in the literature to produce SPs. The extent of polymerization and material properties of SPs are strongly dependent on the association constant of the hydrogen bonding motif. Several examples have been reported in the literature.

Nucleobases based hydrogen bonding motifs constitute a weak hydrogen bonding motif and generally work well for homogenous polymer blends; and with cooperativity effect can give thermoplastic elastomers. Ureidopyrimidone (UPy) derivatives owing to their high dimerization constant, simple synthetic procedure and efficient functionalization with telechelic oligomers have become one of the commonly used hydrogen bonding motifs in the SPs. The SPs using UPy motif have a wide range of applications in many fields depending on the type of linking oligomer or polymer. In the last two decades, significant advancements have been made in synthesis, characterization of solution and solid-state properties of UPy based SPs. More recent studies focus on determining factors affecting UPy dimerization, and

further association and eventually aggregations. However, the understanding of the bulk material properties of SPs and their correlation to molecular structures is still evolving.

## 1.9 References


(1) Carothers, W. H. *Chem. Rev.* **1931**, *8*, 353.

(2) Flory, P. J. *Principles of Polymer Chemistry*; Cornell University Press: Ithac, New York, 1953.

(3) Cram, D. J.; Cram, J. M. *Acc. Chem. Res.* **1978**, *11*, 8.

(4) Cram, D. J. *Angew. Chem. Int. Ed* **1986**, *25*, 1039.

(5) Pedersen, C. J. *J. Am. Chem. Soc.* **1967**, *89*, 2495.

(6) Pedersen, C. J. *Angew. Chem. Int. Ed.* **1988**, *27*, 1021.

(7) Dietrich, B.; Lehn, J. M.; Sauvage, J. P. *Tetrahedron Lett.* **1969**, 2885.

(8) Brevard, C.; Lehn, J. M. *J. Am. Chem. Soc* **1970**, *92*, 4987.

(9) Lehn, J.-M. In *Alkali Metal Complexes with Organic Ligands*; Springer Berlin Heidelberg: 1973; Vol. 16, p 1.

(10) Behr, J. P.; Lehn, J. M. *Febs Lett.* **1973**, *31*, 297.

(11) Behr, J. P.; Lehn, J. M. *J. Am. Chem. Soc* **1973**, *95*, 6108.

(12) Dietrich, B.; Lehn, J. M.; Sauvage, J. P.; Blanzat, J. *Tetrahedron* **1973**, *29*, 1629.

(13) Dietrich, B.; Lehn, J. M.; Sauvage, J. P. *Tetrahedron* **1973**, *29*, 1647.

(14) Timmerman, P.; Reinhoudt, D. N. *Adv. Mater.* **1999**, *11*, 71.

(15) Zimmerman, N.; Moore, J. S.; Zimmerman, S. C. *Chem. Ind.* **1998**, 604.

(16) Fouquey, C.; Lehn, J.-M.; Levelut, A.-M. *Adv. Mater.* **1990**, *2*, 254.

(17) Lehn, J.-M. *Makromol. Chem., Macromol. Symp.* **1993**, *69*, 1.

(18) Lange, R. F. M.; Meijer, E. W. *Macromolecules* **1995**, *28*, 782.

(19) Sijbesma, R. P.; Beijer, F. H.; Brunsveld, L.; Folmer, B. J. B.; Hirschberg, J. H. K. K.; Lange, R. F. M.; Lowe, J. K. L.; Meijer, E. W. *Science* **1997**, *278*, 1601.

(20) Kato, T.; Frechet, J. M. J. *J. Am. Chem. Soc.* **1989**, *111*, 8533.

(21) Kato, T.; Wilson, P. G.; Fujishima, A.; Fr; eacute; chet, J. M. J. *Chem. Lett.* **1990**, *19*, 2003.

(22) Kato, T.; Frechet, J. M. J.; Wilson, P. G.; Saito, T.; Uryu, T.; Fujishima, A.; Jin, C.; Kaneuchi, F. *Chem. Mater.* **1993**, *5*, 1094.

(23) Kato, T.; Ihata, O.; Ujiie, S.; Tokita, M.; Watanabe, J. *Macromolecules* **1998**, *31*, 3551.

(24) Kato, T.; Mizoshita, N.; Kishimoto, K. *Angew. Chem. Int. Ed.* **2006**, *45*, 38.

(25) Kato, T.; Hirai, Y.; Nakaso, S.; Moriyama, M. *Chem. Soc. Rev.* **2007**, *36*, 1857.

(26) Kumar, U.; Fréchet, J. M. J.; Kato, T.; Ujiie, S.; Timura, K. *Angew. Chem. Int. Ed.* **1992**, *31*, 1531.

(27) Fréchet, J. M. J. *Proc. Natl. Acad. Sci. USA* **2002**, *99*, 4782.

(28) Brunsveld, L.; Folmer, B. J. B.; Meijer, E. W.; Sijbesma, R. P. *Chem. Rev.* **2001**, *101*, 4071.

(29) Kotera, M.; Lehn, J.-M.; Vigneron, J.-P. *Tetrahedron* **1995**, *51*, 1953.

(30) Lehn, J.-M. *Supramolecular chemistry : concepts and perspectives*; Wiley-VCH, Weinheim: New York, 1995.

(31) Lehn, J.-M. *Chem. Eur. J.* **1999**, *5*, 2455.

(32) Lehn, J.-M. *Polym. Int.* **2002**, *51*, 825.

(33) De Greef, T. F. A.; Smulders, M. M. J.; Wolffs, M.; Schenning, A. P. H. J.; Sijbesma, R. P.; Meijer, E. W. *Chem. Rev.* **2009**, *109*, 5687.

(34) ten Brinke, G.; Ruokolainen, J.; Ikkala, O. *Adv. Polym. Sci.* **2007**, *207*, 113.

(35) Binder, W. H.; Zirbs, R. In *Hydrogen Bonded Polymers*; Binder, W., Ed.; Springer-Verlag Berlin: Berlin, 2007; Vol. 207, p 1.

(36) Wilson, A. J. *Soft Matter* **2007**, *3*, 409.

(37) Prins, L. J.; Reinhoudt, D. N.; Timmerman, P. *Angew. Chem. Int. Ed.* **2001**, *40*, 2382.

(38) Ciferri, A. *Macromol. Rapid Commun.* **2002**, *23*, 511.

(39) Ciferri, A. *Supramolecular Polymers, Second Edition*; CRC Press: US, 2005.

(40) Berl, V.; Schmutz, M.; Krische, M. J.; Khoury, R. G.; Lehn, J.-M. *Chem. Eur. J.* **2002**, *8*, 1227.

(41) Hirschberg, J.; Beijer, F. H.; van Aert, H. A.; Magusin, P.; Sijbesma, R. P.; Meijer, E. W. *Macromolecules* **1999**, *32*, 2696.

(42) Sijbesma, R. P.; Meijer, E. W. *Curr. Opin. Colloid Interface Sci.* **1999**, *4*, 24.

(43) Lehn, J. M. *Makromol. Chem., Macromol. Symp.* **1993**, *69*, 1.

(44) Elias, V. H.-G. *Makromol. Chem* **1966**, *99*, 291.

(45) Beijer, F. H.; Sijbesma, R. P.; Vekemans, J.; Meijer, E. W.; Kooijman, H.; Spek, A. L. *J. Org. Chem.* **1996**, *61*, 6371.

(46) Beijer, F. H.; Sijbesma, R. P.; Kooijman, H.; Spek, A. L.; Meijer, E. W. *J. Am. Chem. Soc.* **1998**, *120*, 6761.

(47) Folmer, B. J. B.; Sijbesma, R. P.; Versteegen, R. M.; van der Rijt, J. A. J.; Meijer, E. W. *Adv. Mater.* **2000**, *12*, 874.

(48) Pedersen, C. J. *Curr. Cont. Eng. Technol. Appl. Sci.* **1985**, 18.

(49) Shetty, A. S.; Zhang, J.; Moore, J. S. *J. Am. Chem. Soc.* **1996**, *118*, 1019.

(50) Loeb, S. J.; Tiburcio, J.; Vella, S. J. *Org. Lett.* **2005**, *7*, 4923.

(51) Lehn, J. M. *Pure Appl. Chem.* **1978**, *50*, 871.

(52) Lindoy, L. F.; Park, K.-M.; Sung Lee, S. *Supramolecular Chemistry: From Molecules to Nanomaterials.*; John Wiley & Sons, Ltd, 2012.

(53) Connors, K. A. *Chem. Rev.* **1997**, *97*, 1325.

(54) Cram, D. J.; Cram, J. M. *Science* **1974**, *183*, 803.

(55) Cram, D. J. *J. Inclusion. Phenom* **1988**, *6*, 397.

(56) Lehn, J. M. *Science* **1985**, *227*, 849.

(57) Brienne, M. J.; Gabard, J.; Lehn, J. M.; Stibor, I. *J. Chem. Soc., Chem. Commun.* **1989**, 1868.

(58) Lehn, J.-M.; Mascal, M.; Decian, A.; Fischer, J. *J. Chem. Soc., Chem. Commun.* **1990**, *0*, 479.

(59) Lehn, J.-M. *Angew. Chem. Int. Ed.* **1988**, *27*, 89.

(60) Lehn, J.-M. *Chem. Soc. Rev.* **2007**, *36*, 151.

(61) Gellman, S. H. *Acc. Chem. Res.* **1998**, *31*, 173.

(62) Sauvage, J. P.; Collin, J. P.; Chambron, J. C.; Guillerez, S.; Coudret, C.; Balzani, V.; Barigelletti, F.; De Cola, L.; Flamigni, L. *Chem. Rev.* **1994**, *94*, 993.

(63) Seebach, D.; Matthews, J. L.; Meden, A.; Wessels, T.; Baerlocher, C.; McCusker, L. B. *Helv. Chim. Acta* **1997**, *80*, 173.

(64) Castellano, R. K.; Rudkevich, D. M.; Rebek, J. *Proc. Natl. Acad. Sci. U.S.A.* **1997**, *94*, 7132.

(65) Zhang, S.; Marini, D. M.; Hwang, W.; Santoso, S. *Curr. Opin. Chem. Biol.* **2002**, *6*, 865.

(66) Altman, G. H.; Diaz, F.; Jakuba, C.; Calabro, T.; Horan, R. L.; Chen, J.; Lu, H.; Richmond, J.; Kaplan, D. L. *Biomaterials* **2003**, *24*, 401.

(67) Dobb, M. G.; Johnson, D. J.; Saville, B. P. *J. Polym. Sci. Polymer. Phys. Ed.* **1977**, *15*, 2201.

(68) Flory, P. J. *J. Am. Chem. Soc* **1936**, *58*, 1877.

(69) Zhao, D.; Moore, J. S. *Org. Biomol. Chem* **2003**, *1*, 3471.

(70) Goshe, A. J.; Steele, I. M.; Ceccarelli, C.; Rheingold, A. L.; Bosnich, B. *Proc. Natl. Acad. Sci. USA* **2002**, *99*, 4823.

(71) Sivakova, S.; Rowan, S. J. *Chem. Soc. Rev.* **2005**, *34*, 9.

(72) Zeng, H. Q.; Miller, R. S.; Flowers, R. A.; Gong, B. *J. Am. Chem. Soc.* **2000**, *122*, 2635.

(73) Jorgensen, W. L.; Pranata, J. *J. Am. Chem. Soc.* **1990**, *112*, 2008.

(74) Sartorius, J.; Schneider, H. J. *Chem. Eur. J.* **1996**, *2*, 1446.

(75) Murray, T. J.; Zimmerman, S. C. *J. Am. Chem. Soc.* **1992**, *114*, 4010.

(76) Zimmerman, S. C.; Murray, T. J. *Tetrahedron Lett.* **1994**, *35*, 4077.

(77) Blight, B. A.; Camara-Campos, A.; Djurdjevic, S.; Kaller, M.; Leigh, D. A.; McMillan, F. M.; McNab, H.; Slawin, A. M. Z. *J. Am. Chem. Soc.* **2009**, *131*, 14116.

(78) Buhler, E.; Candau, S. J.; Schmidt, J.; Talmon, Y.; Kolomiets, E.; Lehn, J. M. *J. Polym. Sci., Part B: Polym. Phys.* **2007**, *45*, 103.

(79) Alexander, C.; Jariwala, C. P.; Lee, C. M.; Griffin, A. C. *Macrom. Symp* **1994**, *77*, 283.

(80) St.Pourcain, C. B.; Griffin, A. C. *Macromolecules* **1995**, *28*, 4116.

(81) Lillya, C. P.; Baker, R. J.; Hutte, S.; Winter, H. H.; Lin, Y. G.; Shi, J.; Dickinson, L. C.; Chien, J. C. W. *Macromolecules* **1992**, *25*, 2076.

(82) Abed, S.; Boileau, S.; Bouteiller, L.; Lacoudre, N. *Polym. Bull.* **1997**, *39*, 317.

(83) Abed, S.; Boileau, S.; Bouteiller, L. *Macromolecules* **2000**, *33*, 8479.

(84) Abed, S.; Boileau, S.; Bouteiller, L. *Polymer* **2001**, *42*, 8613.

(85) Duweltz, D.; Lauprêtre, F.; Abed, S.; Bouteiller, L.; Boileau, S. *Polymer* **2003**, *44*, 2295.

(86) Kato, T.; Frechet, J. M. J. *Macromolecules* **1989**, *22*, 3818.

(87) Hemp, S. T.; Long, T. E. *Macromol. Biosci* **2012**, *12*, 29.

(88) McHale, R.; O'Reilly, R. K. *Macromolecules* **2012**, *45*, 7665.

(89) Boal, A. K.; Ilhan, F.; DeRouchey, J. E.; Thurn-Albrecht, T.; Russell, T. P.; Rotello, V. M. *Nature* **2000**, *404*, 746.

(90) Frankamp, B. L.; Uzun, O.; Ilhan, F.; Boal, A. K.; Rotello, V. M. *JACS* **2002**, *124*, 892.

(91) Spijker, H. J.; van Delft, F. L.; van Hest, J. C. M. *Macromolecules* **2007**, *40*, 12.

(92) Spijker, H. J.; Dirks, A. J.; van Hest, J. C. M. *J. Polym. Sci., Part A: Polym. Chem.* **2006**, *44*, 4242.

(93) Rowan, S. J.; Suwanmala, P.; Sivakova, S. *J. Polym. Sci., Part A: Polym. Chem.* **2003**, *41*, 3589.

(94) Sivakova, S.; Bohnsack, D. A.; Mackay, M. E.; Suwanmala, P.; Rowan, S. J. *J. Am. Chem. Soc.* **2005**, *127*, 18202.

(95) Sivakova, S.; Wu, J.; Campo, C. J.; Mather, P. T.; Rowan, S. J. *Chem. Eur. J.* **2006**, *12*, 446.

(96) Cheng, S.; Zhang, M.; Dixit, N.; Moore, R. B.; Long, T. E. *Macromolecules* **2012**, *45*, 805.

(97) Mather, B. D.; Baker, M. B.; Beyer, F. L.; Berg, M. A. G.; Green, M. D.; Long, T. E. *Macromolecules* **2007**, *40*, 6834.

(98) Bong, D. T.; Clark, T. D.; Granja, J. R.; Ghadiri, M. R. *Angew. Chem., Int. Ed.* **2001**, *40*, 988.

(99) Chang, S. K.; Hamilton, A. D. *J. Am. Chem. Soc.* **1988**, *110*, 1318.

(100) Garcia-Tellado, F.; Geib, S. J.; Goswami, S.; Hamilton, A. D. *J. Am. Chem. Soc.* **1991**, *113*, 9265.

(101) Geib, S. J.; Vicent, C.; Fan, E.; Hamilton, A. D. *Angew. Chem. Int. Ed.* **1993**, *32*, 119.

(102) Boden, N.; Bushby, R. J.; Hardy, C. *J. Phys., Lett.* **1985**, *46*, 325.

(103) Boden, N.; Bushby, R. J.; Hardy, C.; Sixl, F. *Chem. Phys. Lett.* **1986**, *123*, 359.

(104) Boden, N.; Bushby, R. J.; Clements, J.; Movaghar, B.; Donovan, K. J.; Kreozis, T. *Phys. Rev. B: Condens. Matter Mater. Phys.* **1995**, *52*, 13274.

(105) Boden, N.; Bushby, R. J.; Hubbard, J. F. *Mol. Cryst. Liq. Cryst. Sci. Technol., Sect. A* **1997**, *304*, 195.

(106) Rebek, J. *Science* **1987**, *235*, 1478.

(107) Rebek, J. J. *Chem. Commun.* **2000**, *0*, 637.

(108) Castellano, R. K.; Clark, R.; Craig, S. L.; Nuckolls, C.; Rebek, J. *Proc. Natl. Acad. Sci. U. S. A* **2000**, *97*, 12418.

(109) Corbin, P. S.; Zimmerman, S. C. *J. Am. Chem. Soc.* **1998**, *120*, 9710.

(110) Suarez, M.; Lehn, J. M.; Zimmerman, S. C.; Skoulios, A.; Heinrich, B. *J. Am. Chem. Soc.* **1998**, *120*, 9526.

(111) Kotera, M.; Lehn, J.-M.; Vigneron, J.-P. *J. Chem. Soc., Chem. Commun.* **1994**, *0*, 197.

(112) Berl, V.; Huc, I.; Lehn, J. M.; DeCian, A.; Fischer, J. *Eur. J. Org. Chem.* **1999**, 3089.

(113) Muehldorf, A. V.; Van Engen, D.; Warner, J. C.; Hamilton, A. D. *J. Am. Chem. Soc.* **1988**, *110*, 6561.

(114) Beijer, F. H.; Sijbesma, R. P.; Vekemans, J. A. J. M.; Meijer, E. W.; Kooijman, H.; Spek, A. L. *J. Org. Chem.* **1996**, *61*, 6371.

(115) Palmans, A. R. A.; Vekemans, J. A. J. M.; Havinga, E. E.; Meijer, E. W. *Angew. Chem. Int. Ed.* **1997**, *36*, 2648.

(116) Beijer, F. H.; Kooijman, H.; Spek, A. L.; Sijbesma, R. P.; Meijer, E. W. *Angew. Chem. Int. Ed.* **1998**, *37*, 75.

(117) Folmer, B. J. B.; Sijbesma, R. P.; Kooijman, H.; Spek, A. L.; Meijer, E. W. *J. Am. Chem. Soc.* **1999**, *121*, 9001.

(118) Söntjens, S. H. M.; Sijbesma, R. P.; van Genderen, M. H. P.; Meijer, E. W. *J. Am. Chem. Soc.* **2000**, *122*, 7487.

(119) Zimmerman, S. C.; Corbin, P. S. *Struct. Bonding (Berlin)* **2000**, *96*, 63.

(120) Park, T.; Todd, E. M.; Nakashima, S.; Zimmerman, S. C. *J. Am. Chem. Soc.* **2005**, *127*, 18133.

(121) Park, T.; Zimmerman, S. C.; Nakashima, S. *J. Am. Chem. Soc.* **2005**, *127*, 6520.

(122) Mayer, M. F.; Nakashima, S.; Zimmerman, S. C. *Org. Lett.* **2005**, *7*, 3005.

(123) Park, T.; Zimmerman, S. C. *J. Am. Chem. Soc.* **2006**, *128*, 14236.

(124) Park, T.; Zimmerman, S. C. *J. Am. Chem. Soc.* **2006**, *128*, 13986.

(125) Park, T.; Zimmerman, S. C. *J. Am. Chem. Soc.* **2006**, *128*, 11582.

(126) Zeng, H.; Miller, R. S.; Flowers, R. A.; Gong, B. *J. Am. Chem. Soc.* **2000**, *122*, 2635.

(127) Bong, D. T.; Clark, T. D.; Granja, J. R.; Ghadiri, M. R. *Angew. Chem., Int. Ed.* **2001**, *40*, 988.

(128) Gong, B. *Synlett* **2001**, *2001*, 0582.

(129) Corbin, P. S.; Lawless, L. J.; Li, Z.; Ma, Y.; Witmer, M. J.; Zimmerman, S. C. *Proc. Natl. Acad. Sci. USA* **2002**, *99*, 5099.

(130) Sessler, J. L.; Wang, R. *Angew. Chem. Int. Ed.* **1998**, *37*, 1726.

(131) Sessler, J. L.; Wang, R. *J. Org. Chem.* **1998**, *63*, 4079.

(132) Corbin, P. S.; Zimmerman, S. C.; Thiessen, P. A.; Hawryluk, N. A.; Murray, T. J. *J. Am. Chem. Soc.* **2001**, *123*, 10475.

(133) Lüning, U.; Kühl, C. *Tetrahedron Lett.* **1998**, *39*, 5735.

(134) Lüning, U.; Kühl, C.; Uphoff, A. *Eur. J. Org. Chem.* **2002**, *2002*, 4063.

(135) Corbin, P. S.; Zimmerman, S. C. *J. Am. Chem. Soc.* **2000**, *122*, 3779.

(136) Söntjens, S. H. M.; van Genderen, M. H. P.; Sijbesma, R. P. *J. Org. Chem.* **2003**, *68*, 9070.

(137) Cates, M. E.; Candau, S. J. *J. Phys.:Condens.Matter* **1990**, *2*, 6869.

(138) Folmer, B. J. B., Eindhoven University of Technology, 2000.

(139) J. B. Folmer, B.; Cavini, E. *Chem. Commun.* **1998**, 1847.

(140) Wubbenhorst, M.; Van Turnhout, J.; Folmer, B. J. B.; Sijbesma, R. P.; Meijer, E. W. *IEEE Trans. Dielectr. Electr. Insul.* **2001**, *8*, 365.

(141) Lee, C.-M.; Griffin, A. C. *Macromol. Symp.* **1997**, *117*, 281.

(142) Yamauchi, K.; Lizotte, J. R.; Hercules, D. M.; Vergne, M. J.; Long, T. E. *J. Am. Chem. Soc.* **2002**, *124*, 8599.

(143) Lange, R. F. M.; Van Gurp, M.; Meijer, E. W. *J. Polym. Sci., Part A: Polym. Chem.* **1999**, *37*, 3657.

(144) Elkins, C. L.; Viswanathan, K.; Long, T. E. *Macromolecules* **2006**, *39*, 3132.

(145) Keizer, H. M.; van Kessel, R.; Sijbesma, R. P.; Meijer, E. W. *Polymer* **2003**, *44*, 5505.

(146) Hentschel, J.; Kushner, A. M.; Ziller, J.; Guan, Z. *Angew. Chem. Int. Ed.* **2012**, *51*, 10561.

(147) Huggins, M. L. *Ann. N.Y. Acad. Sci.* **1942**, *43*, 1.

(148) Yamauchi, K.; Lizotte, J. R.; Long, T. E. *Macromolecules* **2003**, *36*, 1083.

(149) Elkins, C. L.; Park, T.; McKee, M. G.; Long, T. E. *J. Polym. Sci., Part A: Polym. Chem.* **2005**, *43*, 4618.

(150) Feldman, K. E.; Kade, M. J.; de Greef, T. F. A.; Meijer, E. W.; Kramer, E. J.; Hawker, C. J. *Macromolecules* **2008**, *41*, 4694.

(151) Feldman, K. E.; Kade, M. J.; Meijer, E. W.; Hawker, C. J.; Kramer, E. J. *Macromolecules* **2009**, *42*, 9072.

(152) Li, J.; Sullivan, K. D.; Brown, E. B.; Anthamatten, M. *Soft Matter* **2010**, *6*, 235.

(153) Feldman, K. E.; Kade, M. J.; Meijer, E. W.; Hawker, C. J.; Kramer, E. J. *Macromolecules* **2010**, *43*, 5121.

(154) De Greef, T. F. A.; Kade, M. J.; Feldman, K. E.; Kramer, E. J.; Hawker, C. J.; Meijer, E. W. *J. Polym. Sci., Part A: Polym. Chem.* **2011**, *49*, 4253.

(155) Celiz, A. D.; Scherman, O. A. *J. Polym. Sci., Part A: Polym. Chem.* **2010**, *48*, 5833.

(156) Celiz, A. D.; Lee, T.-C.; Scherman, O. A. *Adv. Mater.* **2009**, *21*, 3937.

(157) Lewis, C. L.; Anthamatten, M. *Soft Matter* **2013**, *9*, 4058.

(158) Rao, J.; Paunescu, E.; Mirmohades, M.; Gadwal, I.; Khaydarov, A.; Hawker, C. J.; Bang, J.; Khan, A. *Polymer Chemistry* **2012**, *3*, 2050.

(159) Wrue, M. H.; McUmber, A. C.; Anthamatten, M. *Macromolecules* **2009**, *42*, 9255.

(160) McKee, M. G.; Elkins, C. L.; Park, T.; Long, T. E. *Macromolecules* **2005**, *38*, 6015.

(161) McKee, M. G.; Elkins, C. L.; Long, T. E. *Polymer* **2004**, *45*, 8705.

(162) Kuo, S. W.; Tsai, H. T. *Macromolecules* **2009**, *42*, 4701.

(163) Rieth, L. R.; Eaton, R. F.; Coates, G. W. *Angew. Chem. Int. Ed.* **2001**, *40*, 2153.

(164) Guan, Z.; Roland, J. T.; Bai, J. Z.; Ma, S. X.; McIntire, T. M.; Nguyen, M. *J. Am. Chem. Soc.* **2004**, *126*, 2058.

(165) Kushner, A. M.; Vossler, J. D.; Williams, G. A.; Guan, Z. *J. Am. Chem. Soc.* **2009**, *131*, 8766.

(166) Dankers, P. Y. W.; Harmsen, M. C.; Brouwer, L. A.; Van Luyn, M. J. A.; Meijer, E. W. *Nat Mater* **2005**, *4*, 568.

(167) Dankers, P. Y. W.; Zhang, Z.; Wisse, E.; Grijpma, D. W.; Sijbesma, R. P.; Feijen, J.; Meijer, E. W. *Macromolecules* **2006**, *39*, 8763.

(168) Mather, B. D.; Elkins, C. L.; Beyer, F. L.; Long, T. E. *Macromol. Rapid Commun.* **2007**, *28*, 1601.

(169) Dankers, P. Y. W.; Boomker, J. M.; Huizinga-van der Vlag, A.; Wisse, E.; Appel, W. P. J.; Smedts, F. M. M.; Harmsen, M. C.; Bosman, A. W.; Meijer, W.; van Luyn, M. J. A. *Biomaterials* **2011**, *32*, 723.

(170) Abbel, R.; Grenier, C.; Pouderoijen, M. J.; Stouwdam, J. W.; Leclère, P. E. L. G.; Sijbesma, R. P.; Meijer, E. W.; Schenning, A. P. H. J. *J. Am. Chem. Soc.* **2008**, *131*, 833.

(171) Li, J.; Viveros, J. A.; Wrue, M. H.; Anthamatten, M. *Adv. Mater.* **2007**, *19*, 2851.

(172) Anthamatten, M.; Roddecha, S.; Li, J. *Macromolecules* **2013**, *46*, 4230.

(173) Foster, E. J.; Berda, E. B.; Meijer, E. W. *J. Am. Chem. Soc.* **2009**, *131*, 6964.

(174) Kautz, H.; van Beek, D. J. M.; Sijbesma, R. P.; Meijer, E. W. *Macromolecules* **2006**, *39*, 4265.

(175) Appel, W. P. J.; Portale, G.; Wisse, E.; Dankers, P. Y. W.; Meijer, E. W. *Macromolecules* **2011**, *44*, 6776.

(176) Scherman, O. A.; Ligthart, G. B. W. L.; Ohkawa, H.; Sijbesma, R. P.; Meijer, E. W. *Proc. Natl. Acad. Sci. U.S.A.* **2006**, *103*, 11850.

(177) de Greef, T. F. A.; Nieuwenhuizen, M. M. L.; Sibesma, R. P.; Meijer, E. W. *J. Org. Chem.* **2010**, *75*, 598.

(178) Berda, E. B.; Foster, E. J.; Meijer, E. W. *Macromolecules* **2010**, *43*, 1430.

(179) Foster, E. J.; Berda, E. B.; Meijer, E. W. *J. Polym. Sci., Part A: Polym. Chem.* **2011**, *49*, 118.

(180) Chen, Y.; Jones, S. T.; Hancox, I.; Beanland, R.; Tunnah, E. J.; Bon, S. A. F. *ACS Macro Lett* **2012**, *1*, 603.

(181) Chen, Y.; Ballard, N.; Gayet, F.; Bon, S. A. F. *Chem. Commun.* **2012**, *48*, 1117.

(182) Chen, Y.; Ballard, N.; Bon, S. A. F. *Chem. Commun.* **2013**, *49*, 1524.

# Chapter 2: Scope of the Thesis

## 2.1 Proposed research

As described in the introduction, strong hydrogen bonding induced supramolecular polymerization using UPy has been wildly employed in telechelic and side chain oligomers and polymers.[1,2] UPy synthon has very high $K_a$ as determined from solution studies.[3] However, the rate of association and dissociation of hydrogen bonds in the absence of solvent in SPs must be slower due to the interference of linking chain dynamics. Thus, efficiency of reengagement of hydrogen bonding is not only depended on $K_a$, but also strongly depend on the *dynamer equilibrium constant ($K_d$)* in bulk. It is expected that $K_d$ must be equal to $K_a$ in order to have stable reversible SPs that can be used in various potential applications.

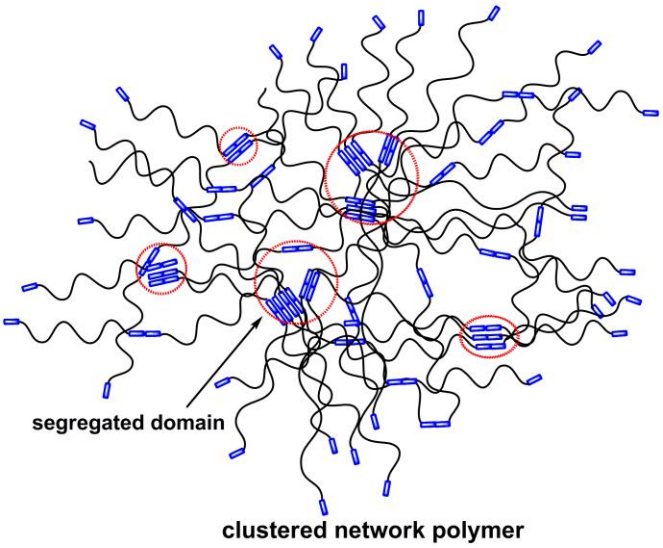



**Figure 2.1:** Presence of micellar-clusters in UPy functionalized polybutadiene supramolecular polymer. The illustration is based on the AFM image obtained in our preliminary studies.

In the literature, a profound effect of SPs based on hydrogen bonding has been shown using non-polar precursor polymers.[2] This may be due to the combination of polar phase separated hydrogen bonded domain formation which is embedded in the non-polar matrix and produces enhanced elastomeric properties for SPs. More importantly, the dynamics of hydrogen bonded domains within the matrix of SPs have not been thoroughly understood yet.[4,5] It is expected that these hydrogen bonded polar sites in bulk polymer will have different types of inter-domain interactions depending on the polarity as well as molecular weight of the

precursor polymer chains. The understanding of SPs using UPy groups is evolving as recent studies have shown evidence of multiple aggregations present along with one-dimensional stacks as claimed by Meijer and co-workers.[5-13] Our preliminary studies indicated that the UPy dimeric associates in SPs may form random or stacked aggregates of rigid cluster network as shown in **Figure 2.1**. *Therefore, it is important to understand the factors affecting the hydrogen bonding, aggregation of UPy groups for a particular linking oligomer chain and to correlate property enhancement in supramolecular systems.*

The primary issues that we addressed in this thesis are the followings: 1) examination of dependence of physical property of SPs on the precursor molecular weight of oligomer or polymer, 2) understanding the UPy interacting domain- dynamics in solution and in bulk, and 3) examine the effect of polarity of the precursor linking chain and attempt to make correction to physical properties of SPs with linking-chain dynamics.

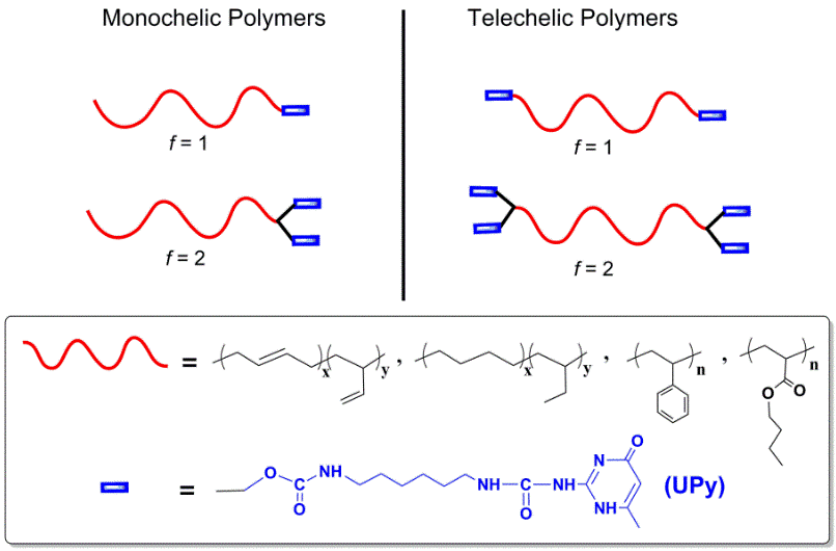



**Figure 2. 2:** Proposed synthesis of mono- and telechelic polybutadienes, polystyrene, and poly(*n*-butyl acrylate) with UPy functionality, *f* = 1, and 2.

We undertook a detailed study of well-defined monochelic and telechelic oligobutadiene functionalized with UPy (**Figure 2.2**). We synthesized monochelic and telechelic polymers and characterized them thoroughly. The polymers with one or two

interacting sites at the chain-ends for examining the effect of concentration of hydrogen bonding on the supramolecular assembly in solution and in bulk (**Figure 2.2**). We examined the influence of high *1,2*-vinyl addition ($T_g$~ -50 °C) and low *1,2*-vinyl addition ($T_g$~ -90 °C) in polybutadiene to evaluate the impact of chain-mobility on SPs and compare with hydrogenated systems. We studied the effect of multiple hydrogen bonded UPy domain, its aggregation in non-polar polybutadiene matrix and also examined the formation of the proposed supramolecular network or physical crosslinks in the SPs.

## 2.2 Outline of the thesis

This thesis is arranged in the following chapters as given below:

**Chapter 3** describes the general overview of the experimental techniques that was used to prepare samples and provide details of the characterization techniques.

**Chapter 4** deals with the micellar cluster association of ureidopyrimidone functionalized monochelic polybutadiene

**Chapter 5** gives the details of synthesis and characterization of telechelic PBds functionalized with UPy: Evidence of polar aggregation of UPy domain in the SPs

**Chapter 6** describes new routes to ureidopyrimidone telechelics by a combination of atom transfer radical polymerization and CuAAC 'Click' Chemistry

**Chapter 7** evaluates critical factors affecting the UPy hydrogen bonded SPs.

**Chapter 8** provides conclusions and future perspective of UPy hydrogen bonded SPs

## 2.3 References


(1) Sijbesma, R. P.; Beijer, F. H.; Brunsveld, L.; Folmer, B. J. B.; Hirschberg, J. H. K. K.; Lange, R. F. M.; Lowe, J. K. L.; Meijer, E. W. *Science* **1997**, *278*, 1601.

(2) Folmer, B. J. B.; Sijbesma, R. P.; Versteegen, R. M.; van der Rijt, J. A. J.; Meijer, E. W. *Adv. Mater.* **2000**, *12*, 874.

(3) Beijer, F. H.; Sijbesma, R. P.; Kooijman, H.; Spek, A. L.; Meijer, E. W. *J. Am. Chem. Soc.* **1998**, *120*, 6761.

(4) te Nijenhuis, K. *Polym. Bull.* **2007**, *58*, 27.

(5) van Beek, D. J. M.; Spiering, A. J. H.; Peters, G. W. M.; te Nijenhuis, K.; Sijbesma, R. P. *Macromolecules* **2007**, *40*, 8464.

(6) Appel, W. P. J.; Portale, G.; Wisse, E.; Dankers, P. Y. W.; Meijer, E. W. *Macromolecules* **2011**, *44*, 6776.

(7) Kautz, H.; van Beek, D. J. M.; Sijbesma, R. P.; Meijer, E. W. *Macromolecules* **2006**, *39*, 4265.

(8) Huggins, M. L. *Ann. N.Y. Acad. Sci.* **1942**, *4*, 1.

(9) Yamauchi, K.; Lizotte, J. R.; Hercules, D. M.; Vergne, M. J.; Long, T. E. *J. Am. Chem. Soc.* **2002**, *124*, 8599.

(10) Yamauchi, K.; Lizotte, J. R.; Long, T. E. *Macromolecules* **2003**, *36*, 1083.

(11) Yamauchi, K.; Kanomata, A.; Inoue, T.; Long, T. E. *Macromolecules* **2004**, *37*, 3519.

(12) Elkins, C. L.; Park, T.; McKee, M. G.; Long, T. E. *J. Polym. Sci., Part A: Polym. Chem.* **2005**, *43*, 4618.

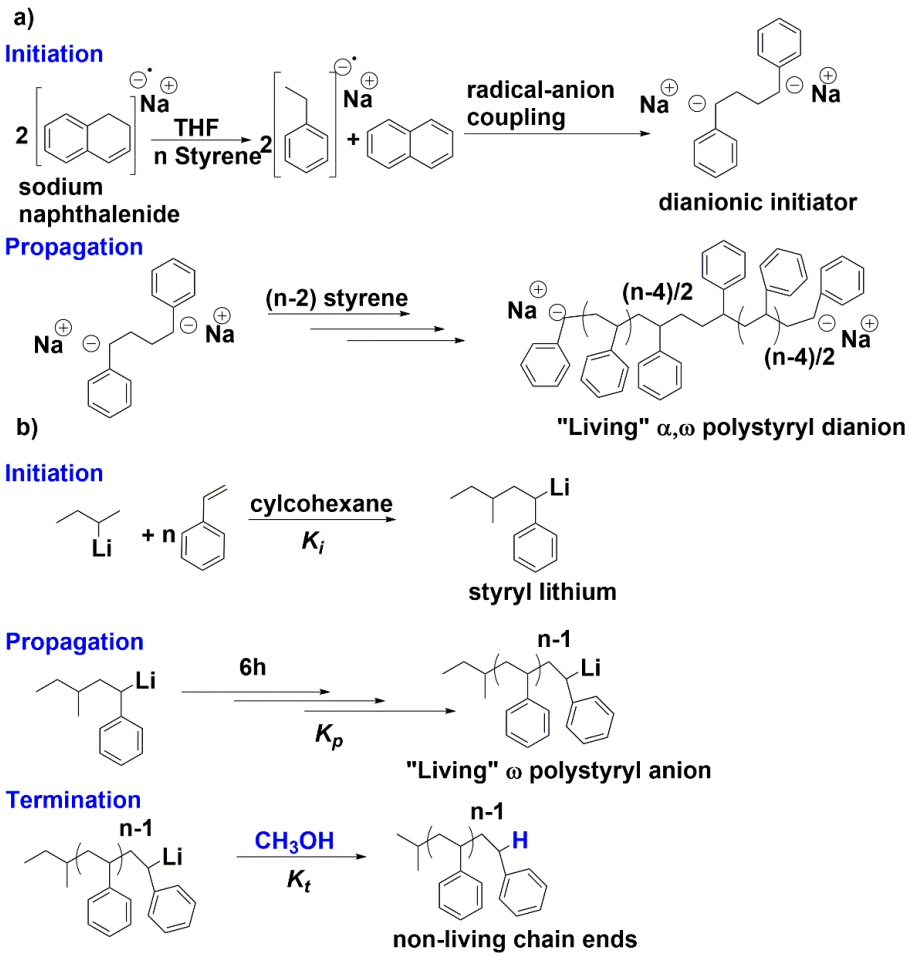
(13) Elkins, C. L.; Viswanathan, K.; Long, T. E. *Macromolecules* **2006**, *39*, 3132.

# Chapter 3: Experimental Techniques and Characterization Tools

## 3.1 Introduction

Living polymerization is a chain polymerization which proceeds in the absence of termination or chain transfer.[1] When the chain polymerization initiation and propagation steps involve an anion (carbanion), it is termed as anionic polymerization. The concept of "living" polymerization was first proved by Szwarc in 1956 by using sodium naphthalenide as initiator to polymerize styrene in THF at -78 °C. [1,2] Living anionic polymerization of styrene was free from termination and transfer reactions under vacuum, and chain end anions were active to reinitiate the polymerization of freshly added monomer. The addition of another type of monomer (i.e. isoprene) gave *tri*-block-*co*-polymer (PI-*b*-PS-*b*-PI) in THF. This interesting development of living anionic polymerization was followed by the anionic polymerization of styrene and dienes in hydrocarbons medium using alkyllithium initiators.[3-11] **Scheme 3.1** illustrates the mechanism of anionic polymerization using a radical anion (sodium naphthalenide) and an anion initiator (alkyl lithium). It is worth mentioning that the earliest application of anions for ionic polymerization was potassium amide used for polymerization of styrene in ammonia.[12]

Monomers subjected to the anionic polymerization must be able to form a stable anionic active center when reacted with suitable radical carbanions, or oxyanions. Monomers that satisfy this condition are styrenic, dienic, alkyl methacrylates and certain cyclic monomers. Styrenic and dienic derivatives stabilize the negative charge by delocalization. Ring opening polymerization of cyclic monomers (epoxide, and lactones) takes place by the ring opening by a nucleophilic attack (alkoxide). In general the carbanions are stabilized by the presence of aromatic rings, double bonds, carbonyl, ester, cyano, and sulfone groups. Obviously the presence of electrophilic substituents results in termination of the living chain ends. These include primary and secondary amines, halides, carboxylic, epoxide, and hydroxyl groups. Such functional groups if present in the monomer needs to be protected with suitable non-interfering group before subjecting them for polymerization. Most importantly appropriate reagents and conditions such as specific counter ions, polar additive, low temperature, and selective initiator are carefully chosen to achieve a successful living anionic polymerization.[13-16]




**Scheme 3. 1:** Anionic polymerization of styrene using sodium naphthalenide as initiator in THF at – 78 °C (a), and anionic polymerization of styrene using sec-butyllithium as initiator in cyclohexane at RT (b)

Alkyl lithium initiators such as secondary lithium (*sec*-BuLi) are most commonly used, but difunctional, trifunctional (multifunctional anionic initiators are derived from either alkyllithium-halide exchange or addition of alkyllithium to plurifunctional diphenylethyelene (DPE) derivatives) have been used in the synthesis of complex macromolecular architecture.[17-28] Initiators with protected functional groups and termination with electrophilic agents have been employed in the synthesis of functional polymers such as monochelic, telechelic and heterotelechelic.[29-32] Protecting groups must be stable under anionic polymerization condition and also be easily removable under mild condition. *Sec*-BuLi initiator is useful because of its solubility in non-polar organic solvents such as cyclohexane and benzene. Steric factors

determine the stability and reactivity of alkyl lithium initiators. Reactivity is largely governed by the dynamics of equilibrium and extent of aggregation in the solution.[33,34] *sec*-BuLi forms carbanion aggregates that are composed of trifunctional, tetrafunctional, and hexafunctional species depending on the medium polarity. It is suitable for the room temperature polymerization of dienes and styrenes in nonpolar solvents. Effect of aggregation can be seen with *n*-butyllithium, which is highly aggregated and its slow equilibrium dynamics with unimer leads to incomplete conversion and poor control of molecular weight distribution.[35] Use of higher reaction temperature or polar additives may help to reduce the aggregation and increase the rate of initiation. The amount of aggregation can be controlled by selection of the initiator species, solvent, and additives. In general initiators follow the general reaction rate hierarchy:

For dienes: Menthyllithium > *s*ec-butyllithium > *ipr*-propyllithium > *ter*-butyllithium > *n*-butyllithum and ethyllithium.

For styrene: Menthyllithium > *sec*-butyllithium > *ipr*-propyllithium > *n*-butyllithum and ethyllithium > *ter*-butyllithium.

For non-polar solvents: toluene > benzene > *n*-hexane > cyclohexane

Two initiator used in this work are *sec*-butyllithium (2°) and (3-(*ter*-Butyldimethylsilyloxy)-1-propyllithium (1°), both of these are well known to polymerize butadiene in cyclohexane to yield well-defined structures, although the latter is not suitable for room temperature polymerization of styrene in cyclohexane, since its structure is similar to *n*-butyllithium (1°).[35]

## 3.2 Controlled Radical Polymerization

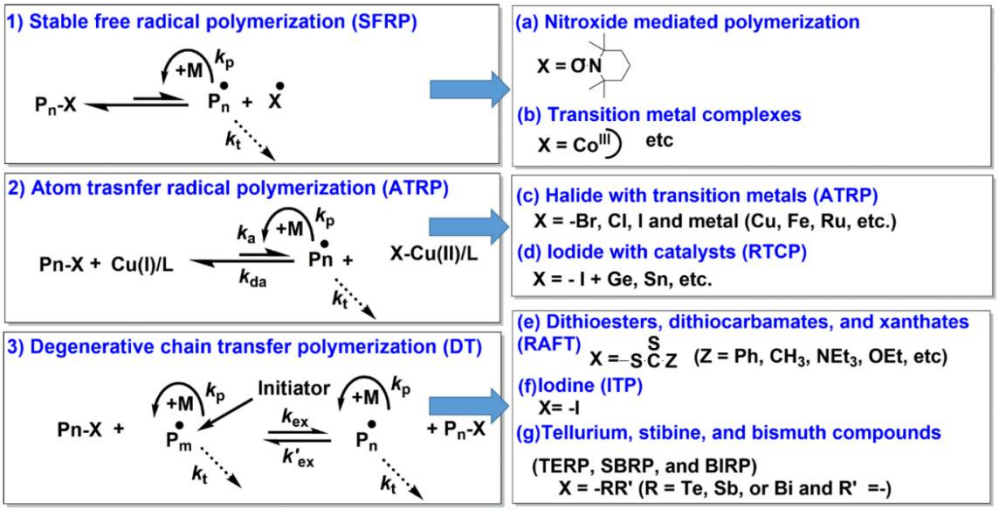
Controlled radical polymerization (CRP) methods, namely atom transfer radical polymerization (ATRP) and reversible addition fragmentation polymerization (RAFT) were also used for the synthesis of telechelic polystyrene and poly-*n*-butyl acrylate. CRP and other organic reactions were performed by using standard Schlenk flask technique using either vacuum or inert gases conditions. Three main mechanism of CRP and their examples involving different radical initiating species are shown in **Scheme 3.2**. Following section will give a short overview of free radical polymerization and controlled radical polymerization (CRP) methods in comparison with classical free radical polymerization (FRP).

FRP consists of four distinct steps: initiation, propagation, termination and chain-transfer. Under a steady state condition, the rate of initiation in FRP is similar to rate of termination, whereas the rate of propagation is $10^3$ times faster than these events. Rate of polymerization ($R_p$) is governed by the concentration of initiator $[I]_o$, and concentration of monomer [*M*], efficiency of initiation (*f*) and rate of radical initiator decomposition ($K_d$), rate of propagation ($K_p$), and termination ($K_t$) (equation 1).

$$R_p = K_p [M] (f K_d [I]_o / K_t)^{1/2} \text{.....(1)}$$

$$DP = K_p [M] (f K_d [I]_o / K_t)^{-1/2} \text{..... (2)}$$

In the FRP growing chain radicals has high reactivity and very short lifetime (~ 1 s). This leads to a significant amount of bimolecular radical coupling or disproportionation by β hydrogen abstraction. Thus, the control of molecular weight, polydispersity; and the synthesis of block-copolymers are difficult and almost impossible in all cases. On the other hand the recently developed CRP methods relies on the phenomenon of reversibly converting radicals into a state of dormancy and thereby reducing the concentration of radicals to suppress termination via coupling or transfer. A dynamic equilibrium between propagating radicals and various dormant species is achieved by using two different principles: trapping the active radical in activation/deactivation process (SFRP, and ATRP); and "regenerative transfer", degenerative exchange process such as radical addition and fragmentation transfer (RAFT) using di-thioester, iodine (ITP) and transition metal compounds ( **Scheme 3.2)**.[36-38]




**Scheme 3. 2:** Three main groups of controlled radical polymerization based on the mechanism of reversible activation: (1) stable free radical polymerization (SFRP), examples (a), and (b), (2) atom transfer radical polymerization (ATRP), examples (c) and (d), and (3) degenerative chain transfer polymerization (DT), examples e), (f) and (g).

ATRP and RAFT mechanisms are illustrated in the **Scheme 3.3**. ATRP is governed by activation/deactivation mechanism and its key components are: [transition metal halide / ligand] complex as catalyst, and α-halo compounds as initiator (generally α-halo ester or benzyl halides).[39-41] Redox system of metal-ligand complex shuffles (by transfer of an electron) between lower and higher oxidation states of metal atom such as $Cu^{I}$-X/L and $Cu^{II}$-$X_2$/L. This redox process is assisted by α-halo compounds (R-X), during which R-X undergoes homolytic cleavage of R-X bond and give alkyl radical ($R^{\cdot}$), halide ion, and metal with higher oxidation state ($Cu^{II}$)(activation step). In the initiation step, this radical ($R^{\cdot}$) adds to the vinyl group of monomer to generate new radical $P_1^{\cdot}$, which then quickly reacts with ($Cu^{II}$)-$X_2$/ L and generates dormant $P_1$-X and $Cu^{I}$ /L (deactivation step). This step is repeated with repetitive monomer addition, $P_1$-X, $P_2$-X…….to $P_n$-X. The rate of propagation is governed by the steady state equilibrium of $P_1$-X and $P_n^{\cdot}$ radicals. Since, at a given time only few $P_n^{\cdot}$ radicals are present, termination reactions are suppressed to a large extent. This allows one to prepare polymers with good control over $M_n$ and polydispersity. Since all the chains are initiated from the R-X bond of the initiator, molecular weight for an ATRP system is calculated by (weight of

monomer in grams/ moles of initiator (R-X). However, $M_n$ (theory) may differ due to initiator efficiency, and for a given ATRP system the polydispersity is given by equation 3.

$$\frac{Mw}{Mn} = 1+\left(\frac{Kp\,[Pn-X]}{Kdeact\left[X-\frac{Cu(II)}{L}\right]}\right)\left(\frac{2}{p}\right)-1 \quad \text{..... (3)}$$

Where, ($P_n$-X) = concentration of dormant species

(X-(Cu(II)/L) = concentration of deactivator

($K_p$) = rate constants of propagation

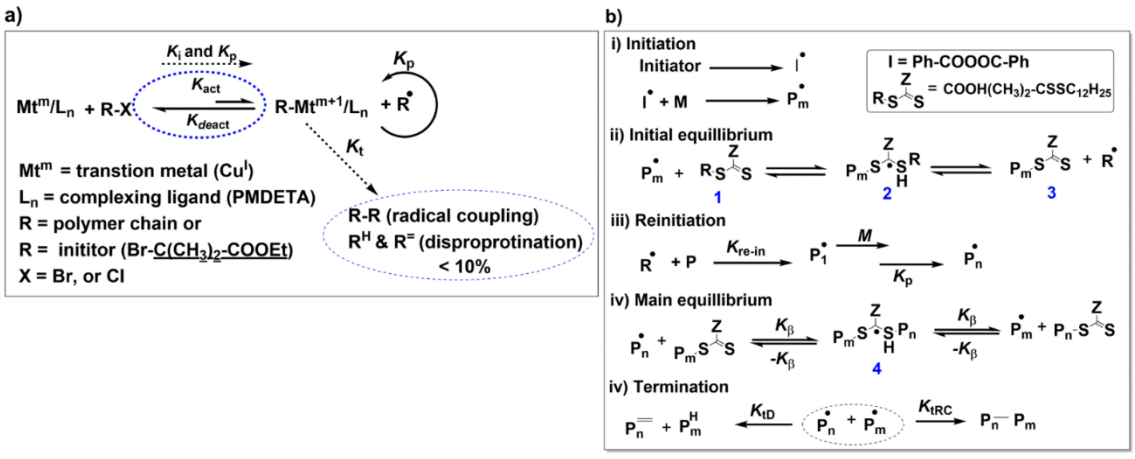
($K_{deact}$), =rate of deactivation

($p$) = monomer conversion

Therefore a combination of monomer, catalyst system, solvent, temperature has different polydispersities.

Moreover, at the end of the reaction polymer still has halo-chain end groups ($P_n$-X), which can be used as macro-initiator in the preparation of block copolymers.[42] Whereas, plurifunctional initiator $(R\text{-}X)_n$ can be used to make star-branched polymers with n-arms.[43,44] Also initiator (R-X) with R group tethered to surface allows preparation of surface grafted polymers.[45,46]

In this work telechelic poly(*n*-butyl acrylate), and polystyrene was prepared by using difunctional initiator, (diethyl-*2,5*-dibromoadipate) and catalyst complex of CuBr(I) and PMDETA.




**Scheme 3. 3:** Key components of ATRP (a) and RAFT (b)

RAFT polymerization is based on a degenerative chain transfer mechanism which is achieved by a RAFT agent, also termed as chain transfer agent (CTA).[47,48] CTA's are thioester, trithiocarbonate and xanthates with Z, and R functional groups. Functional group Z helps in stabilization of intermediate radical (**Scheme 3.3b**, (2) whereas, carbon-sulfur double bonds helps to trap the radical chain ends. Polymerization is initiated by photolysis and thermal imitators such as azobisisobutyronitrile (AIBN), and benzoyl peroxide (BPO). Growing polymer chain ends reacts with CTA, to generate new radical. This radical then adds monomer and also undergoes reversible addition fragmentation steps with another CTA-adduct. Since the fragmentation is largely controlled by the CTA, at a given time very few growing radicals are present which allow control over molecular weight and molecular weight distributions. ATRP reactions can be carried out at room temperature since it relies on redox mechanism which can occur at room temperature. RAFT generally employs thermal initiator, thereby requires much higher reaction temperature (>70 °C). Polymer chain ends are functionalized by CTA groups, therefore similar to ATRP it is also used in the preparation of block copolymers and star-branched polymers.[49]

In this work, RAFT was used in the unsuccessful synthesis of PBd-*b*-$(HEA_{(UPy)})_n$ (n is 4-6).Hydroxyl terminated PBd-OH was converted into macro-CTA (by esterification with *S*-1-dodecyl-*S*′-(α,α′-dimethyl-α″-acetic acid)trithiocarbonate (DDMAT) and used in the polymerization of HEA-UPy monomer. HEA-UPy was prepared by isocyanate coupling of HEA and UPy-synthon. More about the UPy-synthon will be discussed in **Chapter 3**.

## 3.3 Experimental

Anionic polymerization can be carried out under inert atmosphere in Schlenk tubes, in glove-box, and in pressurized stainless steel reactors, but it cannot match with the perfection offered by the high vacuum break-seal techniques.[50,51] Importance of the high vacuum technique is underlined by the synthesis of variety of model macromolecules having a high degree of structural, compositional and molecular weight homogeneity needed to elucidate structure-property relationships, which are critical for the understanding of industrially important polymeric materials.[52,53] In spite of the fact that it is laborious, time-consuming and results in limited quantity of polymers, it has a tremendous potential for designing well-defined architectures needed for specific application. Various types of microstructure can be achieved

by the polymerization of styrenic acrylic, and dienic monomers in a well-controlled manner using high-vacuum techniques.[52,54,55]

In this work, low molecular weight, ω-hydroxyl functional, and α, ω- dihydroxyl functional polybutadienes are synthesized by anionic polymerization of butadiene followed by end capping with ethylene oxide.

### 3.3.1. Typical Schlenk Technique for ATRP and RAFT

In a typical ATRP or RAFT procedure, purified reagents; monomer, solvent, initiator and catalyst/ligand or chain transfer agent were added to a modified Schlenk reactor (**Figure 3.1**). Subsequently polymerization mixture was carefully degassed by three FPT cycles using high-vacuum line. Flask was allowed to cool to room temperature and kept in the preheated oil bath. After desired conversion was achieved, polymerization was quenched by cooling the flask with liquid nitrogen. Polymer was isolated by precipitation in four-time excess non-solvent. Polymer prepared by ATRP contains small amount of Cu/L complex, which was removed by passing the dilute polymer solution through a neutral alumina column.

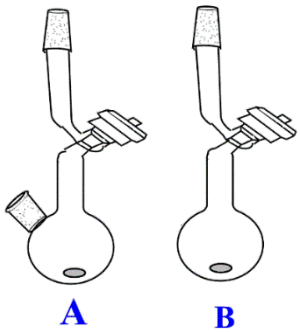



**Figure 3. 1:** Schlenk reactor with ground glass joint for attaching to high-vacuum line and with the Young's Teflon stopcocks (B), and flask with additional joint for septum.

## 3.4. High Vacuum Techniques for Anionic Polymerization

Polybutadiene synthesized in this work and polymer chain end modification reactions were performed using high vacuum techniques combined with the construction of custom made glass reactors. (Inert reaction conditions of nitrogen or argon was used wherever applicable.) The vacuum line consists of manifold made up of two parallel glass tubes connected periodically with Teflon stopcocks (Young). The upper rig is connected to a vacuum source

obtained by a combination of two pumps, a Silicone oil diffusion pump and mechanical oil pump, operated in series. The lower rig of the manifold provides ground glass joints for attachment of the solvent reservoirs and glass reactors. A vacuum trap was cooled by liquid nitrogen to prevent organic solvents from entering the silicone oil diffusion pump and eventually the mechanical oil vacuum pump. The mechanical oil pump used was a Welch model #1402W-01 duo seal pump. To maintain high vacuum in the manifold it is recommended to use liquid nitrogen for cooling trap. Silicone oil is susceptible to degradation by oxidation with air and reacts to organic vapors at high temperature. Therefore, the mechanical pump oil was changed once every three months. J. Young Teflon stopcocks, in particular in-line tap type stopcock with a Teflon piston and O-ring seals have been employed for the operation of manifold.

A representative drawing of the vacuum line is shown in **Figure 3.2**. Glass apparatus was attached to the line using matching ground glass joints greased with Dow Corning high vacuum grease. A Tesla coil was used to perform a leak or pinhole test. The test involves taking a powered Tesla coil close to the surface of vacuum line and hearing the difference in the high frequency noise of the coil. The absence of discharge (louder noise) indicates attainment of the high vacuum ($<10^{-5}$ Torr) inside the line. The vacuum line operation involves the following steps. The mechanical oil pump was started while the silicon pump is isolated from the vacuum line by closing all the three stopcocks (# 1, 2, and 3, **Figure 3.1**). Subsequently, liquid nitrogen was filled in the vacuum trap condenser Dewar and stopcock #1 opened and the manifold is flame dried under vacuum. After half an hour, stopcocks #2, # 3 are opened and one is closed (# 1 is three way connector and by closing it connects manifold via diffusion pump). This allows both pumps to operate in a series, and a high vacuum is achieved by heating the silicone oil until it refluxes inside the pump body.

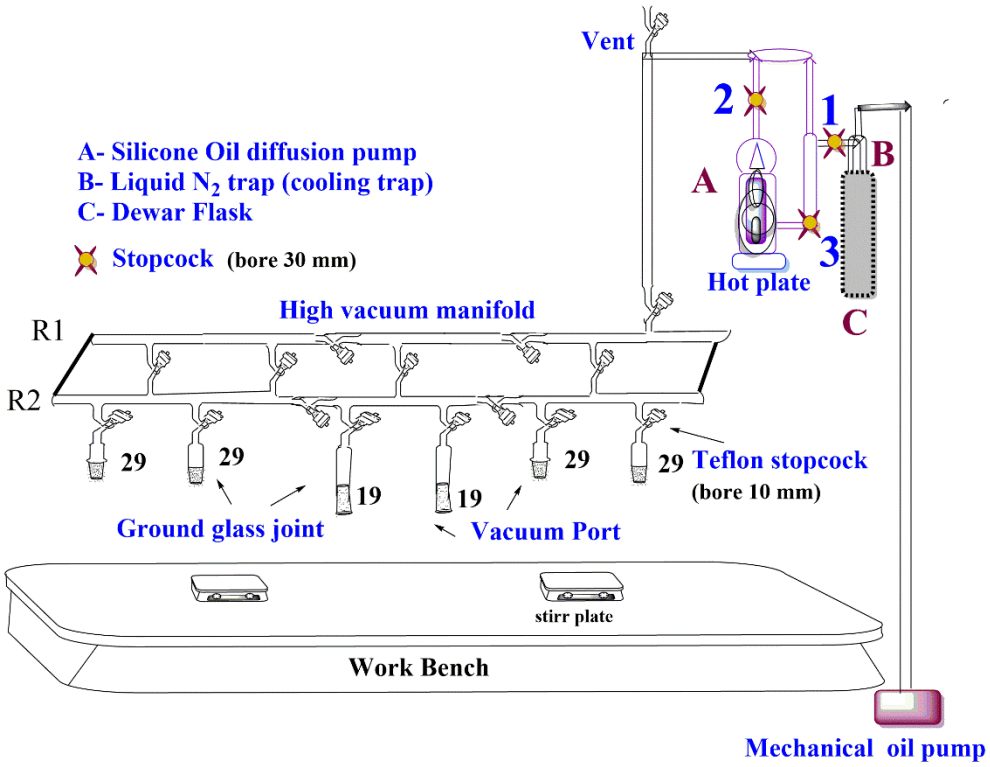



**Figure 3. 2:** High vacuum line set up

## 3.5 Apparatus

Anionic polymerization was performed using custom-made glass reactors using glass constrictions and break-seals (**Figure 3.3**).[50,51] All the glass reactors was subjected to annealing in a furnace at 535 °C to release stresses created by glass blowing. The glass constriction is used to cut/seal a portion of the reactor with flame under vacuum. Break-seals are useful due to the fact that they allow storage of reagents in pure form and facilitate addition of reagents into the reactor without exposing them to contaminants.

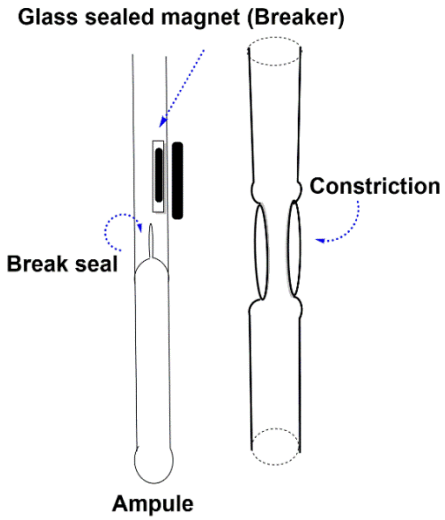



**Figure 3. 3:** Break-seal and glass constriction

## 3.6 Purification of Solvents

### 3.6.1 Benzene

Two separate methods were employed for the purification of benzene depending on the grade of commercial benzene. When a reagent grade benzene was used, it was allowed to stir over the concentrated sulfuric acid for a period of at least one week. This step removes trace amounts of alkylated benzene derivatives such as toluene and heteroaromatics like thiophenes. The benzene was subsequently decanted into a separatory funnel, and washed with deionized water until neutral pH, dried over calcium chloride, and was stirred over calcium hydride for 12 h in a round bottom flask (RBF). The benzene was directly distilled into a calibrated cylinder (14 mm =100 mL) with the help of liquid nitrogen cooling as shown in **Figure 3.4.** To this cylinder small amount styrene (~0.1 ml) (Sigma Aldrich, unpurified) and 10 ml of 2.5 M *n*-butyllithium in hexanes were added (Sigma Aldrich) to purify the solvent under the flux of $N_2$. Then the cylinder was quickly attached to the vacuum line and degassed thoroughly by using three freeze-pump thaw cycles.

In the second method, anhydrous grade benzene (99.9 % purity) was directly taken in the calibrated cylinder and purified as described above. During degassing, warming the benzene solution (~45 °C) with heat gun helps accelerate the reaction of *n*-butyllithium with dissolved gases and protic impurities. The heating also accelerates the formation of yellow-orange colored polystyryllithium. After further degassing a persistent orange color develops

and its intensity may change to dark orange-red over a period of time. The persistence of yellow-orange color indicates the benzene is satisfactorily pure for anionic polymerization. The benzene over polystyryllithium was stirred for at least three days before used in the polymerization to make sure all the styrene has reacted. The use of anhydrous benzene without the treatment of concentrated sulfuric acid appears to cause no significant issues with the anionic polymerization, as long as a sufficient amount of *n*-butyllithium is present in the solvent reservoir.

### 3.6.2 Hexanes

Reagent grade hexane was obtained from Fisher Scientific and was purified in a manner similar to benzene without treatment with sulfuric acid. A few drops of styrene and 10 mL of *n*-butyllithium (2.5 *M*) were used to generate yellow-pale to light-orange color of polystyryllithium.

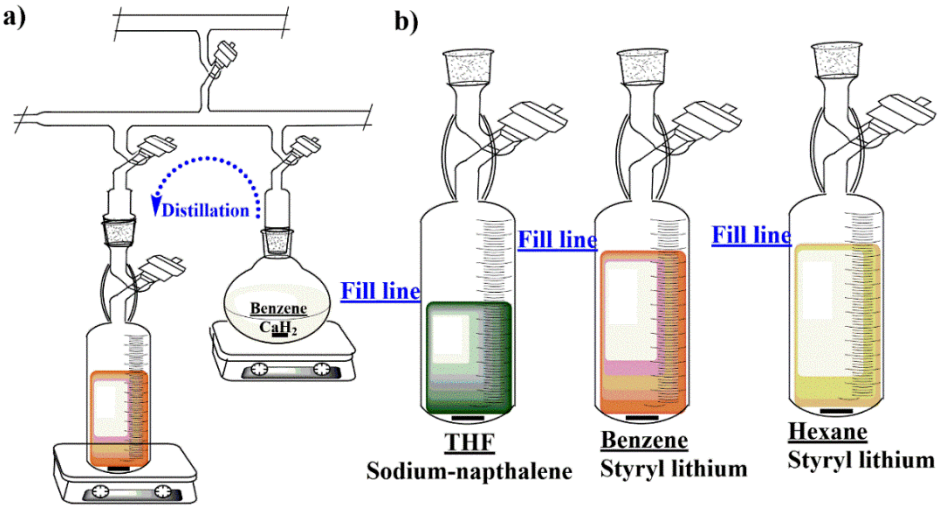



**Figure 3. 4:** Purification of benzene for anionic polymerization (a), removable solvent reservoir with stopcock and color indication for pure solvents with recommended solvent fill line to prevent bumping of solvent onto stopcock (b) (necessary for THF)

### 3.6.3 Tetrahydrofuran

Purification of THF was done by two different types of purification agents. In the first method, THF was initially refluxed over sodium metal and distilled into a flask containing $CaH_2$. The

THF degassed three times and allowed to stir overnight (**Figure 3.4**). Subsequently, the THF was distilled to a solvent storage cylinder-reservoir that contains sodium-potassium (NaK) alloy. The alloy is liquid at room temperature and it is made from 1:3 mixture of sodium and potassium as given below. Sodium and potassium metals were cleaned from oil by using dry hexane to prevent oxidation of the metal. (Caution: hexane must be dry prior to this operation or first clean sodium metal in hexane and then use same hexane for cleaning of potassium metal). The metal oxides are scraped off the metals using forceps and a knife and then cut into small pieces. Clean metals are transferred quickly into the cylinder-reservoir and vacuum was applied immediately. Glass covered magnets stir bars was used for stirring. Then, the cylinder-reservoir was slowly heated by a mild blue flame using a glass blowing torch, until the sodium starts to melt under vacuum. Once the sodium begins to melt the magnet is used to mix the potassium and sodium to form the alloy. The alloy was cooled to room-temperature and the THF was then distilled over calcium hydride into the cylinder-reservoir over NaK. The distilled THF was degassed by three freeze-thaw cycle, and was allowed to stir until a blue color (solvated electrons of metal-ether coordination) was observed.

During degassing cycle's glass encased magnet must be moved above the THF solution level, to avoid possible cracking and breaking. In second method, THF was distilled over calcium hydride into cylinder-reservoir containing pieces of sodium and naphthalene (1:0.8) and stirred under vacuum at room temperature until green color of sodium naphthalide was formed. THF purified by this way is sufficiently pure enough for the chain end modification reactions. However, use of NaK alloy method is recommended when THF is used as solvent for the anionic polymerization. **Figure 3.4 (b)** shows desired color for the dry solvents and recommended filling capacity of the reservoir for individual solvents.

### 3.6.4 Methanol

Reagent grade methanol was obtained from Fisher Scientific and stirred over calcium hydride. It was thoroughly degassed by three freeze-pump-thaw cycles using the vacuum line, and ~ 2 mL of methanol was then distilled into several uncalibrated ampule.

## 3.7 Purification of monomers

### 3.7.1 Butadiene

1,3-Butadiene (Bd) is a gas at room temperature. Extreme caution is required while purifying this monomer. The Bd monomer is supplied in a gas cylinder by Sigma Aldrich. Bd monomer

was purified twice by treating it with *n*-butyllithium and distilled using a short path distillation set up as shown in **Figure 3.5**. To both the flame dried 500 mL RBF-A and RBF-B, ~ 3 mL of *n*-BuLi (2.5 M) was added through a rubber septum under vacuum. After sealing the constriction, the residual hexane was pumped off. Then, Bd gas was allowed to condense into a RBF-A (~ 200 mL) by slowly opening the gas regulator and cooling the flask with a dry ice/acetone bath (-78 °C).

After condensing required amount of Bd, the flask was kept at -78 °C, and allowed to stir for half an hour. Although the polymerization of Bd with *n*-BuLi is very slow at -78 °C, the overall operation does oligomerize ~ 5-10 g of monomer. Therefore an excess (15-20 mL) excess Bd over the required amount should be condensed for purification. Then, the dry ice/acetone bath was removed and replaced with an ice/salt ($CaCl_2$) bath to maintain temperature -10 °C. (Bd boil at -4.5 °C, therefore, bath temperature should be maintained ~ -10 °C) The flask-B was then cooled with dry ice/acetone bath, and Bd was distilled from the flask-A into the flask-B. Bd was stirred for half an hour at ice/salt bath and distilled into flame dried ampule (C) by cooling with dry ice/acetone bath. After distilling 80 mL Bd (0.74 g/mL at -78 °C), the cooling bath was replaced with a liquid nitrogen bath and ~200 mL of benzene was distilled in through the vacuum manifold. The diluted Bd ampule was flame cut from the line and stored at -30 °C. It is recommended to use dilution with double amount of solvent is preferred, though 1.5 times of benzene may also work. The dilution with benzene sufficiently lowers the vapor pressure of the butadiene which allows the break seals to maintain their integrity at room temperature.

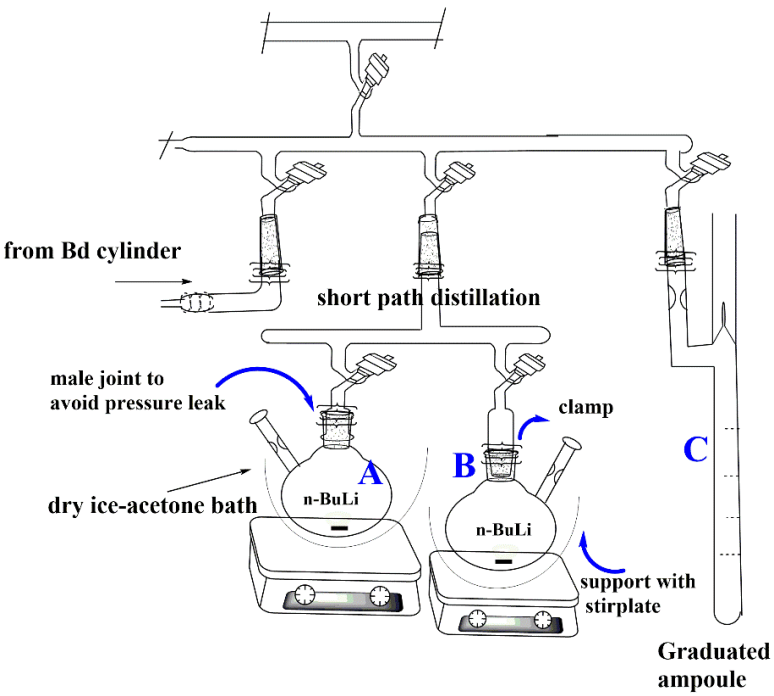



**Figure 3. 5:** Apparatus for the distillation of butadiene

### 3.7.2 Styrene

Reagent grade styrene (boiling point 145 °C) was obtained from Sigma Aldrich and subjected to a two-step purification process. The styrene was purified by using a short path distillation apparatus similar to the Bd purification; except that the single ampule was replaced with an apparatus containing multiple calibrated ampules (**Figure 3.5**). In the first step, the styrene was passed through a neutral alumina column and then stirred over calcium hydride in the flask-A (no constriction required). The system was degassed by three freeze-pump-thaw cycles. It is advised to pass the monomer from the column if the viscosity of the monomer indicates that it contains substantial amount of polystyrene. Meanwhile to the flask-B ~ 4 mL of dibutyl magnesium (1.0 M in heptanes, Sigma-Aldrich) was added through a rubber septum under vacuum and hexane was distilled off before sealing the constriction. A thick wall tubing is used instead of the constriction to the ampule. Then the styrene was distilled from flask-A to flask-B by cooling with liquid nitrogen. The solution of styrene over dibutyl magnesium generates a very faint yellow color; this solution was allowed to stir for one hour. Meanwhile flask-A was replaced with an apparatus containing multiple ampules (**Figure 3.6**).

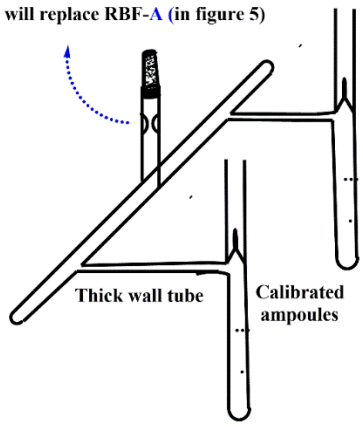



**Figure 3. 6:** Ampules for distillation of styrene

After flame drying the ampules under vacuum, the required amount of styrene was distilled at room temperature into the calibrated ampules by using liquid nitrogen bath and degassed before heat sealing the heavy wall tubing (10 mm diameter). The ampules were stored in the freezer (-30 °C) and used within two months because the highly pure styrene can undergo spontaneous polymerization in the ampule.

### 3.7.3 Ethylene oxide

Ethylene oxide (boiling point 10.7 °C) is gas and is supplied in a cylinder by Aldrich. It was purified in a similar manner to the butadiene monomer. However, similar to styrene multiple ampule were used. No solvent dilution is required. The purified monomer was stored in a freezer at -30 °C.

## 3.8 Ampulization of initiator solution

Two different kinds of alkyl lithium initiators were used in this work. For ω- hydroxyl functionalized polymer synthesis *sec*-butyl lithium was used. A hydroxyl protected propyl lithium initiator (3-(*ter*-butyldimethylsilyloxy)-1-propyllithium) was used for the synthesis of α, ω- dihydroxyl functionalized polybutadiene. Commercial products of these initiators were diluted and ampulized by using the split-down apparatus (**Figure 3.7**) to make the desired and workable final initiator concentrations. In the first step ~ 50 mL of the initiator was added to the flask-A through the septum under $N_2$ and subsequently degassed under vacuum. The constriction was rinsed and flame sealed. A ~ 50 mL of dry hexane was distilled in through the vacuum manifold. The initiator solution was thoroughly degassed by three freeze-pump-thaw cycles.

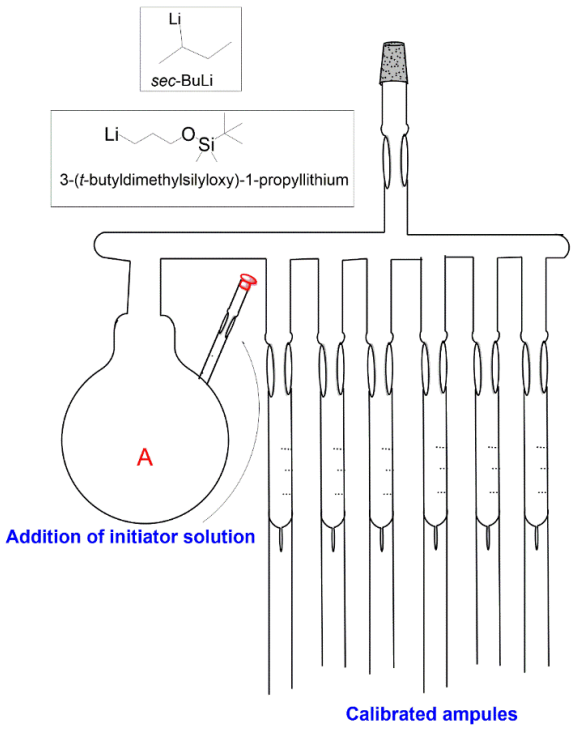



**Figure 3. 7:** Split-down apparatus for the dilution of initiator (structures of *sec*-butyllithium and 3-(*ter*-butyldimethylsilyloxy)-1-propyllithium are shown in the inset)

*Sec*-butyllithium solution (1.4 M Sigma-Aldrich) has a tendency to develop haziness due to the presence of hydrides and oxides. Although it does not affect the course of the polymerization, the presence of such impurities may have a dramatic effect, especially, on the chlorosilane coupling reaction commonly used in the synthesis of complex macromolecular architecture. In addition, these impurities can alter the microstructure of polydienes. Therefore, prior to ampulizing the initiators, they were first filtered through a membrane filter (0.45 μm pore size) while adding to the flask-A. It is advised to filter the solution to reduce the effects of these impurities in the polymerization. 3-(*ter*-butyldimethylsilyloxy)-1-propyllithium was also ampulized by following a similar procedure. The concentration of the initiator solution was calculated by polymerizing a known amount of styrene under high-vacuum break seal conditions and using the following relationship: molarity of initiator = weight in grams of polystyrene/ (SEC $M_n$ of polystyrene x mL of initiator for the polymerization)

## 3.9 Polymerizations

The procedure described herein using the custom made glass apparatus is applicable to the polymerization of styrene, butadiene, and isoprene in nonpolar solvents. For the polymerization in THF medium, tubular type reactors are preferred. The basic reactor for polymerization in benzene is depicted in **Figure 3.8**. Glass reactor was assembled with required numbers of reagent ampules. Initiator, monomer and terminating agent ampules were attached with the glass concealed magnet to the reactor on the day of the polymerization to avoid degradation of the initiator and monomer. Once the reactor was completely assembled, it was connected to the vacuum line and thoroughly flame dried and checked for any pinholes. The reactor was then charged with *n*-BuLi as a purging agent. Constriction-1 was rinsed with hexanes using liquid nitrogen wet towel and flame sealed. The flask was cooled with liquid nitrogen and pure benzene was then distilled into the apparatus. The required amount of benzene was distilled in to make the final concentration of the monomer to ~ 15 % (*w/v*) solutions. This concentration works well for polymers with MW's lower than 10,000 g/mol. For the polymerization with $M_n$ greater than 50,000 g/mol, especially for the butadiene, < 10 % weight solution is used to avoid high viscosity of the polymerization solution.

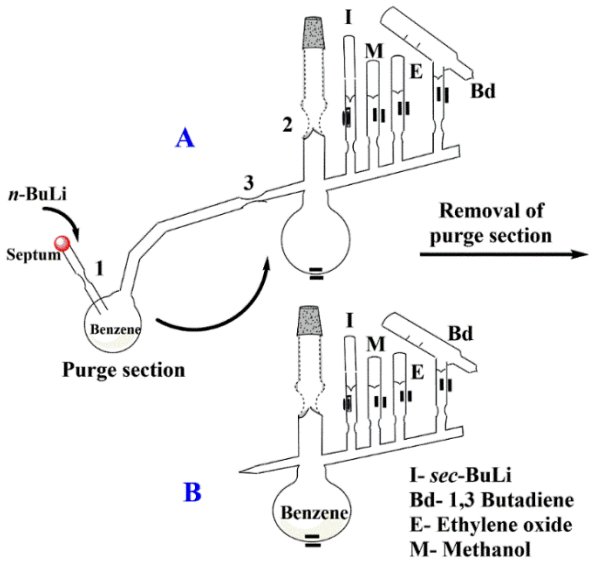



**Figure 3. 8:** Polymerization reactor (A) with purge section and (B) after detaching from the vacuum line and distilling pure benzene from purge section.

After the required amount of benzene was distilled to the purge section from the storage reservoir, the solvent was frozen completely with liquid nitrogen and degassed carefully, and detached from the vacuum line at constriction-2 using heat sealing (**Figure 3.8)**. The solution of *n*-butyllithium and benzene was allowed to thaw in a warm water bath. The entire reactor was washed with the solution. The glass breakers were moved carefully at this point to ensure that the glass between the breakers and the wall of the reactor is also cleaned. After rinsing the reactor, *n*-BuLi containing benzene was collected back into the purge section. The purge section was then submerged in a warm water bath (~50 °C) and the reactor was washed with pure benzene via condensation produced by wrapping wet liquid $N_2$ towel at the outside of the reactor. This step ensures that all of the *n*-BuLi is recovered in the purge section. Any excess *n*-BuLi can also take part in the polymerization, and since it reacts slower than *sec*-BuLi the polydispersities of the polymer being synthesized will be altered. It will also affect targeted molecular weight. Therefore, washing should be performed thoroughly. During the washing process, the solvent collected in the main reactor flask is periodically transferred back to the purge section, this is usually done every 2 to 3 wash cycles. The entire apparatus was washed a total of ten times with the towel dipped in liquid nitrogen (takes ~2h). After the last wash the purge section was cooled with liquid nitrogen to ensure that all of the solution was condensed back to the purge section. The main reactor flask was then cooled with liquid nitrogen and the solution in purge section was maintained at warm water (~45 °C). Room temperature water could be used if the solution bumps into the cleaned reactor. If this occurs the reactor must again undergo the washing step listed previously. Teflon coated or a glass encased magnet can avoid bumping and facilitate the distillation, but this step is optional.

Once the distillation was completed the constriction-3 was flame sealed between the reactor and the purge section leaving a pristine reactor B in which the anionic polymerization can conducted. At this point, the heat seal constriction and frozen benzene were allowed to come to room temperature and then the initiator break seal was broken. The initiator solution was thoroughly mixed with benzene (in the case of styrene polymerization one can add monomer first and it can act as indicator if any residual *n*-butyllithium is left). Subsequently, the monomer break seal was broken and a thorough mixing of the initiator, benzene, and monomer was done by stirring. When using butadiene it is necessary to cool (~5 °C) the benzene as well as Bd ampule with cotton strips dipped in liquid nitrogen before adding the

monomer. The vapor pressure inside this ampule is high, which can force the breaker into the constriction above the ampule causing the glass to crack or break the entire reactor. Cooling the ampule before opening break-seal prevents a large difference in pressures and ensures a much gentler addition of the monomer to the vessel.

The presence of a constriction before the ampules not only enhance the washing procedure (constriction enhance reflux of solvent) but also helps to protect slipping of the breaker into the main reactor. At this point the monomer, the initiator and solvent all stay in the main reactor. After the addition of Bd, the reactor was either manually agitated for a few minutes or kept under stirring with a magnetic stir bar. The reactor was covered with the aluminum foil and left overnight to allow the polymerization to occur. After the polymerization was completed the polymer was end capped with ethylene oxide and terminated with methanol. The polymer terminated was isolated by precipitation into acidic methanol (0.1 M HCl), usually five times the volume of the polymer solution. The methanol is pretreated with a small amount of antioxidant (0.1 %), butylated hydroxyl toluene (BHT). Solvent was decanted and viscous polymer was dried in vacuum at 50 °C. Dried PBd still contains residual methanol which can be removed prior to chain end modification reactions by heating the flask containing PBd at 70-80 °C for 2 h.

The purge section serves the purpose of cleaning protic impurities on the glass surface. Since large amounts of Bd were polymerized in this work, the reaction was conducted in a reactor without the purge section. Use of slight excess of initiator solution (~5 mol %) and baking of the reactor under vacuum line for a longer duration gave the produced polymer with target molecular weight. If purge section is excluded, it is necessary to anneal reactor every time to make sure there are no unwanted impurities on the glass surface (it also burns any polymeric or organic residue on the glass surface).

## 3.10 Polymer Characterization Methods

For the verification of the synthesis of chain end functional polymers and to analyze the effect of chain end groups on the association behavior of the supramolecular polymers, both solution and solid state methods of characterization were employed. In this section, the necessary background behind a some of characterization techniques among size-exclusion chromatography (SEC), static light scattering (SLS), dynamic light scattering (DLS), and atomic force microscopy (AFM), thermal gravimetric analysis (TGA), differential scanning

calorimetry (DSC), viscometry, nuclear magnetic resonance spectroscopy (NMR) and, fourier transform infrared (FTIR)- attenuated total reflectance spectroscopy are discussed. Rheology and dielectric resonance spectroscopy will be described in chapter 5.

## 3.11 Dilute solution viscometry

Solution viscosity is one the most commonly used frictional properties of dilute polymer solutions. Viscosity of the dilute polymer solution is considerably higher than that of the pure solvent as well as dilute solution of low molecular weight compounds. Measurement of the viscosity of dilute solutions provides information regarding polymer chain dimensions, molecular shape, molecular weight, and polymer-solvent interactions. **Table 3.1** gives the common terms used in the dilute solution viscosity. The specific viscosity determines the contribution of the solute to the viscosity of the solution. The reduced viscosity provides a measurement of the polymer's capacity for increasing the solution viscosity. This viscosity intensifying effect is characterized by intrinsic viscosity and it is important for polymer characterization and it relates the intrinsic ability of the polymer to increase the viscosity of a particular solvent at a given temperature. For measurements of intrinsic viscosity two factors are necessary, no chain entanglement and all the polymer coils are well solvated.

**Table 3. 1:** Common terms used in definition of viscosity[56,57]

| Common name | Symbol and definition[a] |
|---|---|
| Relative viscosity | $\eta_r = \eta/\eta_0$ |
| Specific viscosity | $\eta_{sp} = \eta_r - 1$ |
| Reduced viscosity | $\eta_{red} = \eta_{sp}/c$ |
| Inherent viscosity | $\eta_{inh} = \eta_{rel}/c$ |
| Intrinsic viscosity | $[\eta] = \lim_{c \to 0} (\eta)_{red}$ |
| [a]$\eta_0$ is the viscosity of the pure solvent and $\eta$ is the viscosity of a polymer solution of concentration (g/dL). | |

Several mathematical equations are available in the literature for determining the intrinsic viscosity $[\eta]$ of a polymer solution. Most of these equations use graphical

extrapolation, for example, Huggins equation, Kraemer equation, Martin equation, Schulz-Blaschke equation, as shown in (**Table 3.2**).

Specific viscosity ($\eta_{sp}$) of a solution of concentration $c$ is related to intrinsic viscosity $[\eta]$ by a power series of $[\eta]$c.[58]

$\eta_{sp} = k_0[\eta]c + k1[\eta]^2c^2 + k_2[\eta]^3c^{3+} k_3[\eta]^4c^4 + \ldots$ ……(4)

Where, $k_0$, $k_1$, $k_2\ldots$ are dimensionless constant, and $k_0 = 1$

Dividing equation (4) by concentration, for dilute solutions equation 3can be reduced only to the second term, it results in well-known form of the Huggins equation (5).

$\eta_{sp}/c = [\eta] + k_H[\eta]^2c$ ……(5)

Huggins equation is valid for $[\eta]c << 1$.The constant $k_H$ is termed the Huggins constant and it is essentially independent of molar mass and its value fall in the range 0.3 (in good solvents) to 0.5 (in poor solvents).[56] It contains information about hydrodynamic and thermodynamic interactions between coils in solution. A plot of the reduced viscosity, extrapolated to zero concentration yields the intrinsic viscosity. From the slope and intercept value of $k_H$ is obtained.

**Table 3. 2** Common equations used for determination of intrinsic viscosity [η][59]

| | |
|---|---|
| Huggins | $\eta_{sp}/c = [\eta] + k_H[\eta]^2 c$ |
| Kraemer | 1. $\ln \eta_r/c = [\eta] - k''[\eta]^2c$ |
| Martin | $\ln \eta_{sp}/c = \ln [\eta]_m + k_m[\eta]_m c$ |
| Schulz-Blaschke | $\eta_{sp}/c = [\eta]_{sb} + k_{sb}[\eta_{sb}]\eta_{sp}$ |

Intrinsic viscosity can also be obtained by linear plot of $(\ln \eta_{rel})/c$ versus polymer concentration, described by the Kraemer equation (6).

$(\ln \eta_{rel})/c = [\eta] + k''[\eta]^2c$……(6)

$k''$ = Kraemer constant, is generally negative, often around –0.152

$k' - k'' = 0.5$

Concentration of dilute polymer solution should be such that it gives values of $\eta_r$ in the range of 1.2 to 1.8. As lower concentration may impose measurement difficulty and at higher

concentration linearity of the plots are lost. For example, differences of less than 20 % between solvent and solution are difficult to measure, and differences greater than 80 % may lead to curvature.

### 3.12 Mark-Houwink-Sakurada Equation

The Mark-Houwink equation (7) describes the relationship between intrinsic viscosity and the viscosity-average molecular weight of a polymer.[56] The value of the exponent "a" is related to polymer/solvent interactions and polymer stiffness. For Gaussian coils, "a" varies between 0.5 for a theta solvent and 0.8 for a good solvent. Stiff molecules exhibit higher "a" values with a theoretical value of 2 for completely rigid rods. A theta solvent is a solvent in which the free energies of solvent-solvent interactions, solvent-polymer interactions, and polymer-polymer interactions are same. The values of $K$ are typically in the range of $10^{-3}$-$10^{-1}$ $cm^3g^{-1}$ and for flexible polymer chains the values decrease with increase in values of "a".

In this work $K$ = 0.00039dL/g, and "a" = 0.713 values are used for the PBd to compare the value of intrinsic viscosity.[60]

$[\eta] = KM_v^a$ ..... (7)

### 3.13 Measurement of solution viscosity

Absolute measurement of viscosity is not needed in dilute solution viscometry rather viscosity of the polymer solution relative to that of pure solvent is measured.

Viscosity of solution is given by using Poiseuille's equation and its simplified form is given as, $\eta = A\rho t$

Where $A$ is a constant for a given viscometer, $\rho$ is the density and $t$ is flow time.

So, relative viscosity is given as,

$\eta_r = \eta_s/\eta_0 = \rho_s t_s/\rho_0 t_o$

Where, $\eta_s$ and $\eta_0$ are the viscosities, $\rho_s$ and $\rho_0$ are the densities, $t_s$ and $t_o$ are the flow times of a polymer solution of concentration $c$ and of the pure solvent, respectively.

In practice densities of dilute polymer solution and solvent are considerably equal therefore, in order to calculate the relative viscosity flow times of the polymer solution and solvent are calculated by using a viscometer and timer.

Relative viscosity was calculated by using a modified Ubbelholde viscometer with a larger reservoir bulb for dilution using a Schott Instruments viscometer. The viscometer is

automated for recording the flow time and it also does required periodic dilutions. Relative viscosity was calculated by ratio of flow time of polymer solution and pure solvent (toluene or chloroform) at 25 °C and then related to other terms by concentration. Plots of reduced viscosity ($\eta_{sp}/c$) versus concentration ($c$) were used to calculate intrinsic viscosity by extrapolation to zero concentration and Huggins parameters were obtained from slope and intercept. These values were used to characterize the effect of non-covalent interactions on the polymer association behavior.

### 3.14 Size Exclusion Chromatography

Size Exclusion Chromatography (SEC) (also referred to as Gel Permeation Chromatography (GPC) when organic solvents are used as mobile phase, though preferred nomenclature is SEC) is a prime tool for the characterization of the polymer number average molecular weight ($\overline{Mn}$) and polydispersity index ($\overline{Mw}/\overline{Mn}$). In SEC a dilute polymer solution is injected in the mobile phase which then passes through a column packed with beads of porous gel. In this work three different SEC configurations were used for the polymer characterization. SEC employs the use of a high performance liquid chromatography pump and SEC columns usually packed with a stationary phase made up of porous crosslinked polystyrene beads. These beads are the fundamental source of the separation of polymers by hydrodynamic volume. The separation is based on the virtual size of the macromolecules and not the chemical affinity to the substrate.[59]

Generally sample concentration of 1 mg/mL and injection volume of 100-200 μL are used. After injection of the polymer solution larger MW polymer chains avoid entering into the small porous material, therefore the larger chains move faster and are eluted in shorter time whereas, smaller MW chains diffuse through small porous beads, their movement is slowed by the cross linked polystyrene; therefore smaller molecules take longer time to elute. The eluent used in all the experiments was THF. In certain cases THF with 5 % triethylamine (TEA) was added to break down the aggregation of polymer chain end groups and prevent adsorption of material to the columns. (This is particularly useful for polymers containing polar and reactive functional groups like amines such as polyvinylpyridine, and carboxylic acid such as polymethacrylates, polyacrylates etc.) The first SEC system used in this work consisted of two SEC columns from Polymer Standard Service (PSS); a linear S 5 μ 8 x 600 mm column and a SDV 100 Å 8 x 600 mm, both kept at ambient temperature. Columns were attached to a Knauer K-501 HPLC pump and two detectors a Knauer K-2301 differential refractive index (DRI)

detector and a Knauer K-2501 variable ultra violet (UV) detector set at a wavelength of 255 nm. Since in this SEC the columns are without thermostat small amount of toluene was used as flow marker. The second SEC instrument used was a Polymer Laboratories (PL) GPC-120 equipped with four columns: Polymer Laboratories PLgel; 7.5 x 300 mm; 10 μm; 500, $10^3$, $10^5$, and $10^6$ Å. The GPC-120 is equipped with a Precision Detector PD2040 (two angle static light scattering, 15° and 90°), Precision Detector PD2000DLS (dynamic light scattering), Viscotek 220 differential viscometer, and a Polymer Labs refractometer. Pre-filtered HPLC grade THF from Fisher Scientific was used as the mobile phase. Both of these SEC units operated with flow rates of 1.0 mL/min. A third SEC unit used in this study was a Tosoh EcoSEC which has a 100 sample capacity auto-sampler. It consists of the three columns, two Tosoh TSK gel Super Multipore HZ-M; 4.6 x 150 mm; 4 μm; and one TSKgel SuperMultiporeHZ-M guard. It operates at flow rates of 0.35 ml/min. Both the GPC120 and EcoSEC measurements were performed at 40 °C. All the SEC units were calibrated over the MW range of 600 to 7,500,000 g/mol using either PS or PMMA standards. All the samples were pre-filtered (0.45 μm) before injecting onto the column.

### 3.15 Dynamic Light Scattering

Interaction of electromagnetic radiation with a nonabsorbing, nonionizing material induces an oscillating dipole of the same frequency in the material. This accelerating dipole then radiates (scatters) energy of the same frequency in all directions.[61,62] This scattered light forms the basis of light scattering techniques widely used for the analysis of dilute solution polymer properties such as static light scattering (SLS) and dynamic light scattering (DLS). In SLS scattered intensity from scattering particles or macromolecules are measured as a function of various angles and concentrations. Angular variation of scattered intensity gives information about the molecular weight, size, and shape of the scattering macromolecular particles. Concentration dependence of light scattering gives the second virial coefficient, which determines the strength of attractive and repulsive forces between solute particles and the solvent.

In DLS relatively slow fluctuations in the intensity of the scattered light caused by the Brownian motion of the scattering particles are measured.[63] Intensity fluctuation and spectral distribution may be used to determine dynamical properties of macromolecules such as translational and rotational diffusion coefficients and intramolecular relaxation times may be obtained. In general scattered light is detected at a single angle (most commonly at 95°) and

analyzed with an autocorrelator to generate a normalized first-order autocorrelation function $g^{(1)}\tau$. For monodisperse spherical particles with size smaller than the wavelength of the incident beam, the autocorrelation function is given by following equation (8), and it is calculated by fitting the autocorrelation curve to an exponential function with D being proportional to the lifetime of the exponential decay.

$$g^{(1)}\tau = \exp(-Dq^2\tau) \quad \ldots\ldots\ldots\ldots (8)$$

Where: $\tau$ is the decay time,

$(q = (4\pi n/\lambda_0)(\sin(\theta/2))$ is the scattering vector,

$n$ is refractive index of the medium

$\lambda$ is the wavelength of incident light

$\theta$ is the scattering angle.

The translational diffusion coefficient of the particle $(D)$ in a dilute solution is determined by particle geometry. The hydrodynamic radius $(R_h)$ of spherical particles and their diffusion coefficient $(D)$ are related by the Stokes-Einstein equation$(9)$[64].

$$D = k_B T/6\pi\eta R_h \quad \ldots\ldots\ldots..(9)$$

Where: $k_B$ is the Boltzmann constant

$T$ is the absolute temperature

$\eta$ is the viscosity of the solution

For non-spherical particle apparent hydrodynamic radius $R_h^{app}$ is given as,

$$R_h^{app} = k_B T/6\pi\eta D^{app}$$

Where: $D^{app}$ is the diffusion coefficient measured in the DLS experiment

For polydisperse particles, or particles with size approaching the wavelength of the incident beam, the autocorrelation function is a sum of contributions from the various particle sizes and diffusional modes. Particle size distributions from experimental $D^{app}$ are then obtained from fitting autocorrelation functions using programs like cumulants fit and CONTIN.

Polydispersity can arise due to aggregation of the polymer solution or due to the presence of impurities. This may lead to non-single exponential correlation function of scattered light.

For larger particles DLS probes not the pure diffusive brown Brownian motion of the scattering particles but also other dynamic fluctuation in the solution. Theoretical multimodal correlation function and single exponential correlation function and their corresponding relaxation times are shown in **Figure 3.9.**

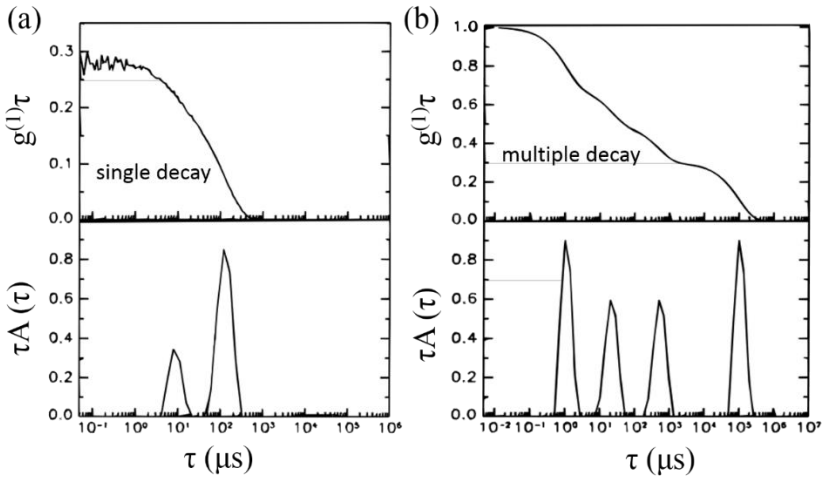



**Figure 3. 9:** Correlation function and corresponding spectrum of relaxation times for, single exponential decay (a), and theoretical multimodal curve for associating polymers with corresponding spectrum of relaxation times (b)[65]

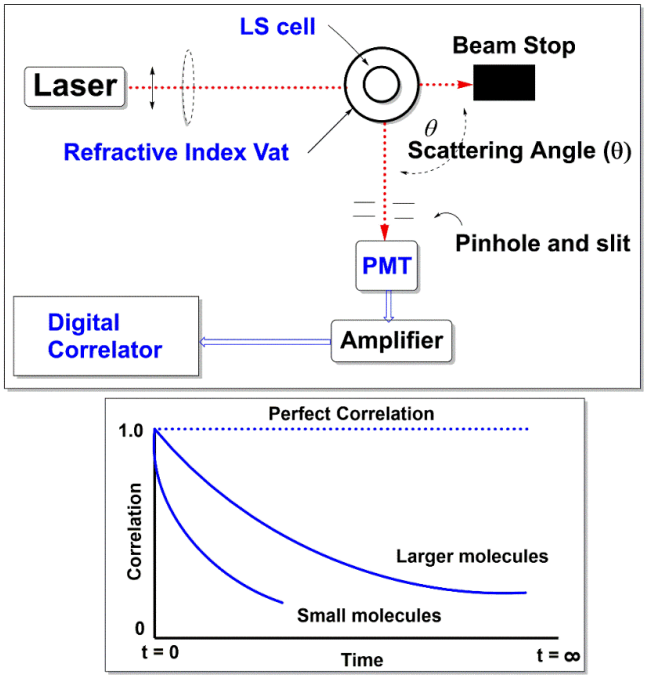



**Figure 3. 10:** Schematic diagram of light scattering apparatus and theoretical correlation as a function of size

DLS analysis was performed (at 95°) using a Precision Detectors PD Expert multi-angle light scattering instrument (PDE). A schematic diagram of the PDE instrument is shown in **Figure 3.10**. In this instrument sample solution is kept in the cylindrical glass cuvette which is surrounded by cylindrical vat filled with similar solvent used for the sample preparation to avoid laser flair at the glass/air interface. Polymer solution was prepared either in toluene or tetrahydrofuran, although toluene was preferably used. Sample concentration was varied until a good correlation curve was obtained. Sensitivity of the instrument and scattering intensity at 95° are low in comparison to the recent back scattering detectors (173°).[66] In this work synthesized polymers have molecular weights less than 10 kg/mol. Some of the samples (even at much higher concentrations) analyzed with PDE were unable to generate good correlation curves, which is attributed to both the low sensitivity of the instrument (at 90°) and oligomeric nature of the polymer, especially such discrepancy are seen in case of ω-UPy functionalized polybutadienes. However, same sample which was unable to give good correlation curves with PDE when analyzed with more sensitive and advanced Zeta-sizer DLS instrument (Malvern Instrument)[66]. It also gave the similar results. Therefore such abnormal behavior is due to the

sample structure, molecular weight and chain-end functionality and not because of the limitation of the DLS instrument.

## 3.16 References


(1) Szwarc, M. *Nature* **1956**, *178*, 1168.

(2) Szwarc, M.; Levy, M.; Milkovich, R. *J. Am. Chem. Soc.* **1956**, *78*, 2656.

(3) Worsfold, D. J.; Bywater, S. *Can. J. Chem.* **1960**, *38*, 1891.

(4) Worsfold, D. J.; Bywater, S. *Can. J. Chem* **1964**, *42*, 2884.

(5) Bywater, S.; Worsfold, D. J. *J. Organomet. Chem.* **1967**, *10*, 1.

(6) Roovers, J. E. L.; Bywater, S. *Macromolecules* **1968**, *1*, 328.

(7) Morton, M.; Rembaum, A. A.; Hall, J. L. *J. Polym. Sci., Part A: Gen. Paper.* **1963**, *1*, 461.

(8) Morton, M.; Fetters, L. J.; Bostick, E. E. *J. Polym. Sci., Part C: Polym. Symp.* **1963**, *1*, 311.

(9) Morton, M.; Fetters, L. J. *J. Polym. Sci., Part A: Gen. Paper.* **1964**, *2*, 3311.

(10) Morton, M.; Bostick, E. E.; Livigni, R. A.; Fetters, L. J. *J. Polym. Sci., Part A: Gen. Paper.* **1963**, *1*, 1735.

(11) Van Beylen, M.; Bywater, S.; Smets, G.; Szwarc, M.; Worsfold, D. In *Polysiloxane Copolymers/Anionic Polymerization*; Springer Berlin Heidelberg: 1988; Vol. 86, p 87.

(12) Higginson, W. C. E.; Wooding, N. S. *J. Chem. Soc.* **1952**, *0*, 760.

(13) Henry L. Shieh, R. P. Q. *Anionic Polymerization Principles and Practical Applications*; Marcel Dekker, Inc: New York, USA, 1996.

(14) Baskaran, D.; Müller, A. H. E. *Prog. Polym. Sci.* **2007**, *32*, 173.

(15) Baskaran, D.; Müller, A. H. E. In *Controlled and Living Polymerizations*; Wiley-VCH Verlag GmbH & Co. KGaA: 2010, p 1.

(16) Baskaran, D.; Müller, A. H. E. In *Polymer Science: A Comprehensive Reference*; Editors-in-Chief: Krzysztof, M., Martin, M., Eds.; Elsevier: Amsterdam, 2012, p 623.

(17) Tung, L. H.; Lo, G. Y. S.; Beyer, D. E. *Macromolecules* **1978**, *11*, 616.

(18) Tung, L. H.; Lo, G. Y. S. *Macromolecules* **1994**, *27*, 2219.

(19) Lo, G. Y. S.; Otterbacher, E. W.; Gatzke, A. L.; Tung, L. H. *Macromolecules* **1994**, *27*, 2233.

(20) Tung, L. H.; Lo, G. Y. S. *Macromolecules* **1994**, *27*, 1680.

(21) Lo, G. Y. S.; Otterbacher, E. W.; Pews, R. G.; Tung, L. H. *Macromolecules* **1994**, *27*, 2241.

(22) Nugay, T.; Küçükyavuz, S. *Polym. Int.* **1992**, *29*, 195.

(23) O'Driscoll, K. F.; Ricchezza, E. N.; Clark, J. E. *J Polym Sci Part A: Gen Pap* **1965**, *3*, 3241.

(24) Matmour, R.; Lebreton, A.; Tsitsilianis, C.; Kallitsis, I.; Héroguez, V.; Gnanou, Y. *Angew. Chem. Int. Ed.* **2005**, *44*, 284.

(25) Quirk, R. P.; Ma, J.-J. *Polym. Int.* **1991**, *24*, 197.

(26) Quirk, R. P.; Tsai, Y. S. *Macromolecules* **1998**, *31*, 8016.

(27) Nikopoulou, A.; Iatrou, H.; Lohse, D. J.; Hadjichristidis, N. *J. Polym. Sci., Part A: Polym. Chem.* **2009**, *47*, 2597.

(28) Matmour, R.; More, A. S.; Wadgaonkar, P. P.; Gnanou, Y. *J. Am. Chem. Soc.* **2006**, *128*, 8158.

(29) Schulz, D. N.; Halasa, A. F.; Oberster, A. E. *J Polym Sci Part A: Polym Chem* **1974**, *12*, 153.

(30) Quirk, R. P.; Jang, S. H.; Yang, H.; Lee, Y. *Macromol. Symp.* **1998**, *132*, 281.

(31) Pispas, S.; Pitsikalis, M.; Hadjichristidis, N.; Dardani, P.; Morandi, F. *Polymer* **1995**, *36*, 3005.

(32) Quirk, R. P.; Ma, J.-J.; Lizarraga, G.; Ge, Q.; Hasegawa, H.; Kim, Y. J.; Jang, S. H.; Lee, Y. *Macromol. Symp.* **2000**, *161*, 37.

(33) Hsieh, H. L. *J Polym Sci Part A: Gen Pap* **1965**, *3*, 163.

(34) Selman, C. M.; Hsieh, H. L. *Polym. Lett.*, **1971**, *9*, 219.

(35) Hsieh, H. L.; McKinney, O. F. *Polym. Lett.*, **1966**, *4*, 843.

(36) Greszta, D.; Mardare, D.; Matyjaszewski, K. *Macromolecules* **1994**, *27*, 638.

(37) Braunecker, W. A.; Matyjaszewski, K. *Prog. Polym. Sci.* **2007**, *32*, 93.

(38) Goto, A.; Fukuda, T. *Prog. Polym. Sci.* **2004**, *29*, 329.

(39) Matyjaszewski, K. *Isr. J. Chem.* **2012**, *52*, 206.

(40) Xia, J.; Matyjaszewski, K. *Macromolecules* **1997**, *30*, 7697.

(41) Wang, J.-S.; Matyjaszewski, K. *J. Am. Chem. Soc.* **1995**, *117*, 5614.

(42) Mühlebach, A.; Gaynor, S. G.; Matyjaszewski, K. *Macromolecules* **1998**, *31*, 6046.

(43) Gao, H.; Matyjaszewski, K. *Macromol. Symp.* **2010**, *291-292*, 12.

(44) Jankova, K.; Bednarek, M.; Hvilsted, S. *J. Polym. Sci., Part A: Polym. Chem.* **2005**, *43*, 3748.

(45) Olivier, A.; Meyer, F.; Raquez, J.-M.; Damman, P.; Dubois, P. *Prog. Polym. Sci.* **2012**, *37*, 157.

(46) Foster, O.; Soeriyadi, A. H.; Whittaker, M. R.; Davis, T. P.; Boyer, C. *Polymer Chemistry* **2012**, *3*, 2102.

(47) Moad, G.; Rizzardo, E.; Thang, S. H. *Polymer* **2008**, *49*, 1079.

(48) Chiefari, J.; Chong, Y. K.; Ercole, F.; Krstina, J.; Jeffery, J.; Le, T. P. T.; Mayadunne, R. T. A.; Meijs, G. F.; Moad, C. L.; Moad, G.; Rizzardo, E.; Thang, S. H. *Macromolecules* **1998**, *31*, 5559.

(49) Mayadunne, R. T. A.; Jeffery, J.; Moad, G.; Rizzardo, E. *Macromolecules* **2003**, *36*, 1505.

(50) Hadjichristidis, N.; Iatrou, H.; Pispas, S.; Pitsikalis, M. *J. Polym. Sci., Part A: Polym. Chem.* **2000**, *38*, 3211.

(51) Uhrig, D.; Mays, J. W. *J. Polym. Sci., Part A: Polym. Chem.* **2005**, *43*, 6179.

(52) Hadjichristidis, N.; Pitsikalis, M.; Pispas, S.; Iatrou, H. *Chem. Rev.* **2001**, *101*, 3747.

(53) Rahman, M. S.; Aggarwal, R.; Larson, R. G.; Dealy, J. M.; Mays, J. *Macromolecules* **2008**, *41*, 8225.

(54) Higashihara, T.; Hayashi, M.; Hirao, A. *Prog. Polym. Sci.* **2011**, *36*, 323.

(55) Hadjichristidis, N. *J. Polym. Sci., Part A: Polym. Chem.* **1999**, *37*, 857.

(56) Flory, P. J. *Principles of Polymer Chemistry*; Cornell University Press: Ithaca, New York, 1953.

(57) Young, R. J.; Lovell, P. A. *Introduction to Polymers, Third Edition*; CRC Press: USA, 2011.

(58) Hiemenz, P. C.; Lodge, T. P. *Polymer Chemistry, Second Edition*; CRC Press: USA, 2007.

(59) Lovell, R. J. Y. a. P. A. *Introduction to Polymers Third Edition*; CRC Press: USA, 2011.

(60) Mark, J. E. *Polymer Data Handbook, 2nd edition*; Oxford University Press: New York, 2009.

(61) Brown, W. *Light Scattering Principles and Developement*; Oxford Univsersity Press: New York, 1996.

(62) Schmitz, K. S. *An Introduction to Dynamic Light Scattering by Macromolecules*; Academic Press, Inc.: New York, 1990.

(63) Pecora, R. *Dynamic Light Scattering: Applications of Photon Correlation Spectroscopy*; Plenum Press: New York, 1985.

(64) Teraoka, I. *Polymer Solutions An Introdcution to Physical Properties*; Jhon Wiley & Sons, Inc.: New York, 2002.

(65) Sedlák, M. *Langmuir* **1999**, *15*, 4045.

(66) http://www.malvern.com, (accessed on 2013).

# Chapter 4: Micellar Cluster Association of Ureidopyrimidone Functionalized Monochelic Polybutadiene

## Abstract

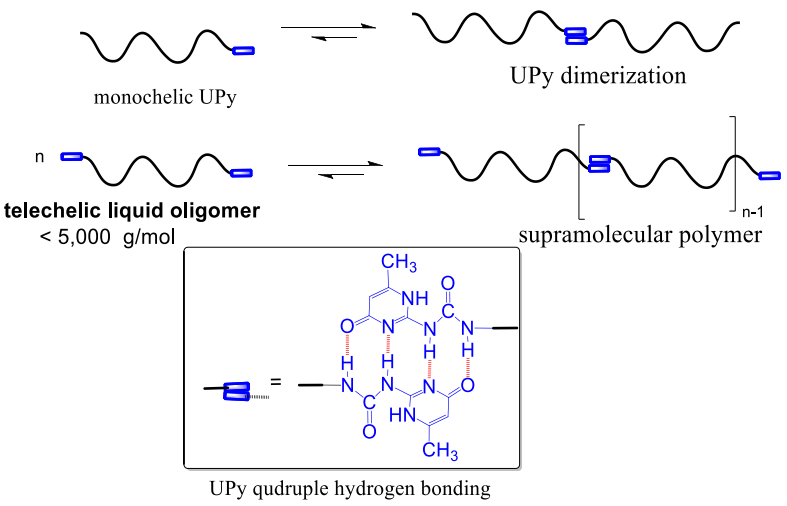
A series of monochelic polybutadienes with ureidopyrimidone terminal group (MPBd-UPy) has been synthesized using anionic polymerization and chain-end transformation via reaction with1-(6-isocyanatohexyl)-3-(6-methyl-4-oxo-1,4-dihydropyrimidin-2-yl)urea(UPy-NCO). Monochelic polybutadiene with two UPy terminal groups, MPBd-$(UPy)_{2,}$ has also been synthesized to study the effect of chain-end concentration on hydrogen bonding association. The transformation of precursor ω-hydroxyl terminated polybutadiene into 2-ureido-4-pyrimidone functionality turns free-flowing liquid samples into semi-solid viscous material due to a well-known quadruple hydrogen bonding ability of UPy. Dimerization association of MPBd-UPy has been studied thoroughly using size exclusion chromatography, intrinsic viscosity, dynamic light scattering. The solutions of MPBd-UPy exhibit high Huggins parameter, $0.40<K_H>0.63$ depending on the molecular weight and number of UPy groups at the chain-end. Studies reveal that along with hydrogen bonded dimers, $(MPBd\text{-}UPy)_2$ also aggregates intermolecularly to form star-like micelles that are in equilibrium with dimers. The presence of multiple populations with $R_h$ of as high as 550 nm, which decreases with increasing temperature in toluene, has been identified. The UPy aggregated micellar clusters have distinct endothermic transitions in DSC, and AFM studies show an evidence of micellar-clusters forming associated parallel line-like structures on a mica surface with the well-defined order. For the first time we show the evidence for multidirectional aggragtion of UPy group.

Part of this work has been published as,
Bobade, S. L.; Malmgren, T.; Baskaran, D.
*Polym. Chem*. **2014**, 5, 910.

## 4.1 Introduction

Non-covalent interactions such as H-bonding, ionic, pi-pi, van der Waals, and other di-polar interactions contribute significantly for the enhancement of macromolecular properties of polymers made of covalent linkages. In the absence of covalent bonding, a certain type of organic molecules or oligomers, that can exert strong non-covalent interactions either bifunctional or multifunctional, exhibits macromolecular properties via supramolecular association. Lehn described such materials derived from complementary binding association via non-covalent interactions as supramolecular dynamers as they are bonded through reversible connections.[1] Hydrogen bonding is an extensively used secondary interaction in supramolecular association. High selectivity and directional-nature of hydrogen bonds are particularly suited for making supramolecular polymers. Lehn and coworkers elegantly demonstrated formation of supramolecular polymers using small molecules that contain bi-functional complementary hydrogen bonding sites (AB and $A_2$ types for hetero-, self-complementary, respectively).[2-9] The strength of a kinetically trapped and thermodynamically controlled hydrogen bonded material is primarily determined by the number, position, and cooperativeness of hydrogen-bonds.[10]

Pioneering work of Meijer, Zimmerman, Griffin, Frechet and Lehn and their co-workers on hydrogen bonded supramolecular polymers indicated that the molecules are linearly connected via hydrogen bonded polymerization.[6,11-21] A well-known and widely used functionality is 2-ureido-4[1H]-pyrimidone (UPy), which has uniquely positioned hydrogen bonding sequence, donor-donor-acceptor-acceptor (DDAA) arrangement for self-complementary interactions. Derivatives of 2-ureido-4[1H]-pyrimidone undergo rapid dimerization via DDAA quadruple hydrogen bonding with high equilibrium constant ($K_{dim}$= $6\times10^7$ $M^{-1}$ in $CHCl_3$ and $6\times10^8$ $M^{-1}$ in toluene).[22] Meijer and co-workers attached UPy functionality at the terminals of telechelic oligomers and produced supramolecular polymers of different kinds.[15,23-25] A complementary quadruple hydrogen bonding with rigid planar geometry for directional interaction with adjacent acceptor molecules is responsible for rendering superior mechanical properties for supramolecular polymers (**Scheme 4.1**).




**Scheme 4. 1:** UPy dimerization in the case of monochelic and linear supramolecular polymerization of telechelic functionalized oligomers.

An enhancement of physical properties in supramolecular polymers formed by telechelic materials functionalized with UPy group is attributed to a strong dimerization of chain-ends leading to high molecular weight linear polymers in several earlier studies.[25] However, recently Long and coworkers showed an evidence that the polymeric system with ureidopyrimidone (UPy) can also form aggregation through multiple and multidirectional hydrogen bonds.[26,27] The hydrogen bonding constant is highly influenced by the nature of the polar or non-polar environment of the linking polymer chain, which in turn will affect the strength of supramolecular polymer. A competitive intramolecular hydrogen bonding from a monomer residue such as oligoethylene oxide has been shown to have an effect upon the UPy-dimerization constant.[28,29]

Recent studies by Meijer and co-workers have focused on the role of urethane and urea linkages on the pre-organization of linear supramolecular polymer held with dimerization of UPy.[30-32] Urea and urethane linkages are formed respectively from the reaction of hydroxyl and amine end-functionalized telechelic oligomer of hydrogenated polybutadiene(X-PE-co-PP-X, where X = -OH or $–NH_2$) with two isocyanate containing UPy groups. Urea and urethane groups are considered to be responsible for lateral H-bonding with one-dimensional stacks leading to aggregation, which is necessary for good material properties, especially in the case of the UPy-(PE-*co*-PB)-UPy system.[33] On the other hand, Rowan and coworkers used weak

hydrogen bonding to form supramolecular thermoplastic elastomers from telechelic oligotetrahydrofuran that are chain-end functionalized with nucleobases.[34,35] Their studies showed the importance of dynamics in hydrogen bonded supramolecular polymers that are critically dependent on physical properties such as $T_g$ and $T_m$ of the connecting chain segment. They also showed the presence of cooperative association and dissociation equilibrium between the secondary interacting end-groups in supramolecular polymer.

In addition to telechelic association equilibrium, the presence of hydrogen bonded domain aggregation also complicates quantitative evaluation of the UPy system. However, in the case of monochelic oligomers that are end-functionalized with one UPy group, the dimerization dynamics could be studied in detail. Accordingly, several groups have used monochelic UPy terminated polystyrene (MPS-UPy), polyisoprene (MPI-UPy), and other block copolymers to exploit the strong dimerization ability of UPy.[36,37] Studies by Long [36] and Karatzas and their coworkers[37], on MPS-UPy, and a series of UPy end functionalized polystyrene-block-isoprene (MPS-*b*-PI-UPy) and (MPI-*b*-PS-UPy) copolymers have shown that these systems undergo aggregation or micellization after dimerization via hydrogen-bonding. Hawker and coworkers have studied blending of well-defined poly (*n*-butyl acrylate) and poly (benzyl acrylate) end functionalized with 2-ureido-4[1H]-pyrimidinone (UPy) and 2,7-diamido-1,8-naphthyridine (Napy) prepared by ATRP initiators containing either UPy or Napy.[38] Furthermore, Hawker and coworkers have shown that 'blocky' random distribution of the UPy groups slows down the dynamics of the UPy groups, producing materials with improved mechanical properties.[39]

In this report, we describe the synthesis and characterization of five different monochelic polybutadienes (MPBd-UPy) varying in molecular weights (900 g/mol $\geq M_n \leq$ 11,500 g/mol) of that are functionalized with the UPy end-group and show the effect of intermolecular dimerization interaction. The existence of association and dissociation dynamics of MPBd-UPy samples in solution and in bulk has been identified. The presence of hydrogen bonded dimers and their aggregation leading to a formation of star-like micelles with polar UPy core and polybutadiene corona has been studied using solution viscosity, dynamic light scattering, differential scanning calorimeter, and atomic force microscopy.

## 4.2 Experimental Section

### 4.2.1 Materials

Styrene (Aldrich, 99%), 1,3-butadiene (Aldrich, 99 %), ethylene oxide (Aldrich), benzene (Aldrich, 99.9 %),methanol (Fisher, ACS certified) were purified according to the standard procedures for the anionic polymerization.[40,41] 1,6-Diisocyanatohexane (1,6-HDI, Acros Organics,>99 %), chloroform (Fisher, ACS certified), 2-Amino-4-hydroxy-6-methylpyrimidine (Acros Organic, 98 %), toluene HPLC (Fischer), dibutyltin dilaurate (DBDTL) (Aldrich) and 2,6-di-tert-butyl-4 methyl phenol (BHT, Aldrich, >99.0 %), were used as received. Benzene (Aldrich) was stirred over sulfuric acid for a week, washed with distilled water until neutral, dried over calcium chloride and finally distilled over $CaH_2$, and stored over a small amount of living polystyryllithium anion. 1,3-Butadiene (Bd) (Aldrich, 99 %) was distilled twice over *n*-BuLi into calibrated ampules with break-seal, diluted with at least two fold excess of benzene and sealed off. Ethylene oxide (Aldrich, 99 %) was distilled in sequence over $CaH_2$ and n-BuLi into calibrated ampules with break-seal. The initiator *sec*-butyl lithium (*sec*-BuLi) 1.4M (Aldrich) diluted with hexane to get a desired final concentration of 0.75 M under vacuum and split into calibrated ampules with break-seal.

### 4.2.2 Characterization

$^1$H NMR spectra were recorded on Varian Mercury Vx 300 spectrometer at 300 MHz. The samples were prepared in C*D*$Cl_3$ without TMS. Polymer number-average molecular weight ($M_n$) and MWD were determined using size exclusion chromatography (SEC)equipped with Knauer's K-501 HPLC pump, K-2301 RI detector, K-2501 UV detector, and with a set of two columns; Polymer Standards Services, SDV-gel, 60-cm length (5 µm) 100 Å and a linear $10^2$–$10^6$ Å. Tetrahydrofuran (THF) with toluene as a solvent flow marker was used as an eluent at a flow rate of 1.0 mL/min, and the SEC was calibrated using polystyrene (PS) standards obtained from Pressure Chemicals (Pittsburgh, USA). The $M_{n,SEC}$ of MPBd-UPy obtained against calibrated PS standards was corrected by multiplying with correction coefficient of 0.50.

Thermogravimetry analysis (TGA) was performed using a TA Q-50 instrument (RT to 1000 °C), with a heating rate of 10 °C/min under nitrogen atmosphere. Dynamic light scattering (DLS) of MPBd-UPy in toluene was performed on a Precision Detectors (PD) Expert instrument at a scattering angle of 95° and at the temperature range of 5 °C to 80 °C.

Data was analyzed with precision Contin analysis software and reported hydrodynamic radius is an average of 10 repetitive measurements (delay time1.5 μsec with 512 channel correlation). Sample concentration was increased until a good correlation curve was obtained as the samples are oligomers.

Atomic force microscopy (AFM) was performed with a Nanoscope IIIa Microscope with Multimode Controller (Veeco Instrument) at ambient temperature. Drop cast films were prepared on a freshly prepared mica surface from a sample concentration of 1 mg/mL in toluene. The tapping mode was employed with an antimony-doped Si tip (radius <10 nm) at a line scanning frequency of 1 Hz.

Dynamic scanning calorimetry (DSC) analysis was performed with a TA-Q1000 instrument from -90 to 150 °C at a scan rate of 10 °C/min. Three repeated heating and cooling scans were run with a 5min isotherm at -90 °C. Solution viscosity in toluene was measured by an automatic viscometer using a Schott Instruments AVS 370 and a type 531-10 viscometer (0.64 mm capillary with K = 0.01)

### 4.3.1 Synthesis of monochelic hydroxyl-polybutadiene (MPBd-OH)

UPy–synthon was prepared using a reported procedure.[42] In a typical reaction, 16 g of 2-amino-4-hydroxy-6-methylpyrimidinewas added into a flame dried round bottom flask and dried under high vacuum at 110 °C for ~4 h to remove traces of moisture. After cooling to room temperature, 1,6-HDI (100 mL) was added into the flask and the reaction mixture was stirred at 110 °C under $N_2$. After 16 h the flask was cooled to room temperature and the reaction mixture was poured into a large excess of *n*-hexane to separate UPy-synthon as a white powder. The UPy-synthon was filtered, washed with a large excess of *n*-hexane to remove traces of 1,6HDI, and dried under vacuum at 50 °C for 12 h. UPy-Synthon $^1$H NMR spectrum is shown in **Figure 4.1**. Yield: 35.2 g (93.95 %);$^1$HNMR (300 MHz, $CDCl_3$): 13.1 (s, 1H, $CH_3C\underline{NH}$), 11.9 (s, 1H,-$CH_2NH(C=O)$ $\underline{NH}$), 10.2 (s, 1H, -$CH_2NH(C=O)$ $\underline{NH}$), 5.8 (s, 1H, -$\underline{CH}$=$CCH_3$),3.3 (m, 4H, NH(C=O) NH$\underline{CH_2}$ + $CH_2NCO$), 2.2 (s, 3H, $\underline{CH_3}C$=CH), 1.6 (m,4H, -$NCH_2\underline{CH_2}CH_2CH_2\underline{CH_2}$-$CH_2N$-), 1.4 (m, -$NCH_2CH_2\underline{CH_2CH_2}CH_2$-$CH_2N$-)

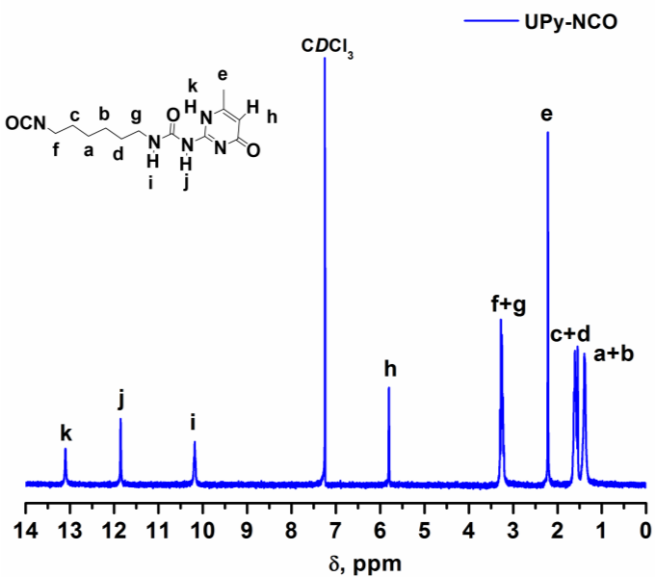
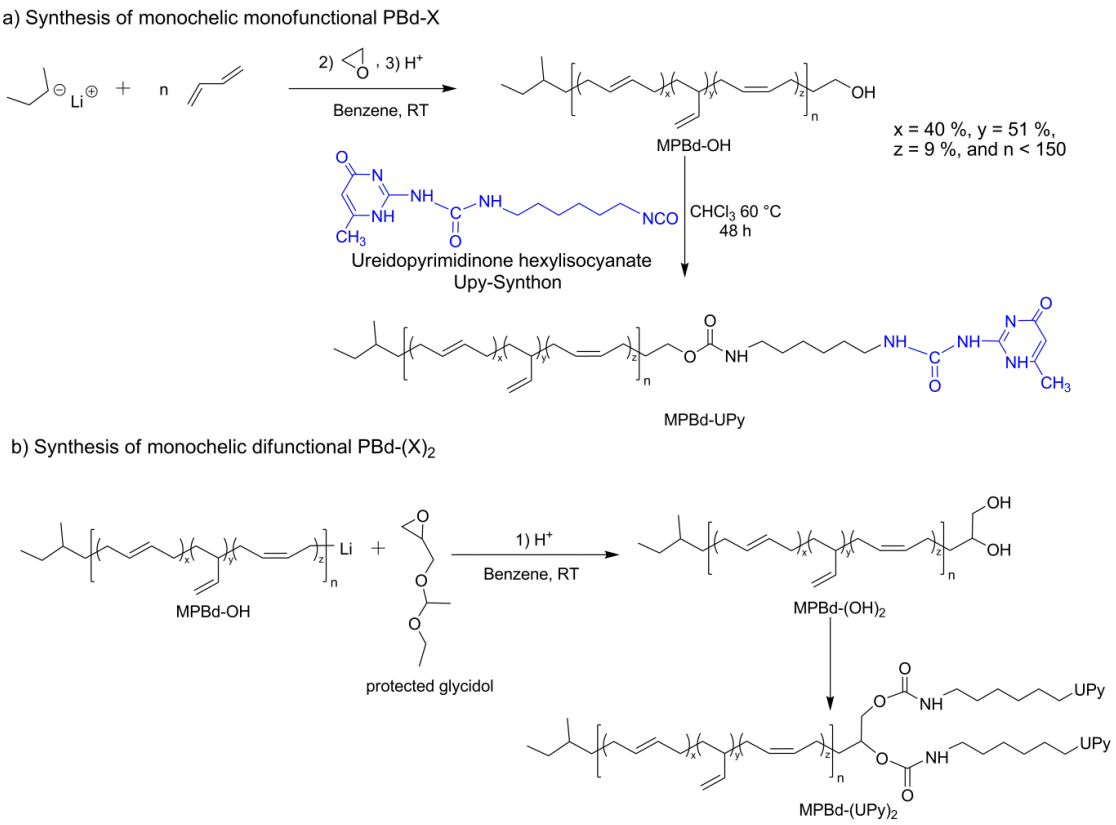



**Figure 4. 1:** $^{1}$H NMR spectrum of UPy- Synthon

### 4.3.2 Synthesis of monochelic UPy-Polybutadiene (MPBd-UPy)

In a typical experiment, to a flame dried round bottom flask, 20.0 g (2.78 mmol) of ω-hydroxyl terminated butadiene, MPBd-OH-4 was added and the flask was attached to a vacuum line. The MPBd-OH-4was dried under vacuum for ~ 4 h at 80 °C to remove traces of methanol and moisture. The flask was cooled with liquid nitrogen and 250 mL of chloroform stored over $CaH_2$ or anhydrous silica was distilled into it and the temperature was allowed to reach 25 $^{o}$C. Upon dissolution of the polymer, the flask was removed from the vacuum line under a purge of $N_2$and closed with a rubber septum. UPy-synthon (1.65 g, 5.63mmol, 2 mol of –OH group) was added along with a few drops of DBDTL catalyst using a syringe. The reaction was stirred at 60 °C and the progress of the reaction was monitored using the $^{1}$H NMR, intermittently. After all the consumption of hydroxyl groups (100 %) over 24 h, the reaction mixture was stirred over silica (15 g) to remove the remaining excess UPy-synthon. The reaction mixture containing ω-UPy terminated monochelic polybutadiene (MPBd-UPy-4) was further purified by passing through silica column and then precipitated in methanol.




**Scheme 4. 2:** Synthesis of monochelic polybutadienes by anionic polymerization and their chain-end transformation with a) monochelic polybutadiene with monofunctional UPy (MPBd-UPy) and b) monochelic polybutadiene with difunctional UPy (MPBd-$(UPy)_2$).

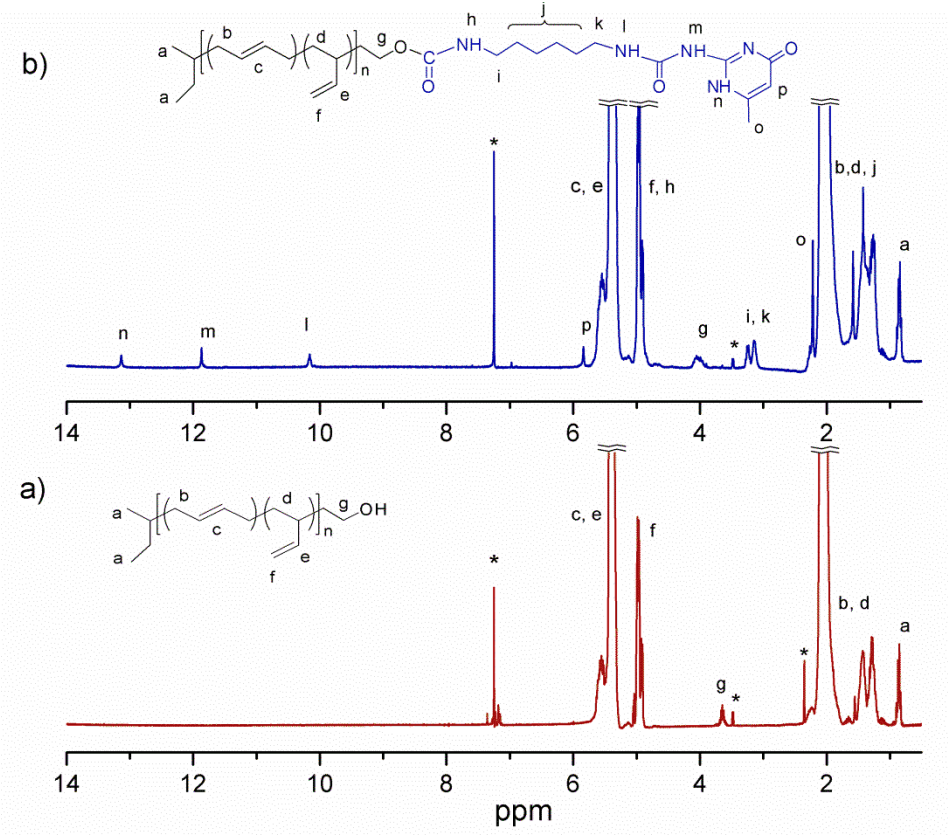



**Figure 4. 2:** [1]H NMR spectrum of a) precursor MPBd-OH-4 and b) after chain-end functionalization with UPy, MPBd-UPy-4. The signals marked as * indicate residual solvent and antioxidant.

## 4.4 Results and discussion

### 4.4.1 Synthesis of Monochelic polybutadienes with UPy tag

Monochelic polybutadienes with hydroxyl end-groups were first prepared using living anionic polymerization of 1,3-butadiene in benzene at room temperature under high vacuum. The polymerization was terminated with a slight excess of ethylene oxide to get polybutadienes with monohydroxyl end-group (MPBd-OH).[41] Similarly, for the synthesis of dihydroxyl terminated polybutadiene, MPBd-$(OH)_2$, the living polybutadiene anion with lithium counterion was reacted with hydroxyl protected glycidol, which adds selectively one unit at the chain-end and subsequently hydrolyzed the protecting group to obtain a desired two hydroxyl functionality (**Scheme 4.2b**). The characterization of MPBd-OHs samples by [1]H NMR and SEC showed that the molecular weight determined by the integral values of the initiator methyl protons (*b*, 0.85 ppm, the head-group) and the methylene protons (*a*, 3.65 ppm,

the end-group) adjacent to the hydroxyl terminal group matches with $M_{n,SEC}$ indicating the hydroxyl functionality is close to one (**Table 4.1, Figure 4.4**).

In a second step, the hydroxyl end-group of the MPBd-OH was coupled with isocyanate functionalized UPy synthon (UPy-NCO), which was prepared by reacting 2-amino-4-hydroxyl-6-methyl pyrimidine and 1,6-HDI. The coupling reaction was optimized since the rate and efficiency of the reaction of UPy-NCO are dependent upon the purity of the solvent. Reactions carried out using distilled chloroform with a slight excess of UPy-NCO produced 100 % coupling efficiency at 60 °C in 24 h. On the other hand, it was observed that the reaction performed using dry, but unpurified chloroform (contains traces of ethanol added as preservative and co-distills along with chloroform) gave a drastic reduction in yield and required an addition of far more excess of UPy-synthon to achieve 100 % coupling efficiency. The presence of protic impurities such as ethanol and moisture in the solvent reacts with UPy-NCO and reduces the efficiency of UPy-NCO coupling.

The recovered MPBd-UPy samples were semi-solid in contrast to their hydroxyl terminated precursors (MPBd-OH), which are free-flowing viscous liquids (**Figure 4.3**). Table 1 gives the $M_n$ and $M_w/M_n$ values of the monochelic hydroxyl and UPy end-functionalized polybutadienes. The $^1$H NMR of MPBd-UPy shows signals corresponding to -NH protons at ~13.1, 11.4, and 10.2 ppm for the dimerized UPy moiety in the polymer (**Figure 4.2b**).The $M_n$ determined by $^1$H NMR using the relative integration of *sec*-butyl, or UPy groups with the polymer backbone is close to the $M_{n\text{-}SEC}$ (PS calibration) when adjusted with the hydrodynamic volume factor.[43] Thermogravimetry analysis (TGA) performed in the presence of nitrogen for MPBd-UPys exhibited a three step decomposition; one at 210 °C ($T_{max\text{-}1}$) corresponding to the chain-end UPy group and a subsequent two steps attributed to the decomposition of polymer backbone at ~375 °C ($T_{max\text{-}2}$) and 458 °C ($T_{max\text{-}3}$). In the case of MPBD-$(UPy)_2$-1(Table 1), which contains two UPy groups at the chain-end, 2.75 % weight loss was observed at $T_{max\text{-}1}$= 210 °C corresponding to double the weight of UPy.



**Figure 4. 3:** Picture of MPBd-OH-2 (liquid) and MPBd-UPy-2 (non-flowing semisolid)

**Table 4. 1:** Characterization of monochelic polybutadiene with hydroxyl (MPBd-OH) and ureidopyrimidone (MPBd-UPy) functional groups

| Sample[a] | [sec-BuLi]$_0$[b] mol/L | [Bd]$_0$ mol/L | MPBd-OH | | | MPBd-UPy | | | Vinyl[f] % |
|---|---|---|---|---|---|---|---|---|---|
| | | | $M_{n,SEC}$[c] g/mol | $M_{n,NMR}$[d] g/mol | $Đ$[e] | $M_{n,SEC}$[c] g/mol | $M_{n,NMR}$[d] g/mol | $Đ$[e] | |
| MPBd-X-1 | 0.323 | 2.852 | 600 | 550 | 1.09 | 700 | 900 | 1.10 | 14.2 |
| MPBd-X-2 | 0.053 | 2.115 | 1,700 | 1,600 | 1.13 | 2,050 | 1,900 | 1.12 | 12.8 |
| MPBd-X-3 | 0.0560 | 1.996 | 2,600 | 2,550 | 1.05 | 3,050 | 2,900 | 1.06 | 13.5 |
| MPBd-X-4 | 0.0187 | 2.460 | 7,200 | 7,200 | 1.03 | 7,300 | 7,700 | 1.03 | 10.6 |
| MPBd-$(X)_2$-1 | 0.0204 | 2.700 | 11,150 | 11,500 | 1.03 | 11,350 | 12,500 | 1.02 | 11.5 |

a) Monochelic polybutadiene with functional group (X), b) polymerization was performed for 12h and terminated with ethylene oxide. c) number average molecular weight ($M_n$) determined based on PS calibration with hydrodynamic volume corrected for PBd (1.99), d) $M_n$ calculated based on *sec*-butyl or UPy end group from $^1$H NMR in $CDCl_3$, e) determined from SEC, and f) % of *1,2* and *1,4* addition in the polymer determined by $^1$H NMR.

### 4.4.2 Aggregation of monochelic PBd-UPys in SEC elution profile

Monochelic PBds with hydroxyl and UPy end-groups were analyzed using SEC in THF. All the MPBd-OH samples exhibited monomodal elution profiles with narrow molecular weight

distributions (MWD). **Figure 4.44a** shows SEC chromatograms of the MPBd-OH precursor and after attachment of UPy-synthon. The free-flowing liquid samples of MPBd-OHs turn into semi-solid materials after attaching the UPy moiety at the chain-ends indicating the formation of dimeric and higher-order association via quadruple hydrogen bonding in the solid-state. The presence of such an associated species in solution can be identified in SEC only when the hydrogen bonding association is stronger than the shear forces operating in the column during the size exclusion process. SEC analyses of MPBd-UPys were performed in THF at a concentration of 1 mg/mL with an injection volume of 100 µL at 30 $^{o}$C. Nevertheless, all the MPBd-UPys exhibited a small high molecular weight hump along with the main peak. The main peak was slightly shifted to a lower elution volume indicating increase of molecular weight corresponding to the attachment of UPy at the chain-end (**Figure 4.4a**).With the exception of the samples MPBd-UPy-1 and, MPBd-UPy-4, all other samples show an increase in the molecular weight by approximately 250-300 g/mol, whereas the MWD remained narrow. Interestingly, the peak maximum molecular weight ($M_p$) of the hump is double the molecular weight of the main peak indicating the presence of dimers in small amounts in THF under normal operating condition (1 mg/mL) of SEC analysis (**Figure 4.4 a and b**).

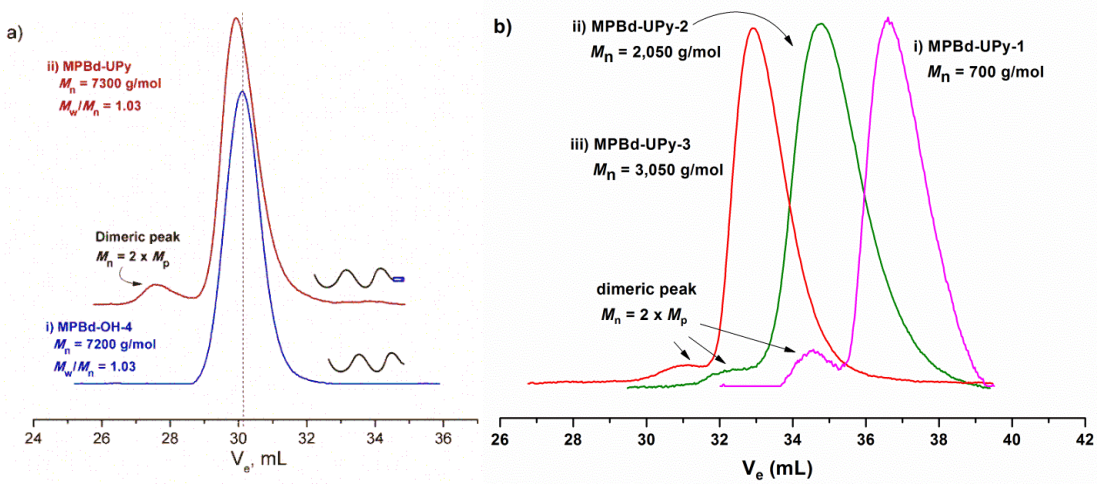



**Figure 4. 4:** GPC traces of a) MPBd-OH-4 and MPBd-UPy-4 and b) other MPBd-UPy samples showing presence of dimeric peak.

The results confirm the existence of MPBd-UPy in equilibrium with dimers in solution even under the influence of shear forces that are present in size exclusion chromatography. Previous reports on the UPy group end-functionalized polymers, for example PS-UPy and PS-b-PI-UPy,[36] did not show such a clear shift in the molecular weight and the presence of a dimer peak in SEC analysis. Although these observations depend upon the efficiency of SEC column resolution, the presence of a dimeric peak could be easily overlooked as its intensity is very low.

Upon increasing the concentration of the solution from 1 mg/mL to 5 mg/mL, the SEC traces of MPBd-UPy-2 showed an increase in the intensity of the dimeric peak and broadening of the main peak, which changes the $M_{n,SEC}$ and $M_p$ values considerably (**Figure 4.5a and Table 4.2**). Nevertheless, an addition of 5 % triethylamine, a hydrogen bonding acceptor, in the mobile phase reduces the peak broadening as well as the amount of dimeric shoulder (**Figure 4.5b**). This suggests that the solution contains not only dimers, but also aggregates of different sizes.

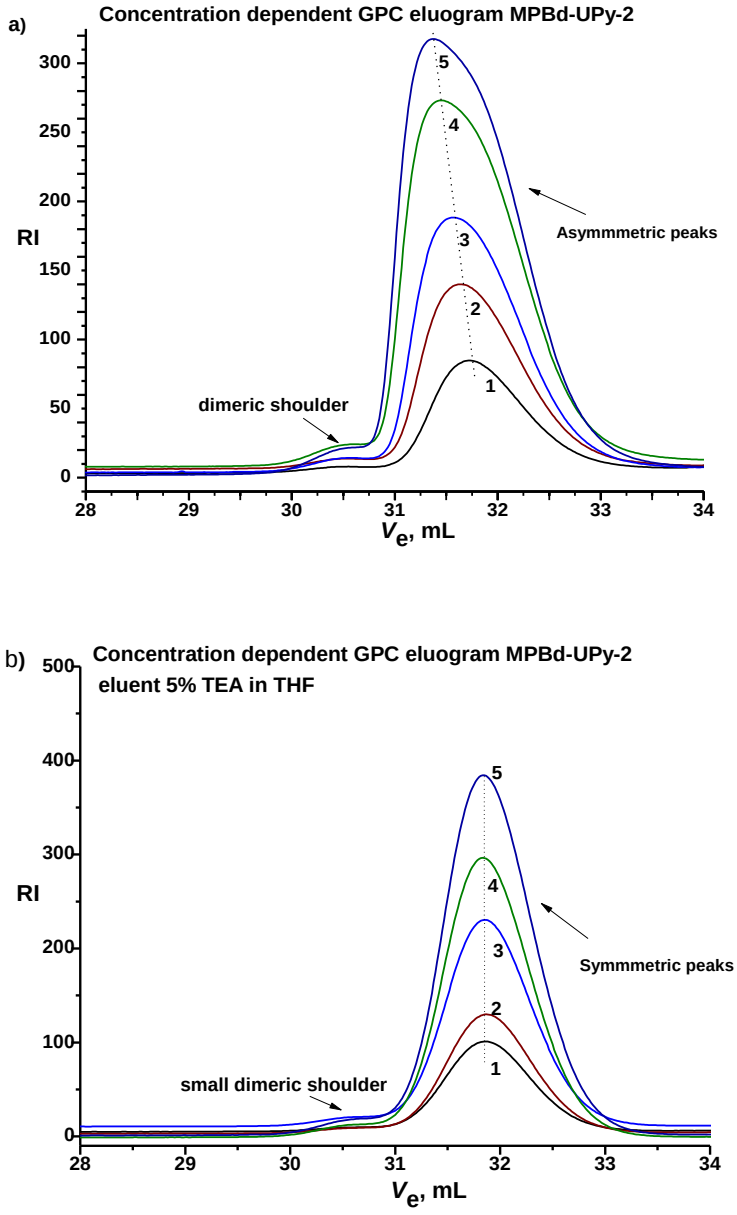



**Figure 4. 5:** Concentration dependent (1-5 mg/mL) GPC eluogram of the MPBd-UPy-2 (a) and MPBd-OH-2 (b)

**Table 4. 2:** Concentration dependent GPC of the MPBd-UPy-2 and MPBd-OH-2

| Sample concentration (mg/mL) | MPBd-OH | | | MPBd-UPy | | |
|---|---|---|---|---|---|---|
| | $M_{n\ SEC,}$ (g/mol) | $M_{n(max)}$ (g/mol) | $M_w/M_n$ | $M_{n,\ SEC}$[c] g/mol | $M_{n,\ (Max)}$ g/mol | $M_w/M_n$ |
| 1 | 1,720 | 1,810 | 1.048 | 1,890 | 2,120 | 1.064 |
| 2 | 1,700 | 1,780 | 1.049 | 1,920 | 2,240 | 1.074 |
| 3 | 1,680 | 1,760 | 1.050 | 1,980 | 2,330 | 1.068 |
| 4 | 1670 | 1,750 | 1.051 | 2,020 | 2,470 | 1.077 |
| 5 | 1670 | 1,750 | 1.052 | 2,590 | 2,590 | 1.077 |

### 4.4.3 Solution viscosity studies and effect of UPy aggregation

The presence of dimers in equilibrium with monomeric chains in solution will affect the solution viscosity depending on the equilibrium dynamics. In order to understand the effect of aggregation of monochelic chains, the solution viscosities of MPBd-UPys (1-4) were measured in toluene in the concentration range of 0.1 g/dL to 1.6 g/dL at 25°C and compared with corresponding precursors (MPBd-OHs). Specific viscosity curves for the MPBd-UPys showed a linear dependence with respect to the concentration. **Figure 4.6a** shows a typical viscosity relation with concentration for MPBd-UPy-2 and MPBd-$(UPy)_2$-1. However, the Huggins parameter, $K_H$, calculated using the slope was distinctly different for UPy functionalized monochelic PBds (**Table 4.3**).

The Huggins parameter ($K_H$) is known to signify intermolecular hydrodynamic interactions, which is governed by the spatial conformation of polymer in a solvent at a constant temperature, independent of the molecular weight.[44-46] For a polymer with linear coil conformation in a good solvent, the $K_H$ value is ≤ 0.40.[47] The obtained $K_H$ values for MPBd-UPys are higher (≥ 0.40) and in the case of MPBd-$(UPy)_2$ (**Figure 4.6 a-iv**), it is 0.63, which

suggest that the solution consists of a polymer with a sphere like conformation. This suggests that dimers of MPBd-UPys interact intermolecularly and form star-like micellar aggregates with a polar hydrogen bonded domain as a core.[48]

**Table 4. 3:** Viscosity measurements of MPBd-OH and MPBd-UPy samples in toluene

| Sample | $M_{n,NMR}$ g/mol | [η] dL/g | $K_H$[a)] | Ratio of $K_H$ $K_{H(MPBd\text{-}Upy)}/K_{H(MPBd\text{-}OH)}$ |
|---|---|---|---|---|
| MPBd-UPy-1 | 900 | 0.07 | 7.23 | NA |
| MPBd-UPy-2 | 1,900 | 0.10 | 0.59 | 1.42 |
| MPBd-UPy-3 | 2,900 | 0.11 | 0.36 | 1.62 |
| MPBd-UPy-4 | 7,700 | 0.28 | 0.50 | 1.32 |
| MPBd-UPy-5 | 12,500 | 0.30 | 0.63 | 1.61 |

a) Determined from viscosity curves, $K_H[\eta]$ = slope $ml^2.\ g^{-2}$

Further, the $K_H$ ratio of MPBd-UPy to MPBd-OH could be used to determine the extent of aggregation in these polymers.[49,50] The ratio of $K_H$ to the precursor is, in all cases, higher than one supporting the presence of micelles in the solution. The determined intrinsic viscosity, [$\eta$] is almost twice for MPBd-UPy as compared to that of the precursor MPBd-OH (**Figure 4.6a**). Such a high viscosity and $K_H$ ($\geq$ 0.40) confirm that the MPBd-UPy samples exist in equilibrium with aggregated dimerized chains in the form of star-like micelles. The $K_H$ ratio of MPBd-UPy-1 to MPBd-OH-1 could not be determined since its precursor has almost a zero value for $K_H$. Interestingly, MPBd-UPy-1 showed an unusual behavior of higher viscosity with lowering the concentration, similar to the behavior of a typical polyelectrolyte solution in water. As this is a low molecular weight ($M_n$ = 700) MPBd-UPy, we believe that the volume ratio of polar to non-polar regions of the molecule is not appropriate to form traditional star-like micelles.

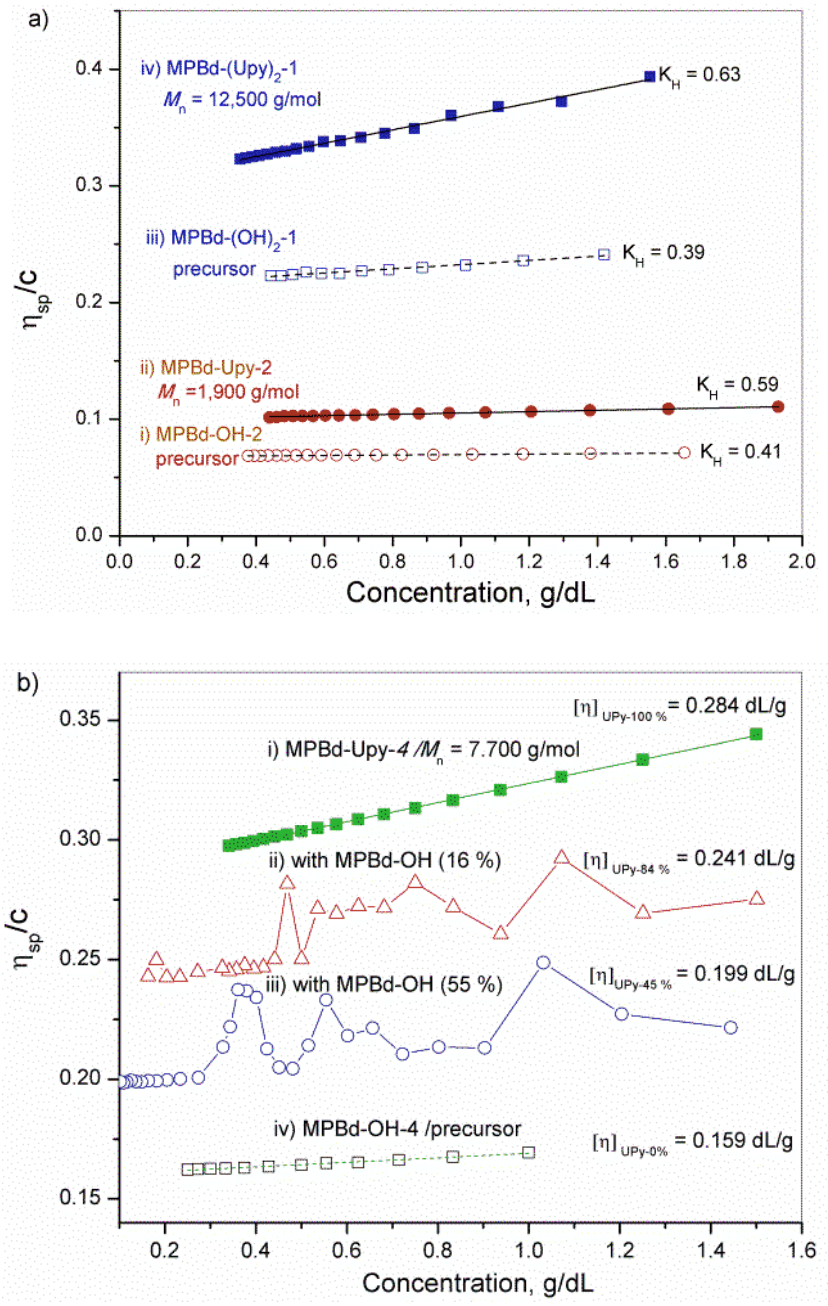
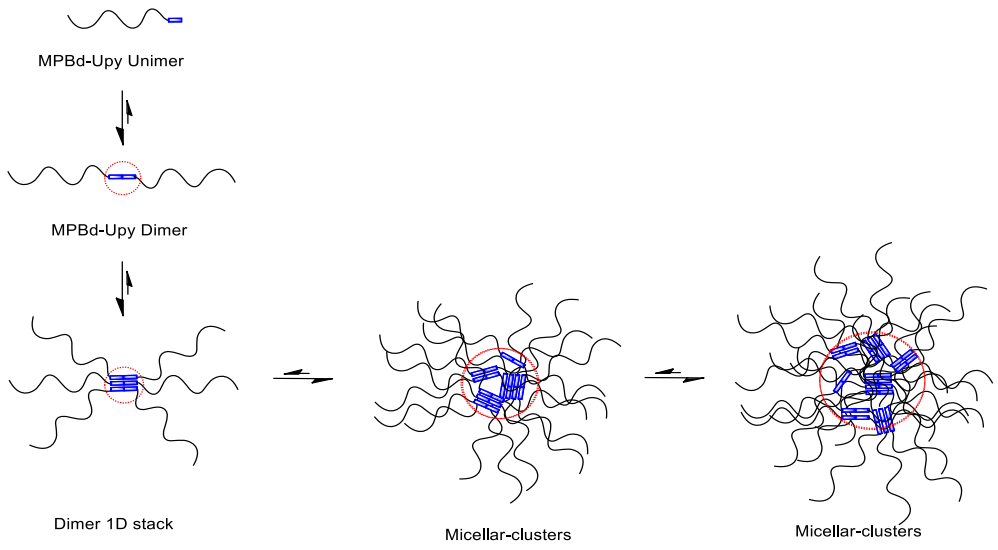



**Figure 4. 6:** Plot of reduced viscosity vs concentration for a) MPBd-UPy-2 (i and ii) and MPBd-$(UPy)_2$-1 (iii and iv) in comparison with respective precursors and b) MPBd-UPy-4 (i and iv) and mixed with 55 wt % and 16 wt % precursor.

High values of the intrinsic viscosity and Huggins parameter indicate that the intermicellar aggregates are stable under the shear forces of viscometry measurement. Karatzas et al[37] reported no significant difference in the values of intrinsic viscosity and $K_H$ for the

monochelic block copolymer, MP(S-*b*-I)-UPy. It is important to note that the PS-*b*-PI used in their study does form micelles themselves in selective solvents, which superseded the effect of UPy interaction. However, in the case of MPBd-UPy, the formation of micelles is primarily driven by UPy chain-end dimerization and aggregation of polar UPy domains in toluene.

A linear correlation of viscosity with concentration suggests that the aggregates are in fast equilibrium with MPBd-UPy dimers (**Figure 4.6a**). The presence of different sizes of micellar-cluster was also confirmed using DLS (discussion in next section, **Figure 4.7**). However, when MPBd-UPy-4 is mixed with 16 % and 55 % by weight of its precursor MPBd-OH, the $\eta_{sp}/C$ was inconsistent fluctuating up and down depending on the concentration (**Figure 4.6b**). Nevertheless, the intrinsic viscosity decreases with increasing amounts of MPBd-OH in the mixture for < 0.3 g/dL (**Figure 4.6 b**). Although, the fluctuation of $\eta_{sp}$ with concentration in the mixed sample is sporadic, a repetition of the experiments confirmed the fluctuation pattern is indeed consistent. Thus, the deviation from the straight line is attributed to an interaction of free MPBd-OH chains entering into the micelles of dimeric MPBd-UPy aggregates and increases abruptly the micellar size at specific concentrations, disrupting the equilibrium of different sizes of aggregated dimers via donating hydrogen bonding (**Scheme 4.3**). This interaction must be slow in order for it to reflect significantly the $\eta_{sp}$ measurement which takes ~ 0.15 min.




**Scheme 4. 3:** Proposed dynamic equilibrium of micellar cluster aggregates in toluene solution of MPBd-UPy

### 4.4.4 Micellar structure and their temperature dependence

Application of static light scattering (SLS) to determine effective $M_n$ and the aggregation number of these star-like micelles was unsuccessful due to the low molecular weight of MPBd-UPy and a dynamic nature of the UPy aggregation. The attempts to measure the $dn/dc$ of these samples were also not successful. However, dynamic light scattering (DLS) studies were conducted in toluene at 25 °C using a 680 nm laser to determine the size of aggregates. The time-correlation function fitted with Contin analysis for MPBd-UPy-1, MPBd-UPy-4, and MPBd-$(UPy)_2$-1 shows evidence for the presence of micelles in the solution. Observed micellar population could be divided into three different populations. However, only one of the populations was predominately present in the solution. Further, the hydrodynamic volume ($R_h$) of these objects is highly dependent on the temperature and the concentration. At 25 °C, MPBd-UPy-1 at a concentration of 35 mg/mL gave three different populations with average sizes of ~2 nm, ~10 nm, and a major population at ~55 nm. The lowest size could result from dimers and other two higher *Rh* populations were attributed to micellar clusters**.** **Figure 4.7** shows the temperature dependent variations of micellar clusters for MPBd-UPy-1 and MPBd-UPy-4.Whereas, MPBd-UPy-2 and MPBd-UPy-3 did not give a good time-correlation function with detectable micellar population.[51] Similarly, no size detection was possible with all the precursor samples of MPBd-OH due to oligomeric nature of the samples and absence of association.

Increasing the measurement temperature gradually decreases the size of populations due to less hydrogen bonding. For example, MPBd-UPy-1 (**Figure 4.7a**), shows only two populations with a substantial reduction in the major population around 30 nm. Similarly, MPBd-UPy-4, and MPBd-$(UPy)_2$-1 (at equal concentrations of 55 mg/mL) show temperature dependent behavior, and the observed highest population sizes at 25 $^oC$ are 310 nm (**Figure 4.7 b**) and 700 nm (**Figure 4.8**), respectively. The presence of increased population size of MPBd-$(UPy)_2$-1 suggests that the two head groups of UPy favor increased aggregation. This indicates the micellar mechanism is solely governed by the UPy group aggregation and urethane linkage. **Figure 5b** shows the effect of temperature on the population sizes for MPBd-UPy-4. It was noticed that the higher size population can be regenerated by decreasing the solution temperature back to 5 °C. This dynamic clearly confirms the presence of equilibrium between different sizes of micellar clusters as shown in the **Scheme 4.3**. Meijer and coworkers

reported a formation of one-dimensional stacks in several types of UPy functionalized telechelic polymers linked via either urea or urethane linkages.[33] The results obtained with monochelic systems (MPBd-UPy) shown here indicate that the formation of long one-dimensional stacks of UPy dimerized domains is highly improbable in toluene.

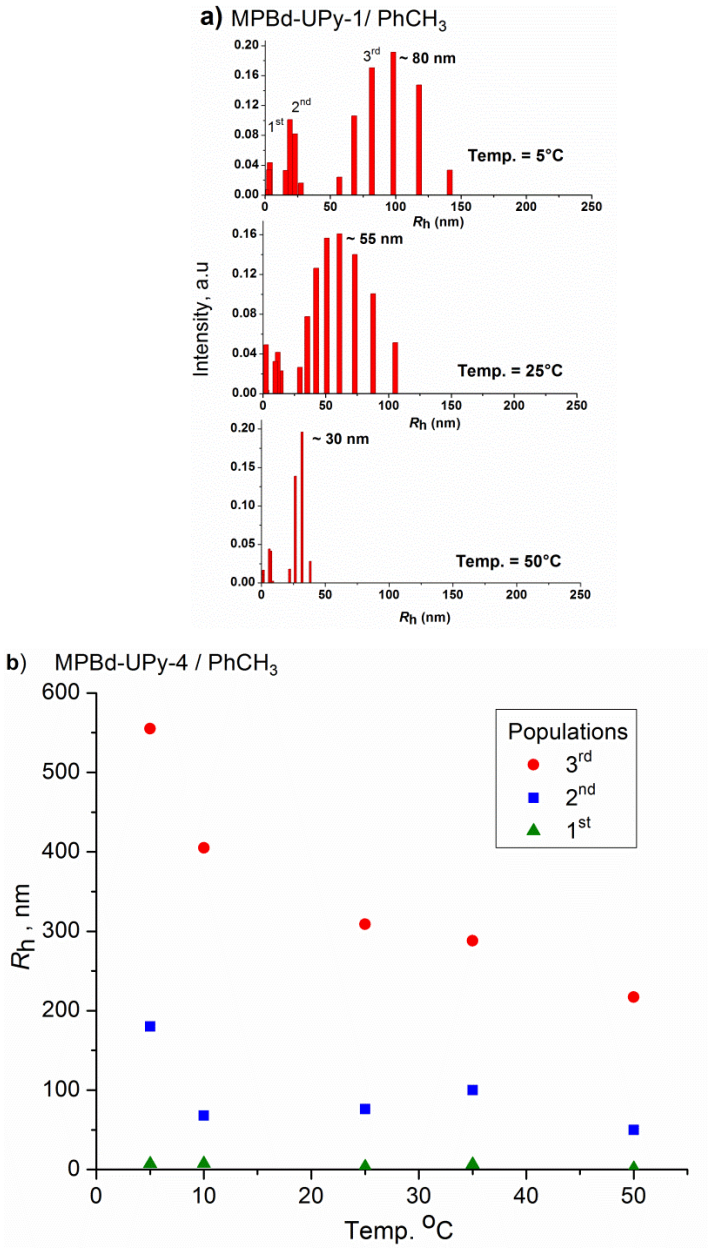



**Figure 4. 7:** Temperature dependent DLS histogram of a) MPBd-UPy-1 and b) plot of $R_h$ over temperature for different populations observed in MPBd-UPy-4.

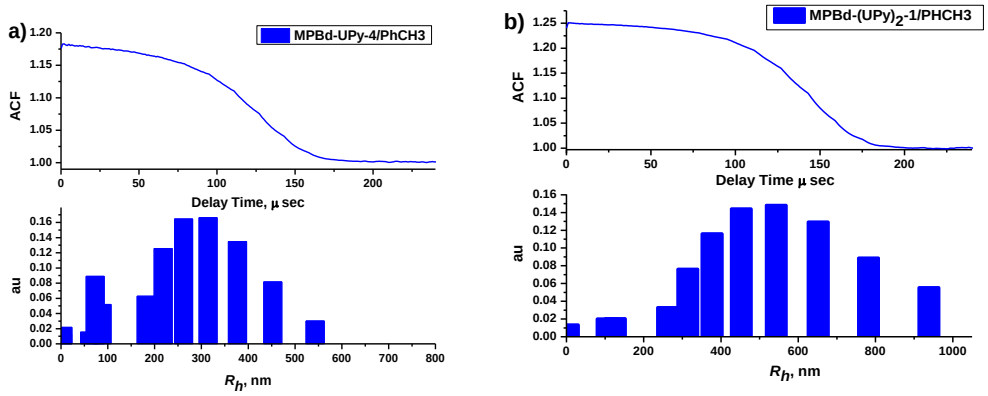



**Figure 4. 8:** Representive histograms of the a) MPBd-UPy-4 and b) MPBd-(UPy)$_2$-1 at 25 °C

### 4.4.5 Solid-state morphology of MPBd-UPy

In order to identify the presence of polar dimeric UPy aggregates, the MPBd-UPy samples were subjected to solid-state analysis by differential scanning calorimetric (DSC) and thin film surface morphology by AFM. DSC of MPBd-UPy shows broad endothermic peaks indicating the presence of an aggregated crystalline domain, which appears as a melting endotherm over a broad temperature range (35-90 °C) (**Figure 4.9**).Whereas, no significant changes are seen in the glass transition temperature ($T_g$) of the non-polar PBd domain. **Figure 4.9a** shows a DSC profile of three heating cycles for MPBd-UPy-1. Some of the samples show the presence of a second melting endothermic peak at a lower temperature than the main peak. The cooling curve shows a broad exothermic peak at a slightly lower temperature than the melting peak corresponding to the re-aggregation or crystallization. The enthalpy associated with the melting of the dimeric aggregated polar domains in the matrix of non-polar PBd is highest for the MBPd-UPy-1with a sharp endothermic peak. Whereas, MBPd-UPy-4 with 7,700 g/mol has a lowest enthalpy (2.64 J/g), and the peak is also very broad indicating a dependence of the polar UPy domain size on the chain length of PBd segment.

The extent of formation and the domain size of hydrogen bonded UPy aggregates depend on the amount of sample used for the DSC indicating that the aggregates are in equilibrium with bulk of dimeric MPBd-UPy chains. The enthalpy of the melting endotherm decreases slightly upon repeated heating cycles (**Figure 4.9a**). Enthalpy values of all the samples at repeated heating cycles show a similar trend (**Table 4.4**). However, the observations made recently by Meijer and Rowan and their coworkers in different hydrogen bonded systems

indicate that the reformation of aggregates are dependent on the aging time and mobility of the non-polar chain attached with UPy moiety.[32, 36] Although, the dimerization of UPy is very fast for low molecular weight compounds in aprotic solvents, the formation of crystalline polar-aggregates in the solid-state needs longer time and this duration is dependent on the chain-mobility in the case of polymeric or oligomeric compounds.

Long and coworkers have studied the molecular weight dependence on glass transition for the monochelic PI-UPy and observed no changes in the $T_g$. However, the rheological analysis showed that the viscosity of the melt is 100 times higher than the functionalized PI, which they attributed to the formation of multiple aggregates.[36] In the case of MPBd-UPy, a low $T_g$ of the PBd facilitates the chain mobility to quickly reform hydrogen-bonding. However, two UPy groups attached in MPBd-$(UPy)_2$-1 showed no appreciable formation of polar aggregates on the second and third heating cycles (**Figure 4.9b**). This could be attributed to a steric restriction imposed on the orientation of the UPy moiety to engage in hydrogen bonding when they are attached adjacent to each other in solid-state. We should note that this sample gave bigger size micellar aggregates in toluene indicating that the chain-mobility places a significant role in solid-state morphology. Interestingly, the solid-sample stored at room temperature for 12 h regenerates almost all the crystalline domains that were melted in the first cycle of heating in DSC (data not given). Therefore, the $T_g$ of the polymer, molecular weight, number and orientation of UPy functionality, and aging time all have significant effect on the formation and the dynamics of star-like micellar UPy domains.

**Table 4. 4:** Enthalpy values of MPBd-UPy

| Sample | Heating cycle | 1st peak | | 2nd peak | |
|---|---|---|---|---|---|
| | | $T_{1deagg}$ (°C) | Enthalpy (J/g) | $T_{2deagg.}$ (°C) | Enthalpy (J/g) |
| MPBd-UPy-1 | 1st | 6.49 | 1.122 | 70.87 | 18.980 |
| | 2nd | 6.69 | 1.245 | 70.62 | 18.430 |
| | 3rd | 7.24 | 1.147 | 70.67 | 18.310 |
| MPBd-UPy-2 | 1st | 20.78 | 0.495 | 52.52 | 6.258 |
| | 2nd | 19.60 | 0.483 | 51.00 | 5.598 |
| | 3rd | 19.20 | 0.462 | 50.61 | 5.80 |
| MPBd-UPy-3 | 1st | 1.69 | 0.273 | 46.77 | 6.564 |
| | 2nd | -2.03 | 0.160 | 48.72 | 6.280 |
| | 3rd | -2.40 | 0.138 | 48.43 | 5.980 |
| MPBd-UPy-4 | 1st | None | None | 48.02 | 2.642 |
| | 2nd | None | None | 51.55 | 2.730 |
| | 3rd | None | None | 53.52 | 2.519 |

In order to confirm the effect of chain-mobility, we synthesized MPBd-UPy (7,000 g/mol) with high *1,2-vinyl* content (94 %) exhibiting high $T_g$ (-10 $^oC$). A relatively low chain-mobility of this polymer compared to high 1,4 MPBd-UPys samples showed enthalpy of melting at 63 $^oC$ with 0.71 J/g. Upon second and subsequent heating cycles showed absence of melting endotherm and required very long period (~ 3 months) of aging at room temperature for regeneration of micellar-aggregates in DSC analysis (**Figure 4.10**).

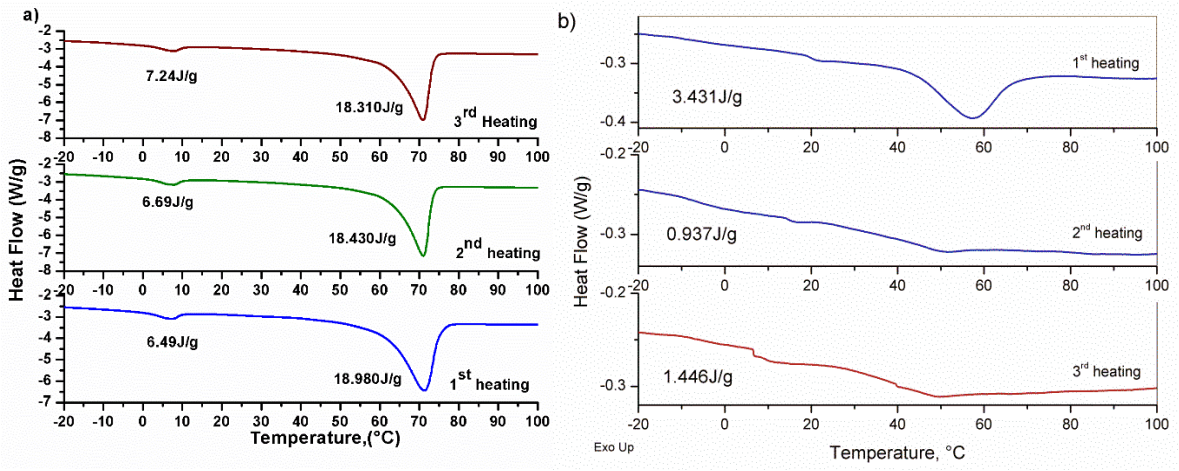



**Figure 4. 9:** DSC traces of repeated heating cycles of (a) MPBd-UPy-1 and (b) MPBd-$(UPy)_2$-1 systems.

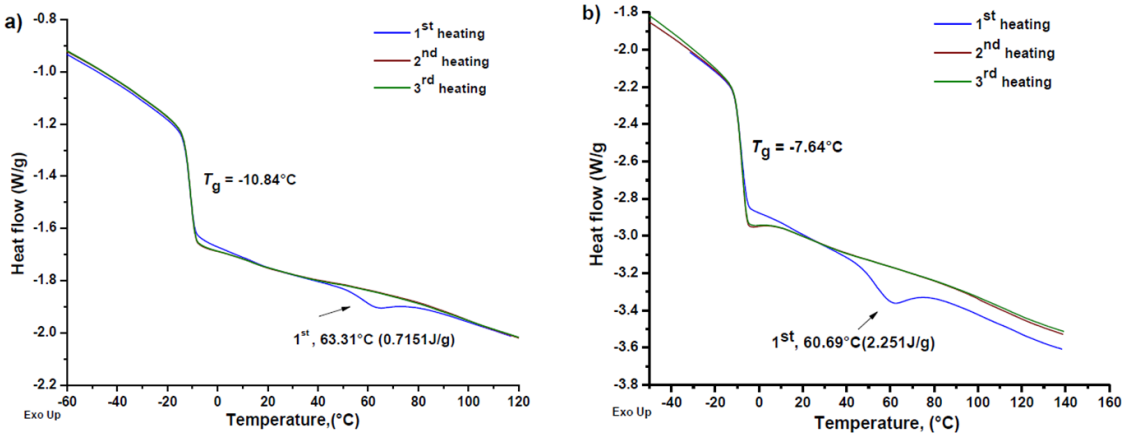



**Figure 4. 10:** DSC profile of MPBd-UPy 7 kg/mol (*1,2 vinyl* contents ~94 %), a) after first run, b) after ~3 months at 30 °C

### 4.4.6 Morphology of MPBd-UPy by Atomic Force Microscopy (AFM)

The solid-state morphology of MPBd-UPys was further examined using AFM. A freshly cleaved disc of mica was used for coating a drop of a toluene solution of MPBd-UPys (1 mg/mL) which was left on the mica for 12 h before imaging. Phase images of all the samples showed a fiber-like morphology arranged in a parallel lines without a long range order (**Figure 4.11 a**). There are some regions in several images wherein large gaps were seen without fibrous structure indicating that these structures are present in a matrix consisting of unassociated MPBd-UPy dimers.

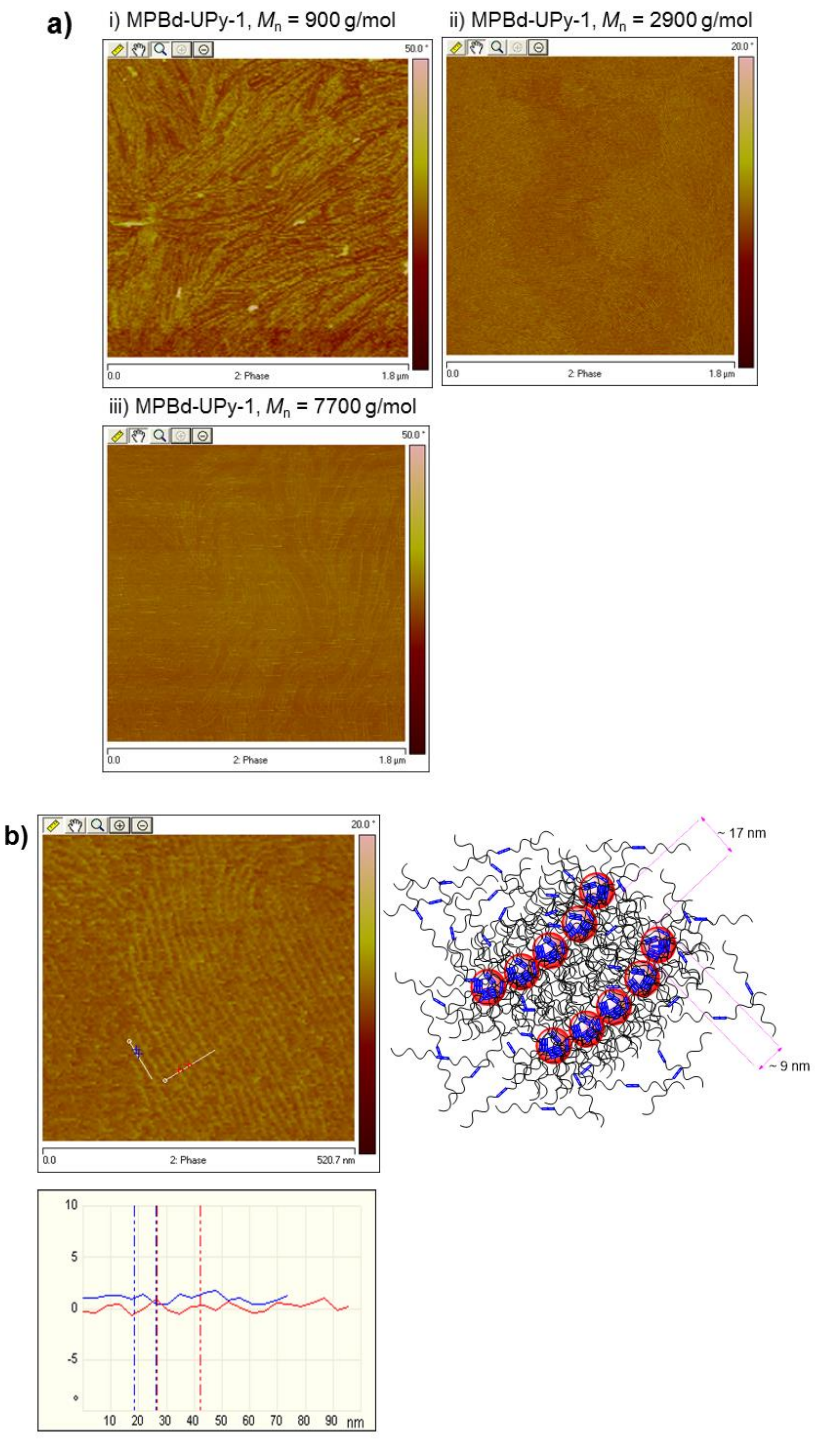



**Figure 4. 11:** Phase images of i) MPBd-UPy-1, ii) MPBd-UPy-3, and iii) MPBd-UPy-4 b) zoomed in image of MPBd-UPy-3 and an illustration representing features of micellar-cluster morphology.

Although the structure looks a like fibrous-like in a large scale image, the fibers are not continuous in nature. Upon careful examination, the image reveals that the parallel lines are composed of individual spherical micellar-clusters lined-up in an organized association with specific interline spacing depending on the molecular weight of MPBd-UPys. The sizes of individual clusters that may possibly contain stacks of randomly oriented UPy-dimers differ depending on the length of the PBd chain. The lower and higher molecular weights MPBd-UPys exhibit micellar-clusters whose sizes are in the range of 20-27 nm (**Figure 4.11a**). On the other hand, MPBd-UPy with an intermediate molecular weight, $M_{n,NMR}$ = 2,900 g/mol, shows a much smaller size of ~ 9 nm with an interline distance of ~ 17 nm (**Figure 4.11b**). This indicates that the hydrogen bonding, aggregation, and chain mobility are all competitively playing a role in driving the system to quasi-equilibrium state morphology at room temperature.

The morphology of MPBd-UPy samples were examined over a period of time up to 48 h. Images taken at different times indicate that the micellar-cluster size and line width increases gradually and smears out into the bulk of unassociated dimers, confirming a constant dynamics between MPBd-UPy unimer or dimers with aggregated polar micellar-clusters (**Figure 4.12**)

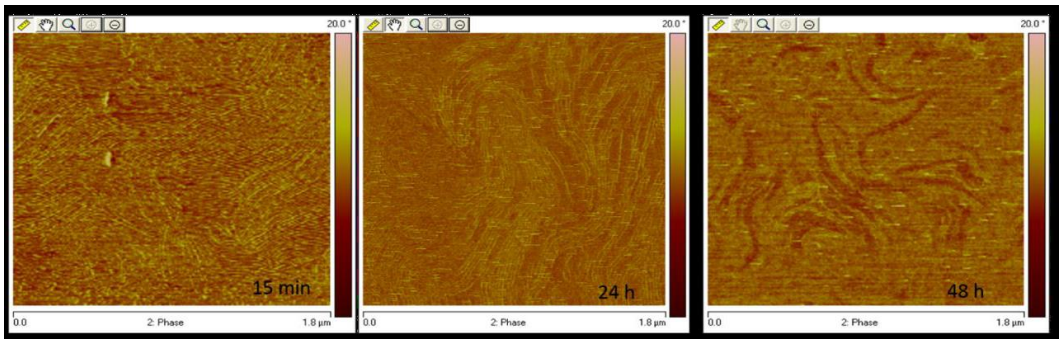



**Figure 4.12:** Time dependent morphology of MPBd-UPy-4 (from left to right, 15 min, 24 h, and 48 h after drop coating a thin film on freshly cleaved mica). The images were taken without changing the position of the sample in the AFM over 48 h. The size of the fibrous looking associated micellar clusters changes gradually over time indicating surface mobility of the associates induced by PBd segments (low $T_g$) at room temperature. Micellar cluster sizes are in the range of ~ 25-27 nm.

## 4.5 Conclusions

Different molecular weights of monochelic polybutadiene carrying 2-ureido-4-pyrimidon chain-end group (MPBd-UPys) have been synthesized and characterized using ω–hydroxyl functionalized polybutadienes (MPBd-OHs) as precursors. The presence of dimers via quadruple hydrogen-bonding of UPy moiety is evident in SEC analysis in THF at 30$^{o}$C. Specific viscosity of MPBd-UPys exhibited higher Higgins constant (> 0.40) confirming presence of micelles in the toluene solution, which consist of dimeric aggregates with hydrogen bonded UPy as core and polybutadiene as corona. Inconsistent specific viscosity of the mixture of MPBd-OH and MPBd-UPy in toluene confirms that the free MPBd-OH chains slowly engage in hydrogen bonding with the core and alter the overall distribution of the different sizes of micelles that are in equilibrium. DLS studies indicated three different sizes of micellar populations were present in toluene, whose intensity and $R_h$ (2 nm <$R_h$< 700 nm), especially the larger micelles, were found to decrease with increasing temperature due to breakage of hydrogen bonding.

A broad endothermic melting corresponding to the micellar clusters over a broad temperature range (35-90 $^{\circ}$C) has been confirmed by DSC for the MPBd-UPys. Reformation of micellar clusters on second and third heating cycles in DSC is strongly dependent on the molecular weight and the chain-mobility of PBd. AFM images of MPBd-UPys confirmed the formation of micellar clusters and their association into discontinuous fibrous-like structures that exist in equilibrium with the bulk of dimers.

The results indicate that the hydrogen-bonding via UPy dimerization, the formation of micellar clusters, their association, the nature of polymeric-chain, and the chain-mobility are all competitively playing a role in driving the system to a quasi-equilibrium state morphology at room temperature. This finding could be useful in understanding the dynamics of UPy-dimers in many telechelic systems.

## 4.6 References


(1) Lehn, J.-M. *Wiley-VCH, Weinheim* **1995**.

(2) Fouquey, C.; Lehn, J.-M.; Levelut, A.-M. *Adv. Mater.* **1990**, *2*, 254.

(3) Lehn, J.-M. *Makromol. Chem., Macromol. Symp.* **1993**, *69*, 1.

(4) Lehn, J.-M. *Polym. Int.* **2002**, *51*, 825.

(5) Kotera, M.; Lehn, J.-M.; Vigneron, J.-P. *J. Chem. Soc., Chem. Commun.* **1994**, *0*, 197.

(6) Lehn, J.-M.; Mascal, M.; Decian, A.; Fischer, J. *J. Chem. Soc., Chem. Commun.* **1990**, *0*, 479.

(7) Kotera, M.; Lehn, J.-M.; Vigneron, J.-P. *Tetrahedron* **1995**, *51*, 1953.

(8) Berl, V.; Huc, I.; Lehn, J. M.; DeCian, A.; Fischer, J. *Eur. J. Org. Chem.* **1999**, 3089.

(9) Lehn, J.-M. *Chem. Eur. J.* **1999**, *5*, 2455.

(10) Jorgensen, W. L.; Pranata, J. *J. Am. Chem. Soc.* **1990**, *112*, 2008.

(11) Park, T.; Todd, E. M.; Nakashima, S.; Zimmerman, S. C. *J. Am. Chem. Soc.* **2005**, *127*, 18133.

(12) Zimmerman, S. C.; Lawless, L. J. *Top. Curr. Chem.* **2001**, *217*, 95.

(13) Park, T.; Zimmerman, S. C.; Nakashima, S. *J. Am. Chem. Soc.* **2005**, *127*, 6520.

(14) Brunsveld, L.; Folmer, B. J. B.; Meijer, E. W. *MRS Bull.* **2000**, *25*, 49.

(15) Brunsveld, L.; Folmer, B. J. B.; Meijer, E. W.; Sijbesma, R. P. *Chem. Rev.* **2001**, *101*, 4071.

(16) Corbin, P. S.; Zimmerman, S. C. *J. Am. Chem. Soc.* **1998**, *120*, 9710.

(17) Corbin, P. S.; Zimmerman, S. C. *J. Am. Chem. Soc* **1998**, *120*, 9710.

(18) Beijer, F. H.; Sijbesma, R. P.; Kooijman, H.; Spek, A. L.; Meijer, E. W. *J. Am. Chem. Soc.* **1998**, *120*, 6761.

(19) St.Pourcain, C. B.; Griffin, A. C. *Macromolecules* **1995**, *28*, 4116.

(20) Alexander, C.; Jariwala, C. P.; Lee, C. M.; Griffin, A. C. *Macrom. Symp* **1994**, *77*, 283.

(21) Kihara, H.; Kato, T.; Uryu, T.; Fréchet, J. M. J. *Chem. Mater.* **1996**, *8*, 961.

(22) Söntjens, S. H. M.; Sijbesma, R. P.; van Genderen, M. H. P.; Meijer, E. W. *J. Am. Chem. Soc.* **2000**, *122*, 7487.

(23) Sibesma, R. P.; Beijer, F. H.; Brunsveld, L.; Folmer, B. J. B.; Hirschberg, J. H. K.; Meijer, E. W. *Science* **1997**, *278*, 1601.

(24) Sijbesma, R. P.; Meijer, E. W. *Curr. Opin. Colloid Interface Sci.* **1999**, *4*, 24.

(25) Greef, T. F. A.; Meijer, E. W. *Nature* **2008**, *453*, 171.

(26) Yamauchi, K.; Lizotte, J. R.; Hercules, D. M.; Vergne, M. J.; Long, T. E. *J. Am. Chem. Soc.* **2002**, *124*, 8599.

(27) Kang, L. H.; Lin, Q.; Armentrout, R. S.; Long, T. E. *Macromolecules* **2002**, *35*, 8738.

(28) Ligthart, G.; Ohkawa, H.; Sijbesma, R. P.; Meijer, E. W. *J. Am. Chem. Soc.* **2005**, *127*, 810.

(29) de Greef, T. F. A.; Nieuwenhuizen, M. M. L.; Sibesma, R. P.; Meijer, E. W. *J. Org. Chem.* **2010**, *75*, 598.

(30) Nieuwenhuizen, M. M. L.; de Greef, T. F. A.; van der Bruggen, R. L. J.; Paulusse, J. M. J.; Appel, W. P. J.; Smulders, M. M. J.; Sijbesma, R. P.; Meijer, E. W. *Chem. Eur. J.* **2010**, *16*, 1601.

(31) Dankers, P. Y. W.; Zhang, Z.; Wisse, E.; Grijpma, D. W.; Sijbesma, R. P.; Feijen, J.; Meijer, E. W. *Macromolecules* **2006**, *39*, 8763.

(32) van Beek, D. J. M.; Spiering, A. J. H.; Peters, G. W. M.; te Nijenhuis, K.; Sijbesma, R. P. *Macromolecules* **2007**, *40*, 8464.

(33) Kautz, H.; van Beek, D. J. M.; Sijbesma, R. P.; Meijer, E. W. *Macromolecules* **2006**, *39*, 4265.

(34) Sivakova, S.; Bohnsack, D. A.; Mackay, M. E.; Suwanmala, P.; Rowan, S. J. *J. Am. Chem. Soc.* **2005**, *127*, 18202.

(35) Sivakova, S.; Rowan, S. J. *Chem. Soc. Rev.* **2005**, *34*, 9.

(36) Yamauchi, K.; Lizotte, J. R.; Hercules, D. M.; Vergne, M. J.; Long, T. E. *J. Am. Chem. Soc.* **2002**, *124*, 8599.

(37) Karatzas, A.; Talelli, M.; Vasilakopoulos, T.; Pitsikalis, M.; Hadjichristidis, N. *Macromolecules* **2006**, *39*, 8456.

(38) Feldman, K. E.; Kade, M. J.; de Greef, T. F. A.; Meijer, E. W.; Kramer, E. J.; Hawker, C. J. *Macromolecules* **2008**, *41*, 4694.

(39) Feldman, K. E.; Kade, M. J.; Meijer, E. W.; Hawker, C. J.; Kramer, E. J. *Macromolecules* **2009**, *42*, 9072.

(40) Uhrig, D.; Mays, J. W. *J. Polym. Sci., Part A: Polym. Chem.* **2005**, *43*, 6179.

(41) Hadjichristidis, N.; Iatrou, H.; Pispas, S.; Pitsikalis, M. *J. Polym. Sci., Part A: Polym. Chem.* **2000**, *38*, 3211.

(42) Folmer, B. J. B.; Sijbesma, R. P.; Versteegen, R. M.; van der Rijt, J. A. J.; Meijer, E. W. *Adv. Mater.* **2000**, *12*, 874.

(43) Runyon, J. R.; Barnes, D. E.; Rudd, J. F.; Tung, L. H. *J. Appl. Polym. Sci.* **1969**, *13*, 2359.

(44) Huggins, M. L. *Ann. N.Y. Acad. Sci.* **1942**, *43*, 1.

(45) Huggins, M. L. *J. Am. Chem. Soc* **1942**, *64*, 2716.

(46) Gundert, F.; Wolf, B. A. *Makromol. Chem.* **1986**, *187*, 2969.

(47) Bohdanecký, M. *Collect. Czech. Chem. Commun.* **1970**, *35*, 1972.

(48) Lewandowska, K.; Staszewska, D. U.; Bohdanecký, M. *Eur. Polym. J.* **2001**, *37*, 25.

(49) Muthukumar, M.; Freed, K. F. *Macromolecules* **1977**, *10*, 899.

(50) Bicerano, J.; Douglas, J. F.; Brune, D. A. *J. Macromol. Sci., Polym. Rev.* **1999**, *39*, 561.

(51) Fetters, L. J.; Hadjichristidis, N.; Lindner, J. S.; Mays, J. W. *J. Phys. Chem. Ref. Data* **1994**, *23*, 619.

# Chapter 5: Synthesis and Characterization of Telechelic Polybutadienes Functionalized with Ureidopyrimidone

## Abstract

Synthesis and characterization of UPy telechelics with a quadruple hydrogen bonding site, 2-ureido-4[1*H*]-pyrimidone (UPy), are described. Anionic polymerization was used to prepare a series of α, ω-dihydroxyl terminated polybutadiene with lower *1,2-vinyl* groups, which was subsequently reacted with UPy-synthon to make UPy-telechelics. Also, UPy-PBd-UPy with higher *1,2-viny*l groups were made. Properties of these polymers were evaluated as a function of *1,2-vinyl* contents. Role of polymer molecular weight, polydispersity, microstructure, and $T_g$ on the property enhancement of UPy telechelics was analyzed by solution viscometry, DSC, and AFM surface and bulk morphology. AFM images give parallel association of micellar clusters. Dynamics of micellar-cluster associated UPy domains (aggregation) with unassociated chain extended dimers (linear chain exntesion) are strogly influenced by *1,2-vinyl* contents.

## 5.1 Introduction

Telechelic oligomers that are chain-end functionalized with self-complementary hydrogen bonding moieties show distinct physical properties like high molecular weight polymers.[1-4] The formation of inter-molecular hydrogen bonding in end-functionalized telechelic oligomers leads to a chain-extension and converts oligomers into high molar mass polymers that exhibit special dynamic mechanical and thermal properties.[4] Meijer and co-workers observed a significant enhancement of physical properties when a strong quadruple hydrogen bonding moiety such as ureidopyrimidone (UPy) is used to functionalize telechelic oligomers.[1,3-7 8,9]

Meijer and group extensively studied the property enhancement of UPy functionalized telechelic oligomers, especially non-polar telechelic hydrogenated polybutadiene, poly(ethyelene-*co*-1-butene) (UPy-(PE-*co*-PB)-UPy).[10] However, various telechelic systems have been studied in the literature with UPy chain-end functionalization, which do not produce enhanced physical properties of UPy-telechelics to a similar extent as that of UPy-(PE-*co*-PB)-UPy.[4,8,10-15] Recent studies gave importance to the effect of lateral hydrogen bonding of urethane and urea groups tandem with UPy hydrogen bonding to form one dimensional stakes.[5,10,16] It was also reported, even in the presence of additional urethane or urea group, a certain type of non-polar polymer with a low $T_g$ backbone does not show a similar physical property enhancement.[17] For example, telechelic *trans*-PBd functionalized with UPy end group, prepared by ring opening metathesis polymerization (ROMP) of 1,5 cyclootadiene with UPy functional chain transfer agent, did not produce thermoplastic elastomeric material similar to UPy-(PE-*co*-PB)-UPy.[17] Noticeably, telechelic polydimethylsiloxane (PDMS) (low $T_g$ and apolar) end-functionalized with UPy group, also failed to give thermoplastic elastomer.[18] Authors attributed this behavior to an incompatibility of soft PDMS with a rigid UPy group. It is worth mentioning here that chemically connected (covalent or hydrogen bonding) incompatible phases in general will produce microphase separation and in the case of hard and soft phases will produce thermoplastic properties. Thus, the poor mechanical properties of these UPy telechelic systems observed by the authors may also be attributed to the efficacy of UPy hydrogen bonding and the molecular properties of the linking oligomer chains.

In **Chapter 4**, we have observed that a well-defined and narrow dispersed monochelic MPBd-UPy system forms micellar clusters of hydrogen bonded UPy-dimers that exist in equilibrium with unimer.[19] It was expected that the monochelic MPBd-UPy would form one-

dimensional dimeric UPy stacks as reported in the literature for other telechelic systems.[10] In contrary, our results clearly indicated that the thermodynamic stability of micellar three-dimensional association competes with the tandem one-dimensional UPy dimer stacks formation. It was also observed that the dynamics of UPy dimer aggregation are strongly governed by the mobility of the PBd chain (low $T_g$ vs high $T_g$).[19] On the other hand, telechelic PBd functionalized with UPy, UPy-PBd-UPy, will have more probability to undergo linear chain extension and may further form networks. Moreover, PBd is a non-polar polymer, and by manipulating its macrostructure one can get PBd with different $T_g$ characteristics. UPy telechelics of PBd with narrow molecular weight distribution will provide an ideal backbone to evaluate the effect of chain dynamics on the UPy chain end association with respect to different $T_g$s. Therefore, examination of different types of telechelic PBd functionalized with UPy is very important.

Hydroxyl telechelic polybutadiene (HO-PBd-OH) with different microstructures and $T_g$s could be prepared using anionic polymerization. A high *1,4*-addition microstructure is formed in non-polar solvents, whereas in the presence of polar additives or in polar solvents, a low *1,4* addition and a high *1,2-vinyl* microstructure is formed in anionic polymerization with lithium as counter ion.[20] In order to understand the UPy hydrogen bonding association dynamics in telechelic PBd system, especially the effect of microstructure on the chain-extension and further association, this chapter will discuss the synthesis and characterization of UPy-PBd-UPy with different microstructures and examine their solution and solid-state properties.

## 5.2 Experimental Section

Telechelic polybutadiene was synthesized by using a similar procedure employed for the synthesis of monochelic polybutadiene, except that the Bd was polymerized in benzene with the hydroxyl protected initiator and end-capped with ethylene oxide to obtain hydroxyl telechelic PBd with low *1,2-vinyl* content. Commercial Krasol-hydroxyl terminated polybutadienes and their hydrogenated analogue were obtained from Cray Valley. The initiator *ter*-butyldimethylsilyloxy (TBDMS) propyl lithium (PFI) (1.0 M) was purchased from Gelest and diluted with known amount of hexane to get a desired final concentration of 0.6 M under vacuum and the solution was split into different calibrated ampules with a break-seal.

### 5.2.1 Synthesis of telechelic hydroxyl-polybutadiene (HO-PBd-OH)

Anionic polymerization of butadiene was conducted in a custom made 1L glass reactor by following a standard all glass high-vacuum technique.[21,22] Details of the operational protocols for high vacuum anionic polymerization are given in Chapter 3. Telechelic hydroxyl polybutadienes (HO-PBd-OH) with predetermined molecular weight were synthesized using appropriate feed ratios of butadiene and hydroxyl protected alkyllithium initiator (PFI, Gelest) in benzene at 25 °C for 24 h. A typical synthetic procedure for HO-PBd-OH-1 is given below.

A 1L glass reactor was attached with ampules of pure reagents containing 108.0 mL (148 mmol) of 1,3-butadiene (dissolved in 220 mL of benzene), 53.0 mL (35.77 mmol) of PFI 0.675M solution in hexane, 5.0 mL of ethylene oxide (160 mmol), and 2.0 mL of methanol (49.5 mmol). The reactor was connected to a high vacuum line with a glass constriction and a ground-glass joint and flame dried under high vacuum for 30 min. About 400 mL of pure benzene was distilled directly into the reactor using liquid nitrogen-bath from the solvent reservoir in the vacuum line. The reactor was removed from the vacuum line by sealing at the glass-constriction, while the solvent was completely frozen under vacuum. After bringing the reactor to room temperature, the initiator (PFI) was introduced into the reactor by breaking the seal of the ampule. Then, the reactor was rinsed and cleaned by using the initiator solution. After collecting all the initiator and benzene into the round bottom of the flask, the reactor was kept in the water bath at ~50 °C. And then, a diluted benzene solution of 1,3-butadiene was added through opening a break-seal. The addition of monomer in general is done at room temperature. As our target molecular weight is oligomeric in nature and in order to obtain narrow molecular weight distribution, monomer was added slowly at higher temperature. ***Extreme caution should be observed while adding low boiling monomer solution into the reactor kept at 50 ºC.*** After the addition, the hot water bath was removed and the polymerization was continued for 12 h at 25 °C.

The living polybutadienyl lithium was chain-end capped with the addition of ethylene oxide at ~5 °C and stirred for 4 h. Upon the addition of ethylene oxide, a colorless living polybutadienyl anion solution in benzene turned into pale yellow, which became colorless after stirring for 2 h at 25 °C. A small portion of the polymer solution was precipitated into methanol in order to determine the molecular weight based on TBDMS group by $^{1}$H NMR. And the rest of the solution was precipitated into an excess methanol containing a small amount of HCl acid

and BHT as antioxidant (0.1 wt % for total polymer). Polymer was washed with methanol until the filtrate became neutral. Methanol was decanted and the polymer was recovered. The entire polymer was dissolved in THF and treated with 10 time's excess tertabutylammonium fluoride TBAF (1M solution in THF) with respect to initiator concentration for deprotection of the TBDMS group. The solution was stirred overnight and the hydroxyl telechelic polymer was precipitated in methanol. In order to completely remove the residual TBAF, the polymer was dissolved in chloroform and passed through a short alumina column. A small amount of antioxidant was added and the chloroform was removed using a rotatory evaporator and the obtained polymer was stored at -20 °C in a tight jar. Theoretical molecular weight for this reaction was, $M_{n,th}$ = 2,230 g/mol, and the obtained $M_{n\,(SEC)}$ = 2,700, ($M_w/M_n$ = 1.06) and $M_{n,NMR}$ = 2,300 g/mol.*)*

### 5.2.2 Synthesis UPy-synthon

UPy-synthon (UPy-NCO) was synthesized by using a reported procedure.[4] Details are given in Chapter 3.

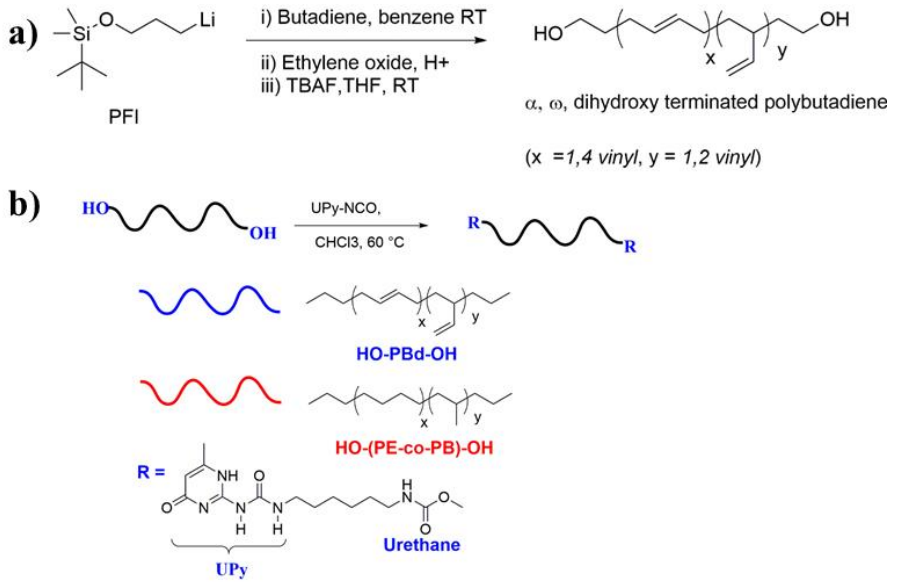
### 5.2.3 UPy functionalization of telechelic Polybutadiene (UPy-PBd-UPy)

Telechelic α, ω-bishydroxyl polybutadiene (HO-PBd-OH) was reacted with UPy-NCO synthon by using a reported procedure.[19] A representative example of the UPy-PBd-UPy-6 is given here, 70.0 g of HO-PBd-OH-6 (42 mmol of hydroxyl groups, $M_{n,NMR}$ = 3,350g/mol, 57 % *1,2-vinyl*) was taken in a 1L round bottom flask, equipped with a ground joint and attached to the vacuum line. The polymer was dried under high vacuum at 70-80 °C for 2 h to remove protic impurities such as water and alcohol. After drying, ~ 750 mL of chloroform was directly distilled into the flask from the vacuum-line (*It is highly recommended to use HPLC grade chloroform or chloroform without ethanol as a stabilizer, since the traces of ethanol may co-distill and react with UPy-synthon; thereby lowering the effective concentration and the efficiency of the functionalization*). The reaction flask filled with nitrogen and removed from the vacuum line under a nitrogen blanket, and then, quickly UPy synthon, 24.6 g (42 mmol), was added along with a few drops of the catalyst, DBDTL. The reaction was stirred at 60 °C for 24 h. The progress of the reaction was monitored using $^1$H NMR. A disappearance of the signal at ~3.64 ppm (-$CH_2$-$\underline{CH_2}$-OH), and an appearance of a new signal at ~ 4.1 ppm (-$CH_2$-$\underline{CH_2}$-O-CONH-), corresponding to the formation of urethane linkage were used to confirm the quantitative conversion (~ 100 %) of end-group.

After the reaction, the excess UPy-NCO synthon and its side products were removed by a treatment with silica gel. The reaction mixture was stirred with 30 g of silica and a few drops of DBDTL at 60 °C for 2 h. The reaction mixture was diluted with 1L of chloroform and filtered. In case of high viscosity, an additional amount (1L) of chloroform was added and the entire solution was passed through a short silica column (column had 10 cm diameter and 15 cm long silica packing). Then, the polymer solution was concentrated under reduced pressure to ~300 mL and precipitated into a 2 L of methanol containing 0.1 % BHT as stabilizer with respect to the polymer weight. The polymer was obtained as a white sticky solid, which upon further washing with methanol and drying in oven at 60 °C for 24 h gave a white transparent solid. Yield: 48.6 g (60 %), $M_{n,th}$ = 3,940 g/mol, $M_{n,GPC}$ /0.50 = 3,430 g/mol, *PDI* = 1.15 $M_{n,NMR}$ = 3,950 g/mol. FTIR/ATR showed an absence of residual UPy-synthon in the final product.

## 5.3 Results and discussion

Anionic polymerization of 1,3-butadiene was performed using a hydroxyl protected alkyllithium initiator, *tert*-butyldimethylsilyloxy-propyllithium (TBDMSPrLi) in benzene at 25 °C. The living oligobutadienyl lithium chains were end-capped with ethylene oxide in order to obtain α, ω-hydroxyl telechelic polybutadiene, HO-PBd-OH with low *1,2-vinyl* microstructure (**Scheme 5.1**) The polymerization was initiated at 50 °C to obtain narrow molecular weight distribution ($Đ$ < 1.10) and the propagation was continued at 25 °C. The protected silyl group, TBDMS, was removed from the polymer using TBAF treatment. As the initiation step was carried out at 50 °C, the obtained polymers have microstructures of approximately 85 % of *1,4* enchainment and 15 % of *1,2-vinyl* contents.




**Scheme 5.1:** Synthesis of hydroxyl telechelic polybutadienes by anionic polymerization (a) and chain-end transformation of various hydroxyl terminated polybutadienes (HO-PBd-OH) and hydrogenated polybutadienes (HO-(PE-*co*-PB)–OH) into UPy-telechelics (b).

The HO-PBd-OH (~ 15 % *1,2-vinyl*) samples with different molecular weights were obtained by varying feed ratios of monomer to initiator (**Table 5.1**). Also, three more samples of HO-PBd-OH with higher *1,2-vinyl* content, ~57 %, and their hydrogenated analogues (HO-(PE-*co*-PB)-OH) were obtained from the Cray Valley. Hydrogenation of HO-PBd-OH (~ 15 % *1,2-vinyl*) sample was performed using *p*-toluenesulfonyl hydrazide by following a reported procedure.[23] Also, hydroxyl terminated PBd, with 24 % *1,2-vinyl*, with $M_n$, 1200 g/mol ($M_w/M_n$ ~2.0) was obtained from Sigma-Aldrich. This polymer was dissolved in THF and precipitated in large excess methanol. After precipitation obtained polymer has $M_{n,SEC}$ /0.50 = 2,400 g/mol, *PDI* = 1.80 $M_{n,NMR}$ = 3,000 g/mol. This was subsequently converted into UPy-PBd-UPy-7. The molecular characterization of the polymers is given in the **Table 5.1**.

The conversion of hydroxyl functionality to the 2-ureido-4[1*H*]-pyrimidone (UPy) quadruple hydrogen bonding group was readily achieved using isocyanate coupling with the UPy-NCO.[24] Upon the chain-end modification with the UPy group, the hydroxyl telechelics

PBds were transformed from viscous liquid into brittle solids for low *1,2-vinyl* and to thermoplastic elastomers for high *1,2-vinyl* content UPy-PBd-UPys.

**Table 5.1:** $^{1}$H NMR and SEC characterization of the functional (X) polybutadienes with the hydroxyl (HO-PBd-OH) and ureidopyrimidone (UPy-PBd-UPy)

| Entry | Samples[a] | vinyl % [b] | HO-PBd-OH | | | UPy-PBd-UPy | | |
|---|---|---|---|---|---|---|---|---|
| | | | $M_{n,SEC}$[e] g/mol | $M_{n,NMR}$[f] g/mol | $Đ$[g] | $M_{n,SEC}$[e] g/mol | $M_{n,NMR}$[i] g/mol | $Đ$[g] |
| 1 | X-PBd-X-1 | 16 | 2,700 | 2,300 | 1.07 | 2,500 | 2,900 | 1.06 |
| 2 | X-PBd-X-2 | 15 | 5,600 | 4,700 | 1.05 | 5,000 | 5,300 | 1.04 |
| 3 | X-PBd-X-3 | 13 | 8,100 | 14,300 | 1.04 | 8,000 | 9,100 | 1.03 |
| 4 | X-PBd-X-4 | 57 | 2,500 | 2,350 | 1.15 | 2,800 | 2,950 | 1.18 |
| 5 | X-PBd-X-5 | 57 | 4,900 | 5,500 | 1.16 | 5,100 | 6,100 | 1.18 |
| 6 | X-PBd-X-6 | 57 | 3,540 | 3,350 | 1.14 | 3,430 | 3,950 | 1.15 |
| 7 | X-PBd-X-7 | 24 | 2,400 | 3,000 | 1.80 | 2,900 | 3,600 | 1.75 |
| 8 | X-(PE-*co*-PB)-X-1 | 16[c] | 3,450 | 2,500 | 1.05 | 3,600 | 3,100 | 1.05 |
| 9 | X-(PE-*co*-PB)-X-4 | 57[d] | 2,900 | 2,400 | 1.13 | 2,800 | 3,000 | 1.16 |
| 10 | X-(PE-*co*-PB)-X-6 | 57[d] | 3,440 | 3,550 | 1.13 | 3,060 | 4,150 | 1.14 |

a) telechelic polybutadiene with functional group (X), b) % of *1,2* and *1,4* addition in the polymer determined by $^{1}$H NMR(error ±1%). c) and d) after hydrogenation, % of isobutylene e) number average molecular weight ($M_n$) of the main peak determined based on PS calibration with hydrodynamic volume corrected for PBd (1.99), f) $M_n$ calculated based on –$CH_2$-$\underline{CH_2}$-OH end group (3.64 ppm) from $^{1}$H NMR in $CDCl_3$, g) determined from SEC, i) $M_n$ calculated based on –$CH_2$-$\underline{CH_2}$-O-CONH- (4.1ppm).

$^{1}$H NMR spectra of HO-BPd-OH-1 and UPy-PBd-UPy-1 (15 % *1,2-vinyl*) are shown in **Figure 5.1**. The methylene proton adjacent to the hydroxyls appears at ~ 3.64 ppm, which upon UPy attachment shifts to ~ 4.1 ppm. In all the samples, the disappearance of this peak after UPy attachment confirms the efficiency of end-group transformation (96-100 %).

Furthermore, the characteristic UPy amide protons appear at 10.12, 11.85, and 13.12 ppm confirming an efficient end-group transformation. The molecular weights calculated based on the –$CH_2$-$\underline{CH_2}$-OH end group (3.64 ppm) are close to the theoretically calculated ones based on the feed ratio of monomer to initiator. Similarly, **Figure 5.2** shows the $^1$H spectrum of the HO-PBd-OH-5 and UPy-PBd-UPy-5 (57 % *1,2-vinyl*). The $^1$H NMRs of UPy functional hydrogenated polymers, UPy-(PE-*co*-PB)-UPy, with the precursor hydroxyl telechelics, HO-(PE-*co*-PB)-OH, are shown in **Figure 5.3** and **Figure 5.4**. All the samples are free from unreacted UPy-NCO as supported by the ATR/FTIR spectra of these samples, which showed the absence of –NCO peak at 2280 cm$^{-1}$.

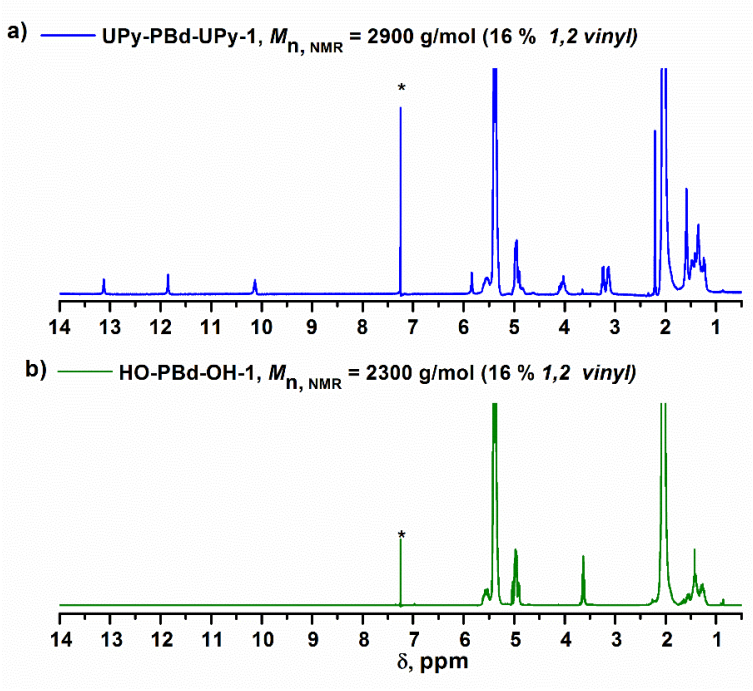



**Figure 5. 1:** $^1$H NMR spectra of a) UPy-PBd-UPy-1 and b) HO-PBd-OH-1

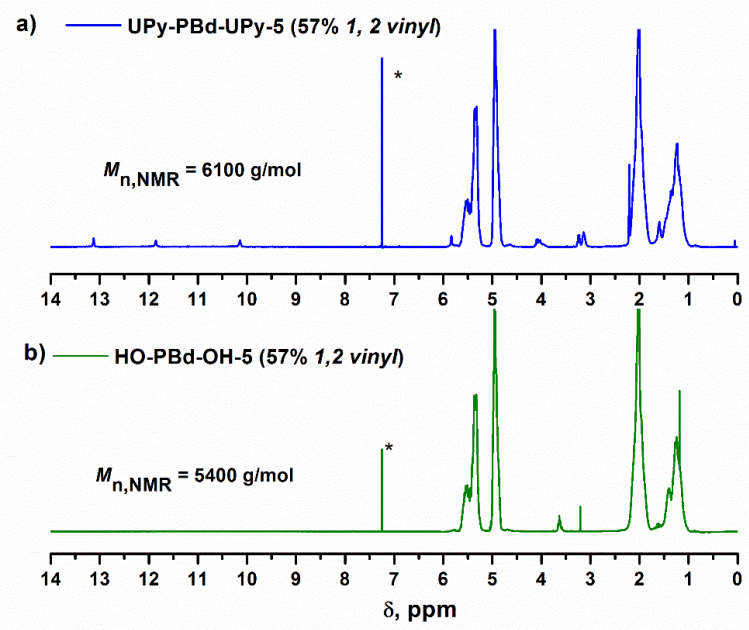



**Figure 5. 2:** $^{1}$H NMR spectra of a) UPy-PBd-UPy-5 and b) HO-PBd-OH-5

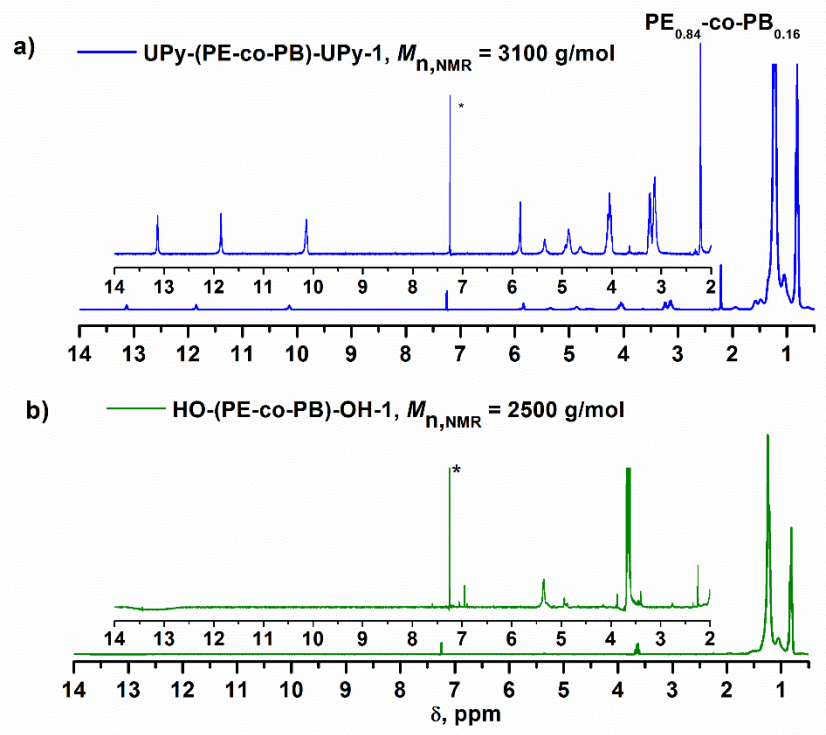



**Figure 5. 3:** $^{1}$H NMR spectrum of a) UPy-(PE-*co*-PB)-UPy-1 and b) HO-(PE-*co*-PB)-OH-1

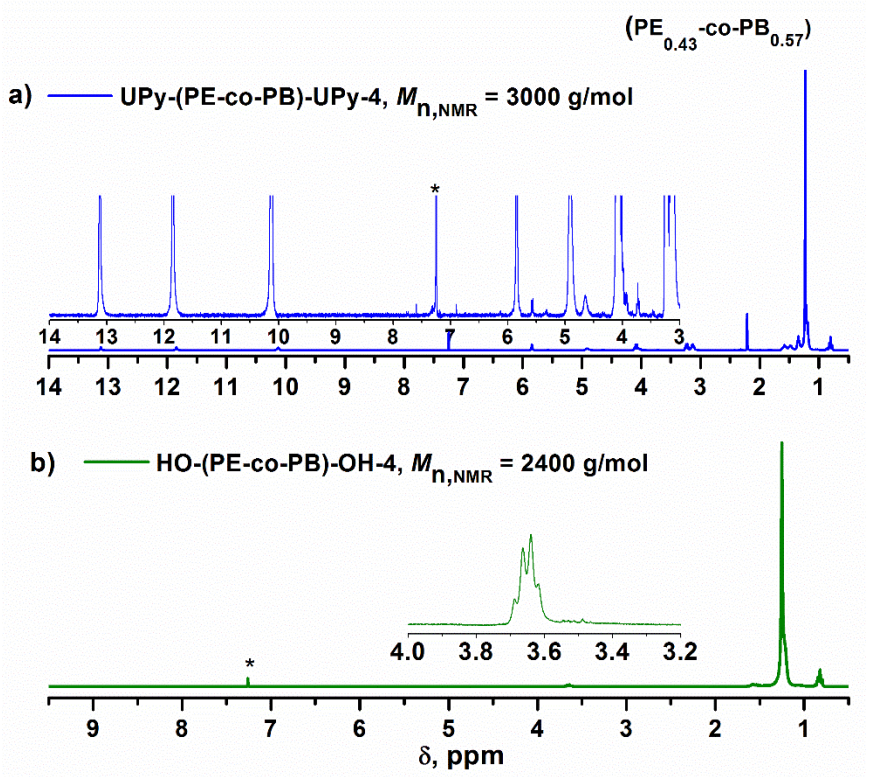



**Figure 5. 4:** [1]H NMR showing a) UPy-(PE-*co*-PB)-UPy-4 and b) HO-(PE-*co*-PB)-OH-4

The SEC traces of HO-PBd-OH and UPy-PBd-UPy with low and high *1,2-vinyl* contents polymers are shown in **Figure 5.5** and **Figure 5.6**, respectively. The attachment of UPy group slightly shifted the elution volume to the right side indicating a decrease in the molecular weight compared to the HO-PBd-OH precursor. The presence of intermolecular hydrogen bonding via UPy dimerization of telechelic PBds would have increased the molecular weight much higher than the precursor HO-PBd-OH. The $M_{n,SECs}$ are not increased, which confirms the absence of chain-extension in THF.

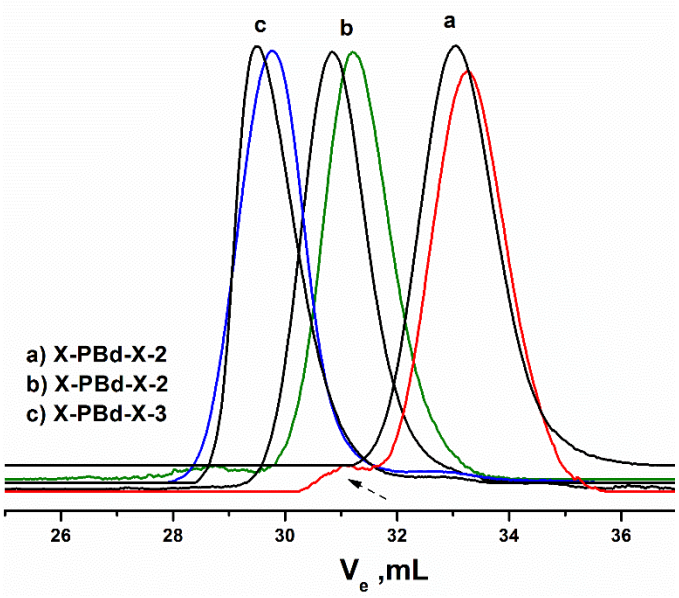



**Figure 5. 5:** SEC traces of telechelic UPy, black like indicates hydroxyl precursor, and colored line indicates UPy functionalized polymers (arrow indicates presence of dimeric peak)

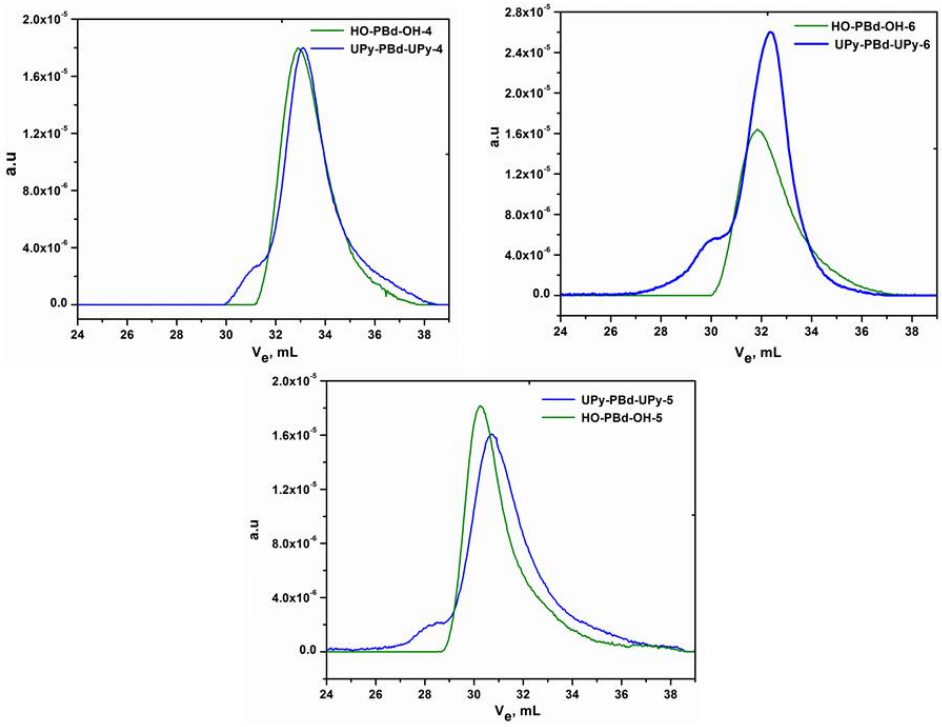



**Figure 5. 6:** SEC traces of hydroxyl and UPy telechelics of PBd with *1,2-vinyl* contents of ~57%

A decrease in the peak maximum molecular weight is contrary to the expectation of a slight increase in the molecular weight after attaching two UPy tags, even in the absence of chain-extension occurring in THF and in the size-exclusion process. The decrease in molecular weight was not uniform and appears to be dependent on the molecular weight and the microstructure. On the other hand, except for a high molecular weight sample (Table 5.1, entry 3), all of the samples showed a small high molecular weight hump with nearly double the molecular weight of the main peak. These observations suggest that a slight reduction in hydrodynamic volume of UPy-telechelics in THF may be attributed to a portion of UPy telechelics forming branched polymer and dimers that are coexisting along with unimers under SEC condition.

### 5.3.1 Intrinsic viscosity of telechelic polymers

The hydrogen bonding in solution is generally promoted in non-polar solvent compared to polar solvent. In the case of SEC, which was performed in a polar solvent (THF), UPy-PBd-UPy samples did not show significant hydrogen bonding association. Thus, the solution viscosity of UPy-PBd-UPy samples was examined in toluene, a non-polar solvent to investigate hydrogen bonding association in solution.

**Figure 5.7a** shows the log-log plot of $\eta_{sp}$ vs [C] for several polymers (**Table 5.1**, entry 3, 4, 5 and 6) in toluene at 25 $^{o}$C. The viscosity behavior of chain-end associating polymers can be explained using Cates model for reversible hydrogen boned polymers.[25] If the double logarithmic plot has a slope value in the range of 3.5-3.7, it is considered as an evidence for the existence of very high molecular weight polymer due to linear chain extension. The viscosity curves show a non-linear behavior (**Figure 5.7**). The viscosity at lower concentration region 3 mM to 10 mM (between log -2.5 to -2.0) has a lower slope dependence whereas at higher concentration region 10 mM to 25 mM (between log -2 to -1.6), it has much higher slope. This slope variation may be attributed to overlap concentration of telechelic oligomers in the solution or this can also be attributed to the extent of UPy hydrogen bonding leading to more branched net-work formation (**Figure 5.7a**). In contrast, UPy-PBd-UPy-7 sample with a broad dispersity, 24 % *1,2-vinyl* groups and $M_n$ in between UPy-PBd-UPy-4 and UPy-PBd-UPy-6 shows a substantial difference. Amongst all the samples, this polymer gave highest viscosity. Furthermore, a distinct region on a curvy plot with a much higher slope values can

be attributed to a broad polydispersity of this sample, alongwith ring-chain equilibrium (**Figure 5.8**).[26]

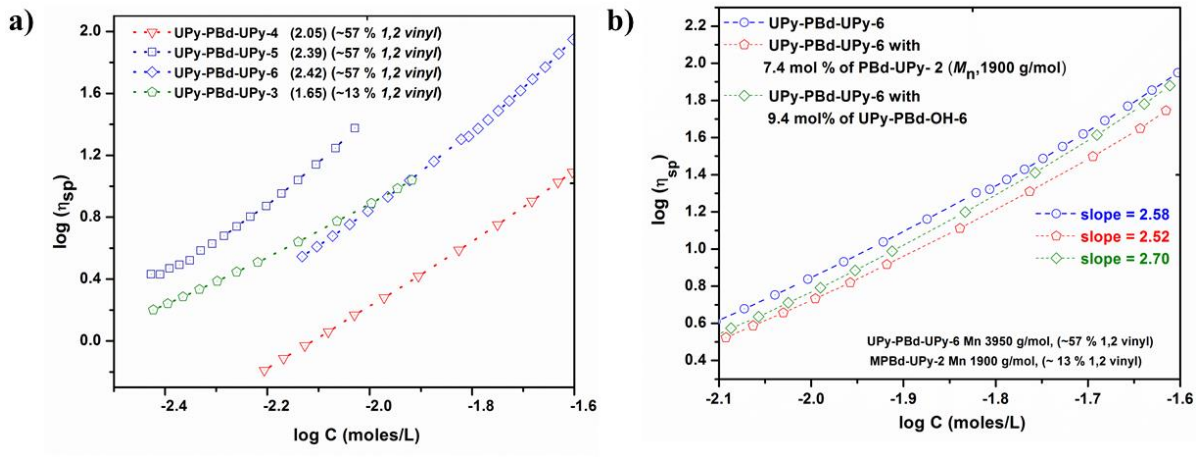



**Figure 5. 7:** Double logarithmic plots for the solution viscosity of UPy-PBd-UPy samples with slope values reported in the bracket are for the similar concentration range for all the polymers (a); and effect of monofunctional impurity (chain stopper) and hydroxyl functional impurities (b)

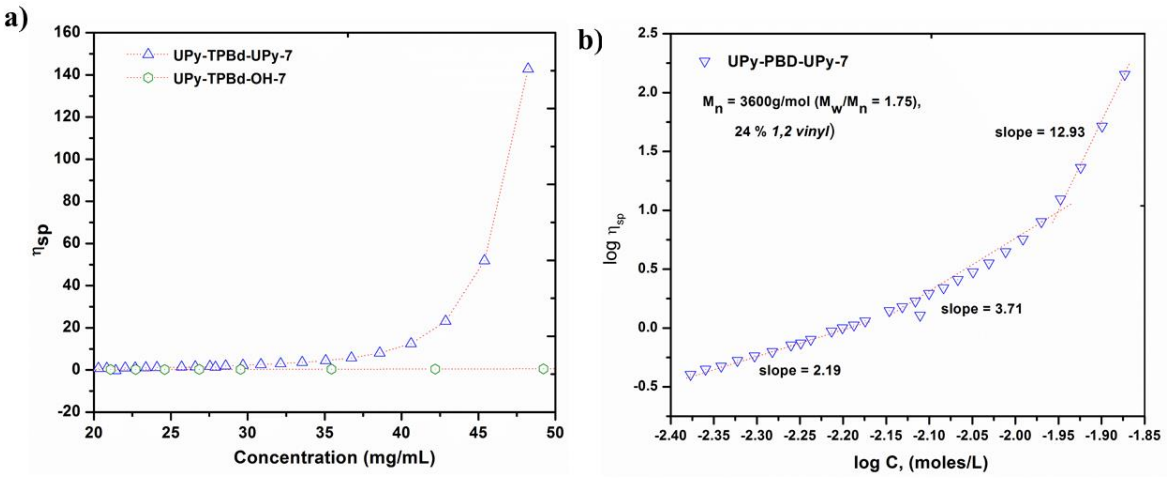
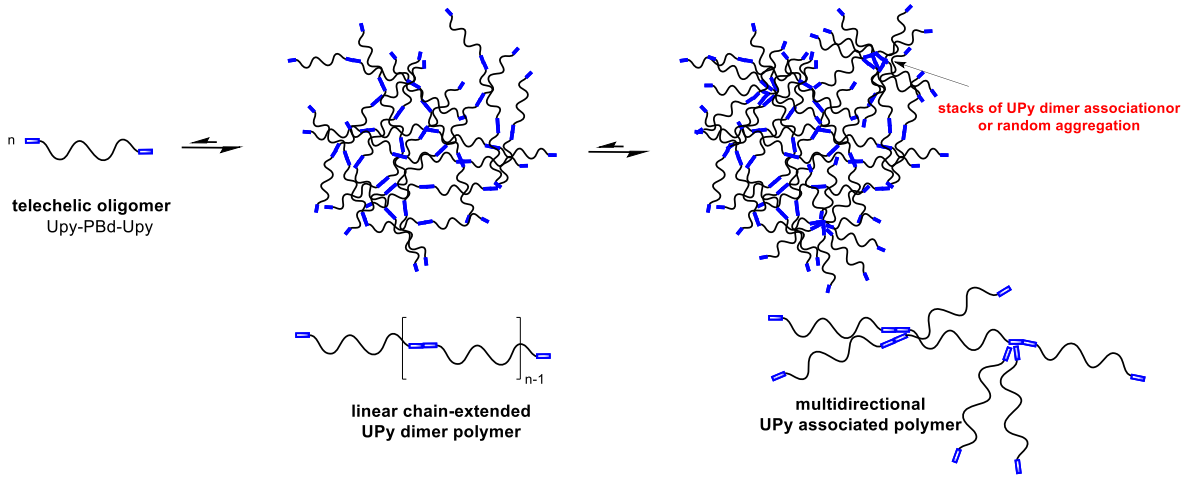



**Figure 5. 8:** Plot of specific viscosity vs concentration for X-PBd-X-7 (a) and double logarithmic plots for the UPy-PBd-UPy-7 with slope value as function of concentration range (b)

It can also be noted that the viscosity of these UPy-PBd-UPy samples show a significant influence of the microstructures. The polymer, UPy-PBd-UPy, with low *1,2-vinyl* content sample (**Table 5.1,** entry 3) shows lower viscosity in spite of the fact that its NMR molecular weight is 9,100 g/mol, whereas a low molecular weight, 3,950 g/mol with the high *1,2-vinyl* content polymer (**Table 5.1**, entry 6) shows higher viscosity. Higher slope values for solution viscosities of UPy-PDMS-UPy and *1,4 trans*-UPy-PBd-UPy could be then assigned to broader polydispersity of these polymers.[9,17] In case of PBd samples, this indicates that the pendent *1,2-vinyl* groups either interacts with UPy hydrogen-bonding unit or alters ring–chain equilibrium leading to higher viscosity. However, similar behavior was seen with hydrogenated PBd, indicating role of pendant *1,2-vinyl* group negligible. The curved nature of the plot which also confirms that a simple chain-extension of UPy telechelics forming very high molecular weight linear polymers is not occurring in the toluene rather a complex multiple UPy associated networks exists in equilibrium (**Scheme 5.2**).




**Scheme 5. 2:** Representation of UPy-PBd-UPy polymers undergoing linear chain-extension via UPy hydrogen-bonding dimerization extending to multiple hydrogen bonded aggregates.

The slope values calculated based on the high and similar concentration regions may be used for correlating to the Cates model for verification of extended chain-end association. The slope values are calculated using the data points at higher concentration region, which are in between 2.05 to 2.42 depending on the molecular weight for high *1,2-vinyl* content polymers as indicated in the **Figure 5.7a**. Although, the slope value of more than 3.5 could be obtained

for a much higher concentration range, the limitation of viscometer doesn't allow viscosity measurement for higher concentration solution. This implies that in order to apply the Cates model, a critical concentration for a given polymer differs based on molecular weight and its microstructure. For example, UPy- (*1,4 trans*-PBd)-UPy prepared by ROMP using UPy functional CTA has a slope value of 3.76[17]. The results obtained here for UPy-PBd-UPy with a high *1,2-vinyl* content exhibit a slope value, close to 2.6 and the UPy-PBD-UPy with low *1,2* vinyl content has much lower slope, i.e.1.65 (**Figure 5.7a**). This further confirms the polymer with higher *1,2-vinyl* groups preferentially undergoes UPy association by linear chain-end extended high molecular weight polymer, which is in equilibrium with a small micellar clusters polymer and unimer telechelics.

### 5.3.2 Effect of addition of end-capping agents in UPy association

Generally lower values of the Cates slope less than 3.5-3.7 are attributed to the presence of impurities, primarily monofunctional UPy oligomers, which can act as a chain-stopper.[27,28] As the functionalization efficiency in our polymers is near 96-100 % as indicated by the absence of chain-end methylene protons (3.64 ppm) adjacent to hydroxyl group from the precursor, the decrease in the slope value can't be attributed to impurities. In order to understand further, the viscosity studies were performed using UPy-PBd-UPy with *57 % 1,2-vinyl* content sample (**Table 5.1**, entry 6) in the presence of monochelic PBd end-functionalized with UPy (MPBd-UPy) with the $M_n$ of 1900 g/mol (~ 13% *1,2-vinyl*), as well as hydroxyl terminated telechelic precursor (HO-PBd-OH).

As seen from **Figure 5.7b**, the addition of end-capping agents does not have a major effect on the slope indicating the interference of these end-capping agents does not alter the molecular weight significantly. For 100 % UPy-PBd-UPy-6, the slope is 2.58 whereas in the presence of 7.4 mol wt. % the chain stopper MPBd-UPy, the value merely drops to 2.52. Surprisingly, the slope in the presence of HO-PBd-OH-6 with 9.4 mol wt % is 2.70. The hydroxyl telechelic precursor, HO-PBd-OH-6 was expected to engage in cross-hydrogen bonding with UPy domains and to increase the size of network association, which should exhibit higher viscosity. Nevertheless, it did not change the slope compared to UPy-PBd-UPy-6. This confirms that the size of UPy associated chains is affected minimally. Accordingly, the solution viscosity reduced slightly in the presence of these end-capping agents in toluene, which is non-polar solvent.

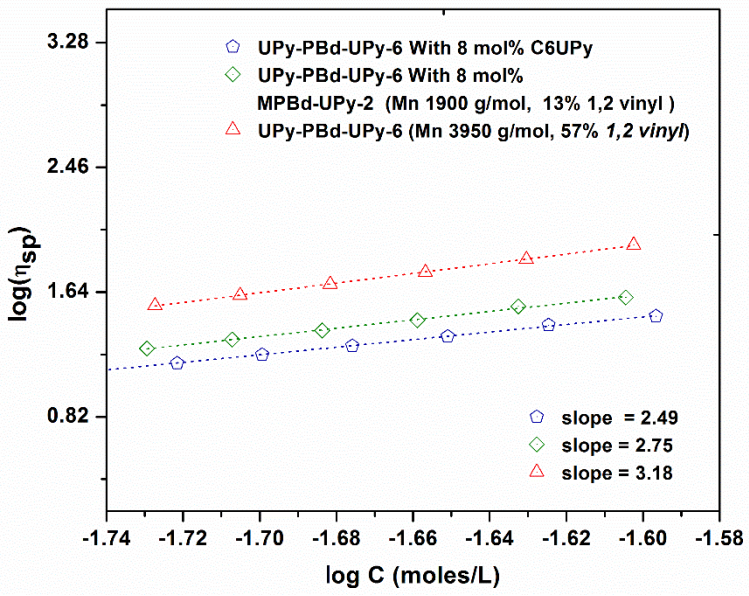



**Figure 5. 9:** Double logarithmic plots of solution viscosity of UPy-PBd-UPy samples in the presence of chain-stoppers in chloroform. (a) in the presence of 8 mol % monofunctional oligomer impurity, MPBd-UPy and b) low molecular weight C6-UPy impurity.

The strength of the hydrogen bonding is also significantly affected by the nature of solvent polarity. For example, when the experiments were performed in chloroform, a moderately polar solvent, the Cates slope values considerably decreased (**Figure 5.9**). The viscosity of UPy-PBd-UPy-6 in chloroform ($K_{dim}$ = 6 x $10^7$ $M^{-1}$) in the presence of the chain stoppers MPBd-UPy-2 and C6UPy, respectively has a linear dependent unlike in toluene and also shows a considerable reduction for low molecular weight stopper (2.49) than oligomeric stopper (2.75). This data underline two things, in chloroform strength of UPy-association is weaker in comparison to toluene and low molecular organic UPy compound acts as a much better chain stopper thereby reducing the size of aggregations, and hence the solution viscosity (**Figure 5.9).**

Although the reduction in the viscosity is directly proportional to the concentration of end-capping agent, the Cates slope value is not changed significantly in non-polar solvent. More importantly, the plots are still curved in the presence of capping agents in toluene. These results support the presence of equilibrium hydrogen bonding of UPy-PBd-UPy telechelics and

their cross-association with end-capping agent more significantly in the non-polar environment (**Scheme 5.2**).

### 5.3.3 Bulk properties of telechelic UPy-PBd-UPy polymers: DSC Studies

The low *1,2-vinyl* containing UPy-PBd-UPy samples (Table 5.1, entry 1-3) are brittle, whereas the high vinyl samples (**Table 5.1, entry 4-6**) are elastomeric solids with the ability to form thermoplastic film from melt. In order to understand the effect of hydrogen bonding interaction and the extent of UPy association in these polymers, telechelic UPy samples were subjected to the solid-state analysis using DSC. The samples were heated at the rate of 10 °C/min upto 150 $^{o}$C and held isothermally for 2 mins and cooled down at 10 $^{o}$C to 25 $^{o}$C. This heating/cooling cycle was repeated for two times. A typical DSC scan is shown in **Figure 5.10**. Melting points and enthalpy values of endothermic peaks observed in the DSC profile of UPy-PBd-UPy samples are reported in the **Table 5.2**.

It is evident that all the low *1,2-vinyl* UPy-PBd-UPy samples show the presence of endothermic melting peak in all the repeated heating cycles. Peak recovery and enthalpy values of endothermic peaks are ~ 80 %, based on the first heating cycle. The presence of endothermic peaks indicates the dissociation of hydrogen-bonded UPy aggregates. A sharp initial (first heating) peak and in some cases multi-modal peaks, which upon subsequent heating/cooling cycles become broader. This type of endothermic peaks may be attributed to the dissociation of aggregated, UPy hydrogen bonded clusters, which may contain a short one dimensional UPy-stacks or disordered aggregates. For the UPy-PBd-UPy samples with 57 % *1,2-vinyl* groups, only UPy-PBd-UPy-4 sample shows a small amount of a melting peak (recovery ~ 12 %) in repeated heating cycles. However, UPy-PBd-UPy-5 and UPy-PBd-UPy-6 do not show any melting peak in second and third heating cycle.

**Table 5. 2** Effect of microstructure of PBd on DSC characterization of UPy-PBd-UPy

| Sample | $M_{n,NMR}$[a] g/mol | $T_g$[b] (°C) | Heating cycle | Endothermic peak | | |
|---|---|---|---|---|---|---|
| | | | | $T_{diss.}$ (°C)[d] | $\Delta H_{diss}$ (J/g )[d] | Recovery (%)[c] |
| UPy-PBd-UPy-1 | 2,900 | -85.25 | 1st | 87.46 | 16.83 | - |
| | | | 2nd | 83.19 | 13.21 | 78.4 |
| | | | 3rd | 82.95 | 12.92 | 76.8 |
| UPy-PBd-UPy-2 | 5,300 | -81.75 | 1st | 55.98 | 9.375 | |
| | | | 2nd | 55.37 | 7.313 | 78.0 |
| | | | 3rd | 55.38 | 7.399 | 78.9 |
| UPy-PBd-UPy-3 | 9,100 | -87.88 | 1st | 46.88 | 5.11 | - |
| | | | 2nd | 46.14 | 4.540 | 88.9 |
| | | | 3rd | 45.88 | 4.67 | 91.4 |
| UPy-PBd-UPy-4 | 2,950 | -38.28 | 1st | 63.08 | 13.33 | |
| | | | 2nd | 58.01 | 1.685 | 12.6 |
| | | | 3rd | 58.55 | 1.437 | 10.8 |
| UPy-PBd-UPy-5 | 6,100 | -45.47 | 1st | 58.33 | 6.395 | - |
| | | | 2nd | None | None | - |
| | | | 3rd | None | None | - |
| UPy-PBd-UPy-6 | 3,950 | -38.38 | 1st | 54.10 | 8.504 | - |
| | | | 2nd | None | None | - |
| | | | 3rd | None | None | - |
| UPy-PBd-UPy-7 | 3,600 | -70.3 | 1st | 71.2 | 14.4 | - |
| | | | 2nd | 64.6 | 1.39 | 9.65 |
| | | | 3rd | None | 0.81 | 5.62 |

a) Determined by ratio of integration of –$\underline{CH_2}$-O-UPy and methyl group of pyridine ring group with polymer backbone, b) determined with DSC, c) with respect to enthalpy values of first heating cycle, d) $\Delta H_{diss}$ is enthalpy change and, $T_{diss}$ is melting temperature of endothermic peak.

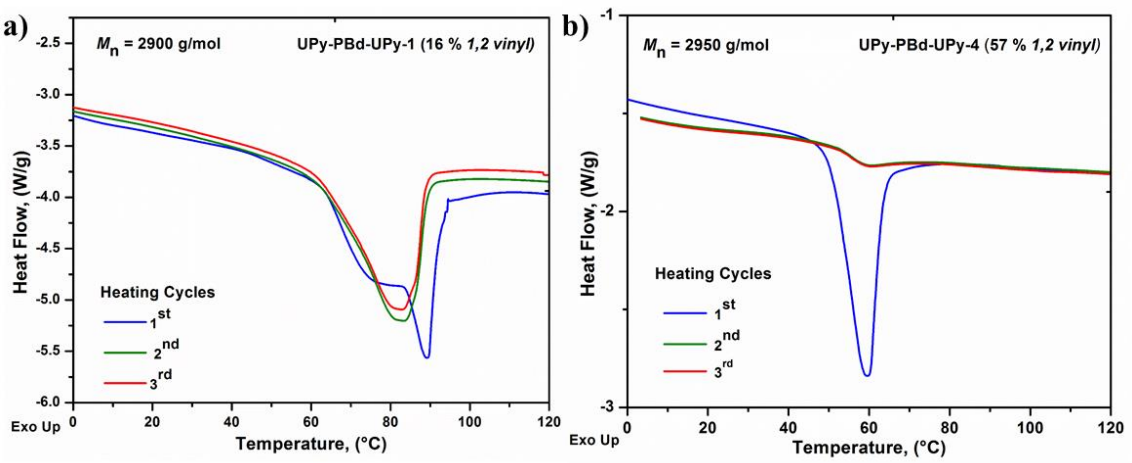



**Figure 5.10:** DSC profile of UPy-PBd-UPy-1 (a) and UPy-PBd-UPy-4 (b)

In the case of low *1,2-vinyl* content telechelics samples, the endothermic peaks are reversible. This reversibility and its specificity with respect to the microstructure indicate the dynamic equilibrium nature of the UPy hydrogen-bonded aggregation. In the case of low *1,2-vinyl* content polymers (**Figure 5.8a**), a low $T_g$ ( ~90 °C) promotes high chain mobility and facilitates UPy at the chain-ends to quickly reaggreates via hydrogen bonding. Actually, 15 % *1,2-vinyl* UPy-PBd-UPy samples (irrespective of the molecular weight and hence % UPy chain end groups) requires very short time to completely reform the original aggregated domains (~12 h); whereas, UPy-PBd-UPy samples with 57 % *1,2-vinyl* require a long duration for the reaggregation (~10 days). The could be associated with high $T_g$ (-45 °C) ) and slow mobility of the chains that limits reaggregation. In contrast, UPy-BPd-UPy-7, with 24 % *1,2-vinyl* groups shows poor peak recovery which was partly attributed to its moderately higher $T_g$ (-70.2 °C) and broad polydispersity. However, all UPy-PBd-UPy samples with 57% *1,2-vinyl* contents reaggreates over a period of week, and DSC profile again shows melting peak in the first heating cycle with similar enthalpy values.

### 5.3.4 Dynamics of UPy domain aggregation in hydrogenated polymers

A similar effect was also seen in the hydrogenated polymer UPy-(PE-*co*-PB)-UPy-1 synthesized from low *1,2-vinyl* content (13 %) precursor, which is a solid semicrystalline polymer and identical to the linear polyethylene with a random short chain branching due to ethyl groups. As a result of a random short chain branching, DSC profile of HO-(PE-*co*-PB)-

OH-1 shows a broad melting point from 40 °C to 100 °C ($T_m$ 88.40 °C, $\Delta H$ = 103.81 J/g, (crystallinity = 36.2 %), whereas UPy-derivative, UPy-(PE-*co*-PB)-UPy-1 has three distinct melting regions, 47.14 °C ($\Delta H$ = 11.43 J/g), 97.94 °C ($\Delta H$ = 1.816 J/g), and a major melting peak at 131.82 °C ($\Delta H$ = 16.71 J/g). Overall, an estimation of 10.4 % crystallinity was found considering all three peaks. The decrease in crystallinity is due to presence of hydrogen-bonded UPy domains and the additional endothermic peaks are attributed to the dissociation of UPy aggregated domains. This sample showed full recovery of endothermic peaks on second and third cycles.

The samples prepared from high *1,2-vinyl* (57 %) content precursors, UPy- (PE-*co*-PB)-UPy-4 ($M_n$ -3,000 g/mol) and UPy-(PE-*co*-PB)-UPy-6 ($M_n$ -4,150 g /mol) show a presence of endothermic peak in first heating cycle. However, the UPy-(PE-*co*-PB)-UPy-4 ($M_{n-}$ 3,000 g/mol) recovered only 40 % of endothermic peak in the second and third heating cycle and the UPy-(PE-*co*-PB)-UPy-6 ($M_n$- 4,150 g /mol) do not show any melting peak in second and third heating cycle. It is worth mentioning here, both these polymer has identical 57 *% 1,2-vinyl* contents, and have identical $T_g$s of ~ -49.13 °C. The absence of melting peak in second heating for these slightly higher molecular weight samples indicates that dynamics of polymer chain ends are further reduced due slow mobility. Also, UPy-(PE-*co*-PB)-UPy-4 sample has higher concentration of UPy chain end groups (11 % vs 8 %). Furthermore, UPy-(PE-*co*-PB)-UPy-4 has much higher peak recovery in second heating cycle in comparison to its unsaturated precursor UPy-PBd-UPy-4 (40 % *vs* 12 %), indicating that the mobility of the hydrogenated chains is higher than the unsaturated chains.

On other hand glass transition temperature of PE is lower than < -100 °C for UPy-(PE-*co*-PB)-UPy-1, therefore has much better chance for reaggregation of the UPy-dimers, and thus shows full recovery of the endothermic peak in second heating cycle. Also, presence of UPy aggregation leads to decrease in the crystallinity of the PE. A similar reduction in the crystallinity of the UPy-(*trans*-PBd-)-UPy has been reported earlier by Scherman and co-workers.[29]

The results indicate that the presence of endothermic peaks that can be attributed to crystalline/or dissociation of aggregated UPy domains in these UPy telechelics. As the UPy domain is a dynamic in nature due to presence of equilibrium with non-aggregated dimers or unimers, to probe the presence of melting or dissociation endothermic peaks, it is crucial to do

a periodic DSC analysis of the sample after first the heating cycle. As, stated earlier the extensively studied UPy-(PE-*co*-PB)-UPy material with $M_n$- 4100 g/mol was reported to have no such melting peaks.[4] The absence of endothermic peak was attributed to the presence of linear chain extension mechanism leading to very high molecular weight polymer. Unfortunately, this DSC values were reported for the second heating cycle with heating rate of 20 °C; therefore it is quite possible that the dynamics of UPy domain aggregation in previously reported for UPy-(PE-*co*-PB)-UPy were not noticed in the literature. However, in recent paper Meijer and coworkers reported presence of small endothermic peak with $T_m$ of 69 °C.[10]

### 5.3.5 Surface morphology of UPy-PBd-UPy samples

Thin films were prepared by drop casting 1mg/mL solution in toluene on polymer on the freshly cleaved mica surface. The surface morphology of thin films of these materials was analyzed using AFM. AFM phase images of UPy-PBD-UPy-2 are shown in **Figure 5.11**. Both the normal and zoomed images of this sample, of ($M_n$ 5,300 g/mol) with ~16 % *1,2-vinyl* microstructure shows features of fiber-like association. Detailed analysis indicate the fiber-like structures are not continuous fibers, but consist of discontinuous assembly of blob like associated individual micellar clusters (similar to the one observed previously with monochelic system). We attribute this discontinuity is caused by the thermodynamic stabilization of micellar UPy association involving one side of the chain-end. The other side of the chain-end can undergo intermolecular association with other micellar clusters. However, such network formation is not observed from the surface morphology. It appears that a competing chain dynamics of PBd at room temperature make the other end of the chain tangle in the matrix of unassociated UPy-PBd-UPy chains.

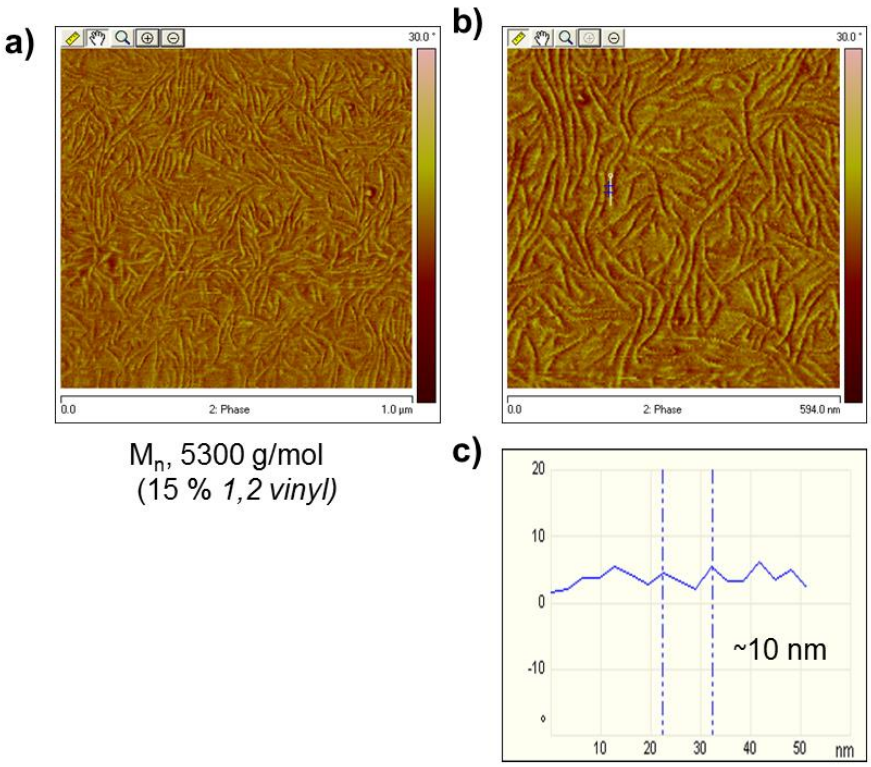
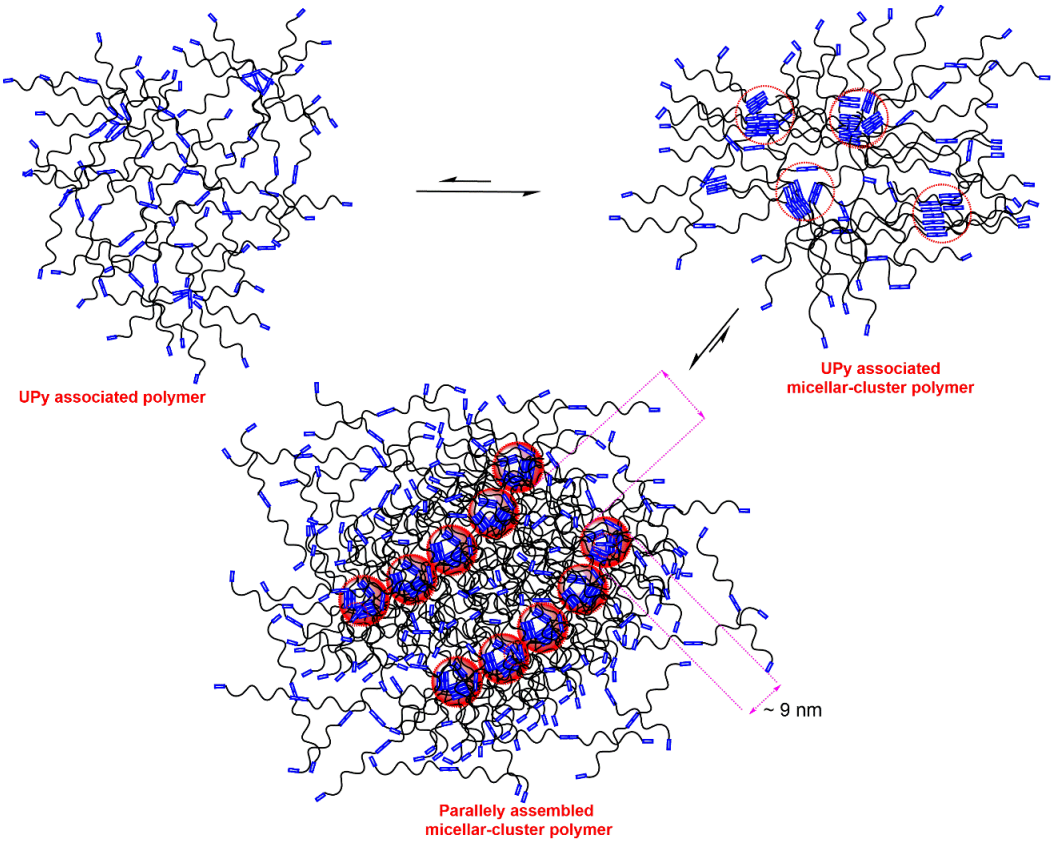



**Figure 5. 11:** AFM phase images of UPy-PBd-UPy-2 (a) Scan size 1µm (b) zoomed image scan size 594 nm, and c) size of cluster domains.

More interesting observation is that the micellar associated clusters further undergo parallel alignment leading to fiber-like structure (**Figure 5.11b**). In the case of monochelic PBd-UPy system, we observed that the sizes of micellar clusters slowly decrease over time at room temperature indicating dynamic nature of the system. Such a dynamic equilibrium between micellar associated clusters with unassociated matrix polymer exists in telechelic system (**Scheme 5.3**). This is also supported by the recovery of endothermic peaks in DSC upon repeated heating/cooling cycles (figure not given)




**Scheme 5. 3:** Proposed equilibrium of associated micellar clusters and their alignment into parallel lines with unassociated linear molecules.

**Figure 5.12** shows a comparison of AFM phase images of UPy-PBd-UPy with molecular weight of ~ 2.9 kg/mol with 16 % and 57 % *1,2-vinyl* microstructures. As seen from the images, the16 % *1,2-vinyl* microstructure sample has a densely packed UPy associated micellar cluster, whereas the sample with 57 % *1,2-vinyl* microstructure has a lesser amount of micellar associated clusters. The portion of the associated micellar cluster is high in the case of low *1,2-vinyl* (16 %) content sample as compared to high *1,2-vinyl* (57 %) content sample. A lower amount of micellar cluster alignment into parallel fiber-like structure is attributed to a higher $T_g$ of high vinyl content PBd and thus, lower chain mobility at room temperature. This indicates that the chain mobility dominates the UPy hydrogen bonding association.

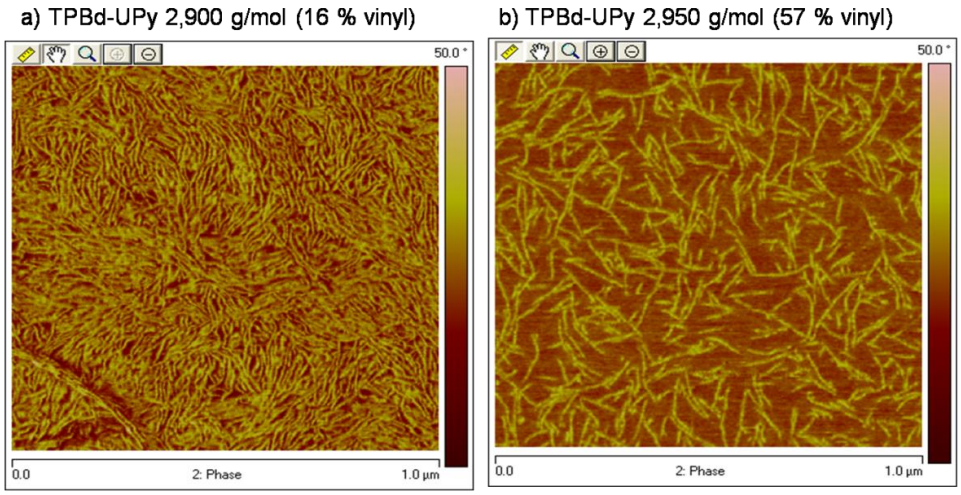



**Figure 5.12:** AFM micrographs of UPy-PBd-UPy-1 (a) and UPy-PBd-UPy-4 (b)

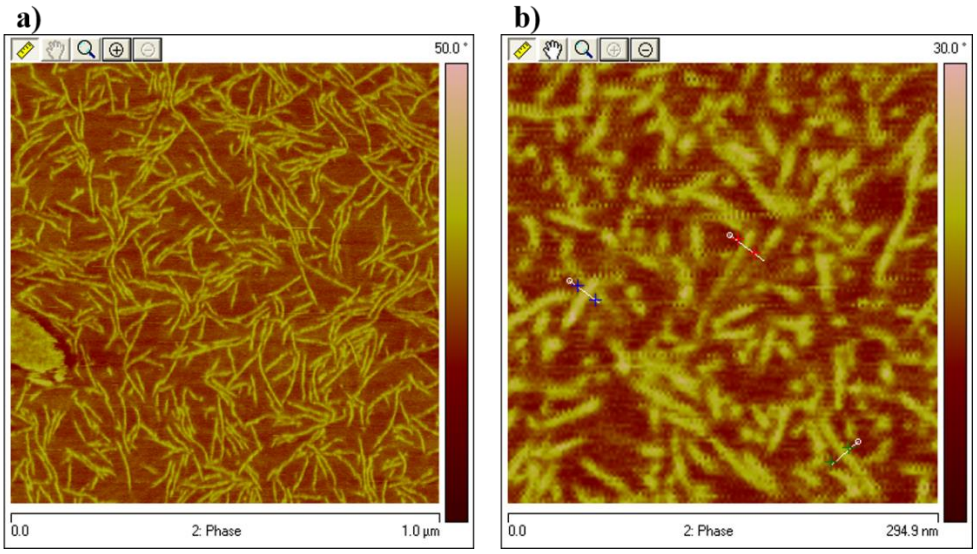



**Figure 5.13**: AFM phase images of UPy-PBd-UPy-4 a) thin film cast on mica surface, and b) bulk morphology (zoomed).

### 5.3.6 Bulk morphology of UPy-PBd-UPy

The development of thin film morphology may be influenced by the multiple interfaces, substrate to sample and sample to air. As UPy-PBd-UPy with high vinyl content samples are elastomeric in nature, it was an interest to know the morphology of the bulk material and compare with the thin film morphology. Thus, the samples were subjected to cryo-cut and the sliced sample was viewed under AFM. The bulk morphology of UPy-PBd-UPy-4 and the

solution caste thin-film morphology are shown in **Figure 5.13**. Form both the phase images, it is clear that the sample with 57 % *1,2-vinyl* microstructure has less dense spherical micellar clusters resulting in fibril like morphology. This confirms that the bulk morphology is similar to the surface morphology observed in the thin film

The bulk morphology of UPy-PBd-UPy-5 also shows much less density of such micellar fibril (**Figure 5.14**). AFM analysis again confirms that the glass transition temperature of PBd plays a significant role on the extent of UPy micellar cluster formation. A high *1,2-vinyl* polymer has relatively higher $T_g$ and making the dynamics of the chain end associated UPy hydrogen bonding slower; thereby a few chain end groups are taking part in the micellar cluster association. The fibrous structure of the aligned micellar clusters interpenetrates the matrix of the unassociated linear polymer, which ultimately results in the formation of strong thermoplastic elastomer (**Figure 5.14 b and c**).

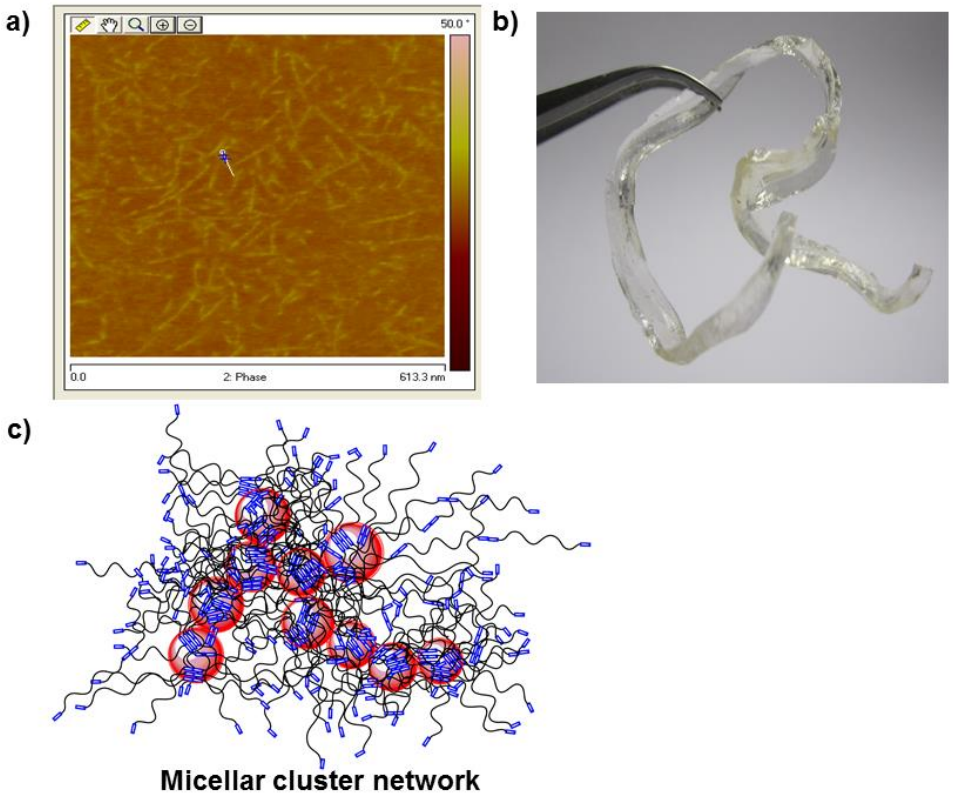



**Figure 5.14:** UPy-PBd-UPy-5, a) AFM of bulk phase from cryo-cut film, b) thermoplastic film forming ability from melt, and c) proposed micellar cluster network formation

## 5.4 Conclusions

Anionic polymerization of butadiene was carried out successfully using hydroxyl protected initiator and terminated with ethylene oxide to obtain telechelic PBds. UPy telechelic of butadiene with various molecular weight and different *1,2-vinyl* contents have been prepared and characterized. Solution viscosity, DSC and AFM analysis reveal the system exist in equilibrium between UPy hydrogen bonded micellar clusters and unassociated linear chain-extended polymer. The extent of micellar cluster network formation is much higher in case of low *1,2-vinyl* content PBd, resulting in brittle film. Whereas, the PBd with high vinyl content has an optimum balance of linear chain extension and micellar cluster alignment giving rise to strong interpenetrated thermoplastic elastomer.

## 5.5 References


(1) Sijbesma, R. P.; Beijer, F. H.; Brunsveld, L.; Folmer, B. J. B.; Hirschberg, J. H. K. K.; Lange, R. F. M.; Lowe, J. K. L.; Meijer, E. W. *Science* **1997**, *278*, 1601.

(2) Beijer, F. H.; Sijbesma, R. P.; Kooijman, H.; Spek, A. L.; Meijer, E. W. *J. Am. Chem. Soc.* **1998**, *120*, 6761.

(3) Hirschberg, J.; Beijer, F. H.; van Aert, H. A.; Magusin, P.; Sijbesma, R. P.; Meijer, E. W. *Macromolecules* **1999**, *32*, 2696.

(4) Folmer, B. J. B.; Sijbesma, R. P.; Versteegen, R. M.; van der Rijt, J. A. J.; Meijer, E. W. *Adv. Mater.* **2000**, *12*, 874.

(5) Lange, R. F. M.; Meijer, E. W. *Macromolecules* **1995**, *28*, 782.

(6) Dankers, P. Y. W.; Harmsen, M. C.; Brouwer, L. A.; Van Luyn, M. J. A.; Meijer, E. W. *Nat. Mater.* **2005**, *4*, 568.

(7) Dankers, P. Y. W.; Zhang, Z.; Wisse, E.; Grijpma, D. W.; Sijbesma, R. P.; Feijen, J.; Meijer, E. W. *Macromolecules* **2006**, *39*, 8763.

(8) van Beek, D. J. M.; Spiering, A. J. H.; Peters, G. W. M.; te Nijenhuis, K.; Sijbesma, R. P. *Macromolecules* **2007**, *40*, 8464.

(9) Botterhuis, N. E.; van Beek, D. J. M.; van Gemert, G. M. L.; Bosman, A. W.; Sijbesma, R. P. *J. Polym. Sci. Part A-Polym. Chem.* **2008**, *46*, 3877.

(10) Kautz, H.; van Beek, D. J. M.; Sijbesma, R. P.; Meijer, E. W. *Macromolecules* **2006**, *39*, 4265.

(11) Mes, T.; Koenigs, M. M. E.; Scalfani, V. F.; Bailey, T. S.; Meijer, E. W.; Palmans, A. R. A. *Acs Macro Lett.* **2012**, *1*, 105.

(12) Appel, W. P. J.; Portale, G.; Wisse, E.; Dankers, P. Y. W.; Meijer, E. W. *Macromolecules* **2011**, *44*, 6776.

(13) De Greef, T. F. A.; Kade, M. J.; Feldman, K. E.; Kramer, E. J.; Hawker, C. J.; Meijer, E. W. *J. Polym. Sci., Part A: Polym. Chem.* **2011**, *49*, 4253.

(14) de Greef, T. F. A.; Nieuwenhuizen, M. M. L.; Sibesma, R. P.; Meijer, E. W. *J. Org. Chem.* **2010**, *75*, 598.

(15) Scherman, O. A.; Ligthart, G. B. W. L.; Ohkawa, H.; Sijbesma, R. P.; Meijer, E. W. *Proc. Natl. Acad. Sci. U.S.A.* **2006**, *103*, 11850.

(16) Nieuwenhuizen, M. M. L.; de Greef, T. F. A.; van der Bruggen, R. L. J.; Paulusse, J. M. J.; Appel, W. P. J.; Smulders, M. M. J.; Sijbesma, R. P.; Meijer, E. W. *Chem. Eur. J.* **2010**, *16*, 1601.

(17) Scherman, O. A.; Ligthart, G.; Ohkawa, H.; Sijbesma, R. P.; Meijer, E. W. *Proc. Natl. Acad. Sci. USA* **2006**, *103*, 11850.

(18) Botterhuis, N. E.; van Beek, D. J. M.; van Gemert, G. M. L.; Bosman, A. W.; Sijbesma, R. P. *J. Polym. Sci., Part A: Polym. Chem.* **2008**, *46*, 3877.

(19) Bobade, S. L.; Malmgren, T.; Baskaran, D. *Polym. Chem.* **2014**, *5*, 910.

(20) Kuntz, I.; Gerber, A. *J. Polym. Sci* **1960**, *42*, 299.

(21) Hadjichristidis, N.; Iatrou, H.; Pispas, S.; Pitsikalis, M. *J. Polym. Sci., Part A: Polym. Chem.* **2000**, *38*, 3211.

(22) Uhrig, D.; Mays, J. W. *J. Polym. Sci., Part A: Polym. Chem.* **2005**, *43*, 6179.

(23) Hahn, S. F. *J. Polym. Sci., Part A: Polym. Chem.* **1992**, *30*, 397.

(24) Keizer, H. M.; van Kessel, R.; Sijbesma, R. P.; Meijer, E. W. *Polymer* **2003**, *44*, 5505.

(25) Cates, M. E.; Candau, S. J. *J. Phys.:Condens.Matter* **1990**, *2*, 6869.

(26) De Greef, T. F. A.; Smulders, M. M. J.; Wolffs, M.; Schenning, A. P. H. J.; Sijbesma, R. P.; Meijer, E. W. *Chem. Rev.* **2009**, *109*, 5687.

(27) Knoben, W.; Besseling, N. A. M.; Bouteiller, L.; Cohen Stuart, M. A. *Phys. Chem. Chem. Phys.* **2005**, *7*, 2390.

(28) Knoben, W.; Besseling, N. A. M.; Cohen Stuart, M. A. *J. Chem. Phys.* **2007**, *126*.

(29) Scherman, O. A.; Ligthart, G.; Ohkawa, H.; Sijbesma, R. P.; Meijer, E. W. *Proc. Natl. Acad. Sci. U.S.A.* **2006**, *103*, 11850.

# Chapter 6: Synthesis and Characterization of Ureidopyrimidone Telechelics by CuAAC "Click" Reaction: Effect of $T_g$ and Polarity

## Abstract

Telechelic oligomers functionalized with 2-ureido-4[1*H*]-pyrimidone (UPy), a quadruple hydrogen bonding group, have been synthesized using a combination of atom-transfer radical polymerization and click reaction. Ureidopyrimidone (UPy) synthons with propargyl and azide functionality were used for clicking with azido and propargyl telechelic oligomers, respectively. The effect of triazole linker and types of oligomers differing in $T_g$ and polarity, such as poly(*n*-butyl acrylate) (P*n*BA), polystyrene (PS), and polybutadiene (PBd) on UPy hydrogen bonding have been examined. High solution viscosity and deviation from the normal terminal relaxation in melt state were observed, suggesting the presence of UPy aggregates that are in equilibrium between linear and network polymers. Differential scanning calorimetry studies confirm dissociation of UPy aggregates as an endothermic peak for PBd system, whereas the polar polymers with high $T_g$ (PS and P*n*BA) had no such peaks associated with $T_m$ indicating the significance of the polymer chain dynamics in supramolecular hydrogen bonding. The triazole linker interferes with the UPy association and reduces the sizes of hydrogen bonded UPy aggregates and thereby improves the physical property of supramolecular polymers.

Part of this work is published as,
Bobade, S..; Wang, Y.; Mays, J.; Baskaran, D,
*Macromolecules*, **2014**, *47* (15), 5040–5050.

## 6.1 Introduction

Supramolecular polymers (SPs)[1] based on self-complementary quadruple hydrogen bonded 2-ureido-4[1H]-pyrimidone (UPy) telechelics oligomers[2-5] exhibit versatile material properties depending on the nature of linking oligomers, and they can be used as thermoplastic elastomers[6], self-healing polymers[7] and in bio-scaffolding applications. A high association constant ($K_{dim}$ = 6 × $10^7$ $M^{-1}$ in chloroform and 6 × $10^8$ $M^{-1}$ in toluene) of UPy groups and inexpensive synthesis using commercial reagents make UPy synthons indispensable for preparation of SPs.[8] Telechelic polymers functionalized with UPy groups are synthesized using chain end modification and often via reaction of hydroxyl terminal groups with a suitable excess UPy-synthon, a compound containing UPy and reactive isocyanate linker (UPy-R-NCO), where R is a linear alkyl chain or cyclic aliphatic chain.[6] By using this approach a variety of UPy telechelics based on low molecular weight oligomers such as, poly(ethylene-*co*-polypropylene oxide) (PEO-PPO)[6], poly(ethylene-*co*-butylene) (PEB)[9,10], polytetrahydrofuran (PTHF)[9], polycarbonates (PC)[6,11] and polyesters[6,12] have been prepared, and their properties are found to vary depending on different polymer backbone. More recently, UPy-NCO approach was employed by Delgado and coworkers in the preparation of UPy-Poly(lactide)-*b*-PBd-*b*-Poly(lactide)-UPy.[13]

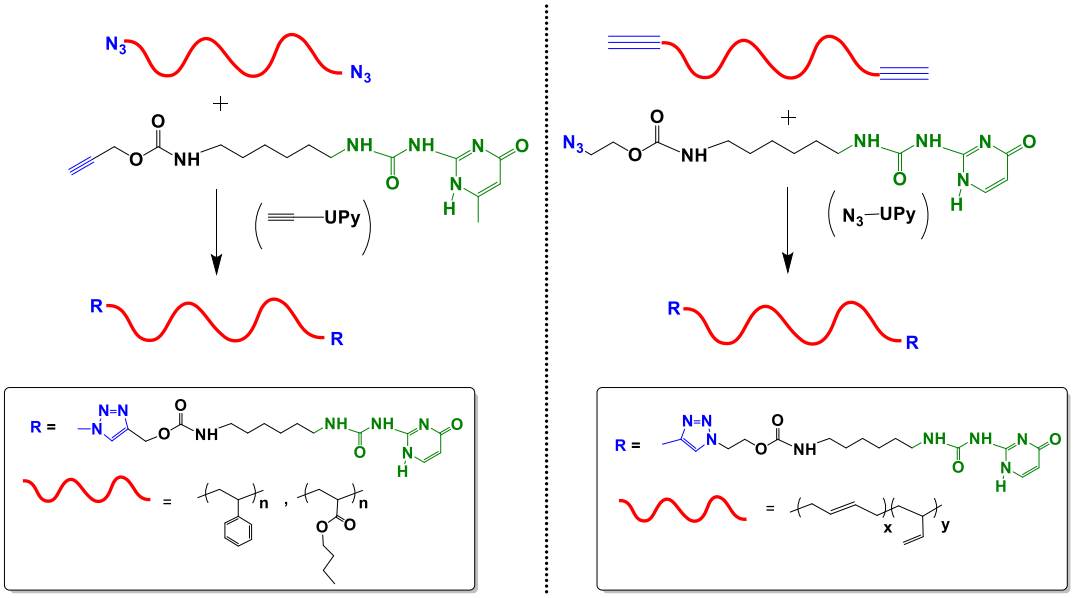
Enhanced properties of SPs resulting from UPy telechelics are, in general, attributed to the linear chain extension resulting to very high molecular weight polymers.[6] Recent studies showed the importance of additional secondary interactions due to urethane or urea linkers and the formation of UPy aggregation contributing to the properties of SPs.[10,14] Our broader focus is to understand and compare the effect of polymer polarity and chain-dynamics on the UPy hydrogen-bonded polybutadiene (PBd) with acrylic and other polymers. However, the synthesis of SPs using UPy functionalized telechelics has a prerequisite that the precursor polymer should have specific chain end functionality (hydroxyl, or amine, or carboxylic). The attachment of UPy synthon becomes problematic for polymers that are difficult to synthesize, or which are not commercially available, with the above mentioned chain end groups. These polymers include, telechelic poly(alkyl) acrylates, poly(alky) methacrylates, and polystyrenic derivatives.

Synthesis of acrylic and styrenic based hydroxyl telechelics by anionic polymerization requires protected initiator, end-capping with ethylene oxide and deprotection. Moreover the

conversion of hydroxyl functionality into UPy using isocyanate functionalized UPy (UPy-NCO) is complicated due to its high sensitive towards polar impurities such as alcohol and water, which are difficult to remove from precipitated polymers. In the literature, excess amount of UPy-NCO has been used to drive the reaction and to improve the functionalization efficiency.[6,13] Although the controlled radical polymerization techniques can produce hydroxyl telechelics[15-17], the transformation of hydroxyl telechelics into UPy telechelic still requires dry reaction condition. Moreover, these reactions often lead to incomplete UPy chain end modifications ($f < 2$) primarily due to atom transfer radical coupling (ATRC) reaction resulting to chains without UPy groups and broad polydispersity index.[18]

On the other hand, using atom-transfer radical polymerization (ATRP), it is possible to prepare monochelic ω-bromide, or telechelic α, ω-*bis*-bromide functionalized polymers from monofunctional or bifunctional initiators, respectively. The α, ω-*bis*-bromide end groups of the telechelics can be easily transformed into azide, which make them ideal candidates for the copper (I) catalyzed alkyne-azide (2 + 3) Huisgen cycloadditon (CuAAC) reaction.[19-26]

Herein, we have used a combination of ATRP and CuAAC click chemistry for the synthesis of telechelic oligomers functionalized with UPy (**Scheme 6.1**). Four different oligomers, with a similar molar mass (< 3.0 kg/mol), were targeted to examine the effect of $T_g$s and the polarity characteristics on the hydrogen bonding association. These oligomers include telechelic polybutadiene (low $T_g$ = -42 °C, non-polar), hydrogenated PBd, ((PE) $_{0.57}$-*co*-PB $_{0.43}$) (low $T_g$ = -48 °C, non-polar), P*n*BA (low $T_g$ = -53 °C, polar), and PS (high $T_g$ = 60 °C, non-polar). Also, UPy telechelics containing hydrogenated PBd, poly(ethylene-*co*-butylene) copolymer (PE-*co*-PB), with triazole linkers and without the Tz linkers was compared for the supramolecular properties.




**Scheme 6. 1:** Synthesis of UPy telechelics of PS, P*n*BA, and PBd by combination of ATRP and CuAAC click reactions

## 6.2 Experimental Section

### 6.2.1 Materials

The reagents CuBr (I), N, N, N', N', N''-pentamethyldiethylenetriamine (PMDETA), tetrahydrofuran (THF, HPLC grade), chloroform (HPLC grade), *n*-hexane, methanol, 2-bromo ethanol, propargyl alcohol, propargyl bromide, sodium hydride (60 %), sodium azide, dimethyl formamide (DMF), *n*-butyl acrylate, styrene, silica gel (230-400 mesh), 2-amino-4-hydroxyl-6-methylpyrimidine (6-Me-Iso), neutral aluminum oxide, diethyl meso-2,5-dibromoadipate (DEBAD), calcium hydride, sodium sulfate, and dibutyltin dilaurate (DBDTL) were purchased from Aldrich. Hydroxyl terminated polybutadiene ($M_n$ = 2,400 g/mol, 57 % *1,2-vinyl*) and hydroxyl terminated hydrogenated PBd , (PE-*co*-PB) ($M_n$ = 3550 g/mol) was kindly donated by Cray Valley. Deuterated chloroform was purchased from Cambridge isotopes laboratories Inc. Monomers were passed through neutral alumina column to remove the inhibitor. Deionized water (DI) was used wherever applied. All other chemicals were used as received unless stated otherwise. All reactions were done under inert condition by using a combination of high vacuum technique and $N_2$ atmosphere.

### 6.2.2 Characterization

$^1$H NMR spectra were recorded on Varian Mercury Vx 300 spectrometer at 300 MHz. The samples were prepared in C*D*Cl$_3$. IR analysis was performed on a Nicolet IS 10 FTI –ATR spectrometer and data were analyzed using OMNIC software. Number-average molecular weight ($M_n$) and polydispersity index ($Đ$) were determined using size exclusion chromatography (SEC) equipped with Knauer's K-501 HPLC pump, K-2301 RI detector, K-2501 UV detector, and with a set of two columns; Polymer Standards Services, SDV-gel, 60-cm length (5 μm) 100 Å and a linear $10^2$–$10^6$ Å. Tetrahydrofuran (THF) with toluene as a solvent flow marker was used as an eluent at a flow rate of 1.0 mL/min, and the SEC was calibrated using polystyrene (PS) standards obtained from Pressure Chemicals (Pittsburgh, USA). The $M_{n,SEC}$ of PBd was obtained against calibrated PS standards and corrected by multiplying with the correction coefficient of 0.50, a value typically used for PBd with *1,2-vinyl* contents less than 10 %.[27] However, Grubbs and co-workers reported that the $M_{n,NMR}$ matches with $M_{n,SEC}$ determined using 0.50 as correction factor for ~90 % *trans*-1,4 PBd.[28] Thus, we used 0. 50 as the correction factor for the synthesized PBd, which has a higher (57 %) *1,2-vinyl* content owing to a close agreement between the $M_{n,SEC}$ and $M_{n,NMR}$. The molecular weight of P*n*BA is reported as apparent and relative to PS calibration. Thermogravimetry analysis (TGA) was performed using a TA Q-50 instrument (25 to 1000 °C), with a heating rate of 10 °C/min under nitrogen atmosphere.

Atomic force microscopy (AFM) was performed with a Nanoscope IIIa Microscope with Multimode Controller (Veeco Instrument) at ambient temperature. Drop cast films were prepared on freshly prepared mica using a sample concentration of 1mg/mL in chloroform; and films were annealed for 24 h at RT. The tapping mode was employed with an antimony-doped Si tip (radius <10 nm) at a line scanning frequency of 1 Hz.

Differential scanning calorimetry (DSC) analysis was performed with a TA-Q1000 and TA Q-2000 instrument from -90 °C to 150 °C at a scan rate of 10 °C/min. Also, heating rates of 5 °C/min and 20 °C/min was used. Three repeated heating and cooling scans were run with a 5 min isotherm at -90 °C. Solution viscosity in toluene was measured by an automatic viscometer using a Schott Instruments AVS 370 and a type 531-10 viscometer (0.64 mm capillary with K = 0.01).

Rheological measurements of PBd-UPy were performed on an AR2000ex rheometer (TA Instruments) with 25 mm disposable parallel plates and an environmental testing chamber (ETC). Nitrogen was used the gas source of ETC to prevent sample degradation at high temperature. Both small amplitude oscillatory shear and creep measurements were used to evaluate the viscoelastic properties of the samples.

Dynamic mechanical spectra were recorded on a TA 800 Dynamic Mechanical Analyzer. A small rectangular bar of the polymer (thin films were prepared from melt), size approximately 2 × 5 × 10 mm were subjected to a sinusoidal deformation at a constant frequency, using the extension clamp method. Measurements were carried out at a frequency of 1 Hz and a heating rate of 3 °C/min. The amplitude of the sinusoidal deformation was kept the same (15 μm) and the static force 10 % more than the dynamic force in order to ensure a good contact between the sample and the probe.

## 6.3 Synthesis of functional UPy tags

### 6.3.1 NCO-UPy

UPy-NCO synthon was synthesized by following the reported procedure.[6] In a typical experiment, 15 g of 6-methyl isocytosine was added into a 250 mL round bottom flask and kept under high vacuum at 110 °C. After 4 h the flask was cooled to room temperature, filled with nitrogen, and 1, 6 HDI was added under nitrogen. The reaction was kept under stirring in an oil bath at 110 °C. After 20 h, the flask was cooled to room temperature and the product was isolated by precipitation in 1L hexane. UPy-synthon was obtained as while solid and thoroughly washed with hexane. Yield 34 g (96.8 %); FT-IR (ATR): υ 1520, 1572, 1664, 1697, 2279, 2931 $cm^{-1,}$

### 6.3.2 Propargyl-UPy (UPy-Pg)

10 g (34 mmol) of NCO-UPy synthon was reacted with 10 g (178 mmol) of propargyl alcohol in 200 mL of dry chloroform at 70 ºC for 5-6 h in the presence of 100 mg of DBDTL. The reaction was monitored using IR until the peak at 2279 $cm^{-1}$ (-NCO group) disappeared completely. After the reaction (6 h), the Pg-UPy was recovered by precipitation in 1 L of hexane. The product was washed with excess hexane and dried at 50 °C under vacuum for 24 h. Yield: 7.5 g (62.9 %), $^1$H NMR (300 MHz, $CDCl_3$): ($\delta$ ppm) 13.13 (s, 1H, $CH_3C\underline{NH}$), 11.86 (s, 1H,-$CH_2NH(C=O)\ \underline{NH}$), 10.12 (s, 1H, -$CH_2NH(C=O)\ \underline{NH}$), 5.88 (s, 1H, -$\underline{CH}=CCH_3$), 5.26 (s, 1H, -$\underline{N}$H-COO-, urethane group), 4.67 (s, 2H, -COO-$\underline{CH_2}$-, propargyl group), 3.1-3.3 (m,

4H, NH(C=O) NH$\underline{CH_2}$ + -$\underline{CH_2}$NHCO), 2.45 (s, 1H, -$CH_2$-C ≡$\underline{CH}$), 2.23 (s, 3H, $\underline{CH_3}$C=CH), 1.5-1.6 (m, 4H,-NCH$_2\underline{CH_2}$CH$_2$CH$_2\underline{CH_2}$-CH$_2$N-), 1.36 (m, -NCH$_2$CH$_2\underline{CH_2CH_2}$CH$_2$-CH$_2$N-). IR (ATR): υ 1526, 1574, 1660, 1706, 2110 (-$\underline{C≡CH}$), 2854, 2931, 3205 cm$^{-1}$

### 6.3.3 Azido-UPy (UPy-N3)

In a first step, 10 g (34 mmol) of NCO-UPy synthon was reacted with 40 g (320 mmol) of 2-bromo ethanol in 200 mL of dry chloroform at 70 °C in the presence of a catalytic amount of DBDTL (0.100 g). The reaction was monitored by IR until all the –NCO groups were consumed. The bromoethanol adduct of UPy was recovered by precipitation in 1L of hexane and washed and dried at 50 °C under vacuum for 24 h. Yield: 11 g, 77.3 %. $^1$HNMR (300 MHz, $CDCl_3$): ($\delta$ ppm) 13.11 (s, 1H, $CH_3C\underline{NH}$), 11.85 (s, 1H,-$CH_2$NH(C=O) $\underline{NH}$), 10.12 (s, 1H, -$CH_2$NH(C=O) $\underline{NH}$), 5.85 (s, 1H, -$\underline{CH}$=$CCH_3$), 5.13 (bs, 1H, -$\underline{N}$H-COO-, urethane group), 4.35 (m, 2H, -NHCOO-$CH_2$-$\underline{CH_2}$Br), 3.50 (m, 2H, -NHCOO-$\underline{CH_2}$-$CH_2$Br) 3.1-3.3 (m, 4H, NH(C=O) NH$\underline{CH_2}$ + -$\underline{CH_2}$NHCO), 2.22 (s, 3H, $\underline{CH_3}$C=CH), 1.5-1.6 (m, 4H,-NCH$_2\underline{CH_2}$CH$_2$CH$_2\underline{CH_2}$-CH$_2$N-), 1.36 (m, -NCH$_2$CH$_2\underline{CH_2CH_2}$CH$_2$-CH$_2$N-).

Subsequently, the bromoethanol UPy adduct, 5.5 g (13.3 mmol) was dissolved in 100 mL of DMF and reacted with 3 g (46 mmol) of sodium azide at 25 ºC for 24 h. The product, azido-UPy was recovered by precipitation in deionized water, washed with excess water to remove traces of DMF, and dried at 50 °C under vacuum for 24 h. Yield: 4.5 g (90.0 %), $^1$HNMR (300 MHz, $CDCl_3$): ($\delta$ ppm) 13.11 (s, 1H, $CH_3C\underline{NH}$), 11.83 (s, 1H,-$CH_2$NH(C=O) $\underline{NH}$), 10.12 (s, 1H, -$CH_2$NH(C=O) $\underline{NH}$), 5.83 (s, 1H, -$\underline{CH}$=$CCH_3$), 5.14 (bs, 1H, -$\underline{N}$H-COO-, urethane group), 4.21 (m, 2H, -NHCOO-$CH_2$-$\underline{CH_2}N_3$), 3.43(m, 2H, -NHCOO-$\underline{CH_2}$-$CH_2N_3$) 3.1-3.3 (m, 4H, NH(C=O) NH$\underline{CH_2}$ + -$\underline{CH_2}$NHCO), 2.22 (s, 3H, $\underline{CH_3}$C=CH), 1.5-1.6(m,4H,-NCH$_2\underline{CH_2}$CH$_2$CH$_2\underline{CH_2}$-CH$_2$N-), 1.36(m,-NCH$_2$CH$_2\underline{CH_2CH_2}$CH$_2$-CH$_2$N-). IR (ATR): υ 1521, 1582, 1665, 1697, 1741, 2095 (azide group), 2861, 2936, 3422 cm$^{-1}$

## 6.4 Synthesis of telechelic functional polymers

### 6.4.1 α, ω-*Bis*-bromo polystyrene (Br-PS-Br)

To a 100 mL clean flame dried round bottom flask equipped with side arm (and teflon stopcock) for attachment to the vacuum line, was added 56 mL of styrene (489 mmol), 6.90 g of DBEAD (1.912 mmol), 0.68 g of PMDETA (3.90 mmol), and 0.56 g of CuBr (I) (3.09 mmol). This reaction mixture was degassed three times by freeze-pump-thaw cycles and the flask was kept in an oil bath maintained at 110 °C. After 110 min, the polymerization was

terminated by cooling the flask with liquid nitrogen. The reaction mixture was diluted in 100 mL of THF and precipitated in 600 ml of methanol.

Recovered polymer was dried and dissolved in 500 mL of THF and passed through alumina column to remove the copper catalyst. The eluted polymer solution was concentrated using rotatory evaporator at 40 °C under reduced pressure. The Br-PS-Br sample was further dried in vacuum oven at 50 °C for 24 h. Yield: 77 %, $M_{n,th}$ = 2,360 g/mol, $M_{n,GPC}$/ = 2,400 g/mol, *PDI* = 1.13, and $M_{n\ NMR}$ = 2,700 g/mol. $^1$H NMR: δ ppm, 0.9-1.9 (aliphatic protons, and -COOCH$_2$-CH$_3$), 3.6-3.9 (-COOCH$_2$-), 4.4 (-PhCHBr), 6.3-7.4 (Ar (H)). FTIR (ATR), υ 1451, 1493, 1600, 1728, 2923, 3025 cm$^{-1}$

### 6.4.2 α, ω-*Bis*-azido polystyrene ($N_3$-PS-$N_3$)

14 g of Br-PS-Br (11.66 mmol of Br) was dissolved in 100 mL of DMF under $N_2$ and reacted with 4.0 g (62.6 mmol) of sodium azide at 25 $^o$C for 24 h. The reaction was monitored by $^1$H NMR and IR. After a 100 % conversion of bromide, the polymer was precipitated in excess water and filtered over buchnner funnel. The polymer was dissolved in chloroform, washed with water, dried over sodium sulfate, and the chloroform was removed using rotatory evaporator to give α, ω azido terminated polystyrene. Yield: 13.5 g, (96.3 %), $M_{n,th}$ = 2,290 g/mol, $M_{n,GPC}$ = 2,500 g/mol, *PDI* = 1.11, and $M_{n,NMR}$ = 2,300 g/mol. $^1$H NMR: δ ppm, 0.9-1.9 (aliphatic protons, and -COOCH$_2$-CH$_3$), 3.6-3.9 (-COOCH$_2$-, and -PhCHN$_3$), 6.3-7.3 (Ar (H)). FTIR (ATR), υ 1452, 1493, 1601, 1728, 2095 (-azide group), 2849, 2924, 3025 cm$^{-1}$

### 6.4.3 α, ω-*Bis*bromo poly(*n*-butyl acrylate) (Br-P*n*BA-Br)

To a 100 mL clean flame dried round bottom flask, equipped with side arm (and teflon stopcock) for attachment to the vacuum line, was added 60 mL of *n*-butyl acrylate (344.5 mmol), 7.0 g of DBEAD (1.944 mmol), 0.68 g of PMDETA (3.90 mmol), and 0.56 g of CuBr(I) (3.90 mmol). This reaction mixture was degassed three times by freeze–pump-thaw cycles and the flask was kept in an oil bath maintained at 70°C ( it is advised to secure the rubber septum tightly by using copper wire, otherwise, due to a large vapor pressure, the integrity of the reactor may be lost). After 60 min the polymerization was terminated by cooling the flask with liquid nitrogen. The reaction mixture was dissolved in 500 mL of THF and passed through a column containing neutral alumina to remove the copper catalyst. The eluted solution was concentrated using rotatory evaporator at 50 °C under reduced pressure to remove the solvent and the residual monomer. Owing to the low molecular weight of the

polymer and its good solubility in the methanol, the precipitation was avoided. Yield: 90 %, $M_{n,th}$ = 2,800 g/mol, $M_{n,GPC}$ = 3,400 g/mol, *PDI* = 1.38. $^1$H NMR: δ ppm, 0.93 (-COOCH$_2$-CH$_2$-CH$_2$-<u>CH$_3$</u>), 1.37-(-COOCH$_2$-CH$_2$-<u>CH$_2$</u>-CH$_3$), 1.57 (-COOCH$_2$-<u>CH$_2$</u>-CH$_2$-CH$_3$), 1.9-2.27 (-CH, and backbone proton), 4.04 (-COO<u>CH$_2$</u>-CH$_2$-CH$_2$-CH$_3$). FTIR (ATR), υ 1454, 1729, 2873, 2933, 2958, cm$^{-1}$

### 6.4.4 α, ω-*Bis*azido poly(*n*-butyl acrylate) (N$_3$-P*n*BA-N$_3$)

25 g of Br-P*n*BA-Br (14.7 mmol) was dissolved in 150 mL of DMF and reacted with 5 g of sodium azide (154 mmol) at 25 ºC. After 24 h, the reaction mixture was precipitated in water, extracted in chloroform, dried over sodium sulfate and the chloroform was removed over rotatory evaporator to obtain 23.5 g of N$_3$-P*n*BA-N$_3$. The product was analyzed using FT-IR to determine the chain end functionality and the functionalization efficiency. The ratio of azide peak to the carbonyl peak was used to calculate the percent of chain end functionalization. Yield: 94 %, $M_{n,th}$= 2,730 g/mol, $M_{n,GPC}$/= 3,660 g/mol, *PDI* =1.35.$^1$H NMR: δ ppm, 0.93 (-COOCH$_2$-CH$_2$-CH$_2$-<u>CH$_3$</u>), 1.37-(-COOCH$_2$-CH$_2$-<u>CH$_2$</u>-CH$_3$), 1.57 (-COOCH$_2$-<u>CH$_2$</u>-CH$_2$-CH$_3$), 1.9-2.27 (-CH, and backbone proton), 4.04 (-COO<u>CH$_2$</u>-CH$_2$-CH$_2$-CH$_3$). FTIR (ATR), υ 1452, 1729, 2109, 2736, 2873, 2934, 2959, cm$^{-1}$

### 6.4.5 α, ω-*Bis*-propargyl polybutadiene (PgO-PBd-OPg)

In a typical experiment, a two neck round bottom flask equipped with a stopcock and a ground joint connectivity to the high vacuum line, 50 g (42 mmol) (2,400 g/mol) of α, ω-bishydroxyl terminated polybutadiene was charged and dried under high vacuum at 70-80 °C for 2 h. After drying the polymer, ~250 mL of THF was distilled in to it, from the vacuum line under reduced pressure using liquid nitrogen as coolant. After dissolution of the polymer at room temperature, 8.34 g of sodium hydride (209 mmol) and 7.0 g of 18-crown-6 ether (26 mmol) was added quickly, through the second neck under $N_2$ flow, and closed with a rubber septum. Immediate hydrogen gas liberation was seen. The reaction mixture was stirred for 1/2 h, while the flask was opened to the vacuum line slightly to remove the liberated hydrogen gas. After observing a complete cessation of hydrogen gas evolution, the flask was removed from the vacuum line and kept under $N_2$ atmosphere. Then, 18.6 mL of propargyl bromide (209 mmol) (80 % in toluene) was added dropwise. Although the reaction goes to completion within ~24-36 h, 18-crown-6 ether (which was not a perfect match for $Na^+$), was used to promote the reaction.

The reaction was monitored by $^1$H NMR. After 48 h, the reaction solution was left standing overnight to precipitate the salt, then the polymer solution was decanted and precipitated in to a large excess of acidic methanol (250 mmol of dilute HCl (6 M HCL) containing 1 % BHT as antioxidant. The recovered dark-brown polymer was further purified by dissolving in chloroform and passing through a short silica column to remove any inorganic solids or suspended impurities. The chloroform was removed using rotatory evaporator to obtain 41 g of brown red colored viscous liquid of PgO-PBd-OPg. Yield: ~ 80 %, $M_{n,th}$ = 2580 g/mol. $M_{n,GPC}$/0.50 = 2,730 g/mol, *PDI* = 1.13 and $M_{n,NMR}$ = 2,500 g/mol. $^1$H NMR: δ ppm, 1.06-1.58 (aliphatic backbone from *1,2-vinyl*), 1.80-2.02 (aliphatic backbone from 1,4 *cis*, and 1,4 *trans*), 2.38 (propargyl –$CH_2$-C≡$\underline{CH}$), 3.50 (PBd-$CH_2$-$\underline{CH_2}$-O-Pg), 4.09-4.12 (PBd-$CH_2$-$CH_2$-O-$\underline{CH_2}$-C≡CH), 4.95 (1,2 vinyl =$CH_2$), 5.33-5.58 (1,4 *cis* and 1,4 *trans*, and *1,2-vinyl* =CH). IR (ATR), υ 1439, 1639, 2844, 2814, 3073 cm$^{-1}$.

### 6.4.6 α, ω-*Bis*-azido poly(ethylene-co--butylene) ($N_3$-P*E-co-PB*-$N_3$)

In the first step, hydroxyl chain end groups were converted to bromo- chain end groups, which were subsequently converted to azide chain end groups in second step. In a typical experiment, 50 g (28.6 mmol) (3550 g/mol) of HO-(PE-*co*-PB)-OH-6 was dissolved in 400 mL dry dichloromethane in 1 L RBF. Flask was cooled in ice water bath and, 11 g of carbon tetrabromide (33.2 mmol) and 10.0 g of triphenylphosphine (38.2 mmol) was added under nitrogen. Pale yellow colored reaction mixture was stirred for 24 h. Then, dichloromethane was removed over rotatory evaporator and product was dissolved in 500 mL hexane and flask was kept in freezer overnight to precipitate the phosphine oxide salt. Salt was filtered and polymer solution was passed through a short silica column. After removal of hexane 48 g of α,ω-*bis*-bromo-(PE-*co*-PB) was obtained, which still contained trace amount of phosphine salts. Without further purification α,ω-*bis*-bromo end functional polymer was dissolved in THF/DMF mixture and reacted with sodium azide at 50 °C for 24 h. After completion of reaction, polymer was precipitated in large excess methanol. Dissolved in chloroform, washed with water, and dried over sodium sulfate. After removal of chloroform 42 g of α,ω-*bis*-azido functional polymer was obtained as colorless liquid.

### 6.4.7 α,ω-*Bis*-UPy polybutadiene (UPy-PBd-UPy)

Telechelic α, ω-*bis*-hydroxyl polybutadiene (HO-PBd-OH) was reacted with UPy-NCO synthon by using reported procedure.[6]

### 6.4.8 α,ω-*Bis*-UPy hydrogenated polybutadiene (UPy-(PE-*co*-PB)-UPy)

Telechelic α, ω-*bis*-hydroxyl hydrogenated polybutadiene (HO-(PE-*co*-PB-OH) was reacted with UPy-NCO synthon by using reported procedure.[6]

## 6.5 UPy functionalization of telechelic polymers using CuAAC click chemistry

In a typical experiment, an equimolar amount of polymer and UPy derivatives with azide or alkyne functionality was taken in an appropriate round bottom flask depending on the amount for reaction. The polymer and UPy derivative was dissolved in DMF or THF and the required amount of PMDETA and CuBr (I) was added. The reaction mixture was stirred at RT for 24 h. In general CuAAC requires a catalytic amount of copper salt (~ 10 %), however, owing to the coordination of the catalyst with UPy group and triazole, the reaction was performed with much higher concentration of copper salt.[29] A typical example is given below wherein the '*polymer*' represents telechelic oligomers (PS, P*n*BA, and PBd) used in this study.

### 6.5.1 Synthesis of UPy-Tz-polymer-Tz-UPy

In a 250 mL round bottom flask, a required amount of $N_3$-polymer-$N_3$ or PgO-polymer-OPg (5.83 mmol) was dissolved in 100 mL of DMF for PS and P*n*BA and toluene for PBd. After obtaining a clear solution, an equivalent amount of Pg-UPy or $N_3$-UPy (5.87 mmol), depending on the functionality of telechelic polymers, CuBr (I) (5.87 mmol), and PMDETA (0.2 or 1 equivalent catalyst-ligand complex) were added into the solution. The reaction mixture was purged with $N_2$ and the dark brownish greenish-brown colored reaction mass was stirred under $N_2$ for 24 h at RT.

Reaction was monitored by FTIR (ATR) until total disappearance of azide peak of either polymer or UPy –$N_3$. Then the product UPy-Tz-polymer-Tz-UPy was precipitated in a large amount of methanol for PS and PBd and water for P*n*BA. The UPy-Tz-polymer-Tz-UPys were isolated and dissolved in 500 mL of chloroform and washed with excess water until a neutral pH, dried over sodium sulfate and passed through a short alumina column to remove the residual copper salt. The solvent was evaporated using rotatory evaporator to give the desired UPy functionalized telechelic polymers.

### 6.5.2 UPy-Tz-PS-Tz-UPy

Yield: ~72 %, $M_{n,th}$ = 2,985 g/mol, $M_{n,GPC}$ = 2,750 g/mol, $PDI$ = 1.10, $M_{n\ NMR}$ = 2,920 g/mol. $^1$H NMR: $\delta$ ppm (chain end group integration are multiplied by two), 13.09 (s, 2H, $CH_3C\underline{NH}$),

11.84 (s, 2H,-$CH_2$NH(C=O) NH), 10.12 (s, 2H, -$CH_2$NH(C=O) NH), 6.33-7.33 (124H, Ar (H), 5.85 (s, 2H, -CH=CCH3), 4.9-5.3 (8H), -CH (2H) (triazole ring), urethane –NH(2H), and –CH-Tz-$CH_2$- (4H)), 3.6-3.9 (-CH-Tz and –COO$CH_2$-$CH_3$). 3.1-3.3 (m, 8H, NH(C=O) NH$CH_2$ + -$CH_2$NHCO), 2.12 (s, 6H, $CH_3$C=CH), 1.5-1.6(m, 8H-NH$CH_2$$CH_2$$CH_2$$CH_2$$CH_2$-$CH_2$N-), 1.36 (8H m,-NH$CH_2$$CH_2$$CH_2$$CH_2$$CH_2$-$CH_2$N-) and aliphatic PS backbone. FTIR (ATR): υ 1521, 1582, 1660, 1698 1724, 2853 3081cm$^{-1}$

### 6.5.3 UPy-Tz-P*n*BA-Tz-UPy

Yield: ~67 %, $M_{n,th}$ = 3,430 g/mol, $M_{n,GPC}$ = 3,200 g/mol, *PDI* = 1.40, $M_{n\ NMR}$ = 5,450 g/mol. $^1$H NMR: $\delta$ ppm (chain end group integration are multiplied by two), 13.09 (s, 2H, $CH_3$CNH), 11.84 (s, 2H,-$CH_2$NH(C=O) NH), 10.12 (s, 2H, -$CH_2$NH(C=O) NH), 7.33 (2H, triazole ring -CH), 5.85 (s, 2H, -CH=$CCH_3$), 5.16-5.25 (bs, 6H, (-NH-COO-, urethane group(2H), and-O$CH_2$-Tz (4H)), 4.04 (-COO$CH_2$-$CH_2$-$CH_2$-$CH_3$ (50H), 3.1-3.3 (m, 8H, NH(C=O) NH$CH_2$ + -$CH_2$NHCO), 0.93 (-COO$CH_2$-$CH_2$-$CH_2$-$CH_3$ (37H)). FTIR (ATR): υ 1525, 1587, 1662, 1729, 2873 2958, 3216 cm$^{-1}$

### 6.5.4 UPy-Tz-PBd-Tz-UPy

Yield: ~79 %, $M_{n,th}$ = 3,300 g/mol, $M_{n,GPC}$ /0.50 = 2,900 g/mol, *PDI* = 1.28, $M_{n\ NMR}$ = 3,160 g/mol. $^1$H NMR: $\delta$ ppm (chain end group integration are multiplied by two), 13.09 (s, 2H, $CH_3$CNH), 11.84 (s, 2H,-$CH_2$NH(C=O) NH), 10.12 (s, 2H, -$CH_2$NH(C=O) NH), 7.56 (2H, triazole ring -CH), 5.80 (s, 2H, -CH=$CCH_3$), 5.33-5.58 ( (54 H) 1,4 cis and 1,4 trans, and 1,2 vinyl =CH) 4.95 (1,2 vinyl =$CH_2$) (57H) and (-NH-COO-, urethane group (2H), 4.57 (8H), Tz-$CH_2$-$CH_2$-urethane), 4.44 ( (4H) -O-$CH_2$-Tz), 3.50 ( 4H), PBd-$CH_2$-$CH_2$-O-Tz), 3.13-3.25 (m, 8H, NH(C=O) NH$CH_2$ + -$CH_2$NHCO), 2.12 (s, 6H, $CH_3$C=CH),1.80-2.02 (aliphatic backbone from *1,4 cis*, and *1,4 trans*), ), 106-1.58 (aliphatic backbone from *1,2-vinyl*), FTIR (ATR): υ 1528, 1588, 1640,1664, 1698, 2846, 2916, 3141 cm$^{-1}$.

## 6.6 Results and Discussion

In order to synthesize UPy functionalized telechelic polymers with different linking chain, we prepared air-stable UPy-synthons with propargyl(Pg) and azido($N_3$) functionalities and used for clicking with azido and propargyl telechelic oligomers, respectively to obtain UPy telechelic polymers (**Scheme 6.1**). Clickable UPy-Pg and UPy-$N_3$ synthons were synthesized from UPy-NCO using an excess propargyl alcohol and 2-bromoethanol, respectively in the presence of dibutyltin dilaurate catalyst at 70 $^o$C. Adduct of bromoethanol was converted to

UPy-$N_3$ using sodium azide. The $^1$H NMR of the products showed all the characteristic signals corresponding to UPy-Pg and UPy-$N_3$ (**Figure 6.1**).

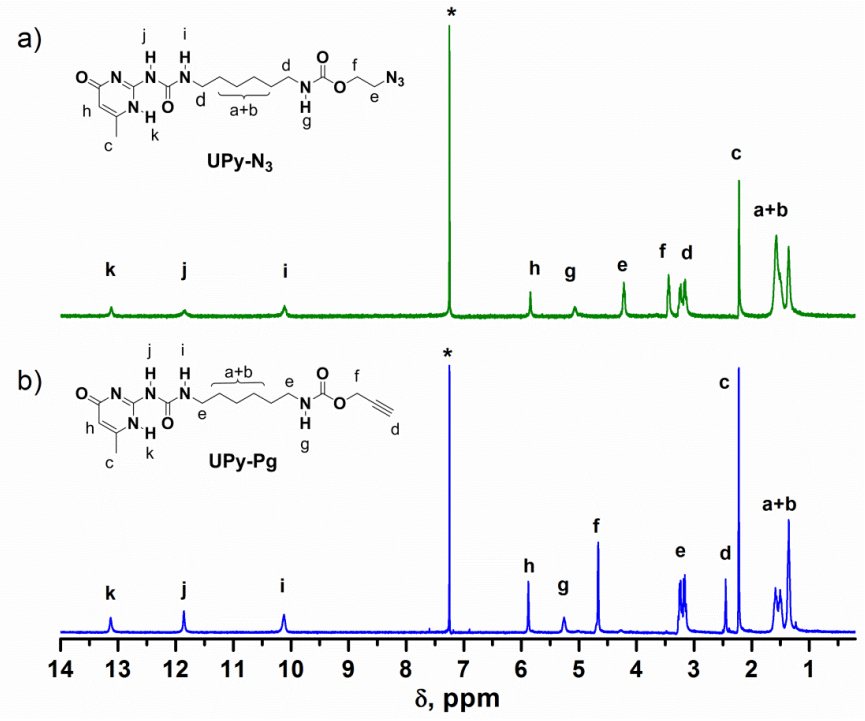
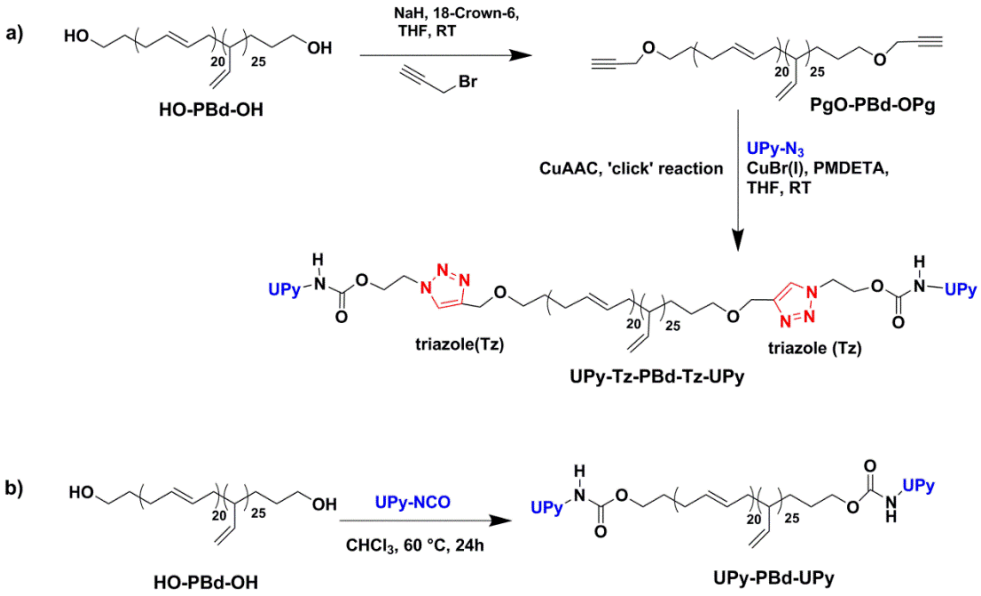



**Figure 6. 1:** $^1$H NMR spectra of (a) UPy-$N_3$ and (b) UPy-Pg. The star (*) indicates residual protons of $CDCl_3$.

The transformation of –NCO group can be seen from the IR spectra ( **Figure A6-1, in Appendix A6**), which showed distinct vibration frequencies associated with –$N_3$ at 2095 cm$^{-1}$ and alkyne at 2110 cm$^{-1}$, for UPy-$N_3$ and UPy-Pg, respectively

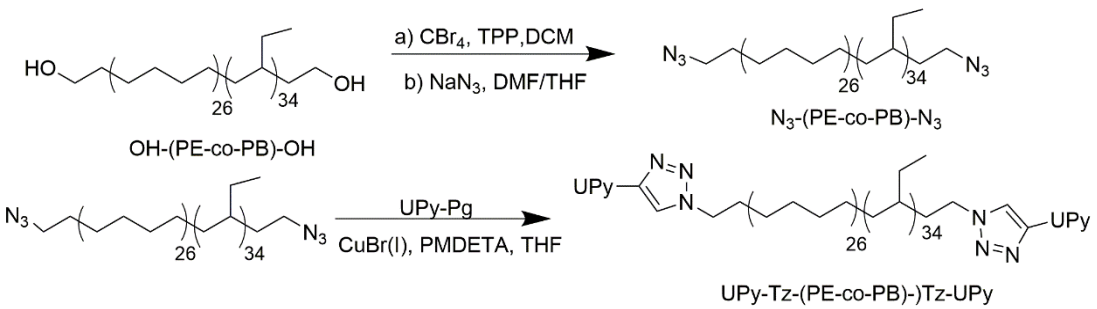
α, ω-*Bis*-azido telechelic PS and P*n*BA were readily prepared by ATRP of styrene and *n*-butyl acrylate, respectively and followed by treatment with sodium azide. Whereas, propargyl end functionalized PBd was prepared by etherification of hydroxyl terminated PBd with propargyl bromide. The propargyl functionalized telechelic PBd was reacted with UPy-$N_3$ to obtain UPy terminal PBd linked via triazole group (**Scheme 6.2a**). Also, hydroxyl terminated PBd was directly reacted with UPy-NCO to obtain UPy-PBd-UPy to evaluate the effect of triazole group on the UPy chain end association (**Scheme 6.2b**). Desired UPy telechelic were then prepared using click reaction in the presence of CuBr-PMDETA complex

(**Scheme 6.1**). Excess of catalyst complex (1:1 mol.) was used in order to compensate coordination of catalyst with UPy and triazole functionality of the product.




**Scheme 6. 2:** Schematic synthesis of UPy telechelic polybutadiene, with and without triazole ring.

In order to obtain non-polar polymer without any double bonds, hydrogenated hydroxyl telechelic polybutadiene was used. Moreover, to evaluate the influence of regiospecificty of the triazole ring substituents, hydroxyl groups were converted into azido functionality (**Scheme 6.3**). The azido functionality was clicked with UPy-Pg to obtain triazole containing hydrogenated PBd telechelics (UPy-Tz-(PE-*co*-PB)-Tz-UPy). The substitution on the triazole ring is different than UPy-Tz-PBd-Tz-UPy sample. Also, this polymer is identical to the PEB-UPy of Meijer and coworkers except two differences, it has higher ethylene groups and it contains triazole group.




**Scheme 6. 3:** Synthesis of triazole containing hydrogenated PBd telechelics (UPy-Tz-(PE-*co*-PB)-Tz-UPy).

The end-group transformations of azido-PS and azido-P*n*BA and propargyl-PBd into UPy group are accompanied by changes in physical characteristics of the polymers. For low $T_g$ polymers, UPy-Tz-PBd-Tz-UPy ($T_g$ = -36 ºC) and UPy-Tz-P*n*BA-Tz-UPy ($T_g$ = -37 ºC), the viscosity enhancement was significant and became semi-solid compared to their liquid precursors, PgO-PBd-OPg, and $N_3$-P*n*BA-$N_3$, respectively. More dramatic changes in the physical properties were seen in low $T_g$ and non-polar polymeric systems. In the case of UPy-Tz-PBd-Tz-UPy, the sample turned into a transparent thermoplastic elastomer. Similarly, UPy-PBd-UPy is a colorless transparent thermoplastic solid and the precursor hydroxyl PBd is a viscous liquid. Whereas, high $T_g$, nonpolar, and low $T_g$, polar polymers have significant increase in the glass transition temperatures without changes in the physical state. The results indicate that the presence of Tz group between UPy and polymer back-bone has significant effect for PBd, a low $T_g$ and non-polar polymer.

**Figure 6.3** shows the $^1$H NMR spectra of the products with the characteristic downfield signals of UPy group (10.2, 11.9, and 13.2 ppm) and triazole -CH group. The efficiency of the end-group transformation is also confirmed by the molecular weight determination by $^1$H NMR and SEC as shown in **Table 6.1**. Propargyl and azide groups were totally absent in the IR spectrum of the polymer; and the ratio of $M_{n,NMR}/M_{n,th}$ in all cases is close to unity indicating almost 100 % functionality of these UPy telechelics.

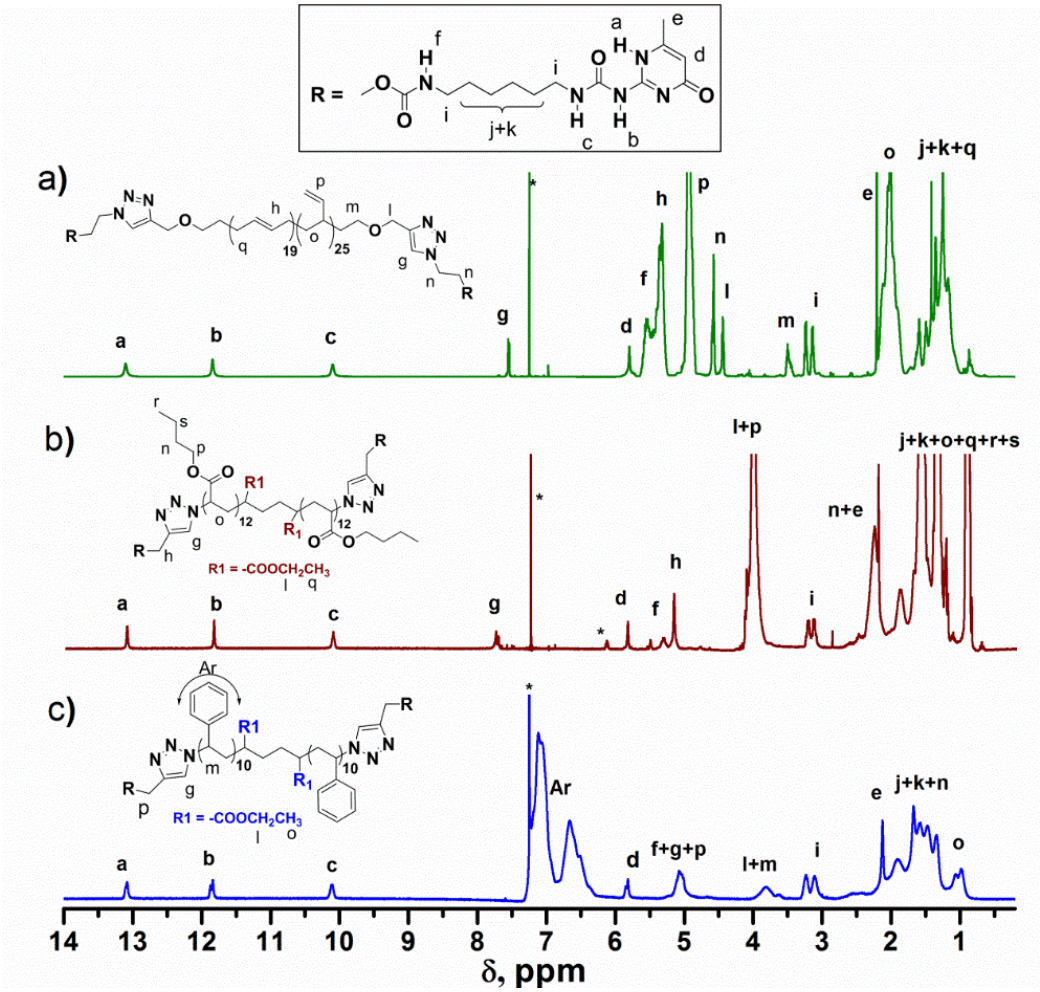



**Figure 6. 2:** $^{1}$H NMR spectra of UPy-telechelics prepared by CuAAC click reaction. a) UPy-Tz-PBd-Tz-UPy, b) UPy-Tz-P*n*BA-Tz-UPy, and c) UPy-Tz- PS-Tz-UPy. The star (*) indicates residual solvent $CDCl_3$.

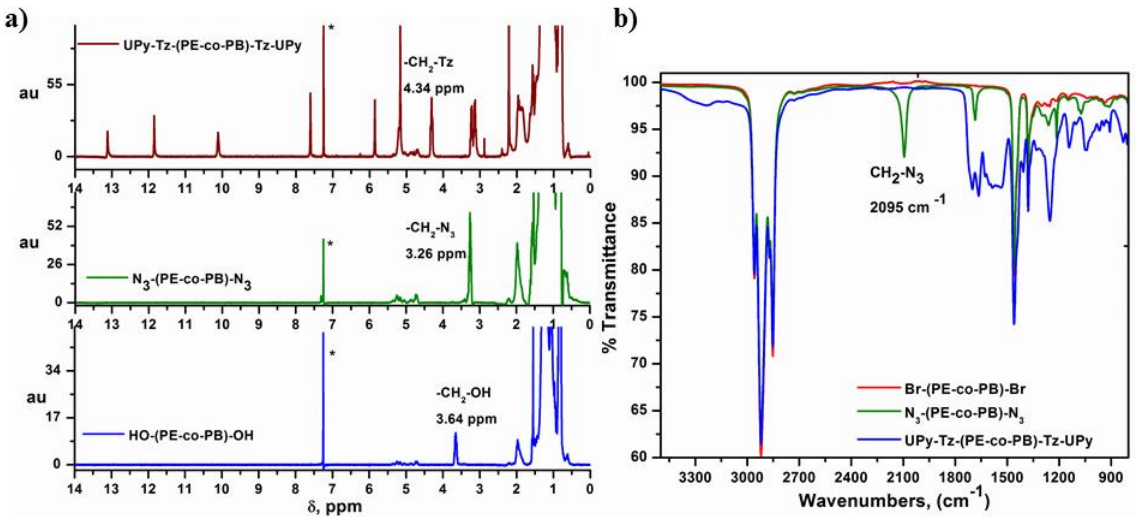



**Figure 6. 3:** a) $^{1}$H NMR and b) ATR-IR spectra of various stages of UPy-Tz-(PE-*co*-PB)-Tz-UPy synthesis.

$^{1}$H NMR of triazole containing hydrogenated PBd telechelics (UPy-Tz-(PE-*co*-PB)-Tz-UPy) shows characteristic UPy groups peaks and triazole ring –CH peak are at 7.61ppm (**Figure 6.3 a**), slightly up field than UPy-Tz-PBd-Tz-UPy (-CH 7.56 ppm. Accordingly, the ATR- FTIR spectra of the polymer show complete disappearance of azide peak at 2095 cm$^{-1}$ **(Figure 6.3 b)**.

**Table 6. 1:** Characterization UPy telechelics prepared by combination of ATRP and CuAAC click reactions

| Polymers[a)] | $M_n$ (kg/mol) of telechelics[b] | | | |
|---|---|---|---|---|
| | $M_{n,th}$[c] | $M_{n,NMR}$[d] | $M_{n,SEC}$[e] | $D$[e] |
| *X*-PS-*X* | | | | |
| Br–~~~–Br | 2.36 | 2.70 | 2.4 | 1.13 |
| $N_3$–~~~–$N_3$ | 2.29 | 2.30 | 2.5 | 1.11 |
| UPy–Tz–~~~–Tz–UPy | 2.98 | 2.92 | 2.75 | 1.10 |
| *X*-P*n*BA-*X* | | | | |
| Br–~~~–Br | 2.8 | - | 3.4 | 1.38 |
| $N_3$–~~~–$N_3$ | 2.73 | - | 3.66 | 1.35 |
| UPy–Tz–~~~–Tz–UPy | 3.43 | 5.45 | 3.2 | 1.40 |
| *X*-PBd-*X* | | | | |
| HO–~~~–OH | 2.0[f] | 2.50 | 2.40 | 1.15 |
| ≡–~~~–≡ | 2.58 | 2.50 | 2.73 | 1.18 |
| UPy–Tz–~~~–Tz–UPy | 3.30 | 3.16 | 2.90 | 1.28 |
| UPy–~~~–UPy | 3.09 | 2.90 | 2.80 | 1.13 |
| X-PE-*co*-PB-X | | | | |
| HO–~~~–OH | 3.00 | 3.55 | 3.44 | 1.13 |
| $N_3$–~~~–$N_3$ | 3.60 | 3.70 | 3.15 | 1.18 |
| UPy–Tz–~~~–Tz–UPy | 4.30 | 4.40 | 4.16 | 1.18 |
| UPy–~~~–UPy | 4.13 | 4.30 | 3.06 | 1.14 |

a) Bulk ATRP of styrene and *n*-butylacrylate were performed at 110 ºC (for 1.8 h with 77 % conversion) and 70 °C (for 1 h with 90 % conversion), respectively using difunctional initiator and telechelic hydroxyl functional PBd and HO-(PE-*co*-PB)-OH was obtained from Cray Valley with 57% *1,2 vinyl* contents, b) Conversion of end–group transformation is 100% based on NMR, the recovered yield is 80-90 % in all cases and reactions performed over 24 h, c) $M_{n,th}$ = (grams of monomer/mol. of initiator) × conversion) + mol. wt. of chain-end functionality, d) $M_n$ calculated based on initiator or end group functionality (UPy, propargyl) from $^1$H NMR in $CDCl_3$, e) determined from SEC, f) based on commercial specification.

### 6.6.1 Multiple aggregation in SEC elution profile

SEC of UPy-Tz-PBd-Tz-UPy shows a small hump on the higher molecular weight (2 × $M_p$) side indicating the presence of dimers in THF solution (**Figure 6.4, b**). Monotelechelic PBd–UPy samples also showed such dimeric peak in SEC eluogram.[30] No such dimeric peaks were observed for PS and P*n*BA telechelic systems; however, when the UPy-Tz-PS-Tz-UPy was analyzed with a SEC equipped with the light scattering detector, it shows additional peaks corresponding to the aggregation of UPy domains, which are dependent on the sample concentration in solution (**Figure 6.4a**). At very high concentration (5 or 6 mg/mL), the elusion profile of the sample would also be influenced by the column overloading.

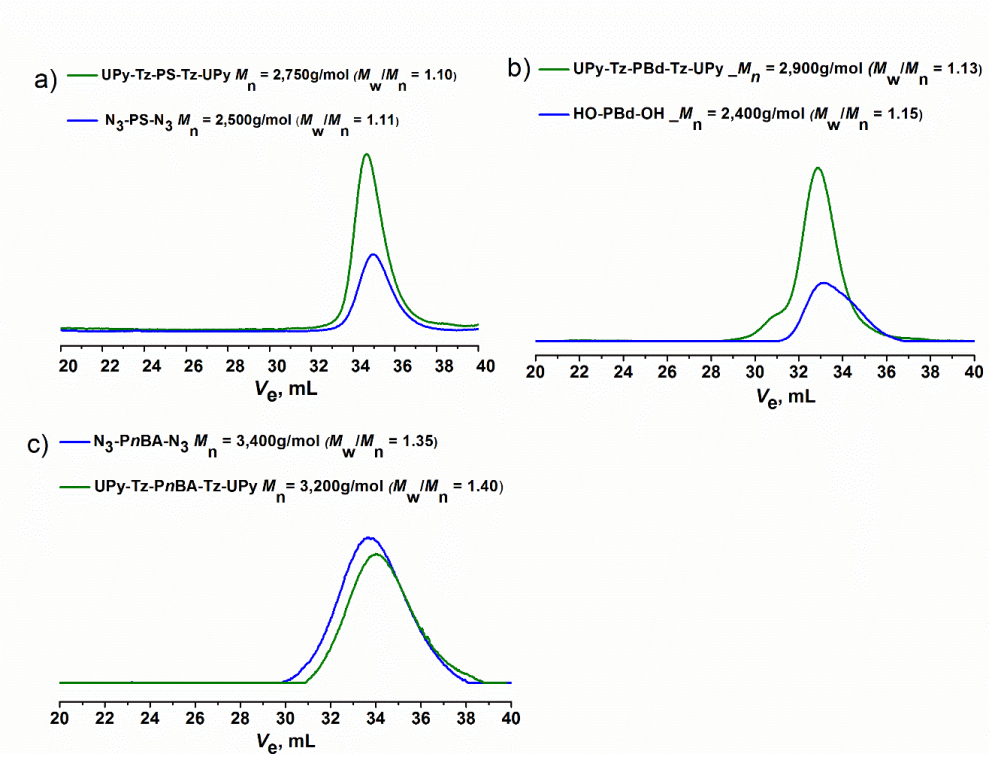



**Figure 6. 4:** SEC eluograms of UPy telechelics prepared by CuAAC click reaction using RI detector. a) UPy-Tz-PS-Tz-UPy-UPy, b) UPy-Tz-PBd-Tz-UPy, and c) UPy-Tz-P*n*BA-Tz-UPy, all SEC sample concentration are 1 mg/mL.

However, the presence of UPy hydrogen-bonded association is evident as the peak-maximum molecular weight increases with increasing sample concentration in SEC (**Figure 6.5b** and **Figure A.2 in Appendix A**). Similar observations were reported by Wrue and co-

workers[31] on telechelic UPy-PS-UPy prepared by a combination of ATRP and ATRC. No such observation was seen with UPy-P*n*BA-UPy, this was partly attributed to a weak hydrogen-bonding in the presence of polar ester pendants of the P*n*BA backbone and a broader molecular weight distribution of the sample.

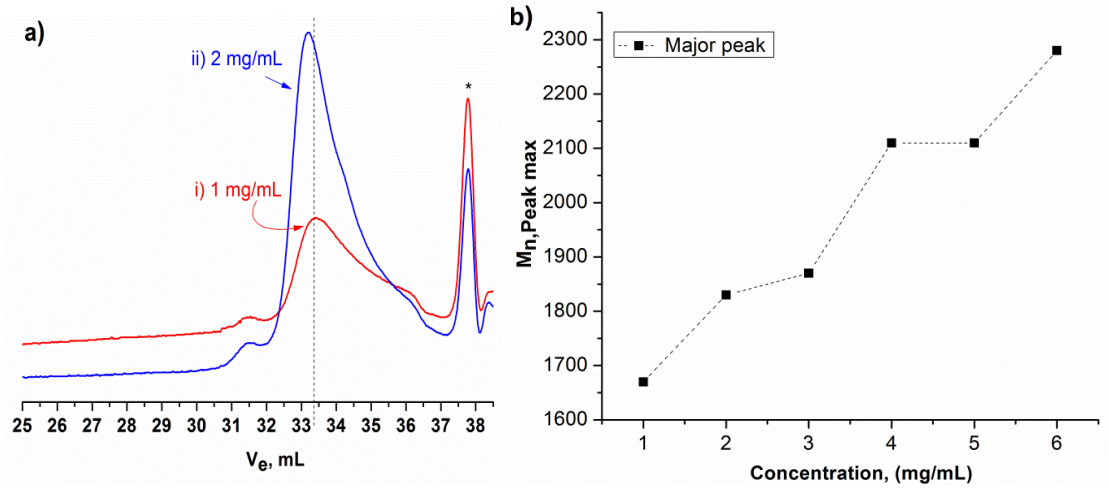



**Figure 6. 5:** a) SEC traces showing effect of concentration on the aggregation of UPy groups in UPy-Tz-PS-Tz-UPy (i) 1 mg/mL and (ii) 2 mg/mL and b) a plot of peak-maximum molecular weight at different injection sample concentration with light scattering detector using $d_n/d_c$ of 0.186.

### 6.6.2 Solution viscosity

Solution viscosity of the triazole containing sample in toluene is much higher than the sample without the triazole linker (**Figure 6.6**). The double logarithmic plot of specific viscosity, $\eta_{sp}$ vs concentration gave slope values of 2.27 and 3.32 for UPy-PBd-UPy and UPy-Tz-PBd-Tz-UPy, respectively in a high concentration region ([C] >18 mM). As per the predictions of Cate's model of the reversibly linked SPs, the viscosity plot for UPy-telechelics with linear chain extension should have a slope in the range of 3.5-3.7, though a slope different than this prediction was also reported in SP networks.[5,32] Furthermore normal viscosity plots, $\eta_{sp}$ vs [C] for PS and PBd SPs show two distinct regions supporting the UPy chain-end network-dynamics change very fast at higher concentration (overlap concentration) indicating the onset

of entanglements (Figure S5). It is evident from the plot, the viscosity increases rapidly above ~15 mM and expected to show a much higher slope > 3.7 at higher concentration ([C] >25 mM). Interestingly, the onset for the entanglement concentration for both the samples is similar ([C] ~ 15 mM). This indicates the chain-end extension is primarily driven by UPy dimerization. At a higher concentration, a much higher slope of UPy-Tz-PBd-Tz-UPy clearly indicating participation of triazole group, which results in much stronger entanglement of the UPy chain-extended network. Also, the crossover concentration can be assumed as an overlap concentration for this sample.[33]

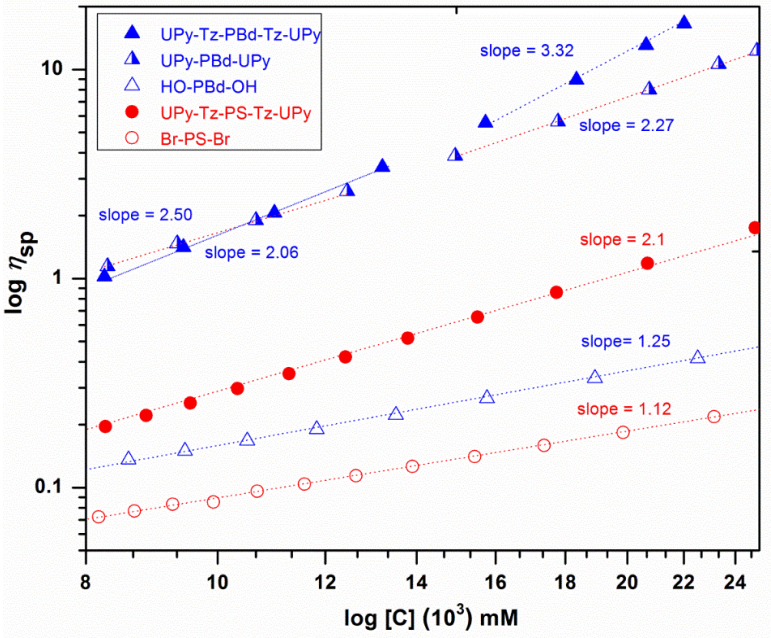



**Figure 6. 6:** Viscosity profile of UPy telechelics and the effect of triazole on UPy chain end association of UPy-Tz-PBd-Tz-UPy and UPy-Tz-PS-Tz-UPy.

On the contrary, the viscosity profile of the UPy-Tz-PS-Tz-UPy sample shows a very minimal increase in comparison to its precursor. This may be related to a low $R_h$ of PS compared to PBd and a much higher overlap concentration of low molecular weight PS. The sample of UPy-Tz-P*n*BA-Tz-UPy was not used for the viscosity study and it is expected to have a similar viscosity behavior like UPy-Tz-PS-Tz-UPy.

### 6.6.3 Effect of heating rate and aging on DSC analysis of UPy Telechelics

Each DSC run has at least three heating and cooling cycles with a heating rate of 5 °C, 10 °C and 20 °C per minute. After the first DSC run, the sample was aged at room temperature for a given time interval before rerunning it for the second and the third heating cycles. The DSC profile of PBd-UPy samples at a heating rate of 10 °C/min shows the presence of endothermic peak at ~ 63 °C for UPy-PBd-UPy and at ~78 °C for UPy-Tz-PBd-Tz-UPy suggesting the presence of aggregated UPy domains (Figure S6).

The UPy-Tz-PBd-Tz-UPy showed a higher melting peak supporting the presence of additional hydrogen bonding interactions involving the triazole group in the UPy domain aggregation. Enthalpy values of endothermic peak decrease in second and third heating cycle. However, a time-dependent DSC analysis of these two samples further supports the participation of triazole affects the reassociation dynamics of supramolecular association as the UPy-Tz-PBd-Tz-UPy sample shows a complete recovery of the melting peak after 6 h, whereas the UPy-PBd-UPy shows only a partial recovery of 33 % in 6 h as evident from the corresponding enthalpies of dissociation (Table 2). This was calculated by using first heating cycle of first run, and values of second and third run were divided by enthalpy values of first cycle of first run.

**Table 6. 2**: DSC analysis of UPy-PBd-UPy, effect of triazole on hydrogen bonded aggregation of UPy groups

| Sample [a] | First run heating cycle | | After 6 h aging | | |
|---|---|---|---|---|---|
| | $T_m$, (°C) | $\Delta H$, (J/g) | $T_m$, (°C) | $\Delta H$, (J/g) | % [b] recovery |
| UPy-Tz-PBd-Tz-UPy | 77.95 | 12.46 | 76.19 | 12.67 | 100 |
| UPy-PBd-UPy | 63.21 | 15.32 | 59.42 | 4.987 | 33.0 |

a) Analysis was performed at a heating/cooling rate of 10 °C, b) calculated based on the enthalpy change ($\Delta H$) of the first heating cycle.

Since the hydrogen bonded UPy dimers are in equilibrium with aggregated domains, the heating rates alter the dynamics significantly. For the heating cycle at 20 °C/min, the endothermic peak recovery is very low for UPy-Tz-PBd-Tz-UPy, and the peak position shifts

from 69.36 °C to 103.5 °C (**Figure 6.7**). For the sample without the Tz linker, the second and third heating cycles do not show any endothermic peak at all. Moreover, the peak recovery is very small for UPy-Tz-PBd-Tz-UPy (4.426 %). This clearly indicates, the time required to regenerate the original volume of UPy aggregated domains is not sufficient for higher heating/cooling rate. Meijer and co-workers in their earlier work on UPy-Kraton-UPy reported an absence of such a melting peak in the second heating cycle (20 °C/min) and considered as absence of crystalline aggregates, and chain extension leading to formation of very high molecular weight polymer was attributed for the thermoplastic elastomeric properties of UPy-Kraton-UPy.[6]

However, the dynamics of linking chain in the present study is much higher due to low $M_n$, it may be possible that the presence of endothermic peak in relatively higher $M_n$ (4100 g/mol*)* material, UPy-Kraton-UPy, could be absent on the experimental timescale since the time in between the subsequent heating and cooling cycles were not sufficient at the rate of 20 °C/min for the formation of UPy aggregates. However, recent work by Kautz and coworkers has shown the presence of a small endothermic peak at 69 °C in UPy-Kraton-UPy sample (DSC run at 10 $^{o}$C/min ramping rate), which was attributed to an incomplete aggregation of lateral urethane group.[10] The sample with a lateral urea linking group has a melting point of 129 °C, due to nanophase aggregated fiber formation by one dimensional staking of urea groups.

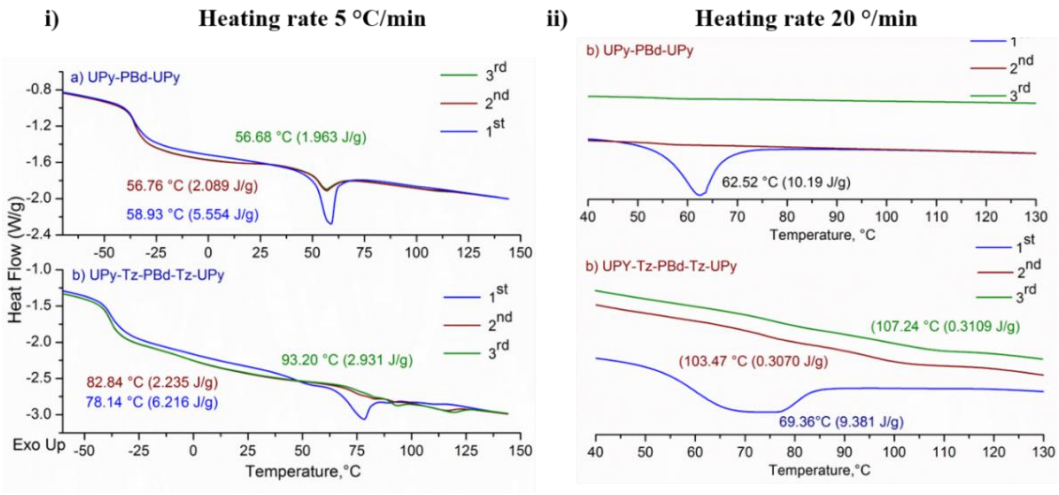



**Figure 6. 7:** DSC profile of telechelic PBd UPy, (i) heating rate (5 °C), UPy-PBd-UPy (a) and UPy-Tz-PBd-Tz-UPy (b); (ii) heating rate 20 °C, UPy-PBd-UPy (a) and UPy-Tz-PBd-Tz-UPy (b).

Our hydrogenated sample, UPy-Tz-(PE-*co*-PB)-Tz-UPy *(*$M_n$, 4300 g/mol), which corresponds to Kraton-UPy ($M_n$, 4100 g/mol) with 7 % higher ethylene contents). UPy-(PE-*co*-PB)-UPy has $T_g$ of -48 °C ad $T_m$ of 56 °C, whereas, Kraton-UPy has $T_g$ of -58 °C and a small emdothermic peak at 69 °C. Difference of $T_m$ of Kraton-UPy and our UPy-(PE-*co*-PB)-UPy, will be aloborated in final chapter. Here it can be directly attributed to the difference in $T_m$, to difference in $T_g$, and eventually towards diferecne of ethylene groups.

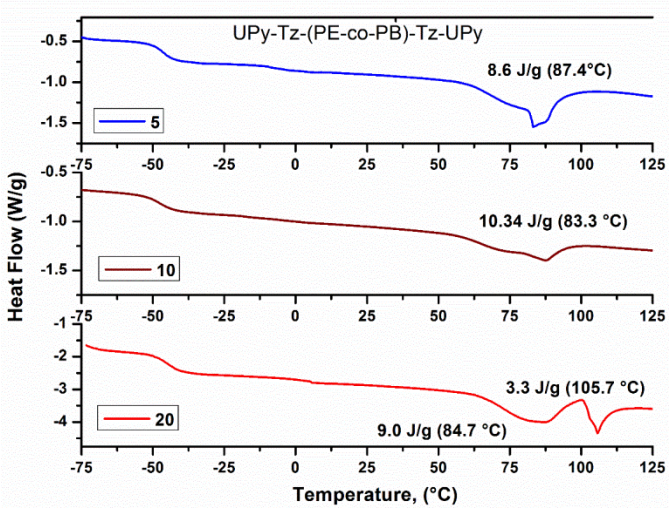
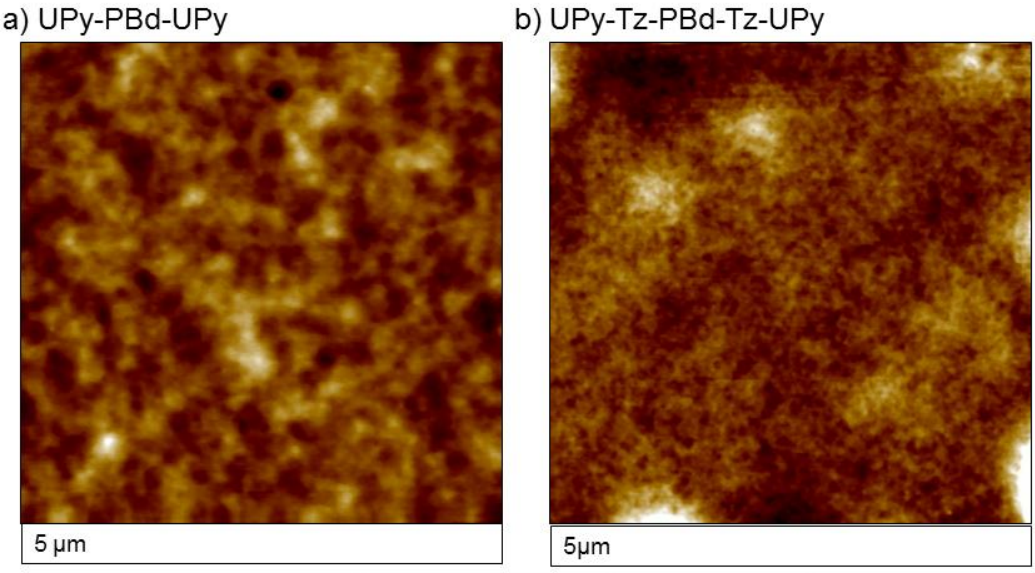



**Figure 6. 8:** DSC plot of UPy-Tz-(PE-*co*-PB)-Tz-UPy

The $T_g$ values of UPy-Tz-PS-Tz-UPy and UPy-Tz-P*n*BA-Tz-UPy are in close agreement with the literature values considering their end-group modification.[29,34,35] Interestingly, there is no endothermic peak in high $T_g$ and non-polar PS sample attributable to the formation of UPy associated domain up to 150 °C. The polar P*n*BA system also has absence of endothermic peak. The combined effect of triazole and UPy association appears to be weak in the case of P*n*BA and PS systems. The polar ester pendants in P*n*BA system can compete with hydrogen bonding and diminishes the UPy hydrogen bonding association.[36] In the case of PS linking chain, the motion of the chains is frozen below the $T_g$, which does not facilitate the growth of extended, and stronger hydrogen bonded domain formation. The hydrogen bonding in this case appears to be limited due to the nature of the polymer chain, especially in solid state. Nevertheless, the existence of UPy associated domain formation is evident in the solution too (**Figure 6.6**).




| Sample | $D_{min}$ (nm) | $D_{max}$ (nm) | $D_{avg}$ (nm) |
|---|---|---|---|
| UPy-PBd-UPy | 49 | 85 | 78.5 |
| UPy-Tz-PBd-Tz-UPy | 34 | 79 | 55.0 |

**Figure 6. 9:** AFM Phase images of UPy-PBd-UPy (a) and UPy-Tz-PBd-Tz-UPy (b), and size of aggregated domains (from chloroform solution).

### 6.6.4 Network structure by AFM and DMTA

Participation of Tz in the UPy network was further supported by AFM analysis of the drop cast film of UPy-PBd-UPy and UPy-Tz-PBd-Tz-UPy. Both samples show a random net-work consisting of micellar aggregated domains indicative of UPy chain end associations. The formation of networks is more favorable at room temperature at which the experiments were performed. However, the sizes of the aggregated domains are smaller in the case of UPy-Tz-PBd-Tz-UPy (**Figure 6.9**). This indicates that the triazole takes part in the chain end association, thereby reducing the UPy micellar cluster sizes in solid-state morphology. However, these images differ slightly from the previous AFM images obtained from toluene solution cast film. (**Chapter 5, Figure 5**. Due to poor solubility of UPy-Tz-PBd-UPy in toluene, polymer solution was made in chloroform. Toluene cast film are more like parallel fibrillar clusters association, whereas, chloroform films are random cluster association.

It is worth mentioning here that model studies carried out with the mixture of $C_6$UPy (made from Me-Iso and hexyl isocyanate) and triazole compound (made from octyl azide and 1-hexyne) indicated only minute changes in $^1$H NMR in diluted concentration (~5 mg/mL) and due to peak merging bands of functional groups, it is difficult to discern the triazole interaction in the FT-IR spectra. Moreover, $^1$H NMR spectrum in C*D*Cl$_3$ shows characteristic UPy peaks indicating triazole does not disturb the dimerization of UPy in solution.

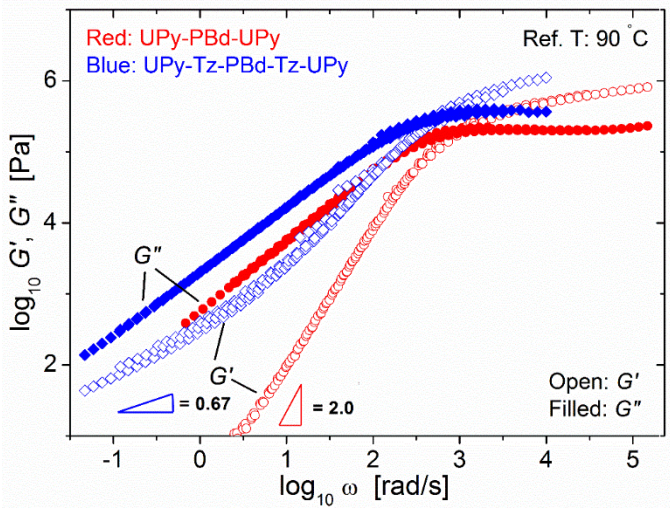



**Figure 6. 10:** Complex viscosity master curves of UPy-Tz-PBd-Tz-UPy and UPy-PBd-UPy at reference temperature 90 °C.

A comparison of the domain sizes indicates the participation of triazole group leading to the formation of smaller domains with uniform distribution across the PBd matrix. However, a high $T_m$ and a modulus (**Figure 6.10**) of triazole containing sample indicate that the net strength of the resulting clusters is higher than UPy-PBd-UPy, probably due to a positive interference either by the hydrogen bonding of the triazole group or steric hindrance around the UPy dimeric clusters.

In order to evaluate the effect of Tz on the UPy group association, both the UPy-PBd-UPy and UPy-Tz-PBd-Tz-UPy samples were analyzed by rheology using 90 °C as reference temperature (**Figure 6.10**). The complex modulus master curves show distinct differences for the UPy-PBd-UPy and UPy-Tz-PBd-Tz-UPy. A higher complex modulus was observed for UPy-Tz-PBd-Tz-UPy compared to the sample without Tz linking group.

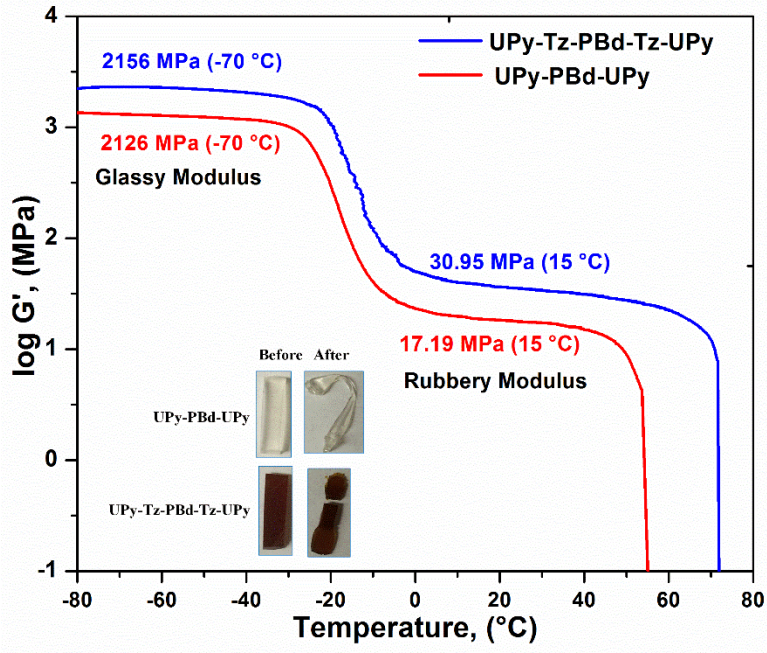



**Figure 6. 11:** Temperature dependence of modulus for UPy-PBd-UPy and UPy-Tz-PBd-Tz-UPy

Moreover, the low-frequency slope 0.67 also deviates from 2 for G' clearly suggesting that the system is not able to completely relax its mechanical stress at low frequency due to network formation. Thus, we believe that the interference of Tz in UPy aggregation domains promotes larger network formation with smaller clusters. The effect of Tz group on the property enhancement was also seen in the DMTA analysis of the thin films of these samples (**Figure 6.11**). Both the glassy ($\Delta G$ = 400 MPa) and rubbery ($\Delta G$= 13 MPa) modulus values of the triazole containing sample are much higher than the sample without the Tz. The value of the rubbery modulus is almost twice for the UPy-Tz-PBd-Tz-UPy. As seen earlier from the DSC analysis, the sample UPy-Tz-PBd-Tz-UPy has a higher $T_m$, which was further confirmed by the DMTA plot. Thin film of UPy-Tz-PBd-Tz-UPy with Tz linker retains its strength up to ~ 70 °C and undergoes brittle-break at ~ 72 °C. Whereas the UPy-PBd-UPy film starts yielding at ~ 54 °C and finally breaks at ~ 57 °C (**Figure 6.11**, inset).

Similarly, the UPy-Tz-(PE-*co*-PB)-Tz-UPy also exhibits enhanced glassy modulus ($\Delta G$ = 74 MPa) and enhanced yield temperature (74.5 °C) compared to non-triazole system (**Figure 6.12**), with no significant change in the rubbery modulus. Unlike Tz-PBd-Tz-UPy, this polymer film retains its shape and DMTA run gets terminated at 87 °C due to softening of

the film at holding points **(Figure 6.12**, inset). Glass and rubbery modulus data of these polymer are given in **Table 6.3**. Although, PE-*co*-PB sample do not differ much in the rubbery modules, strikingly the higher yield temperature allows self-standing film upto 90 °C. Therefore, the preliminary rheology and DMTA studies strongly support the participation of the triazole ring in the hydrogen bonded aggregates of UPy dimers, which changes the size and distribution of UPy aggregated domains as confirmed by AFM images. More detailed studies on the rheology of the UPy telechelics are discussed in **Chapter 7**.

**Table 6. 3:** Modulus enhancement of Triazole linker in UPy telechelics

| Entry | Polymer | Storage Modulus at -60 °C (MPa) | Storage Modulus at 25 °C (MPa) | Yield Temperature (°C)[a] |
|---|---|---|---|---|
| 1 | UPy-PBd-UPy | 2126 | 17 | 54 |
| 2 | UPY-Tz-PBd-Tz-UPy | 2156 | 31 | 72 |
| 3 | UPy-(PE-*co*-PB)-UPy | 1458 | 10 | 52.1 |
| 4 | UPY-Tz-(PE-*co*-PB)-Tz-UPy | 1532 | 9.8 | 74.5 |

a) Determined from the DMTA plot at the point of second tan δ start increasing.

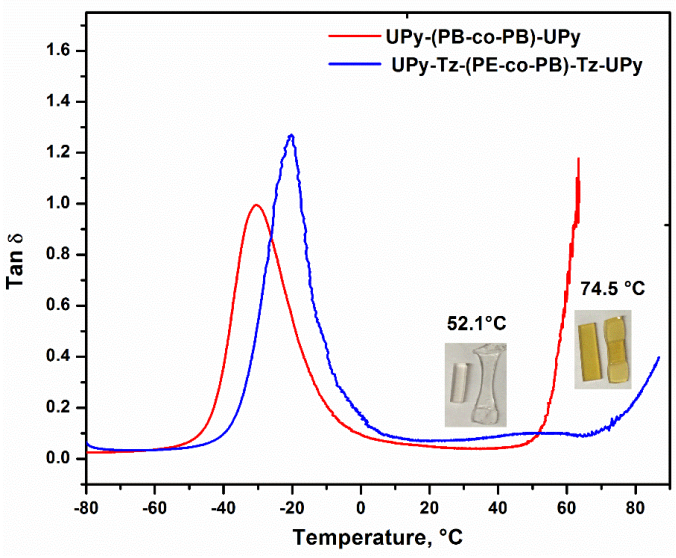



**Figure 6. 12:** DMTA plot of Tan delta for UPy-Tz-(PE-*co*-PB)-Tz-UPy and UPy-(PE-*co*-PB)-UPy

## 6.7 Conclusions

In this chapter, a modular approach for the synthesis of UPy telechelics by combination of ATRP and click reaction has been introduced. Using this approach, four different telechelic polymers of PS, PBd. PE-*co*-PB and P*n*BA have been synthesized and characterized. The presence of triazole group positively interferes with the hydrogen bonding of UPy domains. Solution, melt and solid-state characterizations of triazole containing UPy telechelics indicate that the resulting SPs exhibit higher viscosity and modulus. As ATRP allows preparation of various molecular architectures using block copolymers containing suitable pendant or side-groups, which can be directly used for clicking UPy moiety, this combination of ATRP and click approach would be a very useful synthetic tool. Also, selection of propargyl amine and hydroxyl amine will provide an easy path for UPy telechelic with urea linkage.

## 6.8 Appendix Information

ATR-IR spectra of UPy-NCO, Pg-UPy, and UPy-$N_3$ synthons and UPy-Tz-PBd-Tz-UPy, SEC traces of UPy-Tz-PS-Tz-UPy at different concentration, viscosity plots of UPy-Tz-PBd-Tz-UPy and UPy-Tz-PS-Tz-UPy, DSC of telechelic PBd-UPy and PS-UPy systems with and without Tz linker.

## 6.9 References


(1) Brunsveld, L.; Folmer, B. J. B.; Meijer, E. W.; Sijbesma, R. P. *Chem. Rev.* **2001**, *101*, 4071.

(2) Söntjens, S. H. M.; Sijbesma, R. P.; van Genderen, M. H. P.; Meijer, E. W. *J. Am. Chem. Soc.* **2000**, *122*, 7487.

(3) Hirschberg, J.; Beijer, F. H.; van Aert, H. A.; Magusin, P.; Sijbesma, R. P.; Meijer, E. W. *Macromolecules* **1999**, *32*, 2696.

(4) Beijer, F. H.; Kooijman, H.; Spek, A. L.; Sijbesma, R. P.; Meijer, E. W. *Angew. Chem. Int. Ed.* **1998**, *37*, 75.

(5) Sijbesma, R. P.; Beijer, F. H.; Brunsveld, L.; Folmer, B. J. B.; Hirschberg, J. H. K. K.; Lange, R. F. M.; Lowe, J. K. L.; Meijer, E. W. *Science* **1997**, *278*, 1601.

(6) Folmer, B. J. B.; Sijbesma, R. P.; Versteegen, R. M.; van der Rijt, J. A. J.; Meijer, E. W. *Adv. Mater.* **2000**, *12*, 874.

(7) Hentschel, J.; Kushner, A. M.; Ziller, J.; Guan, Z. *Angew. Chem. Int. Ed.* **2012**, *51*, 10561.

(8) Beijer, F. H.; Sijbesma, R. P.; Kooijman, H.; Spek, A. L.; Meijer, E. W. *J. Am. Chem. Soc.* **1998**, *120*, 6761.

(9) Keizer, H. M.; van Kessel, R.; Sijbesma, R. P.; Meijer, E. W. *Polymer* **2003**, *44*, 5505.

(10) Kautz, H.; van Beek, D. J. M.; Sijbesma, R. P.; Meijer, E. W. *Macromolecules* **2006**, *39*, 4265.

(11) Dankers, P. Y. W.; Zhang, Z.; Wisse, E.; Grijpma, D. W.; Sijbesma, R. P.; Feijen, J.; Meijer, E. W. *Macromolecules* **2006**, *39*, 8763.

(12) Yamauchi, K.; Kanomata, A.; Inoue, T.; Long, T. E. *Macromolecules* **2004**, *37*, 3519.

(13) Delgado, P. A.; Hillmyer, M. A. *RSC. Adv.* **2014**, *4*, 13266.

(14) Nieuwenhuizen, M. M. L.; de Greef, T. F. A.; van der Bruggen, R. L. J.; Paulusse, J. M. J.; Appel, W. P. J.; Smulders, M. M. J.; Sijbesma, R. P.; Meijer, E. W. *Chem. Eur. J.* **2010**, *16*, 1601.

(15) Sarbu, T.; Lin, K.-Y.; Spanswick, J.; Gil, R. R.; Siegwart, D. J.; Matyjaszewski, K. *Macromolecules* **2004**, *37*, 9694.
(16) Tasdelen, M. A.; Kahveci, M. U.; Yagci, Y. *Prog. Polym. Sci.* **2011**, *36*, 455.
(17) Sudo, A.; Hamaguchi, T.; Aoyagi, N.; Endo, T. *J. Polym. Sci. Part A: Polym. Chem.* **2013**, *51*, 318.
(18) Yurteri, S.; Cianga, I.; Yagci, Y. *Macrom. Chem. Phys* **2003**, *204*, 1771.
(19) Kolb, H. C.; Finn, M. G.; Sharpless, K. B. *Angew. Chem. Int. Ed.* **2001**, *40*, 2004.
(20) Vogt, A. P.; Sumerlin, B. S. *Macromolecules* **2006**, *39*, 5286.
(21) Gao, H.; Matyjaszewski, K. *Macromolecules* **2006**, *39*, 4960.
(22) Chen, G.; Tao, L.; Mantovani, G.; Ladmiral, V.; Burt, D. P.; Macpherson, J. V.; Haddleton, D. M. *Soft Matter* **2007**, *3*, 732.
(23) Binder, W. H.; Sachsenhofer, R. *Macromol. Rapid. Commun.* **2008**, *29*, 952.
(24) Iha, R. K.; Wooley, K. L.; Nyström, A. M.; Burke, D. J.; Kade, M. J.; Hawker, C. J. *Chem. Rev.* **2009**, *109*, 5620.
(25) Vora, A.; Singh, K.; Webster, D. C. *Polymer* **2009**, *50*, 2768.
(26) Hasneen, A.; Han, H. S.; Paik, H. J. *React. Funct. Polym.* **2009**, *69*, 681.
(27) Koyama Takahashi, M.; Lima, M.; Polito, W. *Polym. Bull.* **1997**, *38*, 455.
(28) Bielawski, C. W.; Morita, T.; Grubbs, R. H. *Macromolecules* **2000**, *33*, 678.
(29) Feldman, K. E.; Kade, M. J.; Meijer, E. W.; Hawker, C. J.; Kramer, E. J. *Macromolecules* **2009**, *42*, 9072.
(30) Bobade, S. L.; Malmgren, T.; Baskaran, D. *Polym.Chem.* **2014**, *5*, 910.
(31) Wrue, M. H.; McUmber, A. C.; Anthamatten, M. *Macromolecules* **2009**, *42*, 9255.
(32) Seiffert, S.; Sprakel, J. *Chem. Soc. Rev* **2012**, *41*, 909.
(33) van der Gucht, J.; Besseling, N. A. M.; Knoben, W.; Bouteiller, L.; Cohen Stuart, M. A. *Phys.Rev. E* **2003**, *67*, 051106.
(34) Yamauchi, K.; Lizotte, J. R.; Hercules, D. M.; Vergne, M. J.; Long, T. E. *J. Am. Chem. Soc.* **2002**, *124*, 8599.
(35) Elkins, C. L.; Park, T.; McKee, M. G.; Long, T. E. *J. Polym. Sci., Part A: Polym. Chem.* **2005**, *43*, 4618.

(36) De Greef, T. F. A.; Kade, M. J.; Feldman, K. E.; Kramer, E. J.; Hawker, C. J.; Meijer, E. W. *J. Polym. Sci., Part A: Polym. Chem.* **2011**, *49*, 4253.

## Appendix A6

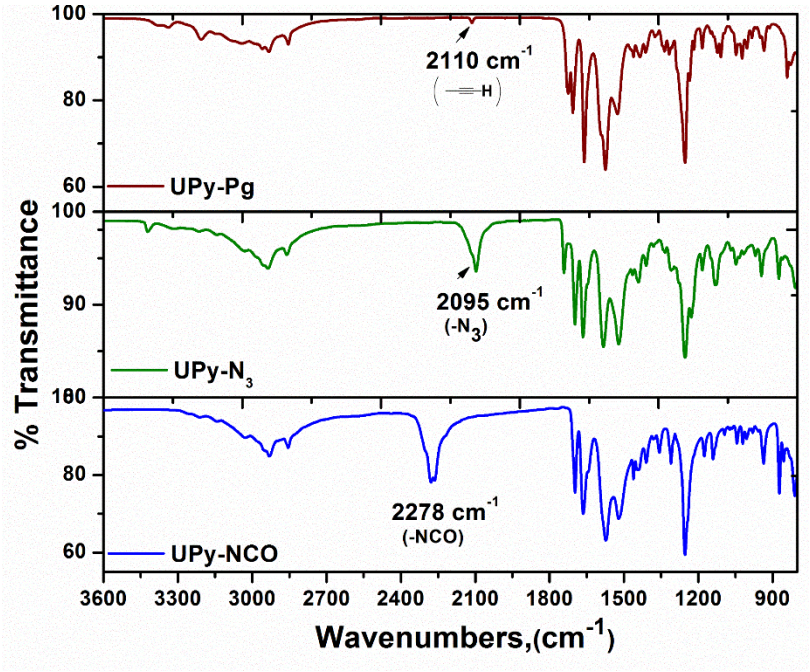



**Figure A6. 1:** FTIR (ATR) spectrums of UPy-Pg and UPy-$N_3$

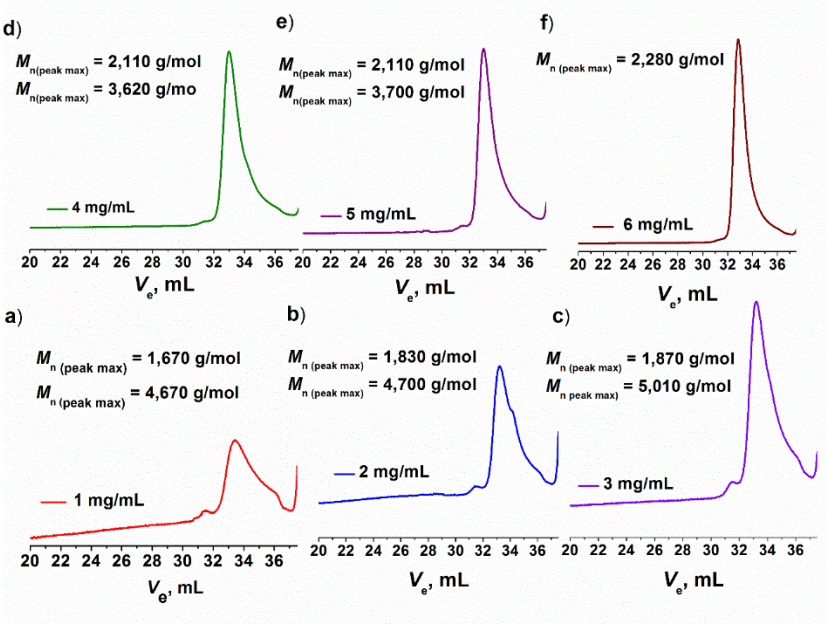



**Figure A6. 2:** SEC traces of UPy-Tz-PS-Tz-UPy, the effect of concentration on the aggregation of UPy groups (1 mg/mL (a) to 6 mg/mL (e) (values are reported with the light scattering detector using $d_n/d_c$ of 0.186)

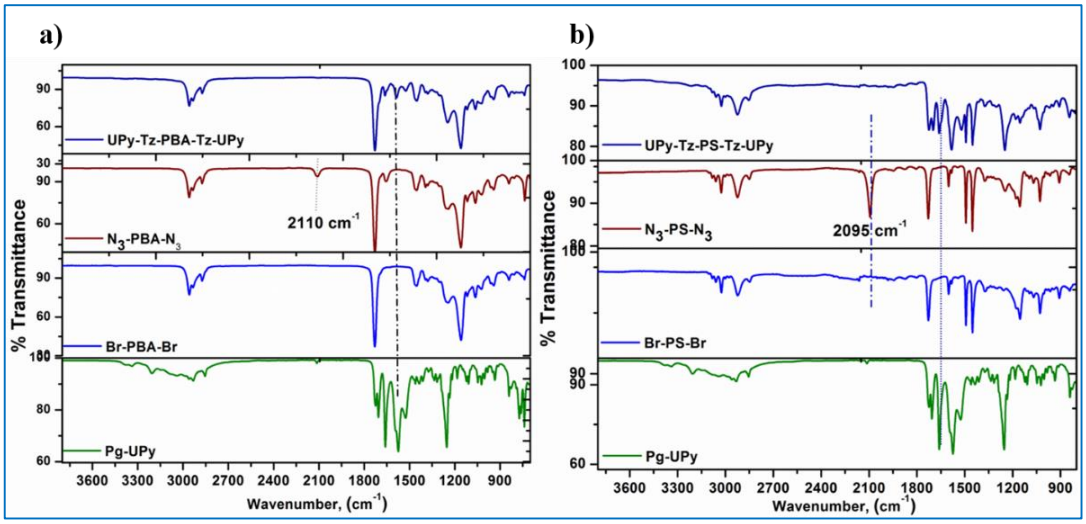



**Figure A6. 3:** FTIR (ATR) spectra of end group transformations. a) UPy-Tz-P*n*BA-Tz-UPY, b) UPy –TZ-PS-Tz-UPy

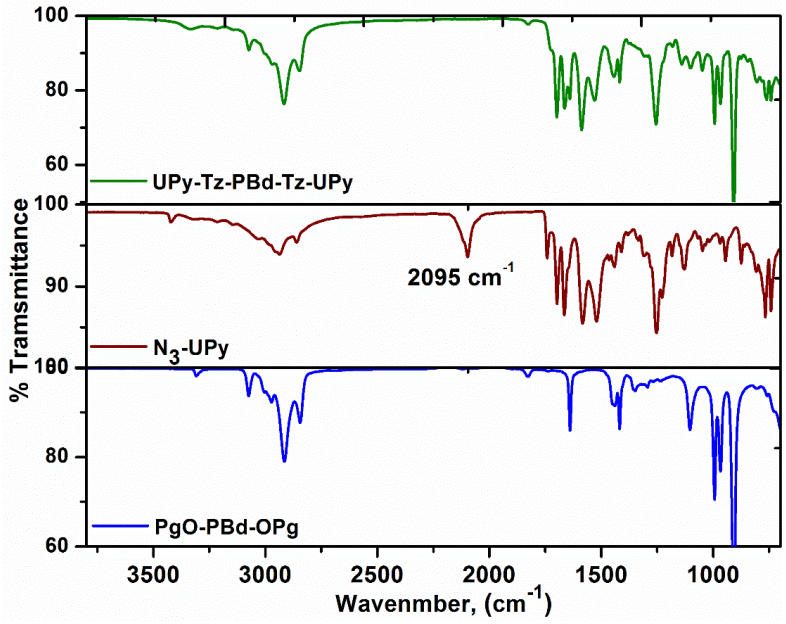



**Figure A6. 4:** FTIR (ATR) spectrum of UPy-Tz-PBd-Tz-UPy

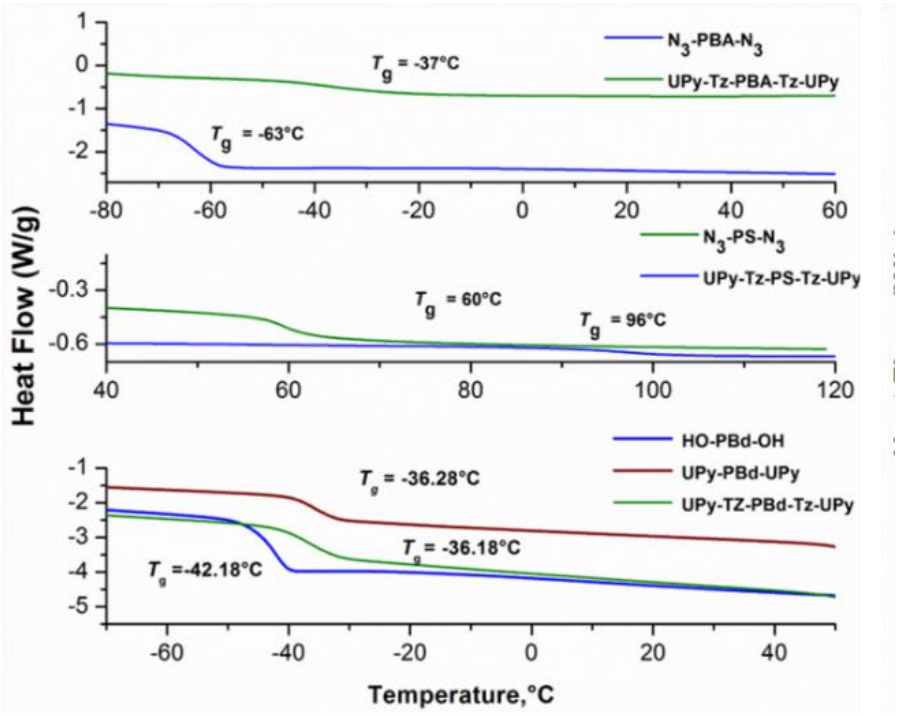



**Figure A6. 5:** Glass transition temperatures of the three polymers prepared by CuAAC click

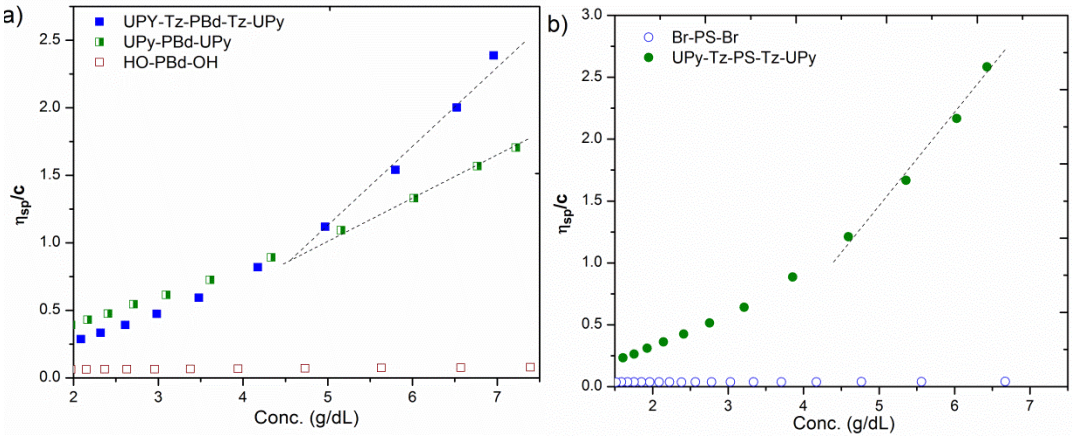



**Figure A6. 6:** Viscosity profile of UPy telechelics and the effect of triazole on UPy chain end association a) UPy-Tz-PBd-Tz-UPy and b) UPy-Tz-PS-Tz-UPy

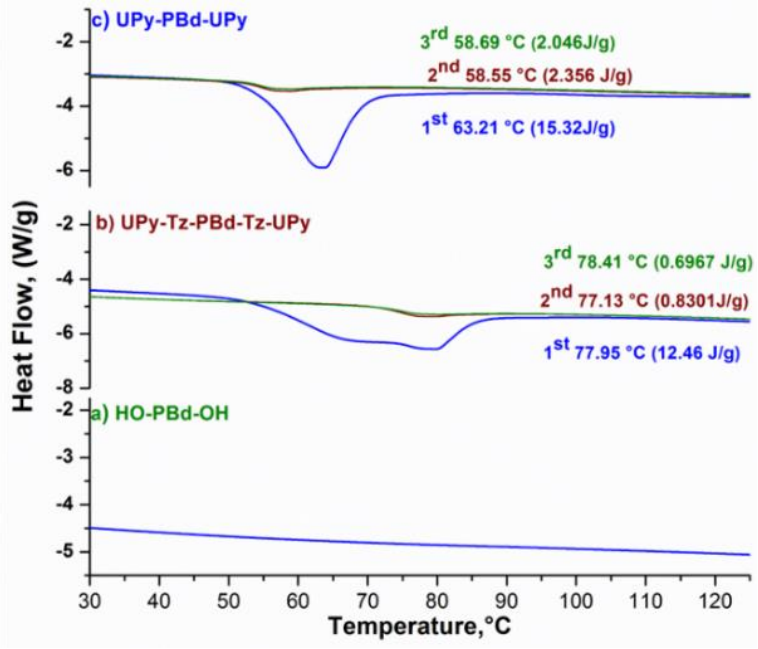



**Figure A6. 7:** DSC profile (at heating rate 10 °C/min) showing effect of triazole on the UPy-group association in the UPy-PBd-UPy

# Chapter 7: Dynamics of Ureidopyrimidone Telechelics: Role of Chain Mobility and Polarity

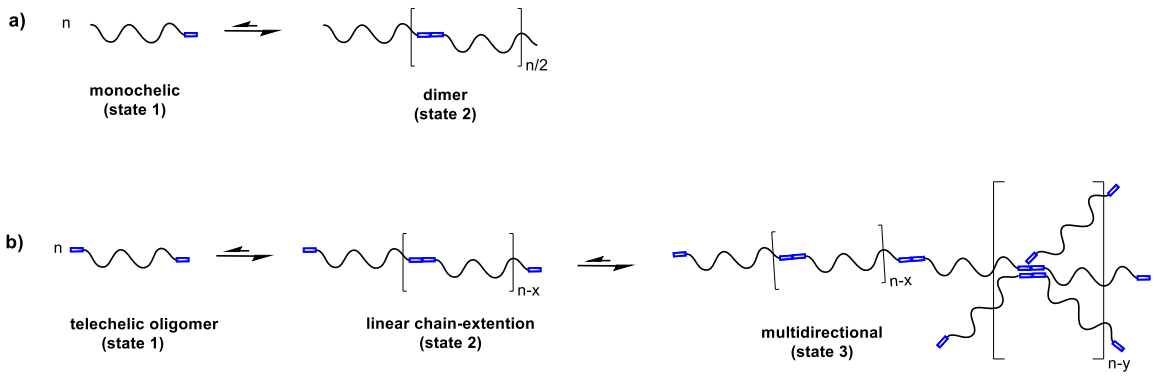
## Abstract

Dyamic mechanical properties of α, ω-di-UPy terminated polybutadienes and their hydrogenated analogue were evaluated as a function of *1,2-vinyl* content. Telechelic UPy-polybutadiene differs strongly in their physical properties, PBd with low $T_g$ (-90 °C) forms semi-solid and brittle material, whereas PBd with moderate $T_g$ (-45 °C) gave strong thermoplastic elastomer. UPy-P*n*BA-UPy with polar linker and low $T_g$ (-37 °C), and UPy-PS-UPy with nonpolar, high $T_g$ (96 °C) linker shows insignificant improvent in the mechanical properties. Whereas, significant enhancement in the properties was seen with nonpolar PBd. Supramolecular gel transition temperature ($T_{SG}$) was identified in rheological studies on various PBd-UPy telechelics. An attempt was made to examine the role of polymer chain mobility and its polarity was used to correlate structure and property with reference to room temperature.

## 7.1 Introduction

Utility of the ureidopyrimidone (UPy) group, a self-complementary quadruple hydrogen bonding unit, in the functionalization of telechelic oligomers has been well established in the literature as numerous SP's with promising properties ranging from thermoplastic elastomers to shape memory polymers have been reported.[1-3] Enhanced properties of UPy telechelic oligomers are widely attributed to the linear chain extension leading to the formation of very high molecular weight polymers with unique UPy hydrogen bonding.[3-9] The dimerization of UPy chain-ends of the telechelic oligomers leads to form uniquely ordered one dimensional stacks, along with disordered multiple aggregates.[10] The degree of polymerization and association of UPy via dimerization hydrogen bonding are influenced by solvent polarity, temperature, and presence of chain stoppers.[11]

Supramolecular polymers via hydrogen bonding system are dynamic in nature and using external stimuli such as temperature, polarity and pH, the properties of SPs can be tuning.[11] Controlled reversibility of hydrogen bonds can be utilized to construct novel drug delivery system. A potential drug loading mechanism can be devised in associated forms of SP and released upon reversing the hydrogen bonds. In order to utilize such a mechanism for any application, the system should possess definite physical state in the application condition. Thus, if the system has two-stage equilibrium as shown in **Scheme 7. 1a**, the equilibrium should be shifted to far right to stabilize and sustain the integrity of the structure. On the other hand, a system consisting of equilibrium involving multiple stages that have a small barrier to cross-over cannot be used employed for application and the material will lose its dimensional stability during application (**Scheme 7.1b**).




**Scheme 7. 1:** Different equilibrium states of mono- and telechelic associating systems.

As demonstrated in the previous chapters, UPy-PBd-UPy system does show distinct hydrogen bonding associations depending on various parameters such as microstructure, $T_g$, and polarity. The presence of multiple UPy dimer associated micellar-cluster and its dynamic equilibrium with unassociated chain-extended dimers have been confirmed using solid-state and solution property characterization.[12,13]

Although the UPy telechelic oligomers produce strong thermoplastic elastomers, the property of elastomeric behavior was not observed for many systems, especially for polar linker chain systems.[3] The reported UPy telechelic system, UPy-(PE-*co*-PB)-UPy, a non-polar oligomer with secondary urea connecting group forms well-defined fibrous structures ($T_m$ = 125 $^oC$).[10] The same system with a secondary urethane connecting group forms ill-defined fibrous structures ($T_m$ = 69 $^oC$).[10] The formation of fibrillar morphology was attributed to unidirectional stacks of tandem hydrogen bonding of UPy dimers with urea and urethane groups as illustrated in **Figure 7.1**.

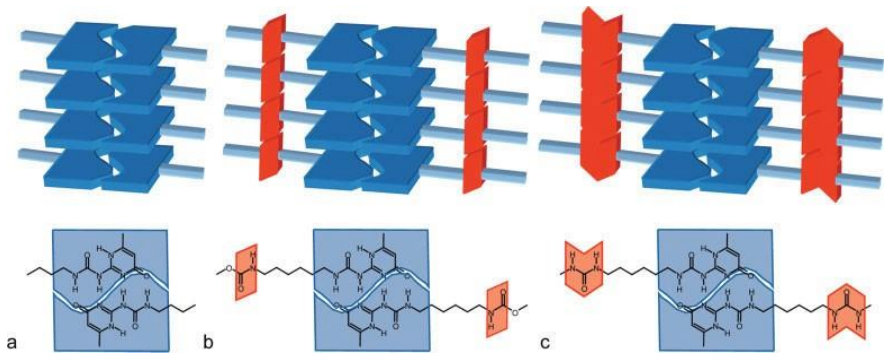



**Figure 7. 1:** Schematic representation of lateral aggregation of UPy dimers: (a) through π–π stacking in hydrogen bonded UPy dimer, (b) additional 1D stacking in H-bonding UPy dimer via a urethane linker, and (c) additional 1D staking by bifurcated H-bonding in UPy coupled via a urea linker.[14]

Even in the presence of additional secondary interactions, several other types of UPy telechelic systems differ in properties. Non-polar linkers namely, polystyrene (PS)[15], *1,4 trans*-PBd[16], hydrogenated PBd (poly(ethylene $_{0.5}$-*co*-isobutylene $_{0.5}$) PEB[3], hydrogenated polyisoprene and (poly (ethylene-co-propylene) PPB[17,18], polydimethylsiloxane (PDMS)[14] and polar linkers such as PEO-*co*-PPO[3], polycarbonates[19], and polyesters[20], Polytetrahydrofuran (PTHF)[21] have been reported in the literature. Many of them does not show distinct material properties.

Elastomeric properties are exhibited by UPy-(PE-*co*-PB)-UPy ($T_g$ = -57 °C), which is a nonpolar polymer. Polyesters ($T_g$ = -50 °C) and polycarbonates ($T_g$ = -20 °C) with polar, semi-crystalline chains also form thermoplastic elastomers. However, non-polar and polar UPy telechelics with very low $T_g$ materials such as PDMS (non-polar, $T_g$ = -119 °C), *1,4* PBd (non-polar, $T_g$ = -90 °C), and PEO-*co*-PPO (polar, $T_g$ = -50 °C) gave high solution and high melt viscosity in comparison to their precursors, but failed to give self-standing elastomeric film.

The results obtained in previous chapters indicated that the UPy-PBd-UPy system forms spherical micellar-clusters, which are in equilibrium with unassociated dimer chains. These findings do not corroborate formation of one dimensional structures claimed in the literature on UPy telechelic systems.[10,22] Thus, the factors responsible for the enhancement of physical properties of the supramolecular UPy associated structures and their dynamics have not been yet thoroughly understood.

Understanding the effect of dynamic interactions of associating/interacting polymeric system to stress is important for applying SPs in various applications. Dynamics of UPy telechelic polymers derived from oligomeric linkers via secondary hydrogen bonding are expected to follow Maxwell model in rheology. In this chapter, the focus is given to the rheology of UPy hydrogen bonded telechelics with an emphasis to examine the effect of different types of linking chains that affect the hydrogen bonding dynamics. UPy-PBd-UPys with different *1,2* and *1,4* microstructures having different transition temperatures will be studied. Along with PBds, PS (non-polar, and high $T_g$) and P*n*BA (polar, and low $T_g$) were also chosen to understand the effect of polar and nonpolar linker chains. Based on the knowledge from the previous chapters and the rheological responses of these materials with supporting DSC studies, criteria for exploiting hydrogen bonded SPs for superior mechanical properties will be discussed.

## 7.2 Experimental section

Synthesis and characterization of UPy telechelic based on PBd, PS, and P*n*BA are given in **Chapter 5** and **Chapter 6**. DSC and AFM characterization of UPy telechelics are given in earlier chapters and will be referred here whenever necessary.

### 7.2.1 Rheology and Dynamic Mechanical Analysis

Rheological measurements of UPy telechelics were carried out on an AR2000ex rheometer from TA Instruments, with a 25 mm disposable parallel plates and an environmental testing chamber (ETC). Nitrogen was used as the gas source of ETC to prevent sample degradation at high temperatures. Creep and small-amplitude oscillatory shear measurements were performed to determine the linear viscoelastic properties of the sample. PBd samples were prepared with small amount of antioxidant Irganox 1010. In an oscillatory shear measurement, the sample is subjected to a small amplitude (~5 %) strain oscillating at angular frequency $\omega$. The complex modulus $G^*$ can be evaluated from the imposed strain $\gamma^*$ and measured stress $\sigma^*$ as $G^* = G' + iG'' = \sigma^*/\gamma^*$. In a creep experiment, a constant stress $\sigma$ is applied to the sample, and the deformation $\gamma$ is monitored as a function of time *t*. The result can be analyzed in terms of the transient creep compliance $J(t)$, defined as $J(t) = \gamma(t)/\sigma$. The zero-shear viscosity value was obtained from the creep measurements as $\eta_0 = \text{limit}\rightarrow\infty(t/J(t))$, where J(t) is the transient shear compliance. DMTA experiments were performed on a TA Instruments, TA Q-800 DMA in

tension mode at a frequency of 1 Hz. The temperature ramp was 3 °C from -100 °C to 40 °C. Rectangular film were cut from melt processed film. Films were annealed for 5 days at 25 °C.

## 7.3 Results and Discussion

### 7.3.1 Gelation in UPy Telechelics

As already shown in the previous chapters DSC analysis reveals the presence of aggregates in the UPy-PBd-UPy samples with a broad melting peak (**Table 7.1**). From **Table 7.1** it is clear that all the UPy-PBd-UPy samples has endothermic peak in between 50-90 °C with a striking difference between two sets of PBd samples. Polymer with ~15 % *1,2-vinyl* contents has slightly higher heat capacity values and higher peak recovery percentages than the 57 % *1,2-vinyl* UPy materials. However, the sample with 24 % *1,2-vinyl* groups and high PDI of 1.75 (UPy-PBd-UPy-7) shows poor recovery of the melting peak. Moreover, this sample is hard and brittle.

The physical states of these materials are different depending on the vinyl content. The sample with ~15 *1,2-vinyl* is semi-solid, which forms transparent brittle film from the melt. Whereas, all the ~57 *1,2-vinyl* samples form transparent strong elastomeric film. The films are transparency initially and the transparency reduces over a period of time. For low molecular weight samples, the film turns slightly hazy over a period of month, whereas for high molecular weight samples, the film has negligible haziness. On the other hand, PS-UPy and P*n*BA-UPy do not show any melting peak in DSC consistent with the literature studies.[15,23] These observations suggest that the UPy-telechelics undergo unique dynamics which varies depending on the temperature and time. A detailed rheological study of these materials were performed to understand dynamics of hydrogen bonded UPy telechelics.

**Table 7. 1:** DSC characterization of UPy-PBd-UPy and UPy-(PE-*co*-PB)-UPy samples

| Sample (*1,2 vinyl* contents) | $M_{n,NMR}$ g/mol | $T_g$ (°C) | Heating cycle | Endothermic peak | | |
|---|---|---|---|---|---|---|
| | | | | $T_{diss}$ .(°C)[a] | $\Delta H_{diss}$ (J/g )[b] | Recovery (%) |
| UPy-PBd-UPy-1 (16 % *1,2-vinyl* ) | 2,900 | -85.25 | 1st | 87.46 | 16.83 | - |
| | | | 2nd | 83.19 | 13.21 | 78.4 |
| | | | 3rd | 82.95 | 12.92 | 76.8 |
| UPy-PBd-UPy-2 (15% *1,2-vinyl* ) | 5,300 | -81.75 | 1st | 55.98 | 9.375 | |
| | | | 2nd | 55.37 | 7.313 | 78.0 |
| | | | 3rd | 55.38 | 7.399 | 78.9 |
| UPy-PBd-UPy-3 (13 %*1,2-vinyl* ) | 9,100 | -87.88 | 1st | 46.88 | 5.11 | - |
| | | | 2nd | 46.14 | 4.540 | 88.9 |
| | | | 3rd | 45.88 | 4.67 | 91.4 |
| UPy-PBd-UPy-4 (57% *1,2-vinyl*) | 2,950 | -38.28 | 1st | 63.08 | 13.33 | |
| | | | 2nd | 58.01 | 1.685 | 12.6 |
| | | | 3rd | 58.55 | 1.437 | 10.8 |
| UPy-PBd-UPy-5 (57 %*1,2-vinyl* ) | 6,100 | -45.47 | 1st | 58.33 | 6.395 | - |
| | | | 2nd | None | None | - |
| | | | 3rd | None | None | - |
| UPy-PBd-UPy-6 (57 % *1,2-vinyl*) | 3,950 | -38.38 | 1st | 54.10 | 8.504 | - |
| | | | 2nd | None | None | - |
| | | | 3rd | None | None | - |
| UPy-PBd-UPy-7[a] (24 % *1,2-vinyl*) | 3,600 | -70.3 | 1st | 71.17 | 14.40 | |
| | | | 2nd | 64.62 | 1.392 | 9.67 |
| | | | 3rd | 64.09 | 0.8069 | 5.60 |
| UPy-(PE-*co*-PB)_-UPy-4 (57 % *1,2-vinyl* ) | 3,100 | -46.26 | 1st | 59.6 | 10.83 | |
| | | | 2nd | 52.68 | 3.441 | 31.8 |
| | | | 3rd | 51.99 | 3.229 | 29.8 |
| UPy-(PE-*co*-PB)-UPy-6 (57 % *1,2-vinyl*) | 4,150 | -47.96 | 1st | 56.29 | 8.50 | |
| | | | 2nd | -- | -- | -- |
| | | | 3rd | -- | -- | -- |

a) $T_{diss}$ endothermic melting peak, b) $\Delta H_{diss}$ enthalpy of endothermic peak

The high-temperature viscoelastic behavior of these samples resembles that of linear polymer melts. For example, the blue filled and open squares in **Figure 7.2** represents the storage and loss modulus of UPy-PBd-UPy-4 ($M_n$ = 2,900 g/mol) with 57% *1,2-vinyl* groups at 35 °C. A well-defined terminal relaxation can be observed at low frequencies or terminal flow region, with a Maxwellian scaling behavior of $G'(\omega) \sim \omega^2$, and $G''(\omega) \sim \omega$. This confirms that the material behaves like a linear chain. However, when the experiment was performed at lower temperature, 25 °C, the low frequency relaxation completely disappeared. The modulus almost became independent to frequency variations. This behavior suggests that the material has turned into gel by simply reducing the temperature from 35 °C to 25 °C. Such an abrupt sol-gel transition is a result of linear chain extended hydrogen bond UPy chains forming associated micellar-cluster and their higher order networks.

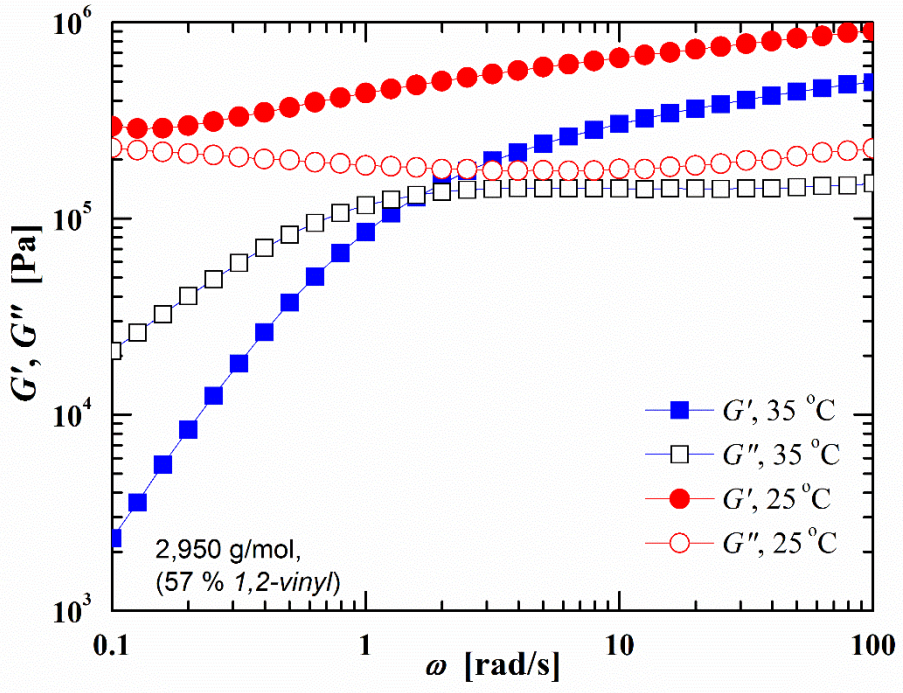



**Figure 7. 2:** Dynamic mechanical spectra of UPy-PBd-UPy-4, 57% *1,2-vinyl* before and after gelation

AFM studies have confirmed that at or above 25 °C, this material exist in the form equilibrium between interpenetrated parallel associated micellar-cluster and linear chain-

extended UPy dimers. It appears the transition is very sharp upon cooling from 35 $^{o}$C. Similar transition was also observed for other samples. The transition temperature depends on the nature of the oligomeric precursor chains. Different *T*gs of precursor oligomers show different transition temperature.

It was also observed that the transition depends on both the thermal and deformation history of the sample and is hard to be determined precisely. On the contrary, the sol-gel transition for UPy-PBd-UPy-1, with 16 % *1,2-vinyl* group is not immediately detectable at 80 °C, but only becomes obvious after sufficient annealing of several hours. On the other hand, the transition can also be accelerated by a large deformation, under rheological experimental conditions. Therefore, the gelation temperatures listed in **Table 7.2** should be regarded as rough estimates defined by a typical experimental time scale of a few minutes. The UPy-(PE-*co*-PB)-UPy-4 and its hydrogenated analogue UPy-(PE-*co*-PB)-UPy-4 have a similar transition temperature around 30 °C. In contrast, the low *1,2-vinyl* PBd has a much higher gelation temperature around 70 °C. The structure of UPy-(PE-*co*-PB)-UPy-1, 16 % *1,2-vinyl* is very similar to polyethylene with short chain branching of ethyl groups and has a high tendency to crystallization. Therefore, it has the highest transition temperature of 135 °C.

A slightly higher molecular weight (3,950 g/mol) precursor sample UPy-PBd-UPy-6, with higher vinyl content 57 % *1,2-vinyl* and its hydrogenated sample, UPy-(PE-*co*-PB)-UPy-6 show gelation temperatures of 20 °C and 25 °C, respectively. It appears that the gelation temperature also depends on the molecular weight of the oligomer precursor. After the rheology experiments, the UPy-PBd-UPy samples were analyzed by SEC to confirm absence of thermal degradation, while doing experiment. The $SEC_{trans}$ showed no change in the molecular characteristics of the precursor and confirmed no covalent crosslinking occurred in the sample. This also indicates the reversibility of the dynamics.

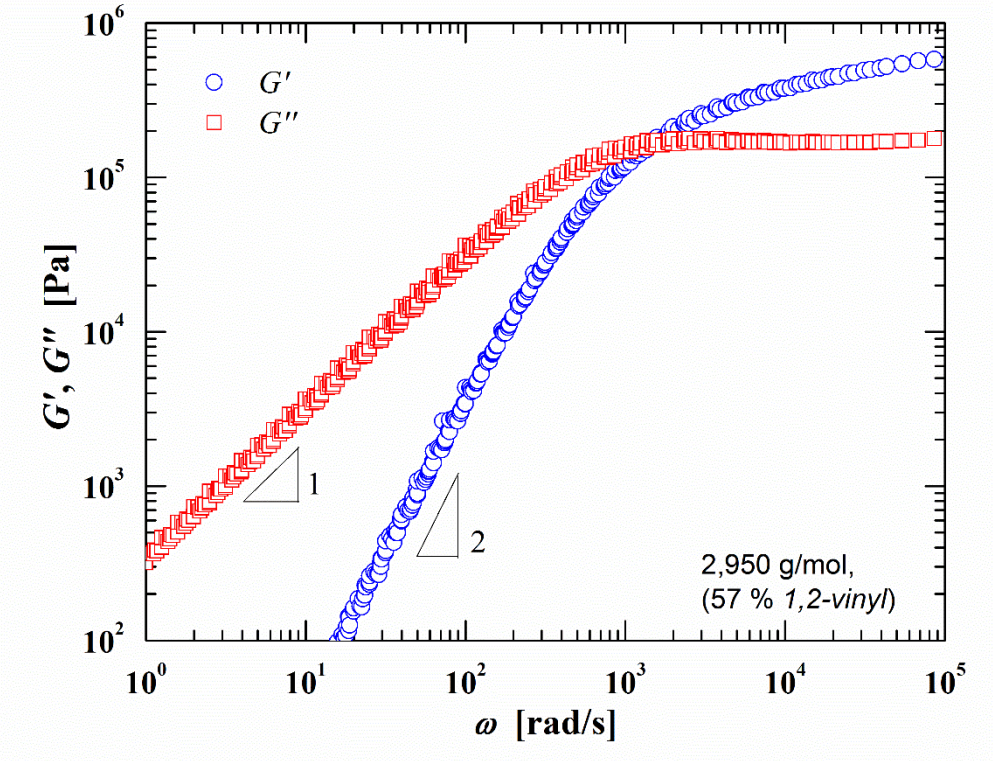



**Figure 7. 3:** Linear viscoelastic data of UPy-PBd-UPy-4 before gelation. SAOS measurements were performed at every 5 °C between 95 and 35 °C. The data are shifted to 90 °C according to the time-temperature superposition principle. Circles: Storage modulus (G′); Squares: Loss modulus (G″).

**Figure 7.2** presents the linear viscoelastic data of UPy-PBd-UPy-4, 57% *1,2-vinyl* before gelation. The dynamic mechanical spectra at different temperatures can be super-imposed according to well-known time-temperature superposition (TTS) principle. This suggests that there is no abrupt structural change before gelation (**Figure 7.3**). The molecular weight of the PBd backbone is 2,350 g/mol, which is still slightly below the critical entanglement molecular weight for PBd. However, the mechanical spectrum of UPy-PBd-UPy-4, 57% *1,2-vinyl* resembles that of high molecular weight entangled polymers. Such an increase of apparent molecular weight is clearly a result of hydrogen bonding formation among neighboring chains. The apparent entanglement molecular weight (network mesh size) can be estimated from the classical rubber elasticity theory as:

$$M_e = \frac{\rho RT}{G}, \quad (1)$$

where $\rho$ is the polymer melt density, $R$ is the universal gas constant, $T$ is the absolute temperature, and $G$ is the plateau modulus. This gives $M_e$ of approximately 4.6 kg/mol.

It should be noted that the plateau modulus $G$ of UPy-PBd-UPy-4, 57% *1,2-vinyl* is significantly lower than that of a high molecular weight PBd. This might be related to the fact that chain length of the hydrogen-bonding supramolecular polymers has a broad distribution: both long chains and short chains co-exist in the system. The short chains cannot form entanglements and act as solvents. The volume fraction of relatively long chains can be estimated as:

$$\phi = (G / G_0)^{\frac{1}{2.3}}, \quad (2)$$

according to the well-established scaling's for entangled polymer solutions. Here $G_0$ is the plateau modulus of neat PBd melts. This estimation yields a volume fraction of roughly 0.8 for long chains.

Furthermore, the rubber plateau width of a linear entangled polymer is related to the ratio of $M$ and $M_e$ as:

$$\omega_{\text{High}} / \omega_{\text{Low}} = (M / M_e)^{3.4}, \quad (3)$$

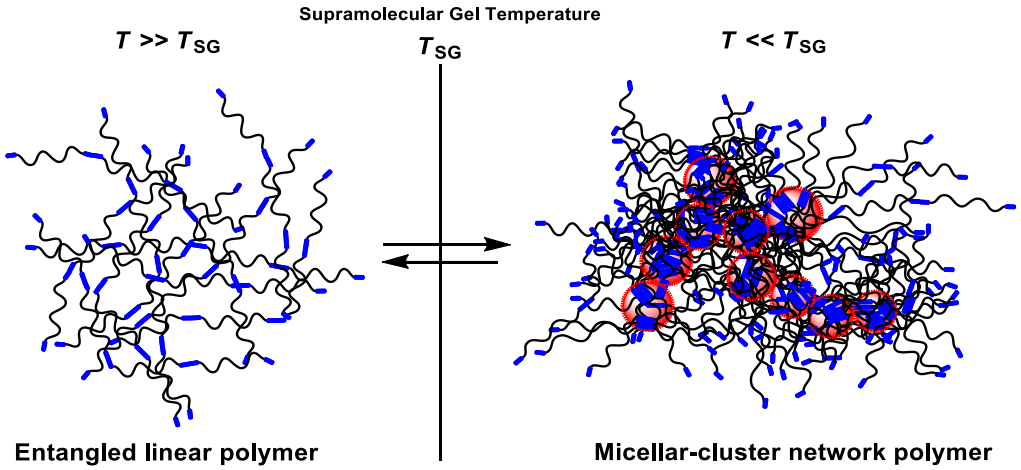
Where $\omega_{\text{High}}$ is the high crossover angular frequency of $G'$ and $G''$, and $\omega_{\text{Low}}$ is low-frequency one. In principle, this relation could allow us to estimate the apparent molecular weight of the supramolecular polymer. Unfortunately, due to both gelation and the frequency limit of the spectrometer, the high-frequency spectrum is not available for UPy-PBd-UPy-4- 57% *1,2-vinyl*

**Table 7. 2** Gelation temperature for UPy-PBd-UPy and UPy-(PE-*co*-PB)-UPy

| Entry | Sample[a] | Supramolecular Gelation Temperature [°C] $T_{SG}$ |
|---|---|---|
| 1 | UPy-PBd-UPy-4, (57% *1,2-vinyl* ) | 30 |
| 2 | UPy(PE-*co*-PB)-UPy-4 (57% *1,2-vinyl*) | 30 |
| 3 | UPy-PBd-UPy-1 (16% *1,2-vinyl*) | 70 |
| 4 | UPy-(PE-*co*-PB)-UPy (16% *1,2-vinyl*) | 135[†] |
| 5 | UPy-PBd-UPy-6 (57% *1,2-vinyl*) | 20 |
| 6 | UPy-(PE-*co*-PB)-UPy-6 (57% *1,2-vinyl*) | 25 |
| 7 | MPB-UPy-2 (15% *1,2-vinyl*) | 40 |

[†] Crystallization temperature, a) values of *1,2-vinyl* groups refer to either 1,2 ethylene groups in PBd or ethyl groups in hydrogenated PBd.

Gelation temperature of the PBd-UPy polymers as a function of *1,2-vinyl* contents are given in **Table 7.2**. Below gelation temperature ($T_{SG}$) there is transition from a linear entangled networks to micellar clustered network. Gelation temperature is strongly affected by the linker *T*g, whereas, with molecular weight of the linking chain plays less significant role. UPy-PBd-UPy with low *1,2-vinyl* group has low $T_g$'s, ~ -90 °C and UPy-PBd-UPy with higher *1,2-vinyl* groups has high $T_g$ ~ -45 °C. UPy-PBd-UPy-1 has $T_{SG}$ around 70 °C and UPy-PBd-UPy-4 has $T_{SG}$ of 30 °C. This explains the strong difference in the physical properties of these two samples at room temperature. High $T_{SG}$ sample UPy-PBd-UPy-1 at room temperature has presence of large extended micellar cluster network giving a brittle solid, whereas UPy-PBd-UPy-4 gives self-standing elastomeric film due to absence of large extended micellar cluster network. **Scheme 7.2** illustrates the extended micellar clusters and linear concatenated polymer. UPy-PBd-UPy-4 sample with higher *T*g has slower molecular motion of the linker which prevents it from formation of strong micellar cluster network, whereas UPy-PBd-UPy-1 with lower $T_g$ has sufficient mobility of linker chain to allow formation of micellar cluster network.




**Scheme 7. 2:** Proposed structures of UPy-PBd-UPy as function of supramolecular gelation temperature

### 7.3.2 Effect of *1,2 vinyl* contents and hydrogenation on the melt viscosity of UPy telechelics

The temperature dependence of zero-shear viscosity of sample UPy-PBd-UPy-4 and its hydrogenated counterpart UPy-(PE-*co*-PB)-UPy-4 is presented in **Figure 7.4** Viscosity of UPy-PBd-UPy-4 and its hydrogenated counterpart has very similar temperature dependence, implying that the dynamics before gelation is not strongly affected by the hydrogenation (**Figure 7.5**). From **Figure 7.4** it is clear that at a given temperature, UPy-terminated polymers have much higher viscosities than hydroxyl-terminated polymers. Also, Hydrogenation seems to have a relatively small but detectable effect on viscosity. Also, monochelic sample with one UPy group at one chain end gives much higher viscosity than an ideally expected dimerization of UPy group resulting in polymer with twice the $M_n$.

UPy-PBd-UPy-6 samples with 57 % *1,2-vinyl* content shows similar behavior to UPy-PBd-UPy-4. However, in the case of $M_n$ 2,350 g/mol, the viscosity of UPy-PBd-UPy is higher than its hydrogenated counterpart and the two samples appear to have the same temperature dependence for viscosity. In the case of UPy-PBd-UPy-6, the hydrogenated UPy sample has higher viscosity and UPy-PBd-UPy-6 and UPy-(PE-*co*-PB)-UPy-6 exhibit different temperature dependence for viscosity (**Figure 7.5**).

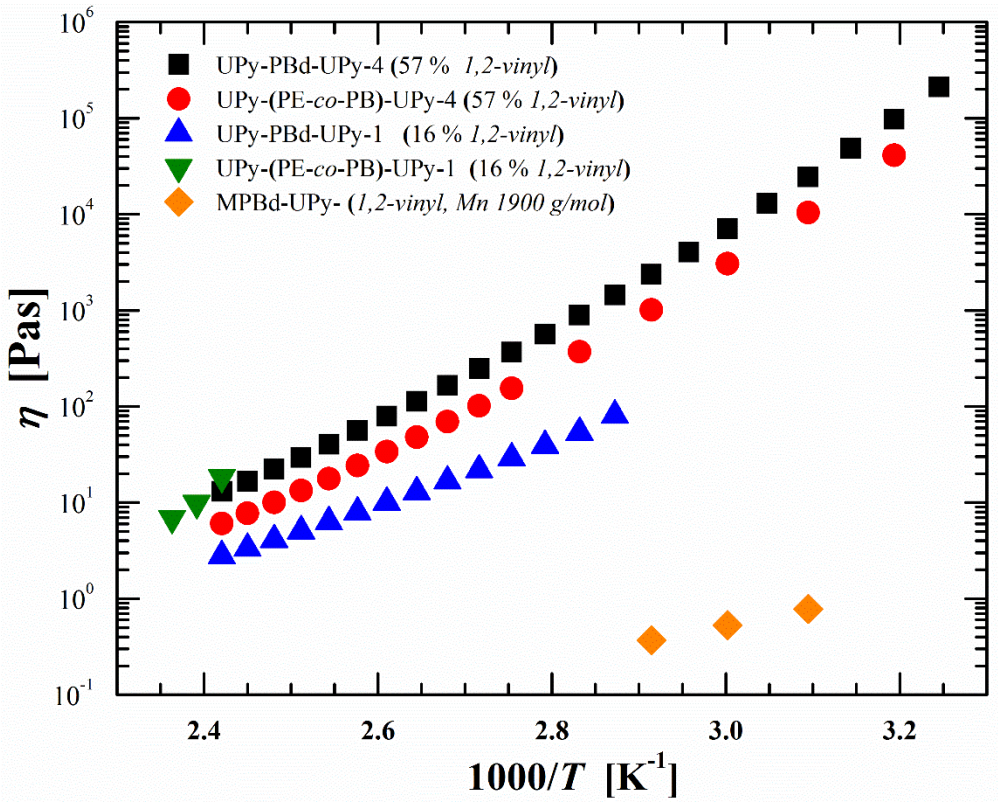



**Figure 7. 4:** Temperature dependence of zero-shear viscosity (η). UPy-(PE-*co*-PB)-UPy-1 (16 % *1,2-vinyl* could not melt completely at the three testing temperatures (150, 145, and 140 °C), and did not strictly exhibit Newtonian behavior. The data for UPy-PBd-UPy-16 % *1,2-vinyl* should only be regarded as rough apparent viscosities.

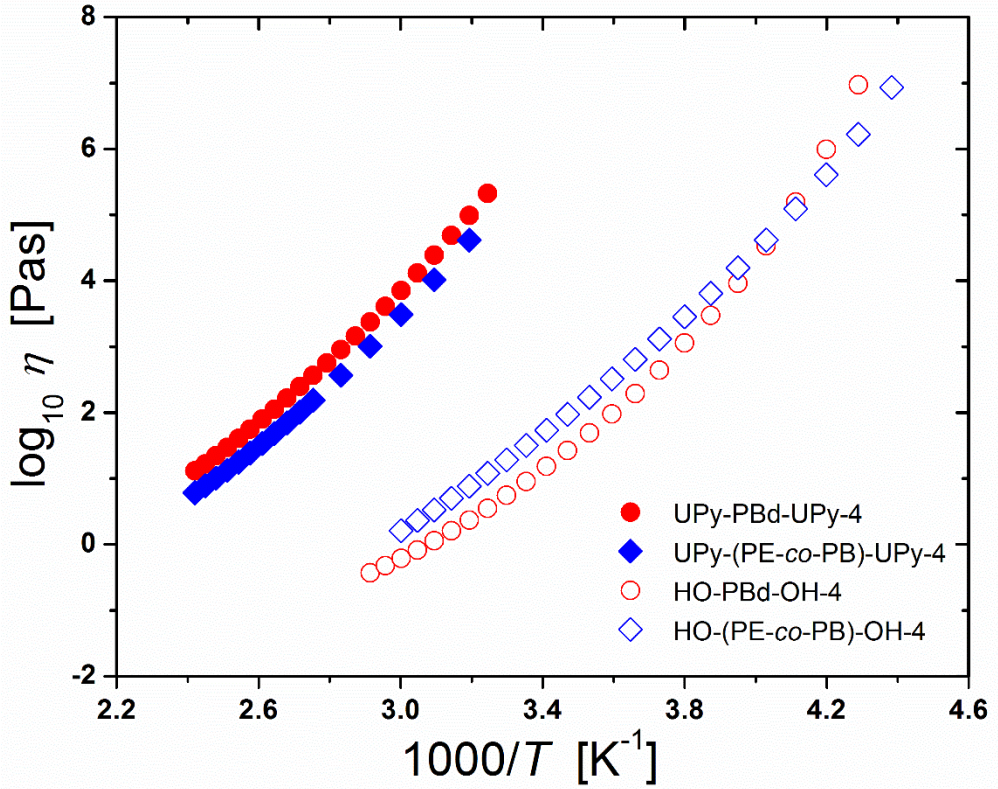



**Figure 7. 5:** Temperature dependence of viscosity for PBd-based (57 % *1,2-vinyl*) polymers. Solid symbols: UPy-terminated telechelic polymers. Open symbols: hydroxyl-terminated telechelic polymers. Red circles: polybutadienes (PBd). Blue diamonds: hydrogenated polybutadienes (PE-*co*-PB).

Polybutadiene with 16 % *1,2-vinyl* structure and its hydrogenated analogue shows significant increase in the viscosity after UPy chain end modification (**Figure 7.6**). Unfortunately, viscosities of UPy-PBd-UPy and UPy-(PE-*co*-PB)-UPy cannot be compared at the same temperature. This is partially due to the fact that the 16 % *1,2-vinyl* UPy-(PE-*co*-PB)-UPy has a relatively high gelation temperature. The hydrogenated PBd with hydroxyl terminal groups has a high melting point and its viscosity is not reported here. Moreover, the melting point is very broad. Although, HO-(PE-*co*-PB)-OH-1 made by hydrogenation using (tosyslhydrazone) TSH method may influence the rheological behavior due to incorporation of smaller polar functionality group from TSH. However, the difference between UPy-(PE-*co*

PB)-UPy-1 and HO-(PE-*co*-PB)-OH-1 can be considered as result of UPy chain end modification, with negligible contribution by tosyl groups.

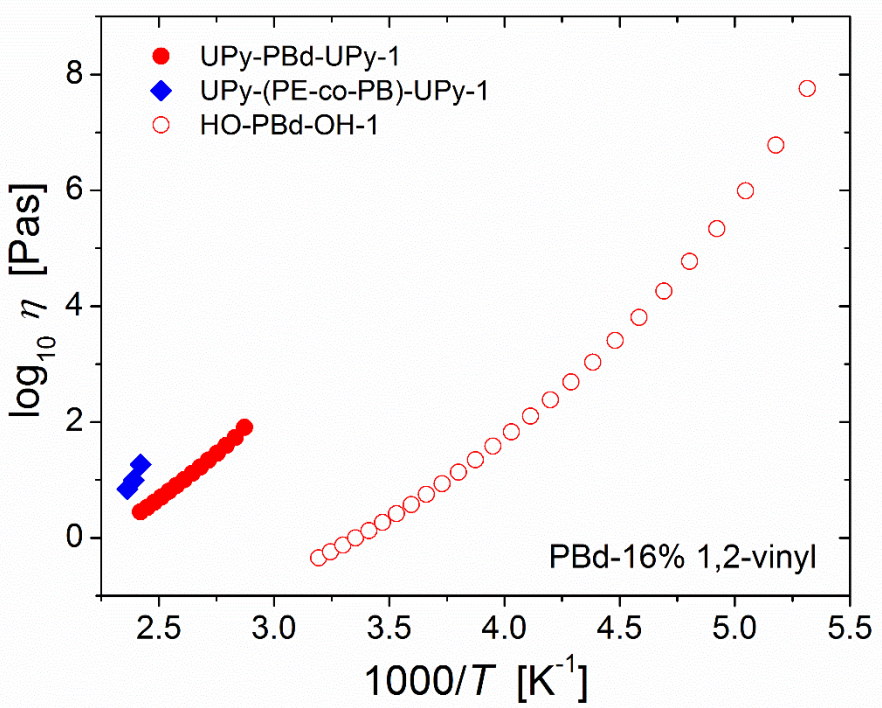



**Figure 7. 6:** Temperature dependence of viscosity for PBd-based (16 % *1,2-vinyl*) polymers. Solid symbols: UPy-terminated telechelic polymers. Open symbols: hydroxyl-terminated telechelic polymers. Red circles: polybutadienes (UPy-PBd-UPy-1). Blue diamonds: hydrogenated polybutadienes (UPy-(PE-*co*-PB)-UPy-1).

The polydispersed UPy-PBd-UPy-7 with $M_n$ of 3,600 g/mol and $M_w/M_n$ = 1.75 has ~24 % *1,2-vinyl* content. Therefore, it is not surprising that the viscosity of its -OH-terminated precursor falls in between 16 % and 57 % *1,2-vinyl* PBds ($M_n$ ~ 2.9 K and 4.1 K respectively) (**Figure 7.7**). In general, PBds with higher *1,2-vinyl* content tend to have higher viscosity. This is because higher *1,2-vinyl* content typically leads to higher glass transition temperature and

slower molecular motion. HO-PBd-OH-4 ($M_n$, 2,350 g/mol) and HO-PBd-OH-6 ($M_n$, 3,350 g/mol) has similar viscosity values.

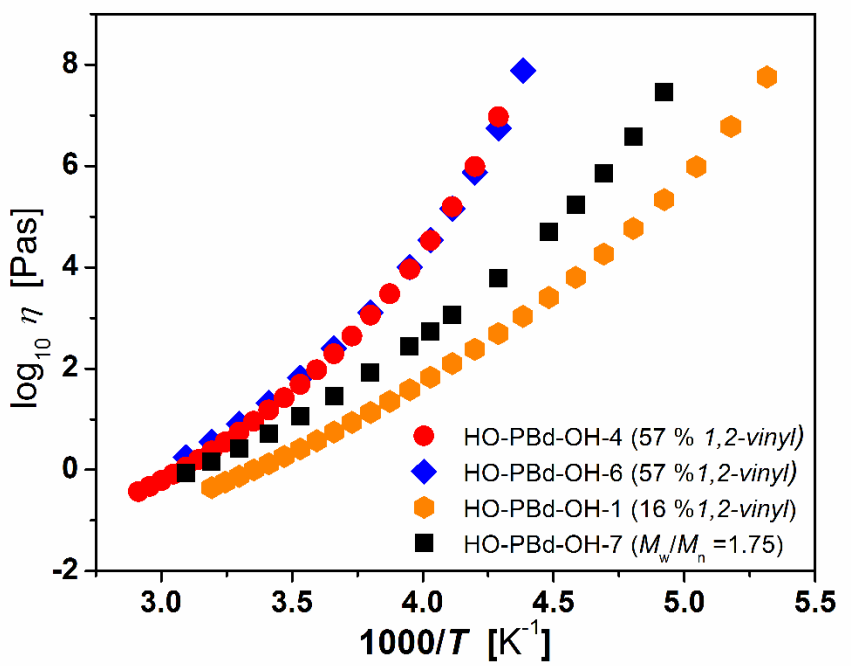



**Figure 7. 7:** Comparison of the viscosities of different PBd precursors.

However, the same trend is not observed in UPy-PBd-UPy samples. The polydispersed UPy-PBd-UPy-7 has the highest viscosity among all the samples (**Figure 7.8**). This result suggests that polydispersity also plays an important role in the formation of supramolecular polymer. Moreover, UPy-PBd-UPy-4 and UPy-PBd-UPy-6, samples shows identical viscosity profile. Whereas, their hydrogenated analogue UPy-(PE-*co*-PB)-UPy-6 has higher viscosity than UPy-(PE-*co*-PB)-UPy-4 (**Figure 7.9**).

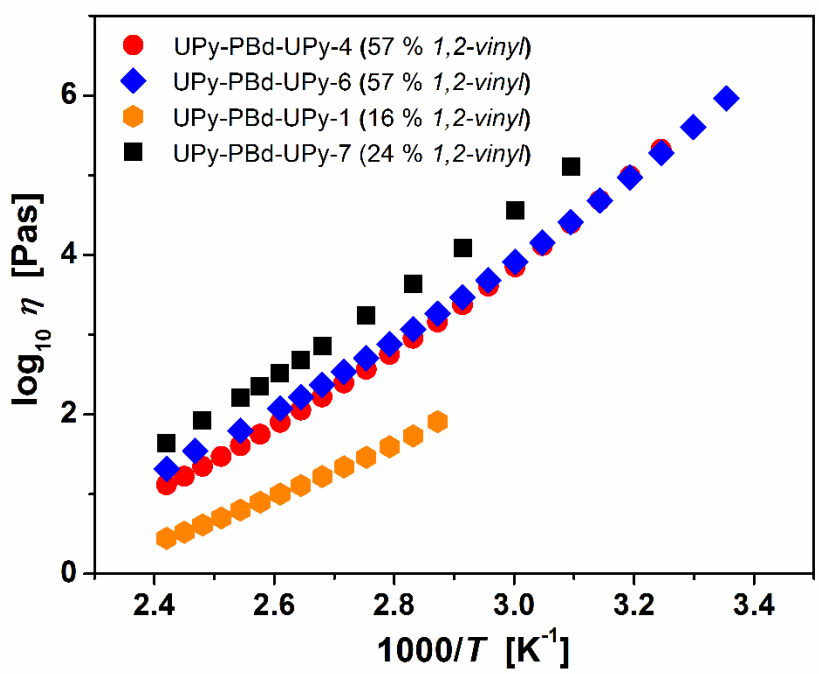



**Figure 7. 8:** Comparison of the viscosities of PBd-UPys of different microstructures and molecular weight distributions

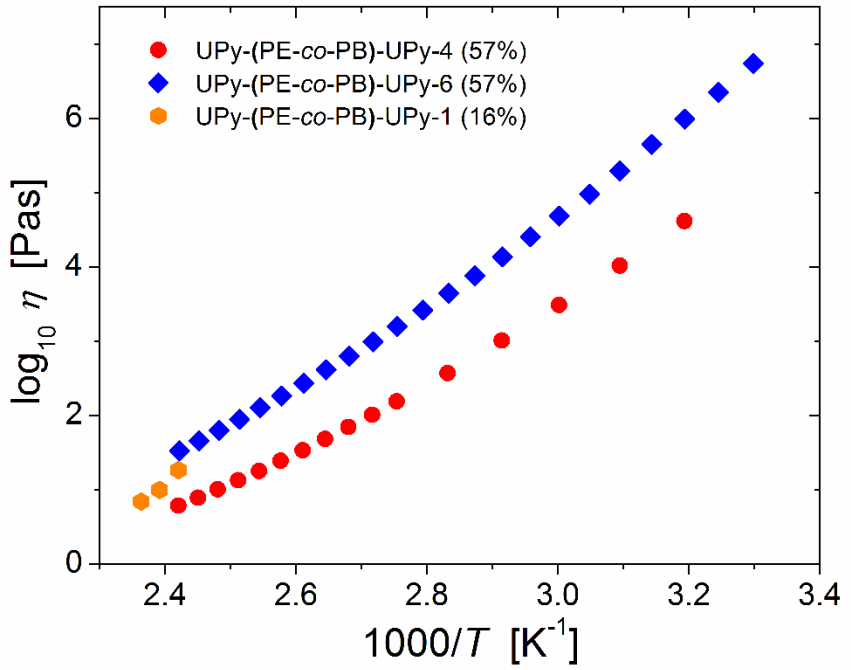



**Figure 7. 9:** Comparison of the viscosities of different hydrogenated PBd-UPys

Although, melt viscosity of the sample UPy-PBd-UPy-4 and UPy-PBd-UPy-6 are almost identical, when these samples were analyzed by DMTA. It shows different behavior. In **Figure 7.10**, logarithmic plot of storage modulus *vs* temperature for three UPy-PBd-UPy samples with similar 57% *1,2-vinyl* groups are shown. Both glassy modulus and rubber modulus has higher values for lower molecular weight sample, UPy-PBd-UPy-4. Also, UPy-PBd-UPy-5 and UPy-PBd-UPy-6 has similar glassy modulus, but their elastic modulus differ by a factor of two. Since, UPy-PBd-UPy-4 has much higher wt % UPy (11.5% vs 8.5%) groups, this polymer would have higher lateral interaction due to urethane groups, which can act as physical crosslinks to give stronger network in the solid state. Whereas, in the melt lateral urethane interaction did not play significant role for UPy-PBd-UPy-4 and UPy-PBd-UPy-6 and their dynamics are governed by the linear chain extended polymer.

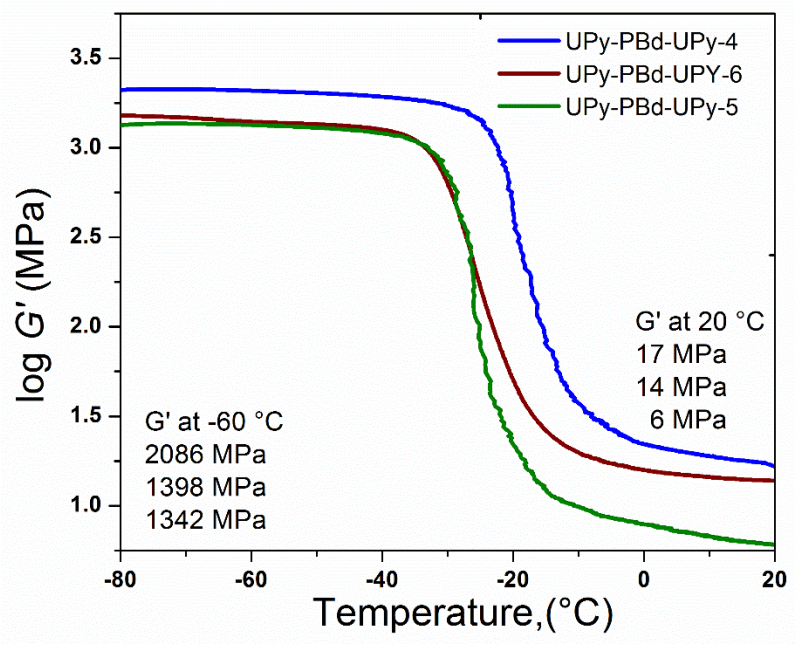



**Figure 7. 10:** DMTA curve of UPy-PBd-UPy with 57 % *1,2-vinyl* groups and with different molecular weight.

### 7.3.3 Influence of low $T_g$, polar and high $T_g$, nonpolar linker

All the UPy-PBd-UPy and UPy-(PE-*co*-PB)-UPy samples have comparatively low $T_g$, nonpolar backbone and shows dramatic improvement in the physical properties, such as much higher solution and melt viscosities. Although, telechelic P*n*BA and PS-UPy samples has much

higher $T_g$ values than its precursor samples they do not shows dramatic improvement in the solution viscosities (**Figure 7.11**). These samples were analyzed by rheology to evaluate the influence of the chain end group on their viscosity. Although, azide terminated PS was used in the CuAAC click reaction, bromo telechelic samples were used for rheology analysis to avoid any thermal degradation due to azide group. CuAAC also introduces additional triazole group in between the linker and UPy group. As seen in the **Chapter 6,** triazole group enhance the supramolecular association. Therefore PS-UPy and P*n*BA-UPy samples can be treated as model polymer to study the effect of nonpolar high $T_g$ backbone, and low $T_g$ polar backbone respectively.

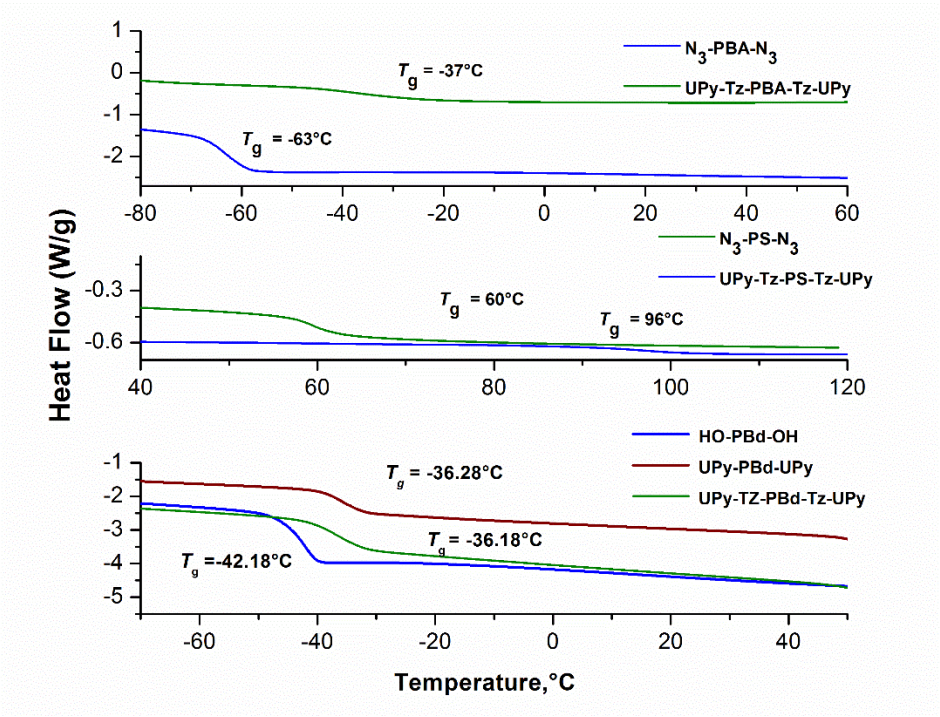



**Figure 7. 11:** Glass transition temperature of PBd-UPy-4 and PS-UPy and P*n*BA-UPy

UPy-terminated P*n*BA and PS has much higher viscosity than Br-terminated P*n*BA and PS, respectively. Appendix 6A, a **Figure 6A.1** and **Figure 6A.2** demonstrates the viscosities of P*n*BA-UPy and PS-UPy and their precursor. Surprisingly, both these polymer do not have any melting endothermic peak. Feldman and co-workers reported absence of any melting peak in side chain P*n*BA-UPy with much higher weight percentage of UPy groups.[23] Whereas, Yamauchi and co-workers also reported absence of melting peak in PS-UPy.[15] Implying that

in this system no additional physical crosslinks arise from UPy group associations. Therefore, increase in the viscosity of these two polymer can be attributed to the change of glass transition temperature. UPy-PBd-UPy-1, UPy-PBd-UPy-4, PS-UPy and P*n*BA-UPy samples have almost identical molecular weight, differ strongly in their properties, however.

Both PBd-UPy behaves like high molecular weight entangled polymers with a well-defined rubbery plateau while P*n*BA-UPy and PS-UPy display Rouse-like dynamics of low molecular weight polymers (**Figure 7.12**). Because the modification of the end group and the formation of supramolecular polymer may change the glass transition temperature of the system, a better way to compare the viscosities of the precursor and UPy-terminated polymer is to use the $T_g$-normalized temperature ($T_g/T$). Therefore, **Figure 7.13**) gives plot of $\log_{10}\eta$ as a function of $T_g/T$ for all the four series of polymers. It is immediately evident that the polymer backbone structure plays a very important role in the formation of supramolecular polymer. On the $T_g$-normalized plot, there is a significant difference between viscosity of the UPy and OH terminated PBds, irrespective of the *1,2-vinyl* contents. On the other hand, the differences in the P*n*BA and PS series are much smaller.

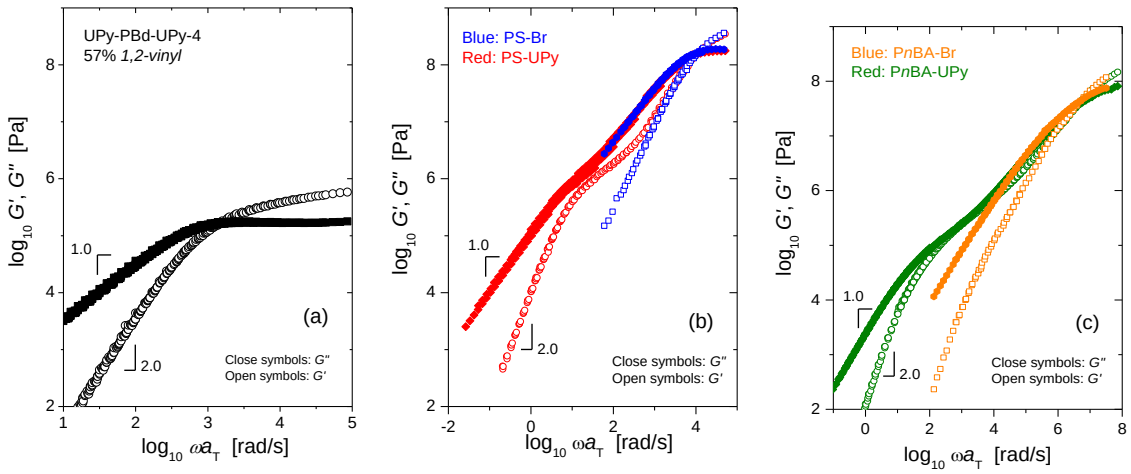



**Figure 7. 12:** Comparison of the viscoelastic spectra of UPy-based supramolecular polymers of different backbones. (a) PBd-4. (b) PS. (c) P*n*BA.

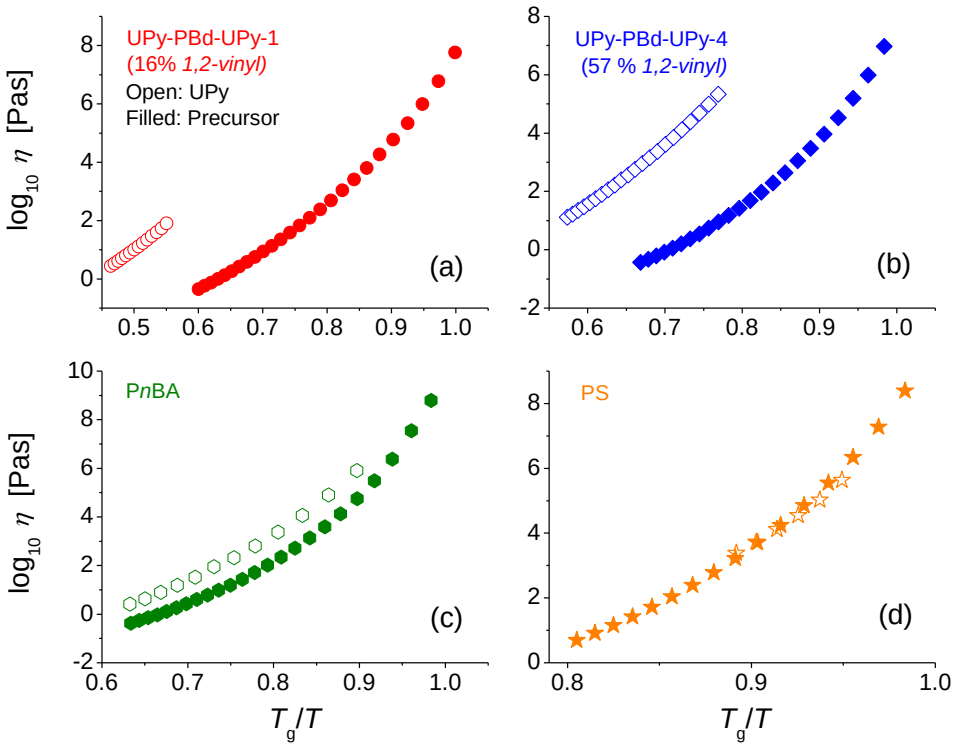



**Figure 7. 13:** Temperature dependence of viscosity for UPy-based supramolecular polymers of different backbones. (a) 2.3 kg/mol Polybutadiene (PBd) with 16 % *1,2-vinyl* groups. (b) 2.4 kg/mol PBd with 57 % *1,2-vinyl* groups. (c) 3.2 kg/mol Poly(*n*-butyl acrylate) (P*n*BA). (d) 2.4 kg/mol Polystyrene (PS)

## 7.4 Dynamics of UPy-Supramolecular Associations

Dynamics of the UPy-telechelics from linear supramolecular associated chains to gel networks due to hydrogen bond association/dissociation equilibrium can be seen clearly from the existence of $T_{SG}$ for the different polymers studied. Influence of the dynamics on the polymer properties is seen for three distinct polymers with non-polar and low *T*g linker, polar and low $T_g$ linker and non-polar and high $T_g$ linker oligomers. Moreover, previous studies have already underlined the importance of the presence of nanophase separation by either due to large amount of nano-fibrillar formation, or insufficient nano fibrillar formation via 1D UPy dimer stacking from lateral urea or urethane groups' tandem cooperation and multiple UPy aggregation.[10] The results in obtained herein do not support the formation of 1D UPy stacks. Evidence for the presence of multiple aggregation of spherical micellar UPy associations and

their dynamic higher order associations to network or gel formation in presented for various PBd materials.

Comparison of PBd and hydrogenated PBd linker chains indicates that chain-dynamics dictates the properties. For example, UPy-PBd-UPy-6, UPy-(PE-*co*-PB)-UPy and Meijer's PEB-UPy all have similar molecular weight and have similar UPy chain end group concentration, except there is a slight difference of *1,2 vinyl* content. The reported PEB-UPy has 50 % ethylene groups (from 50 % *1,2-vinyl* groups), whereas UPy-(PE-*co*-PB)-UPy has 43 % ethylene groups. Meijer's PEB-UPy has $T_g$ of -50 °C (DSC $T_g$ is -57 °C, $T_m$ 69 °C) and rubbery modulus of 7 MPa for solvent cast film and 5 MPa for melt pressed film can be attributed to the subtle differences in $T_g$ characteristics of the materials in comparison to the samples studied herein. Whereas, storage modulus values of PEB-UPy (from 57% *1,2-vinyl*), UPy-(PE-*co*-PB)-UPy-6 are 1458 MPa at -60 °C and 10 MPa at 10 °C. On other hand its precursor PBd, UPy-PBd-UPy-6 has storage values of 1398 MPa at -60 °C and 14 MPa at 25 °C; alongwith higher $T_g$ of -22.5 °C (DSC $T_g$ is -38.8 °C, $T_m$ 54 °C), which gave stronger material.

On comparison of material properties of different types of linker chains (UPy-PBd-UPy, P*n*BA-UPy, and PS-UPy), it is clear that only non-polar linkers with moderately higher $T_g$ were able to form strong thermoplastic elastomeric films at or close to room temperature. This is also related to supramolecular gelation temperature ($T_{SG}$) observed for these materials. This temperature is very important in determining the material property for temperature window for application. A higher $T_{SG}$ was seen for UPy-PBd-UPy system with lower $T_g$ (-90 °C), which means that this polymer remains in gel form until ~ 70 °C. Moreover, physical crosslinks due to lateral urethane start melting around ~ 60 °C. Therefore, below this temperature, and also at room temperature, this polymer is semi-solid and does not form free forming film. Above 70 °C, physical crosslinks provided by lateral urethane groups are broken and polymer behaves as high molecular weight material..

Driving force for the gelation is favorable enthalpy associated with polar hydrogen-bonding interactions of UPy multiple association, which is strongly assisted by the mobility of the linker chain. Much lower $T_g$ of ~ 16 % *1,2-vinyl* groups provides higher probability chains to move and find other chain-ends or UPy domain to engage hydrogen bonding. Whereas, for ~ 57 *1,2-vinyl* UPy-PBd-UPy samples with a moderately higher $T_g$, the probability for chains

to find UPy domain is reduced. This also reduces dissociation dynamics of UPy domain leading to lower $T_{SG}$.

## 7.5 Conclusions

The presence of UPy domains formation via hydrogen bonding is evident in all polymers studied irrespective of $T_g$ characteristics. The concentration of micellar associated UPy domain relative to unassociated extended chains in the matrices, association of micellar-clusters to form parallel alignment of fiber-like morphology, and interpenetration to form extended gel are critical factors which determine the physical properties of UPy telechelics. These critical factors govern the superior mechanical property of UPy telechelics. More importantly, the dynamic nature of these factors must be considered for constructing dimensionally stable materials based on UPy telechelics.

A consideration of application or service window is important as the properties of SPs based on hydrogen bonding depend on the properties such as the polarity of the polymer and $T_g$ characteristics of linking oligomers. Preferred characteristics of the oligomer linkers to observe superior elastomeric property at ambient temperature are non-polar oligomer with moderate $T_g$ to exhibit low $T_{SG}$ for hydrogen bonded SPs.

## 7.6 References


(1) Guan, Z.; Roland, J. T.; Bai, J. Z.; Ma, S. X.; McIntire, T. M.; Nguyen, M. *J. Am. Chem. Soc.* **2004**, *126*, 2058.

(2) Guan, Z. *Polym. Int.* **2007**, *56*, 467.

(3) Folmer, B. J. B.; Sijbesma, R. P.; Versteegen, R. M.; van der Rijt, J. A. J.; Meijer, E. W. *Adv. Mater.* **2000**, *12*, 874.

(4) Sijbesma, R. P.; Beijer, F. H.; Brunsveld, L.; Folmer, B. J. B.; Hirschberg, J. H. K. K.; Lange, R. F. M.; Lowe, J. K. L.; Meijer, E. W. *Science* **1997**, *278*, 1601.

(5) Beijer, F. H.; Sijbesma, R. P.; Kooijman, H.; Spek, A. L.; Meijer, E. W. *J. Am. Chem. Soc.* **1998**, *120*, 6761.

(6) Beijer, F. H.; Kooijman, H.; Spek, A. L.; Sijbesma, R. P.; Meijer, E. W. *Angew. Chem. Int. Ed.* **1998**, *37*, 75.

(7) Hirschberg, J.; Beijer, F. H.; van Aert, H. A.; Magusin, P.; Sijbesma, R. P.; Meijer, E. W. *Macromolecules* **1999**, *32*, 2696.

(8) Lange, R. F. M.; Van Gurp, M.; Meijer, E. W. *J. Polym. Sci., Part A: Polym. Chem.* **1999**, *37*, 3657.

(9) Söntjens, S. H. M.; Sijbesma, R. P.; van Genderen, M. H. P.; Meijer, E. W. *J. Am. Chem. Soc.* **2000**, *122*, 7487.

(10) Kautz, H.; van Beek, D. J. M.; Sijbesma, R. P.; Meijer, E. W. *Macromolecules* **2006**, *39*, 4265.

(11) De Greef, T. F. A.; Smulders, M. M. J.; Wolffs, M.; Schenning, A. P. H. J.; Sijbesma, R. P.; Meijer, E. W. *Chem. Rev.* **2009**, *109*, 5687.

(12) Bobade, S. L.; Malmgren, T.; Baskaran, D. *Polym. Chem.* **2014**, *5*, 910.

(13) Bobade, S.; Wang, Y.; Mays, J.; Baskaran, D. *Macromolecules* **2014**.

(14) Botterhuis, N. E.; van Beek, D. J. M.; van Gemert, G. M. L.; Bosman, A. W.; Sijbesma, R. P. *J. Polym. Sci. Part A-Polym. Chem.* **2008**, *46*, 3877.

(15) Yamauchi, K.; Lizotte, J. R.; Hercules, D. M.; Vergne, M. J.; Long, T. E. *J. Am. Chem. Soc.* **2002**, *124*, 8599.

(16) Scherman, O. A.; Ligthart, G. B. W. L.; Ohkawa, H.; Sijbesma, R. P.; Meijer, E. W. *Proc. Natl. Acad. Sci. USA* **2006**, *103*, 11850.

(17) Elkins, C. L.; Viswanathan, K.; Long, T. E. *Macromolecules* **2006**, *39*, 3132.

(18) Mather, B. D.; Elkins, C. L.; Beyer, F. L.; Long, T. E. *Macromol. Rapid Commun.* **2007**, *28*, 1601.

(19) Dankers, P. Y. W.; Zhang, Z.; Wisse, E.; Grijpma, D. W.; Sijbesma, R. P.; Feijen, J.; Meijer, E. W. *Macromolecules* **2006**, *39*, 8763.

(20) Yamauchi, K.; Kanomata, A.; Inoue, T.; Long, T. E. *Macromolecules* **2004**, *37*, 3519.

(21) Shokrollahi, P.; Mirzadeh, H.; Huck, W. T. S.; Scherman, O. A. *Polymer* **2010**, *51*, 6303.

(22) Appel, W. P. J.; Portale, G.; Wisse, E.; Dankers, P. Y. W.; Meijer, E. W. *Macromolecules* **2011**, *44*, 6776.

(23) Feldman, K. E.; Kade, M. J.; Meijer, E. W.; Hawker, C. J.; Kramer, E. J. *Macromolecules* **2009**, *42*, 9072.

## Appendix 7A

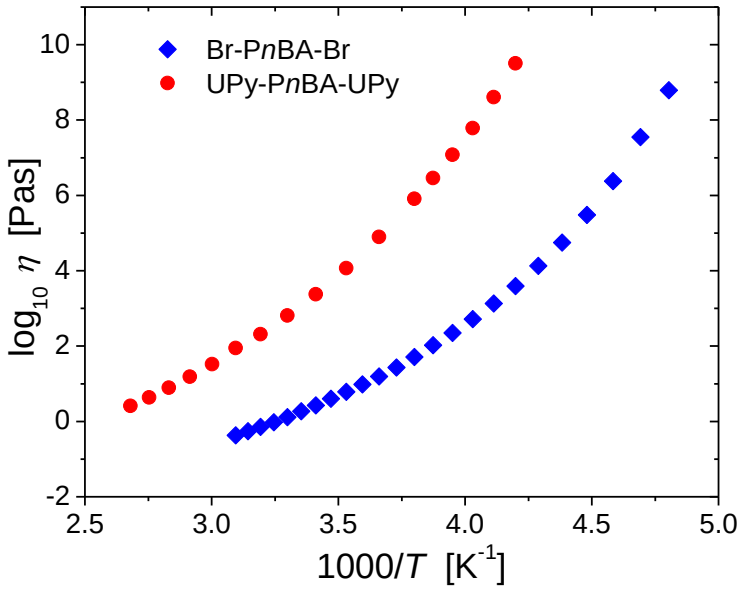



**Figure 7A. 1:** Temperature dependence of viscosity for P*n*BA-UPy and P*n*BA-Br.

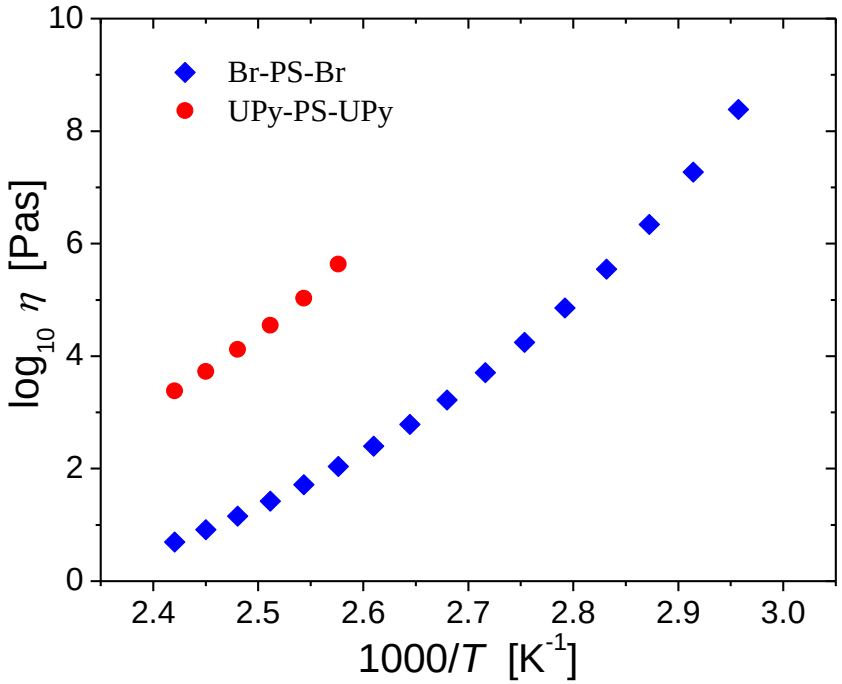



**Figure 7A. 2:** Temperature dependence of viscosity for PS-UPy and PS-Br.

# Chapter 8: Conclusions and Feature Perspective of UPy Hydrogen Bonded SPs

This work was carried in order to evaluate the role of polymer chain mobility on the UPy chain end association. Anionic polymerization was applied to synthesize a series of narrow dispersed ω-monohydroxyl α, ω dihydroxyl terminated polybutadiene. Upon chain end modification the obtained monochelic PBd-UPy samples became waxy solid, whereas the telechelic PBd-UPys became semisolid to strong free-standing elastomer. Physical properties of the MPBd-UPys indicate the presence of micellar-clusters dissociating or melting over a broad temperature range (35-90 °C). Reformation of micellar-clusters on second and third heating cycles in DSC is strongly dependent on the molecular weight and the chain-mobility of PBd. AFM images of MPBd-UPys confirmed the formation of micellar clusters and their association into discontinuous fibrous-like structures that exist in equilibrium with the bulk of dimers.

Anionic polymerization of butadiene was carried out successfully using hydroxyl protected initiator and terminated with ethylene oxide to obtain telechelic PBds. UPy telechelic of butadiene with various molecular weight and different *1,2-vinyl* contents have been prepared and characterized. Solution viscosity, DSC and AFM analysis reveal the system exist in equilibrium between UPy hydrogen bonded micellar clusters and unassociated linear chain-extended polymer. The extent of micellar cluster network formation is much higher in case of low *1,2-vinyl* content PBd, resulting in brittle film. Whereas, the PBds with high *1,2-vinyl* content have an optimum balance of linear chain extension and micellar cluster alignment giving rise to strong interpenetrated thermoplastic elastomer at or close to room temperature.
A new approach for the synthesis of UPy telechelics by a combination of ATRP and click reaction was introduced. Using this approach, four different telechelic polymers of PS, PBd. PE-*co*-PB and P*n*BA have been synthesized and characterized. The presence of triazole group positively interferes with the hydrogen bonding of UPy domains. Solution, melt and solid-state characterizations of triazole containing UPy telechelics indicate that the resulting SPs exhibit higher viscosity and modulus.

The presence of UPy domain formation via hydrogen bonding is evident in all the polymers studied irrespective of $T_g$ characteristics of their precursor oligomers. The concentration of micellar associated UPy domain relative to unassociated extended chains in the matrices, association of micellar-clusters to form parallel alignment of fiber-like morphology, and interpenetration to form extended gel are the critical factors, which determine the physical properties of UPy telechelics. These critical factors govern the superior

mechanical property of the UPy telechelics with reference to the application temperature. More importantly, the dynamic nature of these factors must be considered for constructing dimensionally stable materials based on UPy telechelics.

A consideration of the application or service window is very important in designing SPs based on hydrogen bonded system as the properties significantly depend on the polarity of the polymer and $T_g$ characteristics of linking oligomers. Preferred characteristics of the oligomer linkers to observe superior elastomeric property at ambient temperature are non-polar oligomer with moderate $T_g$ to exhibit low $T_{SG}$ for hydrogen bonded SPs.

Application of these findings to develop supramolecular polymeric assemblies based on ionic interactions such as pi-pi interaction, and metal-ion interaction will be very interesting. Though, considering each non-covalent interaction has its own specificity, directionality, and cooperative effect, application of above parameters may not be as straight forward, it will help to predict a general criterion to construct superior supramolecular materials for a defined application process window.

# Vita

Sachin Bobade was born on Jun 15th, 1983 Osmanabad, Maharashtra, India. He is the elder son of Sh. Laxman. P. Bobade and Smt. Hirabai Bobade. He has three younger siblings, two sisters Archana and Kalpana, and brother Nitin. In Dec 2013 he got married to his loving wife Laxmi Avatade.

After his high school he obtained his Bachelors of Science degree in Chemistry in 2003 from K. M. Agrawal College, Kalyan, affiliated with University of Mumbai. He continued his studies in the field of Chemistry at the University Department of Chemistry, University of Mumbai, India, and was awarded Masters of Science in Chemistry with major in Organic Chemistry in Jun 2005. After his M.Sc he worked as Research Chemist at Galaxy Surfactants Limited, at Galaxy Research Centre, India. He was awarded with junior research fellowship by CSIR, Delhi, India, which allowed him to join National Chemical Laboratory in August 2006, Pune with full time fellowship for five years. At NCL he started his doctoral studies in Polymer Chemistry under the guidance of Dr. D. Baskaran and Dr. Wadgaonkar. In Jan 2009 he moved to University of Tennessee, Knoxville and continued his doctoral research under the guidance Dr. Jimmy Mays and Dr. D. Baskaran. Sachin successfully defended his dissertation on 4th August, 2014.